AN EXAMINATION OF DEEP STABLE LAYERS IN THE INTERMOUNTAIN REGION OF THE WESTERN UNITED STATES

Paul G. Wolyn

Thomas B. McKee

Atmospheric Science
PAPER NO.
409

US ISSN 0067-0340

DEPARTMENT OF ATMOSPHERIC SCIENCE
COLORADO STATE UNIVERSITY
FORT COLLINS, COLORADO

AN EXAMINATION OF DEEP STABLE LAYERS IN THE INTERMOUNTAIN REGION OF THE WESTERN UNITED STATES

Paul G. Wolyn

Thomas B. McKee

This research was supported by
the National Science Foundation
under grant number ATM-8304328.

Department of Atmospheric Science
Colorado State University
Fort Collins, Colorado 80523

December 1986

Atmospheric Science Paper No. 409

ABSTRACT

AN EXAMINATION OF DEEP STABLE LAYERS IN THE INTERMOUNTAIN REGION OF THE WESTERN UNITED STATES

The definition of a deep stable layer used in this report is 65% of the lowest 1.5km of the 1200 GMT sounding having a lapse rate of 2.5°Ckm^{-1} or less. Deep stable layers are associated with one important group of days which can potentially cause poor regional air quality in the intermountain region of the western United States. At Grand Junction, CO, Salt Lake City, UT, Winnemucca, NV, and Boise, ID they cause low daytime convective boundary layer heights and can allow for light winds near the surface even if moderate or strong synoptic scale winds aloft are present. A climatology of deep stable layer days showed that at the four intermountain region stations most of the days with deep stable layers occurred in December and January. Using a strict deep stable layer definition and episode criteria, episodes of three days or longer occurred on the average at least once every two years at Salt Lake City and Winnemucca, and at least once a year at Boise and Grand Junction. An analysis of the mixing volumes for five consecutive Decembers at the four intermountain region stations shows that all the deep stable layer days had low mixing volumes.

A deep stable layer episode, which occurred from December 6 to December 23, 1980 at the four intermountain region stations, was examined in-depth to study the life cycle of a deep stable layer episode and to study the importance of different meteorological factors to the

initiation, continuation, and termination of the episode. The initiation of the episode is associated with the movement of a warm ridge aloft into the region and is accompanied by a descending region of rapid warming and strong stability. Synoptic-scale warm air advection and subsidence are both important mechanisms for causing the warming aloft. Weak incoming solar radiation resulting in modest surface heating is important to prevent the destruction of the descending stable region.

When the region of rapid warming descended to 0.5km-1.5km it formed a capping stable layer. In this part of the episode called the continuation phase, a disturbance was able to weaken the deep stable layer but not terminate it. The longwave radiative effects of fog may be important in this phase of the episode.

The termination of the episode is associated with the destruction of the warm ridge aloft and the movement of disturbances into the region. Surface heating may be important for aiding in the termination of the episode. The presence of a thick fog layer can require a stronger disturbance to terminate the episode.

ACKNOWLEDGEMENTS

The authors would like to thank Dr. Roger Pielke and Dr. Robert Meroney for their helpful advice. John Kleist was immensely helpful with the computer work used in this research and his assistance is greatly appreciated. Odie Bliss was very helpful with the preparation of this report and her assistance is also greatly appreciated. Judy Sorbie's drafting of some of the figures is also appreciated.

This research was funded by the National Science Foundation under grant number ATM-8304328.

TABLE OF CONTENTS

TABLE OF CONTENTS (continued)

CHAPTER I

INTRODUCTION

A. Overview of Thesis

Many people's notion of the intermountain region of the western United States is rugged mountains and unpolluted air with visibilities often greater than 50 miles. While this may often be the case, the intermountain region of the western United States is not immune from air quality problems. Many cities such as Salt Lake City, UT, and Boise, ID, occasionally have episodes of very poor air quality. The cities of the western United States, like the cities in the east and midwest, now realize that the atmosphere is not an infinite medium into which pollutants can be emitted and be easily dispersed.

Many studies have attempted to understand how frequently days with potentially poor regional air quality occur and to identify the meteorological conditions causing regional poor air quality. Methods that have been used to calculate the frequency of potentially poor regional air quality include calculating mixing volume for mean or individual soundings or determining the frequency or depth of inversions. The studies examining pollution potential for significant portions of the United States generally conclude that low level subsidence and light synoptic-scale winds cause a high potential for poor regional air quality.

In complex terrain cold air can stagnate near the surface resulting in the poor dispersion of pollutants. Many studies of the different instances of cold-air stagnation have identified mechanisms such as IR cooling of deep fog layer and weak surface heating as being important for the initiation and termination of a cold-air stagnation episode.

This study will examine deep stable layers at cities in the intermountain region of the western United States. The objective definition of a deep stable layer used in this study is that 65% of the lowest 1.5km of an atmospheric vertical sounding has a lapse rate of $2.5°Ckm^{-1}$ or less. Its structure consists of a deep layer having a lapse rate nearly isothermal or smaller above a surface based inversion or fog layer. Deep stable layers are significantly deeper than a typical nocturnal inversion. They are related to cold air stagnation in complex terrain. Deep stable layers can greatly reduce the height of the daytime convective boundary layer height (CBL) and can cause light winds near the surface despite the presence of moderate to strong synoptic-scale winds aloft. The low CBL heights and light surface winds can cause the volume of air into which pollutants are mixed to be small potentially resulting in high concentrations of pollutants in a region.

This thesis begins with a brief examination of the importance of deep stable layers for regional air quality in the intermountain region of the western United States. Then, for the remainder of the thesis the life cycle of a deep stable layer episode will be studied. A brief description of the life cycle of a deep stable layer episode will be given. The potential importance of synoptic-scale vertical motion, synoptic-scale horizontal advection, longwave induced temperature changes, and shortwave heating to the life cycle will be discussed.

The discussion will also investigate how different meteorological phenomenon can cause these physical processes to occur. Then, by performing a case study of a deep stable layer episode which occurred in December 1980, the importance of the different mechanisms to the episode will be discussed. Finally, the results from the case study will be synthesized into a conceptual model of an episode. The better understanding of deep stable layers from this study will aid in the forecasting of episodes of poor air quality and episodes of fog. The results will also provide insight into the different processes which must be included in any attempt to model the phenomenon.

B. Background

1. Studies Assessing Pollution Potential

Many studies have assessed the potential for poor regional air quality. One commonly used concept is the mixing volume (also called ventilation). It estimates the volume of air into which pollutants are emitted. A smaller mixing volume results in a higher pollution potential. A simple way of understanding the mixing volume concept is to imagine the atmosphere near the surface to be a box. During the daytime the top of the convective boundary layer (CBL) is the vertical boundary of the box. In the daytime CBL vigorous vertical motions occur which transport pollutants throughout the depth of the CBL. The top of the daytime CBL is very often capped by an inversion which is very stable and severely hampers vertical motion. Convective plumes can only penetrate a short distance into the inversion.

One of the horizontal boundaries of the box is defined by the length of the pollution emitting area perpendicular to the wind

direction. To simplify matters this boundary is often ignored. Wind speed determines the other horizontal boundary to the box. Faster wind speeds will cause more air to move over the pollution source. If other conditions are similar, the same amount of pollution will be emitted into more air resulting in lower pollution concentrations.

Niemeyer (1960) devised criteria to forecast low mixing volumes. These criteria were surface winds less than 8 knots, winds below 500mb no stronger than 25 knots, subsidence below 600mb, and such conditions persisting for at least 36 hours. Using several case studies in a large area of the eastern United States he showed that when these conditions occurred pollution concentrations were noticeably higher. He also noted that these conditions occurred almost exclusively with high pressure.

Boettger (1961) used the same criteria to forecast bad pollution episodes for the United States east of 105°W. Like Niemeyer (1960) he found that bad pollution episodes occurred when all four criteria were met. In one case he found high pollution concentration when only two of the four criteria were met. He suggested that any pollution forecasting program should not strictly follow all four criteria in determining bad regional pollutant episodes.

Holzworth (1962) examined the pollution potential for the western United States. The region considered was approximated defined to be west of the continental divide. He performed a climatology of mean mixing heights by using monthly averages of temperature at 50 mb intervals for 10 years of 0000 GMT soundings. He chose the height where the adiabatic lapse rate from the monthly mean maximum surface temperature intersects the mean sounding as the mean afternoon mixing height. The mean afternoon mixing heights of all the stations in the

study for January, April, July, and October were compared. The heights were lowest in January and ranged from 150m to 950m. They were the next lowest in October with a maximum height of about 1850m occurring over central Nevada. Along the Pacific coast mean mixing depths less than 1000m occurred for the four months examined. The synoptic situation associated with potentially bad air pollution episodes were also examined. Holzworth (1962) stated that the bad episodes were associated with a "quasi-stationary anticyclone centered over the Great Basin with a warm ridge aloft." In a climatology of bad episodes he noticed that about half of the time the wind at around 500mb exceeded 25 knots. This does not satisfy the low mixing volume forecasting criteria of Niemeyer (1960).

Holzworth (1967) performed an analysis of mean mixing depths for several cities in the United States. He estimated the mean morning mixing depth as where the dry adiabatic lapse rate from of the average minimum temperature plus 5°C intersects the mean monthly sounding. He found that Salt Lake City had a very shallow mean nocturnal mixing depth. The afternoon mixing depth in December and January were about 600m to 700m. These are smaller mixing depths than the other stations examined. The mean morning and afternoon wind speeds in December and January also were lower in Salt Lake City than most of other stations compared.

The mixing volume concept was further elaborated by Hanson and McKee (1983). For the 20 year period from 1959 to 1978, they calculated hourly daytime CBL heights at Grand Junction, CO, and Denver, CO, by using the daily 1200 GMT National Weather Service rawinsondes. An algorithm which calculates the hourly values of incoming solar radiation

was used. They assumed that 30% of the incoming solar radiation is used for CBL growth. The wind profile was estimated by using a logarithmic profile and the 700mb wind at 1200 GMT. Their determination of mixing area uses more than the maximum daytime mixing height. The estimated CBL heights throughout the morning and afternoon were used in the calculation of mixing area. This allowed for a more accurate representation of the actual volume of air into which pollutants are emitted. In their study a mixing area less than $3*10^8 m^2$ was considered to cause potentially poor air quality. Using this criteria, they identified episodes of low mixing volumes. They found there is a 60% chance of an episode of 10 days or longer occurring once a year at Grand Junction. For Denver they found a 60% chance of an episode of 7 days or longer occurring once a year.

Some methods for assessing the potential for poor regional air quality do not directly use the mixing volume concept. In many of these studies climatologies of meteorological factors, such as inversions or wind speeds, which are related to poor regional air quality were performed. Hosler (1961) examined the occurrence of surface based nocturnal inversions using sounding and tower data and found that a high frequency of surface based inversions during the night.

Holzworth (1962) performed a climatology of surface wind speeds for stations in the western United States. He defined a light wind day as having an average wind speed was less than 5.0 mph. He divided the wind climatologies into three categories. The climatology showed that 15% of the stations examined had hardly any light wind days; 60% of the stations had a large number of low wind speed days in the winter sometimes extending into the fall; and 20% of the stations had the

highest occurrence of low wind days in the fall with few low wind days in the winter. Of the stations in this study, Grand Junction, CO, Winnemucca, NV, Boise, ID, and Salt Lake City, UT, were classified as the second category with Boise also being assigned the first category.

Holzworth and Fischer (1979) calculated statistics of lapse rates, wind speeds, moisture, and inversions in the lowest 3.0km of the soundings from 1960 to 1964 for nearly all the stations in the United States which routinely take soundings at 1115 GMT and 2315 GMT. The calculations were performed for the 1115 GMT and 2315 GMT soundings for the winter, spring, summer, and autumn months. The results presented here will only be for the 1115 GMT (0415 MST) soundings in the winter months, which are December, January, and February.

The percentage of soundings with surface based inversions has a maximum of over 90% in southern Nevada. Values at Grand Junction, Salt Lake City, Winnemucca, and Boise are 68% to 86%. The percent of soundings with surface based inversions decreases to a minimum of 30% around the Great Lakes and 20% over the Pacific northwest. The percentage of elevated inversions with bases below 3.0km has nearly an opposite pattern to that of surface based inversions. For the four intermountain stations mentioned previously the percentages of soundings with elevated inversions are 6% to 22%. The sum of percentages of soundings with surface based inversions and elevated inversions are greater than 85% at nearly all the stations.

Figure 1 shows the percentage of soundings with surface based inversions heights exceeding 100m, 250m, 500m, 750m, 1000m, and 1500m. The maximum percentages of surface based inversions exceeding 750m are over 20% and occur around the Four Corners area and the northern plains

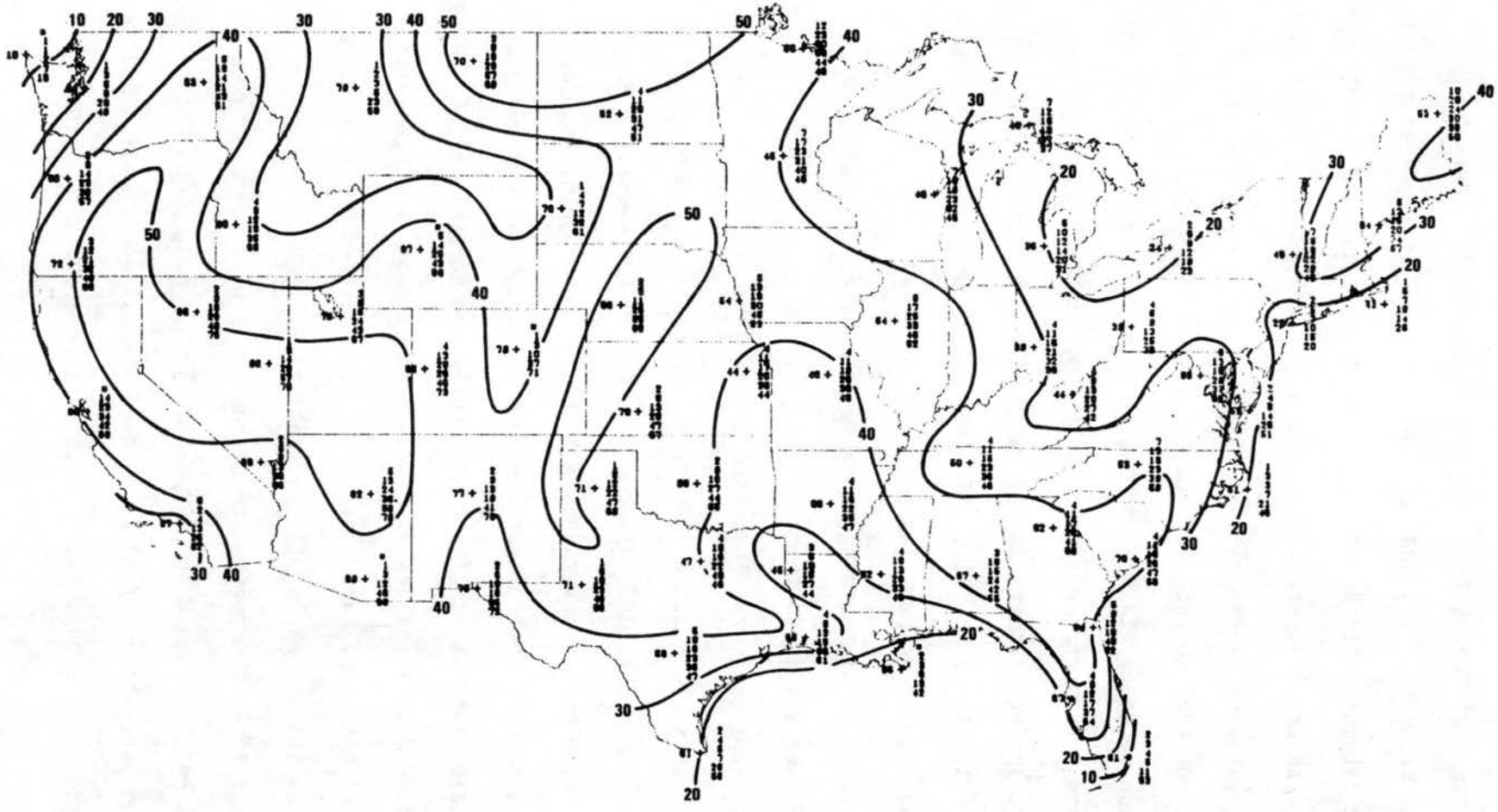

Figure 1. For the months December, January, and February the percentage of 1115 GMT soundings with surface-based inversions (on the left of the station marker) and with surface-based inversions exceeding 100m, 250m, 500m, 750m, 1000m and 1500m (on the right from bottom to top). Isopleths are for tops exceeding 250m. (From Holzworth and Fischer (1979)).

in a triangle defined by northwestern North Dakota, northeastern Minnesota, and north central Illinois. Except for the eastern Great Lakes region and along the mid-Atlantic coast, percentages of soundings with surface base inversion heights exceeding 750m is 10% to 20%. At the four stations in the intermountain region mentioned previously the percentage of surface based inversion heights exceeding 750m is 12% to 20%.

2. Complex Terrain Influences on Stagnation and Dispersion

Many stuidies have examined stagnation and pollution dispersion in complex terrain. This section will describe some of the stagnation and dispersion phenomenon. In the discussion of the different phenomenon the meteorological factors important for causing the stagnation and affecting the dispersion will be mentioned.

One example of the ability of air to stagnate in a wide valley is the occurrence of high inversion fog in the central valley of California. Willett (1928) in a section of his paper described high inversion fog that occurs in Europe and postulated the physical processes causing its formation. High inversion fogs are associated with marked inversions 200m to 2000m above the ground. Fog may extend from the ground to the base of the inversion and may persist for the entire day or dissolve during the daylight hours. There may also be a persistent low stratus deck at the base of the inversion.

Using stations at different elevations, Willett performed a climatology of 21 days of high inversion fog. The average temperatures were -2°C at the surface, -4.7°C at 700m, and 0°C at 1270m. His explanation for the inversion aloft was that subsidence associated with

an anticyclone warmed the air aloft while air near the surface did not sink and warm. He noticed an increase of dust particles in the lower levels with very clean air above the inversion base. The top of the dust layer became an effective radiating surface. Even if the air near the surface initially has a low relative humidity, the radiational cooling occurring over several days may be sufficiently strong to cool the air to its dew point. He noticed that fog also formed after the air mass moved over the coast of Norway. In this case the sea was colder than the air mass so convection did not occur. He concluded that the best conditions for high inversion fog occurs when the air mass has passed over water.

Lockhart (1943) in a technical paper by Byers documented a case of high inversion fog in the central valley of California in December 1928. A maritime air mass entered the valley on the fourteenth. Fog often formed at night but dissipated soon after sunrise. On the nineteenth winds above the top of the barrier up to 9800 feet had an easterly component. Temperature and moisture traces at a station 4209 feet above sea level showed a drying and warming trend while at Fresno, a station in the central valley, no appreciable warming or drying occurred. He noted that even without a strong capping inversion new air did not flow into the valley after the seventeenth. The fog progressively became more intense and often lasted the entire day. The end of this episode occurred when a moist air mass with stronger winds, associated with a storm moving onshore, replaced the warm, dry air in the inversion. The inversion breakup appeared to occur in about eight hours.

Holets and Swanson (1981) reported on observations associated with high inversion fog in the central valley of California in December 1978.

In the fog layer below the inversion the lapse rate was nearly moist adiabatic. At Butte, CA, where meteorological parameters and soundings were routinely taken the 10m wind speed varied from 1.3 to 2.2ms^{-1} and the wind shear in the fog layer was less than 0.3ms^{-1}(100m)$^{-1}$. The mean inversion intensity was 2.9K(100m)$^{-1}$ and the mean wind speed at the base of the inversion was 2.3ms^{-1} compared to 1.8 ms^{-1} at 10m. The mean wind shear in the inversion was only 0.47 ms^{-1}(100m)$^{-1}$. Soundings where taken at other places and they found that wind speeds generally where 5 ms^{-1} or less in the fog layer and overriding inversion layer. Also the inversion above the fog layer had a thickness of 1000m or less and was moderately stable.

Topographic blocking of air can cause low level stagnation. Orgill (1981) summarized the work of many authors who studied topographic blocking. Blocking can simply be described as a terrain induced collection of air on the upwind side of the barrier. The air trapped against the barrier does not have sufficient kinetic energy to rise over the barrier. Major influences affecting upwind blocking of air are geometric characteristics of the barrier, static stability of the air, height of boundary layer, and vertical wind profile. The conditions which are favorable for upstream stagnation are low prevailing wind speed, boundary layer height much lower than the barrier, and stable atmospheric static stability.

Parish (1982) presented the results of an observational study of the damming of cold, stable air against the Sierra Nevada Range in California. Pressure increases of 4mb to 6mb on the upwind side of the barrier associated with the damming were observed. The local pressure

increases were able to induce an along barrier jet with speeds over $20ms^{-1}$.

Using a two-dimensional mesoscale model Bader and McKee (1985) examined effects of different situations on deep mountain valley inversion breakup. One conclusion they made is that the wider the valley the less important the slope flow is in inversion breakup. In their modeling they found that when the valley width (measured from ridgetop to ridgetop) to valley depth ratio is greater than 24, inversion breakup is the same as if the terrain is flat. To measure the effect of higher albedo they reduced the amount of incoming solar radiation by 50% and 80%. The model showed that inversion breakup is similar for lower albedo cases but it occurred more slowly. They commented that high albedo can prevent the daily inversion breakup in deep mountain valleys.

The effects of wind shear above the valley were examined. In one simulation a wind of 10 ms^{-1} was put in at 500m above ridgetop, the model was allowed to come to equilibrium, then the simulated daytime heating in the model began. Inversion destruction proceeded very similarly to the no imposed wind case. They only noticed a slightly less stable stable core and that slightly less time was needed for inversion breakup.

Yu and Pielke (1985) examined the problem of stagnant conditions in the Lake Powell area. They performed a climatology of the synoptic surface weather pattern and found that 65% of the time from October to December the region is under the influence of a stagnant high pressure center. In January and February the frequency is 55%. In an examination of the synoptic situation on days with significant layered haze they

found that most days were under the influence of stagnant high pressure. Figure 2 shows three examples of atmospheric soundings which were taken on days with observed layered haze. The height of 900mb, 800mb, and 700mb are about 1km, 2km, and 3km above mean sea level (MSL), respectively. The layered haze episodes were accompanied by deep layers of significant stability near the surface. A primitive equation model was used to simulate the air flows in the valley filled with stagnant air. The output was used to run a Lagrangian particle dispersion model. The model showed that in this trapping valley the surrounding topography and inversion aloft can cause local recirculations in the valley. The pollution will accumulate in the valley without leaving it. They also suggested that the layered haze episodes are not easily ended and noticed that weak fronts or warm air advection over the valley did not terminate the layered haze episodes.

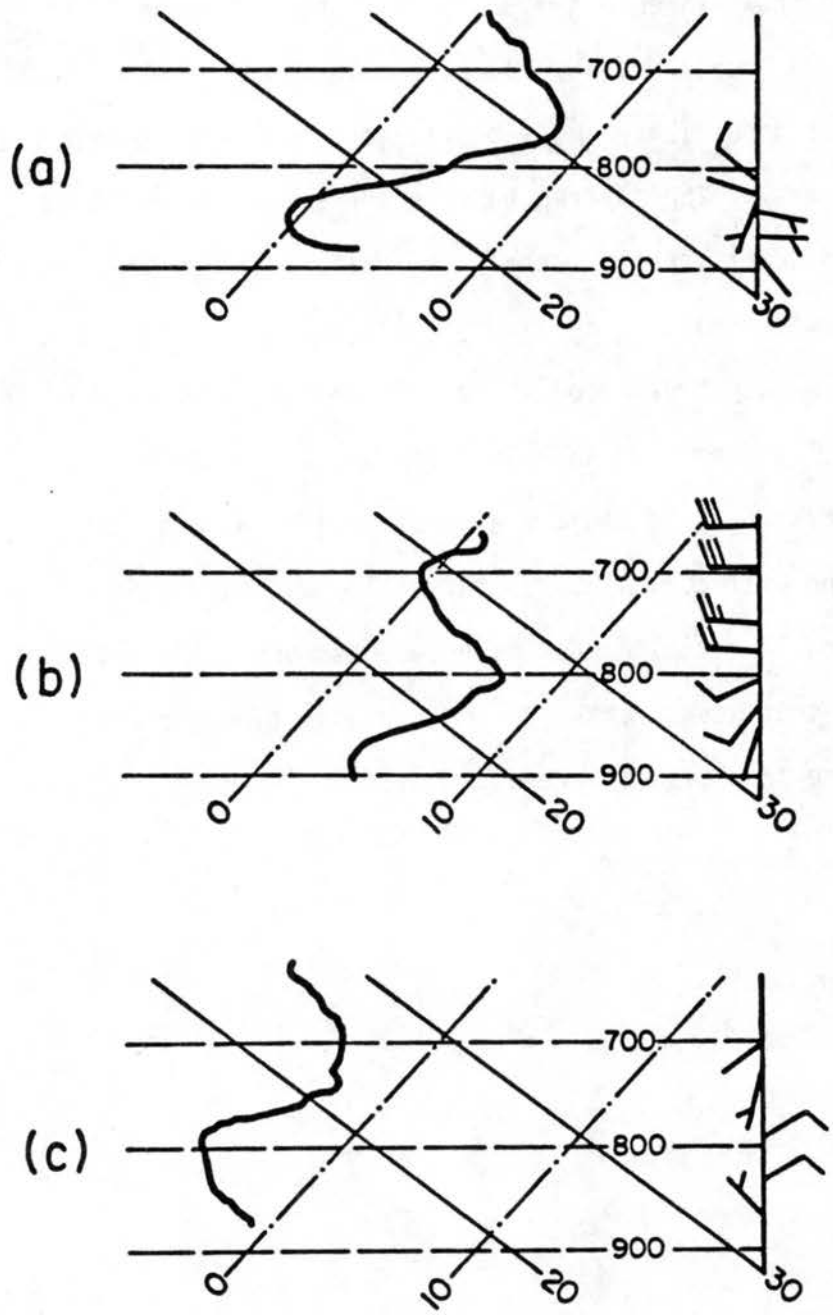

Figure 2. Plots of temperature at 0900 LST on days with observed layered haze in the Lake Powell Region. Diagonal lines which slope upward to the right are isotherms (°C) and lines that slope upward and to the left are adiabats (°C). Dates of the soundings are: (a) Dec. 3, 1979, (b) Dec. 10, 1979, and (c) Dec. 12, 1979. (From Yu and Pielke (1985)).

CHAPTER II

AIR POLLUTION IMPLICATIONS OF DEEP STABLE LAYERS

A. Introduction

In the last chapter many studies which assessed the potential for poor air quality at different locations were discussed. A high potential for regional poor air quality was related to low CBL heights and light winds near the surface. Some studies used the mixing volume to assess the air pollution potential while other studies examined the frequency of inversions or light wind speeds which both are related to potentially poor regional air quality. In complex terrain cold air near the surface can become stagnant in a region and can result in the trapping of pollutants in a small area.

This chapter will discuss the air pollution implications of deep stable layers by first examining the rationale for the deep stable layer definition. Then, the days with deep stable layers will be identified. The sensitivity of the definition to changes in the lapse rate and minimum depth criteria will be shown. Finally, by examining a climatology of deep stable layers and an analysis of mixing volume the importance of deep stable layers to regional air quality in the intermountain region will be determined.

B. Rationale for Deep Stable Layer Definition

The objective definition of a deep stable layer in this study is 65% of the lowest 1.5km of the 1200 GMT sounding has a lapse rate of $2.5°Ckm^{-1}$ or less. The deep layer of low level stability can severely reduce the height of the daytime CBL because a large amount of heating near the surface is needed to form a deep adiabatic layer. The deep layer of low level stability can allow for light winds near the surface with moderate to strong winds aloft. The Richardson number (Panosky and Dutton (1984)) ignoring the Bowen ratio effects is:

$$R_i = \frac{g}{T} \frac{(\gamma_d - \gamma)}{(\partial v/\partial z)^2} \qquad (1)$$

where:

R_i = Richardson number

g = gravity

T = temperature

γ = lapse rate of layer

γ_d = dry adiabatic lapse rate

v = wind speed.

The Richardson number is valid for determining if turbulent mixing of a fluid in a thin layer will occur. For thick layers the Richardson number is less valid, but it can still give a good indication of whether turbulent mixing will occur. For a lapse rate of $2.5°Ckm^{-1}$ and a temperature of 273K a wind shear of $32ms^{-1}km^{-1}$ is needed to reach the critical Richardson number, which is 0.25. This suggests that a deep layer of stability with a lapse rate of $2.5°Ckm^{-1}$ can allow for the

existence of strong wind shears without significant turbulent mixing of momentum.

Decoupling occurs when momentum from synoptic-scale winds aloft do not penetrate to near the surface. With light synoptic-scale winds aloft the wind shears near the surface will be small and decoupling can occur with fairly weak stability. Deep stable layers may allow for decoupling with moderate or strong synoptic-scale winds, because they can allow for the existence of large vertical wind shears. Momentum from moderate or strong synoptic-scale winds above the deep stable may not be able to penetrate to near the surface. With decoupling the winds near the surface will be dominated by surface pressure gradients. In complex terrain if a deep stable layer covers an entire basin and if the synoptic-scale surface pressure gradients are weak, winds caused by mesoscale circulations, which generally are light and do not cause transport of pollutants over long distances, will predominate.

The episodic implications of deep stable layers are important to air quality. In locations where terrain features limit the horizontal movement of air near the surface, deep stable layer episodes can cause the collection of pollution emitted over many days in a small volume. The structure of deep stable layers is favorable for the occurrence of episodes, because deep layers of significant stability are not easily destroyed. If the weather conditions of the atmosphere above the deep stable layer do not drastically change and the air near the surface does not warm substantially, deep stable layers will last for many consecutive days. As seen with the stagnation in the Lake Powell region and the central valley of California, when weather conditions do change deep layer of significant stability may not easily breakup. Holzworth

(1967) in his examination of the air pollution potential for the western United States stated that in many cases a weak disturbance cannot destroy layers of stable air near the surface.

C. Identification of Deep Stable Layers

A computer tape containing the National Weather Service synoptic soundings for Denver, CO, Dodge City, KS, Grand Junction, CO, Salt Lake City, UT, Winnemucca, NV, and Boise, ID, taken at 2315 GMT (1615 MST) and at 1115 GMT (0415 MST) was obtained. Figure 3 shows the location of the stations. The data for each sounding on the tape includes temperature, dew point, wind direction, and wind speed for the mandatory levels; temperature and dew point for the significant levels; and wind speed and wind direction for other heights. Wind speed, wind direction, temperature, and dew point data were also interpolated to provide values at levels of 50 mb increments. The Manual for Radiosonde Coding (1968) states that below 300mb linear interpolation of temperature and dewpoint between significant levels should allow for the sounding to be constructed to an accuracy of 2°C for temperature and 10% for relative humidity. By linearly interpolating between data points the temperature and humidity for any level below 300mb can be found to an accuracy of at least 2°C and 10%, respectively.

Daily sounding data from 1959 to 1983 for the six stations was examined to identify days with deep stable layers. Obviously, the soundings for each day could not be plotted and examined individually to subjectively determine whether a deep stable layer was present on that day. An automated objective method was developed to identify days with deep stable layers.

Figure 3. Map of the western United States showing the locations of the stations in this study.

Figure 4 shows a schematic of how the method was used to determine the existence of a deep stable layer. Beginning at the surface and ending at the first data point at or above 1500m AGL, the lapse rate between two consecutive data points was calculated. If the lapse rate is $2.5°Ckm^{-1}$ or less, the layer is stable. The difference of the heights between the top and bottom data points of a stable layer is the thickness of the layer. If the top data point was above 1500m AGL, the top data point was assumed to have a height of 1500m AGL. If the sum of the thickness of the stable layer was 975m or greater, the sounding has a deep stable layer. The program examined the 1200 GMT sounding on each day. If the 1200 GMT sounding satisfied the deep stable layer criteria, then the day was considered to be under the influence of a deep stable layer.

D. Sensitivity of Deep Stable Layer Definition

The objective definition of a deep stable layer has a minimum depth criteria of 975m and a lapse rate criteria of $2.5°Ckm^{-1}$. As with any objective definition, the number of deep stable layers possibly can be very sensitive to the values of parameters in the definition. Figure 5 shows a plot of the number of deep stable layers for different minimum depth criteria for the six stations. At 975m the changes in number of days with depth criteria are generally small so a minor change in minimum depth criteria will not significantly affect the number of deep stable layers.

Figure 6 shows a plot of the number of deep stable layers for different lapse rate criteria at the six stations. The curves have a more exponential shape than the curves for the different depth criteria.

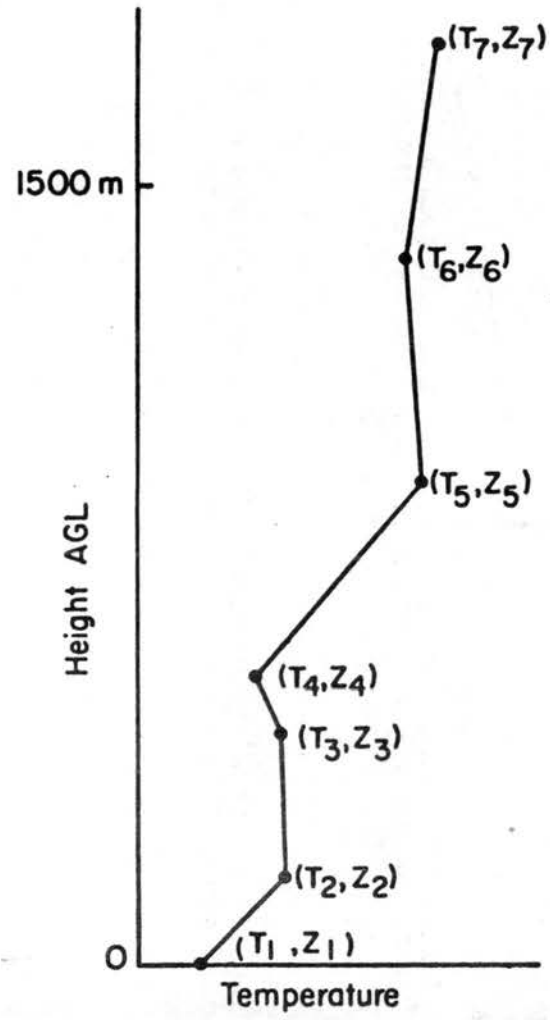

Initially set the sum of the thickness of layers with stable lapse rates (SUMTHK) = 0

For $i = 2, 3, 4, 5,$ and 6

If $\left(\frac{T_i - T_{i-1}}{Z_i - Z_{i-1}}\right) \geq -2.5°\,C\ km^{-1}$ then

$SUMTHK = SUMTHK + (Z_i - Z_{i-1})$

Since $Z_7 \geq 1500m$

If $\left(\frac{T_7 - T_6}{Z_7 - Z_6}\right) \geq -2.5°C\ km^{-1}$ then

$SUMTHK = SUMTHK + (1500 - Z_6)$

If SUMTHK ≥ 975m then a deep stable layer is present.

Figure 4. A schematic of how the presence of a deep stable layer was determined.

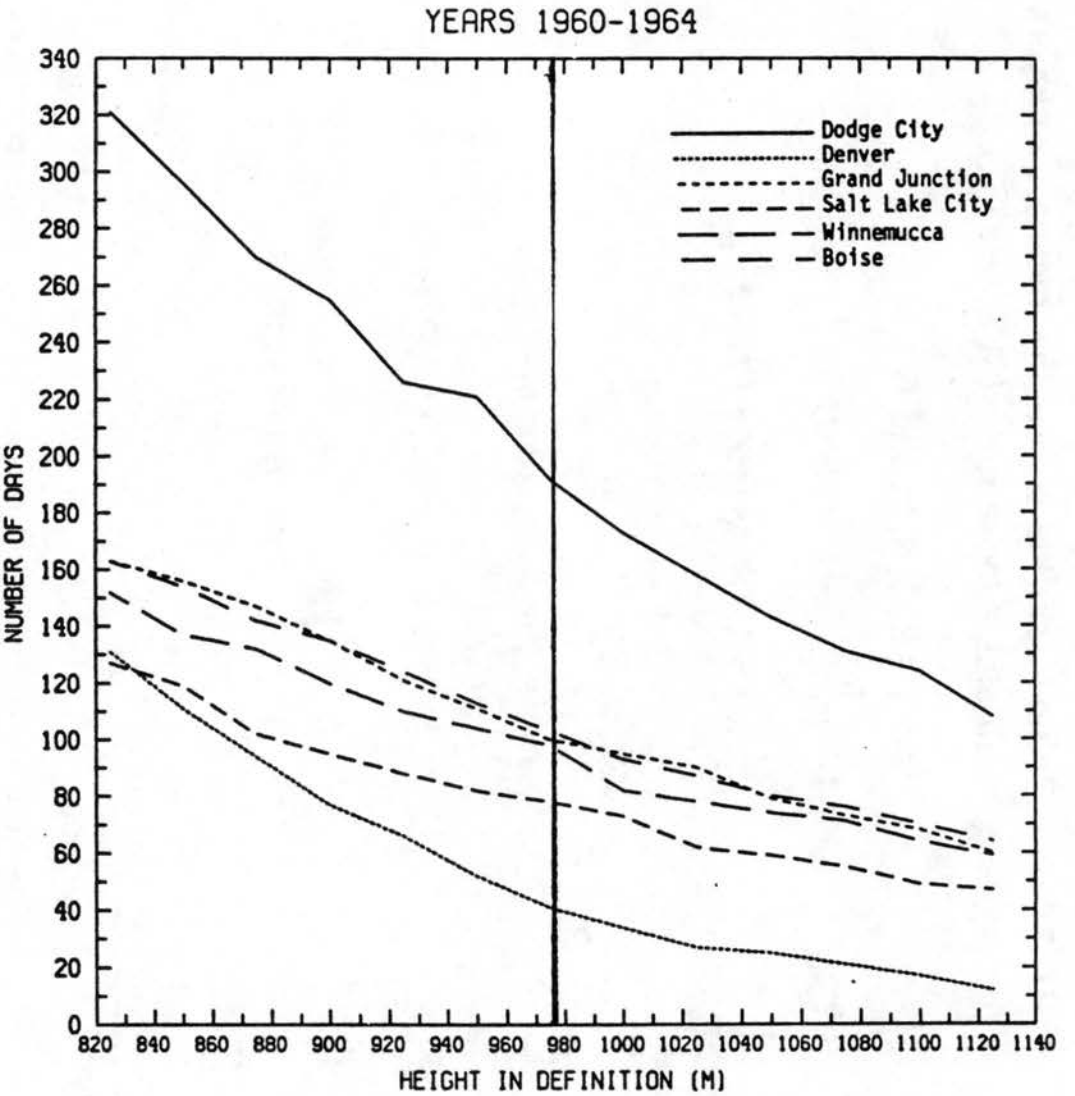

Figure 5. A graph showing the number of deep stable layer days from 1960 to 1964 for different minimum depth criteria.

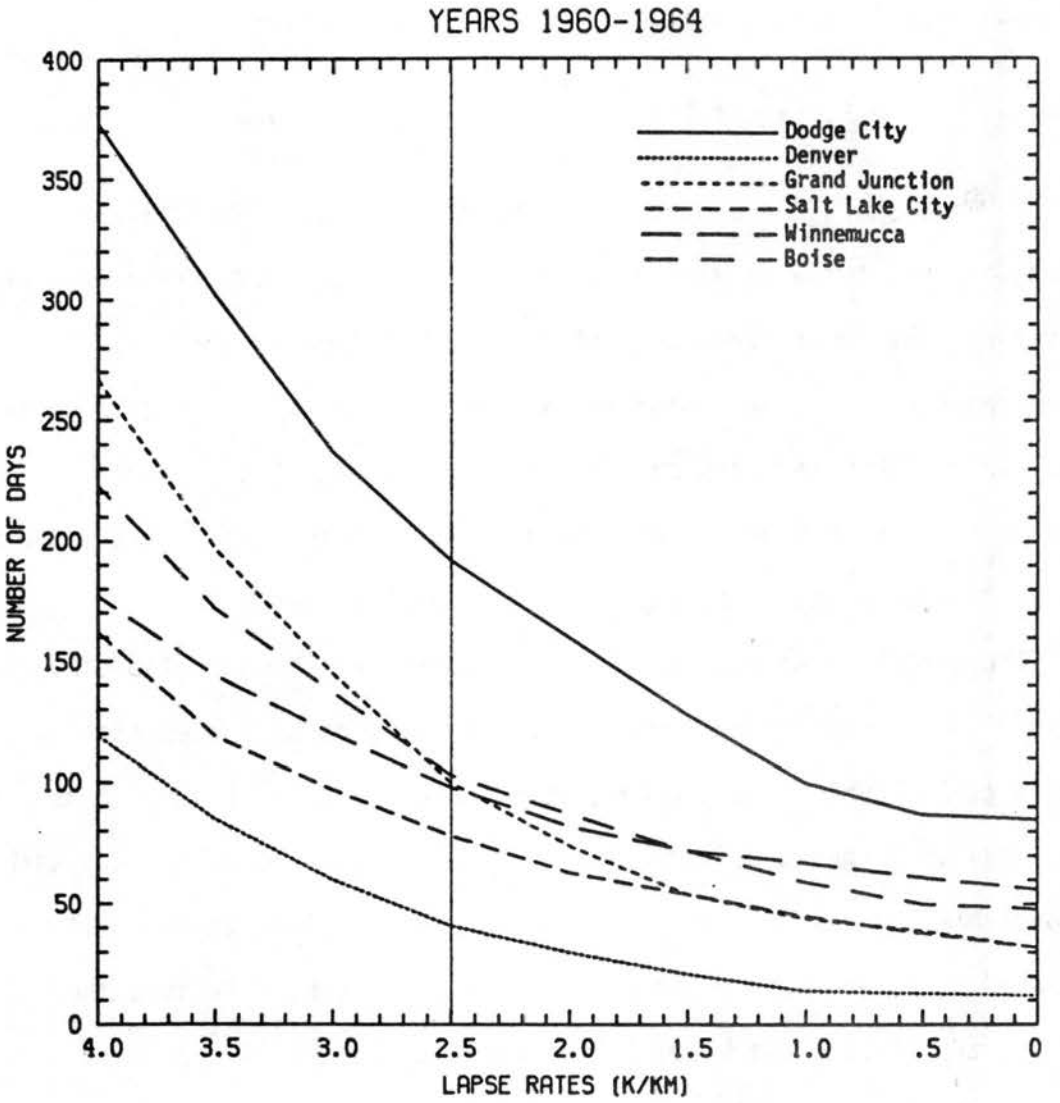

Figure 6. A graph showing the number of deep stable layers days from 1960 to 1964 for different lapse rate criteria.

Generally, around the lapse rate of 2.5°Ckm^{-1} the slope of the curves begin to "flatten" significantly. Using lapse rates less than 2.5°Ckm^{-1} will not greatly alter the number of deep stable layers.

E. Climatology of Deep Stable Layer Days

Table 1 shows the monthly distribution of deep stable layers. Dodge City has twice as many deep stable layers than the other stations. Denver has the lowest frequency of deep stable layers. The four remaining stations show a similar pattern. The most deep stable layers occur in December and January. There are also significant number of days in October, November, and February. During the other months about one percent or less of the days have deep stable layers.

The length of deep stable layer episodes are shown in Table 2. An episode is defined as the number of consecutive days of deep stable layers at 1200 GMT. Missing days were included in an episode if it was four days or longer and if the missing day was sandwiched by days with deep stable layers. At Grand Junction in the 25 years examined 34 episodes of three days or longer occurred. For other stations the numbers are 15 for Salt Lake, 21 for Winnemucca, and 35 for Boise. Episodes three days or longer can occur at least once every two years at Salt Lake City and Winnemucca and at least once a year at Grand Junction and Boise.

Dodge City also shows an interesting trait. For the large number of deep stable layer days, the number of episodes of three days or longer, especially in the winter, is not very different from the other stations. This suggests that many of the deep stable layers at Dodge City may be related to transient synoptic-scale systems. At Denver

Table 1.
Monthly distribution of the number and percentage of days with deep stable layers from 1959 to 1983.

	JAN	FEB	MAR	APR	MAY	JUN	JUL	AUG	SEP	OCT	NOV	DEC	TOTAL
Dodge City													
Number of days	153	112	91	65	52	46	27	30	53	85	98	145	954
Percentage of days	20	16	12	9	7	6	4	4	7	11	13	19	
Denver													
Number of days	30	8	14	4	14	11	13	22	15	22	14	21	188
Percentage of days	4	1	2	1	2	2	2	3	2	3	2	3	
Grand Junction													
Number of days	151	33	4	3	5	6	4	6	9	16	37	143	417
Percentage of days	20	5	1	<1	1	1	1	1	1	2	5	18	
Salt Lake City													
Number of days	83	30	8	3	2	4	3	2	4	25	49	85	298
Percentage of days	11	4	1	<1	<1	1	<1	<1	1	3	7	11	
Winnemucca													
Number of days	119	40	6	0	9	0	4	3	7	35	76	117	416
Percentage of days	15	6	1	0	1	0	1	<1	1	5	10	15	
Boise													
Number of days	118	51	8	6	3	6	14	3	8	53	76	116	462
Percentage of days	15	7	1	1	<1	1	2	<1	1	7	10	15	

Table 2.
Monthly distribution of the length of deep stable layers from 1959 to 1983.

LENGTH	JAN	FEB	MAR	APR	MAY	JUN	JUL	AUG	SEP	OCT	NOV	DEC
Dodge City												
1	85	73	59	48	42	36	28	23	42	63	68	72
2	18	9	15	5	5	4	1	2	5	8	12	19
3	5	4	0	1	0	0	0	1	1	2	1	17
4	3	2	0	0	0	0	0	0	0	0	1	1
5	1	0	0	1	0	0	0	0	0	0	0	2
Denver												
1	24	8	14	3	15	9	13	20	15	21	12	18
2	3	0	0	0	0	1	0	1	0	0	1	0
3	0	0	0	0	0	0	0	0	0	0	0	1
Grand Junction												
1	40	13	2	3	5	6	4	6	10	14	29	41
2	25	4	1	0	0	0	0	0	0	1	2	21
3	10	2	0	0	0	0	0	0	0	0	1	8
4	3	0	0	0	0	0	0	0	0	0	0	2
5	2	0	0	0	0	0	0	0	0	0	0	1
6	2	0	0	0	0	0	0	0	0	0	0	1
7	0	0	0	0	0	0	0	0	0	0	0	1
8	0	0	0	0	0	0	0	0	0	0	0	1
Salt Lake City												
1	29	15	6	3	2	4	3	2	4	19	33	43
2	9	6	1	0	0	0	0	0	0	1	7	16
3	6	1	0	0	0	0	0	0	0	1	0	1
4	1	0	0	0	0	0	0	0	0	0	1	2
5	1	0	0	0	0	0	0	0	0	0	0	0
6	1	0	0	0	0	0	0	0	0	0	0	0
Winnemucca												
1	51	19	6	0	9	0	4	3	7	25	37	59
2	21	6	0	0	0	0	0	0	0	5	11	16
3	7	1	0	0	0	0	0	0	0	0	2	4
4	1	0	0	0	0	0	0	0	0	0	2	2
5	1	0	0	0	0	0	0	0	0	0	0	0
6	0	0	0	0	0	0	0	0	0	0	1	0
Boise												
1	52	20	8	6	3	6	11	3	5	36	40	35
2	11	9	0	0	0	0	1	0	0	6	7	15
3	4	1	0	0	0	0	0	0	1	2	3	11
4	4	0	0	0	0	0	0	0	0	0	2	0
5	3	1	0	0	0	0	0	0	0	0	0	2
6	0	0	0	0	0	0	0	0	0	0	1	0

there are very few deep stable layer days and only one episode of three days or longer occurred. This suggests that the deep layer of moderate stability as defined in this thesis is not a major concern for air quality problems in Denver.

F. Pollution Potential of Deep Stable Layer Days

The wind speeds at the surface and a level from 500m to 750m above ground level for all deep stable layers from 1960 to 1964 were calculated. The means include the 0000 GMT and 1200 GMT data. Tables 3 and 4 show the results. The mean surface wind speeds at Dodge City are almost twice as strong as at any other station, and this is true especially in December and January. The strong wind speeds show that the deep stable layers at Dodge City generally are not associated with stagnant conditions and are not of major concern for air pollution problems. A brief examination of the deep stable layers at Dodge City shows that most of the days are associated with precipitation, low clouds, or shallow continental polar or continental arctic air masses from central Canada.

An analysis of mixing volume for Grand Junction, Salt Lake City, Winnemucca, and Boise for all the days in December from 1976 to 1980 was performed. To estimate the maximum height of the daytime CBL, the height at which an adiabat of the surface maximum temperature first intersects the 0000 GMT sounding was calculated. This parameter is called the calculated convective boundary layer (CCBL) height. This value is often an overestimate because a shallow superadiabatic layer immediately above the surface usually is present and the potential temperature of most of the CBL is less than the potential temperature of

Table 3.
The mean and standard deviation of surface wind speeds on days with deep stable layers for years 1960-1964. The data includes values from the 1200 and 0000 GMT soundings.

	JAN	FEB	MAR	APR	MAY	JUN	JUL	AUG	SEP	OCT	NOV	DEC	MEAN
Dodge City													
Speed (m/s)	6.3	6.6	6.6	7.3	8.4	7.1	5.2	6.3	5.9	5.7	4.9	5.8	6.3
Stand. dev.	2.77	2.83	2.49	4.01	3.51	3.75	1.82	2.97	2.77	2.28	2.44	2.68	
Number of values	55	47	46	27	21	14	15	18	32	28	30	50	
Grand Junction													
Speed (m/s)	2.2	2.8	-	4.5	6.2	4.8	5.8	5.3	4.3	3.3	2.5	2.3	2.8
Stand. dev.	1.48	2.64	-	0.71	2.04	1.60	0.96	2.06	1.71	1.03	1.20	1.29	
Number of values	70	9	0	2	6	6	4	4	4	6	18	51	
Salt Lake City													
Speed (m/s)	3.0	4.0	3.0	3.0	4.0	-	4.2	-	3.0	3.3	4.0	2.9	3.3
Stand. dev.	1.07	2.19	1.41	0.00	1.41	-	1.94	-	1.41	0.71	1.81	1.28	
Number of values	65	11	4	2	2	0	6	0	2	8	24	32	
Winnemucca													
Speed (m/s)	2.7	1.6	4.0	-	5.8	-	3.5	2.5	3.3	2.9	2.2	2.2	2.7
Stand. dev.	2.28	1.33	0.00	-	1.99	-	0.71	0.71	1.53	1.52	2.05	1.76	
Number of values	68	9	2	0	12	0	2	2	3	17	26	55	
Boise													
Speed (m/s)	2.6	2.8	3.2	-	3.5	-	4.2	3.5	4.4	3.4	3.5	2.4	2.9
Stand. dev.	1.59	2.07	2.32	-	0.71	-	2.23	0.71	1.92	0.84	1.83	1.45	
Number of values	65	19	6	0	2	0	6	2	8	23	26	47	

Table 4.
The mean and standard deviation of wind speeds at a level between 500 and 750m AGL for years 1960-1964. The mean heights of the levels are also given. The data includes speeds at 1200 and 0000 GMT.

	JAN	FEB	MAR	APR	MAY	JUN	JUL	AUG	SEP	OCT	NOV	DEC
Dodge City												
Speed (m/s)	10.4	10.1	10.8	12.6	17.4	13.9	7.7	10.1	10.9	10.7	10.8	10.6
Stand. dev.	5.56	5.92	6.36	8.02	7.29	7.85	4.75	6.08	6.60	5.50	5.79	6.43
Mean height (m)	685	663	668	667	683	706	719	711	731	732	724	700
Number of values	51	43	44	22	18	13	14	18	27	24	24	47
Grand Junction												
Speed (m/s)	3.1	5.0	-	6.5	8.0	6.2	7.3	6.5	7.0	2.8	3.0	3.2
Stand. dev.	1.97	3.74	-	0.71	3.03	2.79	0.50	5.45	1.83	1.17	1.41	2.40
Mean height (m)	544	558	-	527	522	512	537	542	546	587	544	556
Number of values	78	8	0	2	6	6	4	4	4	6	17	61
Salt Lake City												
Speed (m/s)	3.1	4.5	3.5	1.5	10.0	-	4.0	-	3.0	2.6	4.9	3.4
Stand. dev.	2.73	3.62	1.29	0.71	2.83	-	1.67	-	1.41	1.51	4.56	2.65
Mean height (m)	759	750	701	668	683	-	752	-	701	782	753	755
Number of values	65	11	4	2	2	0	6	0	2	8	24	32
Winnemucca												
Speed (m/s)	4.4	3.6	2.5	-	6.5	-	4.5	3.0	3.0	3.4	4.5	3.4
Stand. dev.	2.96	1.69	0.71	-	3.21	-	0.71	2.83	1.73	1.50	2.89	2.12
Mean height	727	763	683	-	651	-	714	712	726	744	735	739
Number of values	65	8	2	0	11	0	2	2	3	17	26	55
Boise												
Speed (m/s)	5.7	5.9	4.3	-	4.0	-	7.0	7.0	7.3	3.7	5.8	5.1
Stand. dev.	4.34	3.18	3.20	-	2.71	-	2.71	1.41	2.49	2.19	2.83	2.92
Mean height (m)	670	677	652	-	648	-	638	660	613	693	659	689
Number of values	61	18	4	0	1	0	4	2	8	22	25	43

the surface. The wind speed in the CCBL was calculated by integrally averaging the wind speeds below the CCBL height. The wind speeds are assumed to vary linearly with height between data points.

Table 5 shows the distribution, averages, and standard deviations of the product of CCBL heights and mean wind speed below the CCBL height for days with and without deep stable layers. This product will be called the mixing volume. Table 6 shows the distribution, means, and standard deviations of CCBL heights and mean wind speed below the CCBL height at the four stations. The data shows that all days with deep stable layers have low mixing volumes, all the deep stable layer days have CCBL heights less than 1000m, and nearly all the deep stable layer days have mean wind speeds below the CCBL height less than 4 ms^{-1}. The percentage of days with mixing volumes of $2.0*10^{3}m^{2}s^{-1}$ or less which have deep stable layers are 24% at Grand Junction, 16% at Salt lake City, 39% at Winnemucca, and 29% at Boise. The objective deep stable layer definition identifies one group of potentially poor air quality days. Since deep stable layers occur fairly frequently, can occur in episodes of three days or longer, and are associated with small mixing volumes, deep stable layers are important for air regional air quality in the intermountain region.

The analysis also shows that there are a large number of non-deep stable layer days which have small mixing volumes. Some of the non-deep stable layer days with low mixing volumes may be the result of less stable atmospheric structures that may be able to cause low daytime CBL heights and light winds near the surface. For example, days with deep fog layers capped by a strong, relatively deep inversion, which can cause low CCBL height and decoupling with moderate to strong winds

Table 5.
Distribution, mean, and standard deviation of mixing volumes for days with and without deep stable layers for the month of December from 1976-1980. DSL refers to days with deep stable layers and non-DSL refers to days without deep stable layers.

Mixing Volume	Grand Junction		Salt Lake City		Winnemucca		Boise	
($10^3 m^2 s^{-1}$)	DSL	non-DSL	DSL	non-DSL	DSL	non-DSL	DSL	non-DSL
<1	26	78	12	53	18	24	24	55
1-2	6	23	2	20	8	17	7	20
2-3	0	3	1	17	1	14	1	9
3-4	0	3	0	4	0	9	0	6
4-5	0	1	0	6	0	7	0	7
5-6	0	6	0	7	0	4	0	4
6-7	0	3	0	4	1	3	0	1
7-8	1	1	0	3	0	6	0	1
8-0	0	2	0	3	0	5	0	2
9-10	0	0	0	3	0	3	0	1
10-11	0	1	0	2	0	1	0	2
11-12	0	0	0	1	0	2	0	1
>12	0	4	0	14	0	23	0	12
Mean	655	2158	726	4380	1109	8359	755	4892
Stand. Dev.	396	4432	673	7111	1261	12709	542	10721

Table 6.
Same as Table 5 except values are for CCBL heights and mean wind speeds below the CCBL height.

CCBL Height	Grand Junction		Salt Lake City		Winnemucca		Boise	
(10^2m)	DSL	non-DSL	DSL	non-DSL	DSL	non-DSL	DSL	non-DSL
<2.5	9	35	5	25	3	8	8	38
2.5-5.0	14	44	8	33	13	21	21	28
5.0-7.5	6	15	3	24	9	18	2	24
7.5-10.0	0	13	0	13	6	13	2	11
10.0-12.5	0	3	0	8	0	16	0	4
12.5-15.0	0	4	0	6	0	14	0	3
15.0-17.5	0	4	0	9	0	10	0	5
17.5-20.0	0	3	0	7	0	8	0	2
20.0-22.5	0	1	0	3	0	4	0	1
22.5-25.0	0	1	0	7	0	4	0	0
>25.0	0	2	0	3	0	8	0	6
Mean	350	581	359	865	519	1162	356	669
Stand. Dev.	161	565	140	772	236	794	168	754

Wind Speed	Grand Junction		Salt Lake City		Winnemucca		Boise	
(ms^{-1})	DSL	non DSL	DSL	non-DSL	DSL	non-DSL	DSL	non-DSL
<1	2	2	1	3	3	0	3	3
1-2	13	53	9	49	11	28	12	22
2-3	11	39	2	25	10	15	11	22
3-4	3	15	1	14	1	15	5	14
4-5	0	7	1	18	1	15	0	14
5-6	0	1	1	7	1	6	1	12
6-7	0	1	0	9	0	6	0	6
7-8	0	1	0	4	1	9	0	10
8-9	0	3	0	3	0	5	0	3
9-10	0	2	0	2	0	5	0	2
>10	0	1	0	9	0	14	0	13
Mean	1.9	2.6	1.9	3.9	2.1	5.2	2.0	4.9
Stand. Dev.	0.7	1.9	1.3	3.1	1.5	4.1	1.0	3.9

aloft, may not be identified as a deep stable layer. Other factors such as snowcover, cloudcover, or very light synoptic-scale winds may also be contribute to smaller mixing volumes on the non-deep stable layer days.

CHAPTER III

PHYSICAL PROCESSES IMPORTANT FOR A DEEP STABLE LAYER EPISODE

A. Introduction

Deep stable layers are important for regional air quality in the intermountain region of the western United States. For the remainder of the thesis, the life cycle of a deep stable layer will be examined in depth. In this chapter a brief description of the life cycle of a deep stable layer episode will be given. Then, the potential effects of synoptic-scale vertical motion, synoptic-scale horizontal temperature advection, and diabatic heating on the initiation, continuation, and termination of a deep stable layer episode will be presented. The discussion of diabatic effects on the life cycle will concentrate on how meteorological phenomenon, such as fog and snowcover, can affect the life cycle.

B. Life Cycle of a Deep Stable Layer Episode

The life cycle of a deep stable layer episode will be divided into three phases: the initiation phase, the continuation phase, and the termination phase. The initiation phase is the period of time in which processes which form a deep stable layer episode occur. To form a deep stable layer there must be cooling near the surface or warming aloft. If the air near the surface and aloft both warm or cool similar amounts

then the overall stability of the atmosphere will not increase and the deep stable layer will not form. In this phase cold air near the surface must not be able to rise over the elevated surrounding terrain resulting in the trapping of the cold air in a region. As stated in the first chapter, light winds and a stable atmosphere can greatly reduce the possibility of cold air rising over barriers. The initiation phase ends with the first appearance of a deep stable layer.

The continuation phase of the episode is associated with a persistent deep stable layer. In this phase the deep stable layer may strengthen or weaken, but any mechanism weakening the episode is not sufficiently strong to end it. The termination phase is associated with processes which end the episode. This phase begins when processes terminating the episode are first able to weaken the deep stable layer. The termination of the episode must have cooling aloft, warming near the surface, or mechanisms, such as strong winds or synoptic-scale vertical motion, that can lift the cold air over the surrounding elevated terrain and replace it with warmer air.

C. Possible Physical Processes Affecting the Life Cycle

In the discussion of the life cycle of a deep stable layer episode heating and cooling aloft and near the surface were listed as important factors in the life cycle. In this section physical processes that may be important to the initiation, continuation, and termination of a deep stable layer episode will be given. The discussion will mainly focus on the potential for different physical processes to cause heating or cooling and on identifying possible meteorological phenomenon that can cause the heating or cooling.

The first law of thermodynamics given in Holton (1972) is:

$$c_p \frac{dT}{dt} - \alpha \frac{dP}{dt} = \dot{Q} \qquad (2)$$

where:

c_p = specific heat of dry air at a constant pressure

α = specific volume

P = pressure

$\dot{Q}$ = diabatic heating rate per unit mass.

Using potential temperature, equation (2) becomes:

$$\frac{\partial \theta}{\partial t} = - \underset{\sim}{V} \cdot \nabla \theta - w \frac{\partial \theta}{\partial z} + \frac{\theta}{c_p T} \dot{Q} \qquad (3)$$

where:

θ = potential temperature

$\underset{\sim}{V}$ = horizontal velocity of the air

w = vertical velocity of the air.

The terms from left to right in the potential temperature form of the equation are local change in potential temperature, local potential temperature change by horizontal advection of potential temperature, local potential temperature change by vertical motion, and local potential temperature change by diabatic heating/cooling. Heating or cooling at a location can only be accomplished by vertical motion, horizontal temperature advection, or diabatic effects.

Synoptic-scale vertical motion can be important to the initiation of a deep stable layer episode. Since potential temperature increases with height, synoptic-scale sinking motion can cause warming starting at several hundred meters above the ground. Similarly, rising motion can cause cooling the atmosphere above the surface and likely is an

important mechanism for the termination of an episode. By continuity of mass considerations, rising motion can also terminate a deep stable layer episode by forcing the ascent of cold air near the surface.

Horizontal temperature advection can be another important influence for the initiation or termination of a deep stable layer. Beginning several hundred meters above the ground, warm air advection is a mechanism for the initiation of an episode and cold air advection is a mechanism for the termination of a deep stable layer episode. Horizontal temperature advection near the surface can also be an initiation or termination mechanism. Cold air advection near the surface can aid in the initiation of an episode while warm air advection can aid in the termination of an episode. In complex terrain the advection of air masses near the surface from one basin to another is difficult especially when winds are light and the lower atmosphere is stable.

Diabatic heating can also have important influences on the life cycle of an episode. Diabatic heating can be accomplished by three different physical processes: solar heating, longwave heating or cooling, and condensation heating. It will later be shown that the diabatic effects of condensation do not appear to be significant, so its potential influences on the life cycle will not be discussed. The remainder of this section will mainly concentrate on how different meteorological phenomenon can influence the episode life cycle through diabatic effects.

The atmosphere is poor at absorbing shortwave radiation; therefore, the major effect of incoming solar radiation is to heat the surface forming a daytime CBL. Significant daytime heating of the surface can

greatly warm the air near the surface, and the resulting daytime CBL can mix through a deep layer of stability destroying it.

The time of year is an important factor for surface heating. During low sun months the amount of incoming solar radiation at middle latitudes is much less than the high sun months. With low sun angles the energy from the sun is spread over a larger area resulting in less heating at one point. The low sun angle further reduces the amount of solar radiation reaching the surface because the path of radiation is through a greater depth of the atmosphere.

Snowcover can lessen the heating near the surface from incoming solar radiation. Snow has a high albedo resulting in a large percentage of incoming solar radiation being reflected to space. If incoming solar energy is absorbed some of the energy may be used to melt the snow crystals instead of heating the air near the surface. Similarly, wet ground can reduce the amount of heating near the surface because a significant amount of the incoming solar radiation is can be used to evaporate the moisture at the surface.

The clouds and fog can also can also lessen the surface heating by reducing the amount of solar radiation reaching the surface. Like snowcover, clouds have high albedoes so a significant portion of the incoming solar radiation will be reflected away from the surface.

Longwave properties of snowcover, clouds, and vertical moisture and temperature profiles can affect the life cycle of an episode by causing increased cooling or heating at different heights. Snowcover is an excellent radiator of longwave radiation. With the large loss of longwave radiation by snowcover significant diabatic cooling of the atmosphere near the surface, especially during the nighttime, is likely.

Clouds can aid in the initiation or termination of a deep stable layer episode. Clouds are good emitters of longwave radiation. They may reduce the nighttime longwave cooling of air near the surface. Clouds may also radiatively interact with a fog layer. If the cloud is warmer than the fog layer, the clouds may be able to rapidly heat the cold fog potentially resulting in its dissipation.

Fog, like most clouds, often is an excellent emitter of longwave radiation. The downward IR flux of the fog layer can keep the air immediately above the surface warmer than if the fog layer was not present. However, the large upward IR flux can also result in significant cooling of a large portion of the fog layer. This cooling in the lower portion of the atmosphere can be an important factor in the life cycle of the episode.

The vertical temperature and moisture profiles can possibly lead to diabatic heating or cooling through longwave radiation. The amount of radiation emitted from a layer is larger for higher temperatures and moisture content. The thermal and moisture profiles of cloudless days can have preferred regions of longwave radiation induced diabatic heating or cooling which can aid in the initiation or termination of a deep stable layer episode.

CHAPTER IV

CASE STUDY OF A DEEP STABLE LAYER EPISODE

A. Introduction

In this chapter a deep stable layer episode from December 6 to December 23, 1980 at Grand Junction, Salt Lake City, Winnemucca, and Boise will be examined. Table 7 shows the days which met the objective deep stable layer criteria. The synoptic situation in the western United States during the this time period will be discussed. Using time versus height plots of potential temperature and winds, the temperature changes, wind speeds and wind directions associated with the initiation, continuation, and termination of the deep stable layer episode will be examined. From this case study the importance of synoptic-scale vertical motion, synoptic-scale temperature advection, longwave heating or cooling, and shortwave heating in the initiation, continuation, and termination of the deep stable layer episode will be examined. The examination will determine which meteorological phenomenon are important for causing the occurrence of the different physical processes. An analysis of decoupling and pollution potential for the episode will also be presented.

B. Terminology

To simplify the discussion in this chapter and the remainder of the thesis, some terms will be defined. The sounding taken at about 1115

Table 7.
The days from December 6-23, 1980 at Grand Junction, Salt Lake City, Winnemucca, and Boise which satisfied the objective deep stable layer definition.

December	Grand Junction	Salt Lake City	Winnemucca	Boise
6				
7				
8				
9			X	X
10		X	X	X
11	X		X	X
12		X		X
13	X		X	X
14	X	X	X	
15	X	X		X
16	X	X		X
17	X	X		X
18	X			X
19				X
20				
21				
22				
23				

GMT (0415 MST) will be referred to as the morning sounding, and the sounding taken at about 2315 GMT (1615 MST) will be referred to as the afternoon sounding. The days in the case studies are defined by the calendar day at the station. The word daytime refers to the time period from the 1115 GMT sounding to the 2315 GMT sounding. At stations in the western United States this period includes most of the daylight hours. The time period from the 2315 GMT sounding on the previous day to the 1115 GMT sounding on the present day will be referred to as nighttime. In the western United States this time period includes most of the evening of the previous day and early morning of the present day. In figures and tables "M" or "A" listed with a date refers to the morning or afternoon sounding of that date respectively. Unless otherwise stated, the times in this discussion will be local standard time.

Many of the days in the continuation phase of the deep stable layer episode to be examined satisfied the deep stable layer criteria. As stated in Chapter II, there are a significant number of non-deep stable layer days which have small mixing volumes. To simplify the discussion of the episode, days which have deep layers of moderate stability but do not satisfy the objective deep stable layer criteria will still be referred to as deep stable layers.

C. Synoptic Situation

Figures 7 and 8 show the temperatures at 500mb and 700mb, respectively, for December 6 to December 23, 1980 at Grand Junction, Salt Lake City, Winnemucca, and Boise. The 500mb, 700mb, and surface maps appear in Appendix A. On the sixth there was a deep, cold trough in southwest Canada with temperatures at its center below -35°C at 500mb

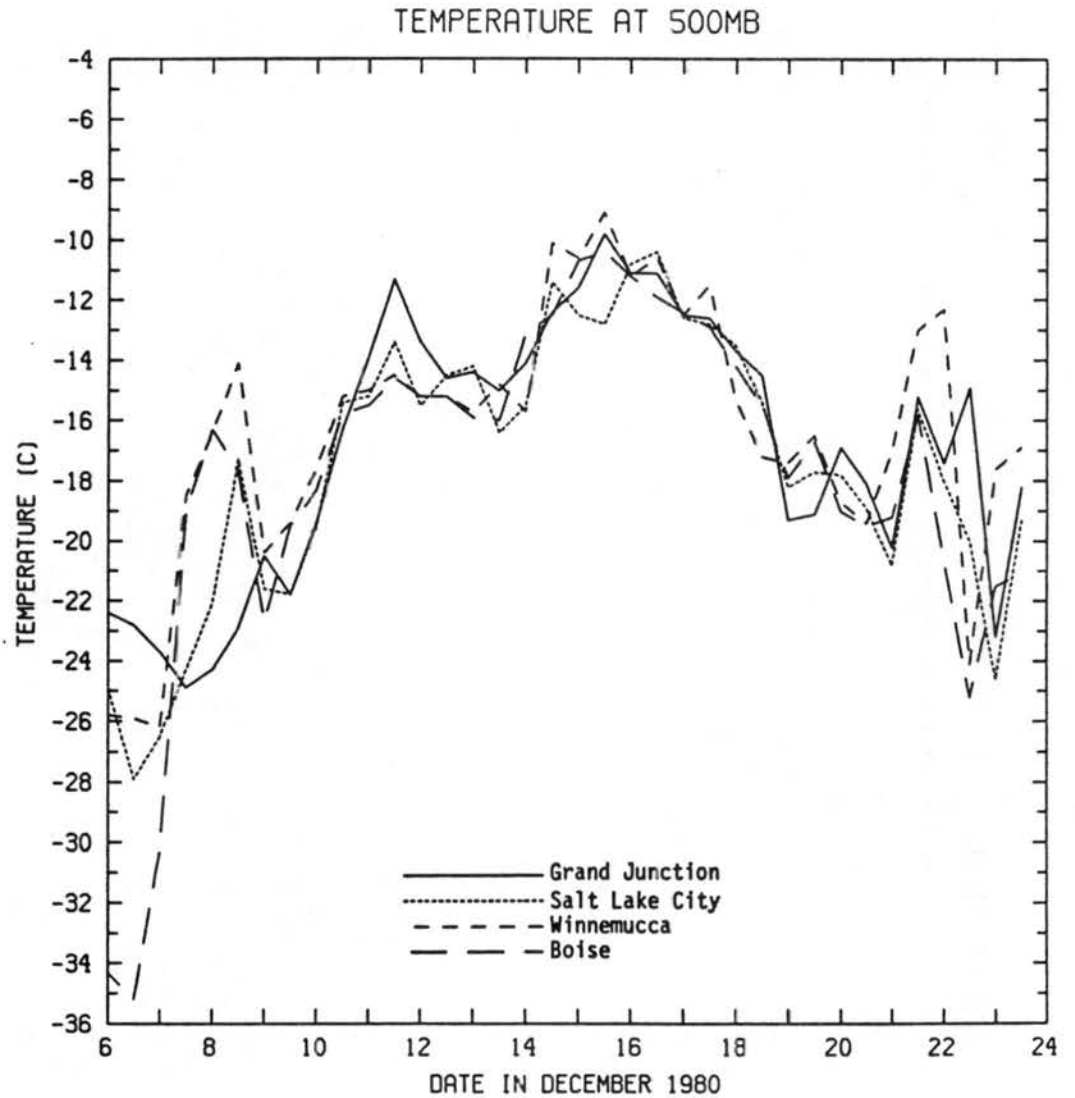

Figure 7. The temperature at 500mb from December 6-23, 1980 at Grand Junction, Salt Lake City, Winnemucca, and Boise. The values above the date number are for the morning sounding and values between the date numbers are for the afternoon soundings.

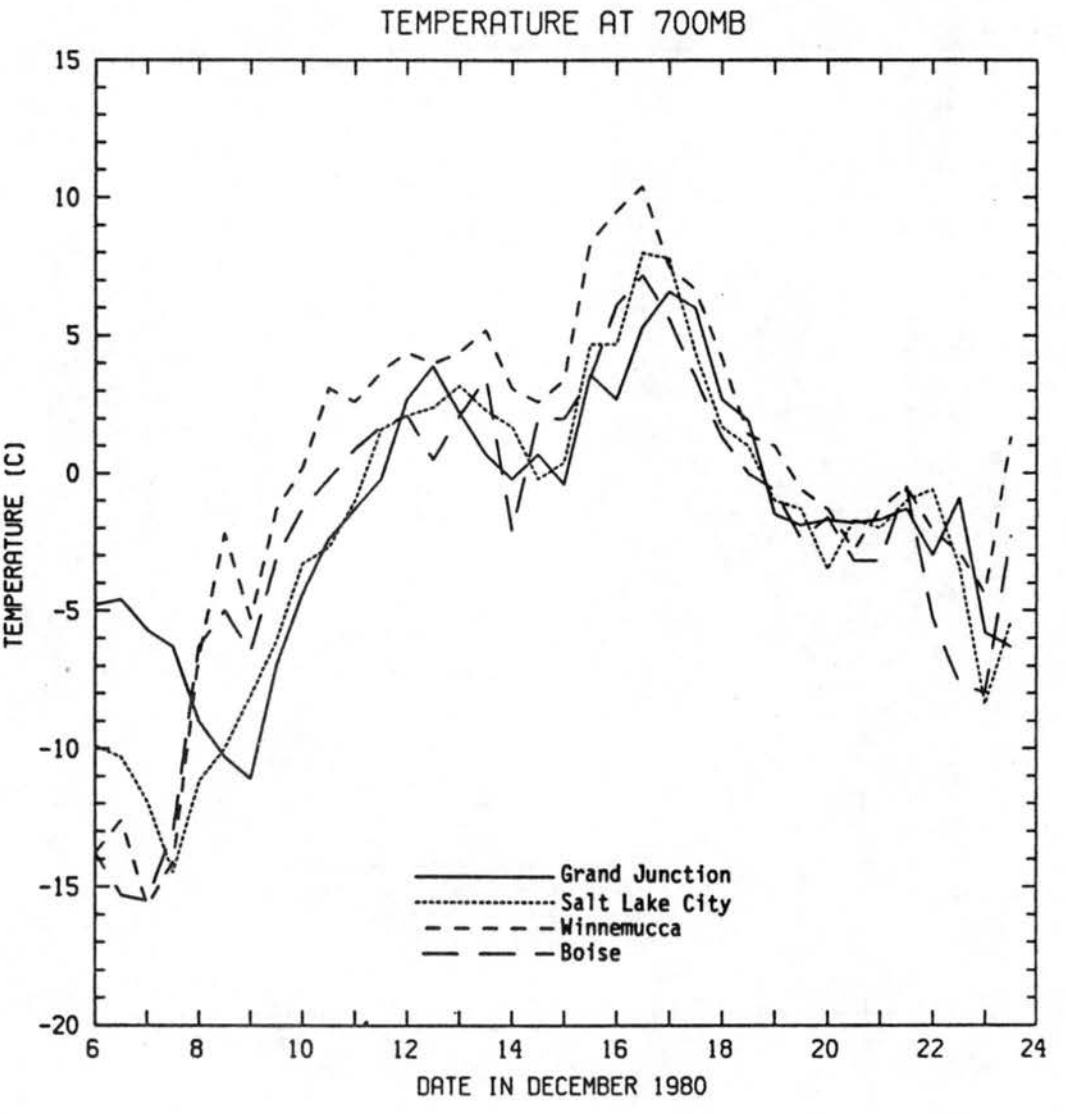

Figure 8. Same as Figure 7 but for 700 mb.

and below -15°C at 700mb. On the seventh and eighth the strong trough moved southward over the intermountain region. The surface maps shows general storminess in the western United States. By the eighth the storm had moved eastward with Boise and Winnemucca having generally clear skies. By the ninth the upper level trough had moved eastward and southward with Salt Lake City and Grand Junction still being generally cloudy in the early part of the day. The surface map shows high pressure centered over Idaho.

For the next several days the ridge at 500mb and 700mb built into the area with generally light winds and continued warming at these levels. The surface maps show a persistent high pressure center over the region around Idaho. On the thirteenth and fourteenth a weak 500mb "cut-off" low moved eastward with its center passing over Arizona and New Mexico. The 500mb and 700mb highs appear to be moving westward and to be merging with a ridge in the Pacific Ocean. By the fifteenth the 500mb and 700mb ridge moved onshore into the western United States, but the center of the high pressure aloft was further west than the previous days. The winds at Boise at 500mb and 700mb increased to around 45 knots and could be associated with a short wave moving through Idaho, Montana, and Wyoming. There was no noticeable surface feature over the western United States associated with the increased winds. On the sixteenth the ridge aloft had moved eastward and was associated with lighter winds aloft at Boise and the other stations. At the surface high pressure over the region persisted.

On the seventeenth the ridge aloft began to weaken. The surface high over Idaho also showed noticeable weakening and temperatures at 500mb and 700mb began to cool. On the nineteenth an eastward moving

trough was present over Utah and Colorado. On the twentieth despite the considerable weakening of the ridge aloft, the winds aloft at the four stations were still fairly light. The surface map shows no trace of a high over Idaho and shows a Pacific storm moving onshore.

The 500mb and 700mb maps on the twenty-first shows a nearly zonal pattern over the western United States with a weak trough over western Colorado extending into Arizona. The temperatures at 500mb and 700mb were continuing to cool with strengthening winds at these levels. The surface maps shows a weak high over northern Utah with the fronts associated with the Pacific storm onshore. By the twenty-second the winds at 500mb were strong and zonal with the surface showing the Pacific front through the intermountain region.

D. Adiabatic Diagrams

1. Introduction

To aid in understanding the initiation phase, continuation phase, and termination phase of the episode, plots of potential temperature and winds on time versus height diagrams were constructed. Some of the diagrams are shown in Figures 9 and 10 with the remainder being in Appendix B. The diagrams are contoured with adiabats at 2K intervals. The wind barbs show the direction from which the wind is blowing and give the speed. Each small barb indicates speeds of 2-3ms^{-1}. Each full barb indicates speeds of 4-6ms^{-1}, and a flag represents speeds of 24-26ms^{-1}. Since 1ms^{-1} approximately equals two knots, the wind barbs in the diagrams have almost the same meanings as the ones used by the National Weather Service on its synoptic maps. On the adiabatic diagrams adiabats that slope downward with time indicate warming while

adiabats which slope upward with time shows cooling. The larger the number of adiabats over a vertical depth there are; the more stable the atmosphere is. Adiabatic diagrams with regions having dew point depressions of 3°C or less shaded also are in Appendix B. A brief description of the topography surrounding the four stations is given in Appendix C.

2. Salt Lake City

Figure 9 shows the adiabatic diagram extending up to 5.0km AGL for Salt Lake City for December 6-23, 1980. The initiation phase of the episode began during the daytime of the seventh when rapid warming was occurring between 4.2km and 5.0km with cooling below 2.5km. The region of rapid warming descended, and by the morning of the eleventh it was between 0.5km and 1.0km.

The continuation phase began on the morning of the tenth when a deep stable layer was first present. The adiabats from 0.4km to 0.8km are nearly horizontal signifying little warming in the region. The region of strong stability from 0.4km to 0.8km is called the capping stable layer. The change in potential temperature through the capping stable layer is about $25Kkm^{-1}$. On the thirteenth a fog layer developed and lasted until the afternoon sounding of the twenty first.

During the nighttime of the fourteenth significant cooling occurred between 0.5km and 2.0km. This cooling was probably the result of a weak 500mb "cut-off" low moving to the south of the region and the development of a trough to the east of the region. This disturbance weakened the capping stable layer but was not sufficiently strong to

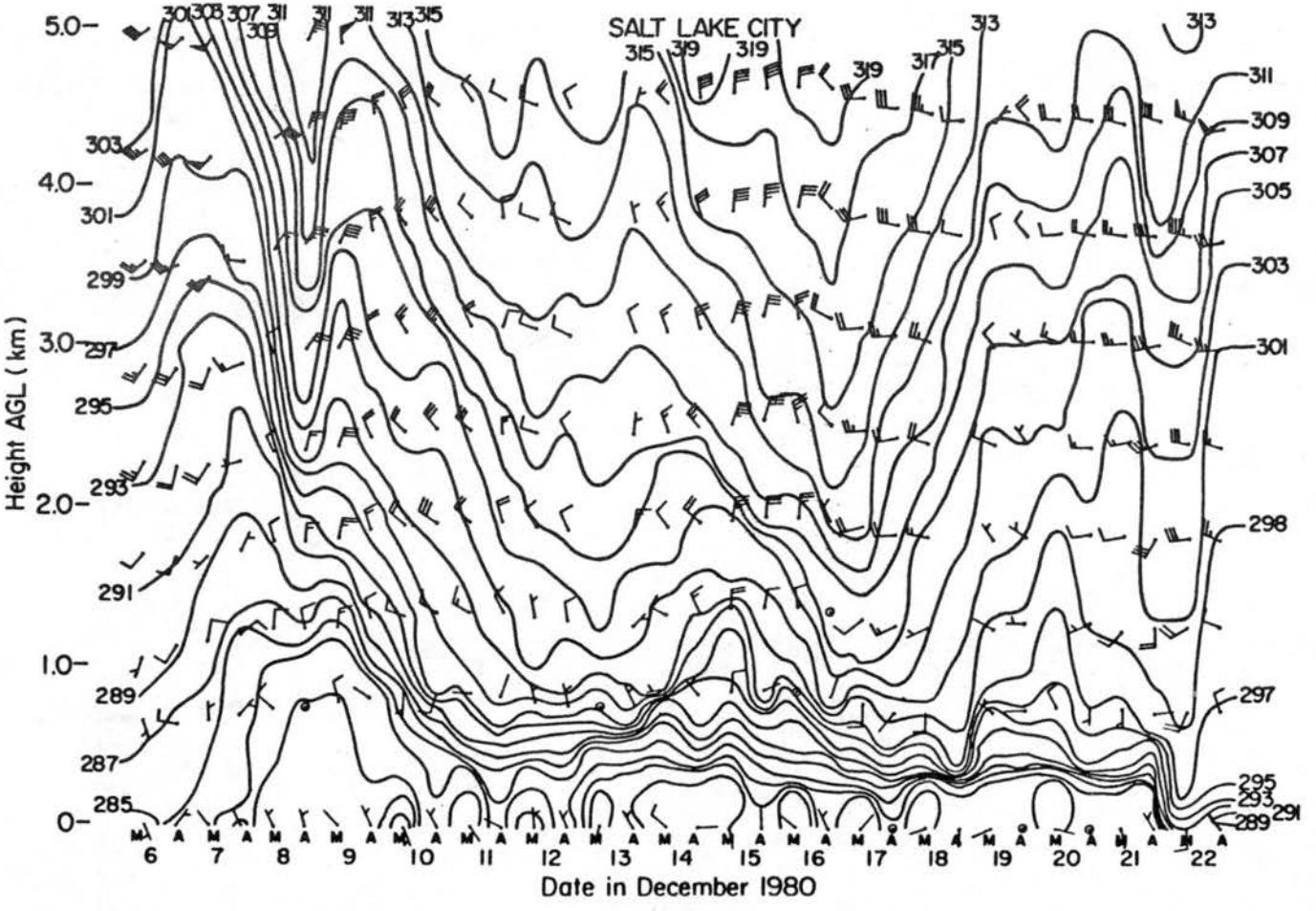

Figure 9. A time versus height plot of potential temperature and winds from December 6-23, 1980 for Salt Lake City.

destroy it. By the afternoon sounding of the fifteenth warming was occurring between 0.5km and 2.0km.

The termination phase of the episode began the morning of the seventeenth with cooling above 1.0km. During the nighttime of the nineteenth there was rapid cooling between 0.4km and 0.9km causing a significant weakening of the capping stable layer. The fog layer capped by a weaker stable layer remained until the afternoon of the twenty-first. The weakening of the ridge and movement of a weak disturbance over the area apparently were not able to end the episode. During the nighttime of the twenty-second a strong storm moved onshore from the Pacific and the capping stable layer and fog layer were destroyed. The destruction was preceded by some warming above 1.3km which suggests that significant synoptic scale lifting was involved in the destruction of the fog layer.

The synoptic-scale winds during the initiation phase of the episode were not weak. Wind speeds of 10-20ms^{-1} were associated with the descending region of rapid warming. Similar speeds were also associated with the warming which occurs on the fifteenth. During other times in the episode the wind speeds were generally light with stronger wind speeds on the twenty-second associated with the destruction of the fog layer.

3. Winnemucca

Figure 10 is the adiabatic diagram extending up to 5.0km AGL for Winnemucca for December 6-23, 1980. The initiation phase of the episode had a descending region of rapid warming. By the afternoon of the tenth, this region had reached 0.5km to 1.0km.

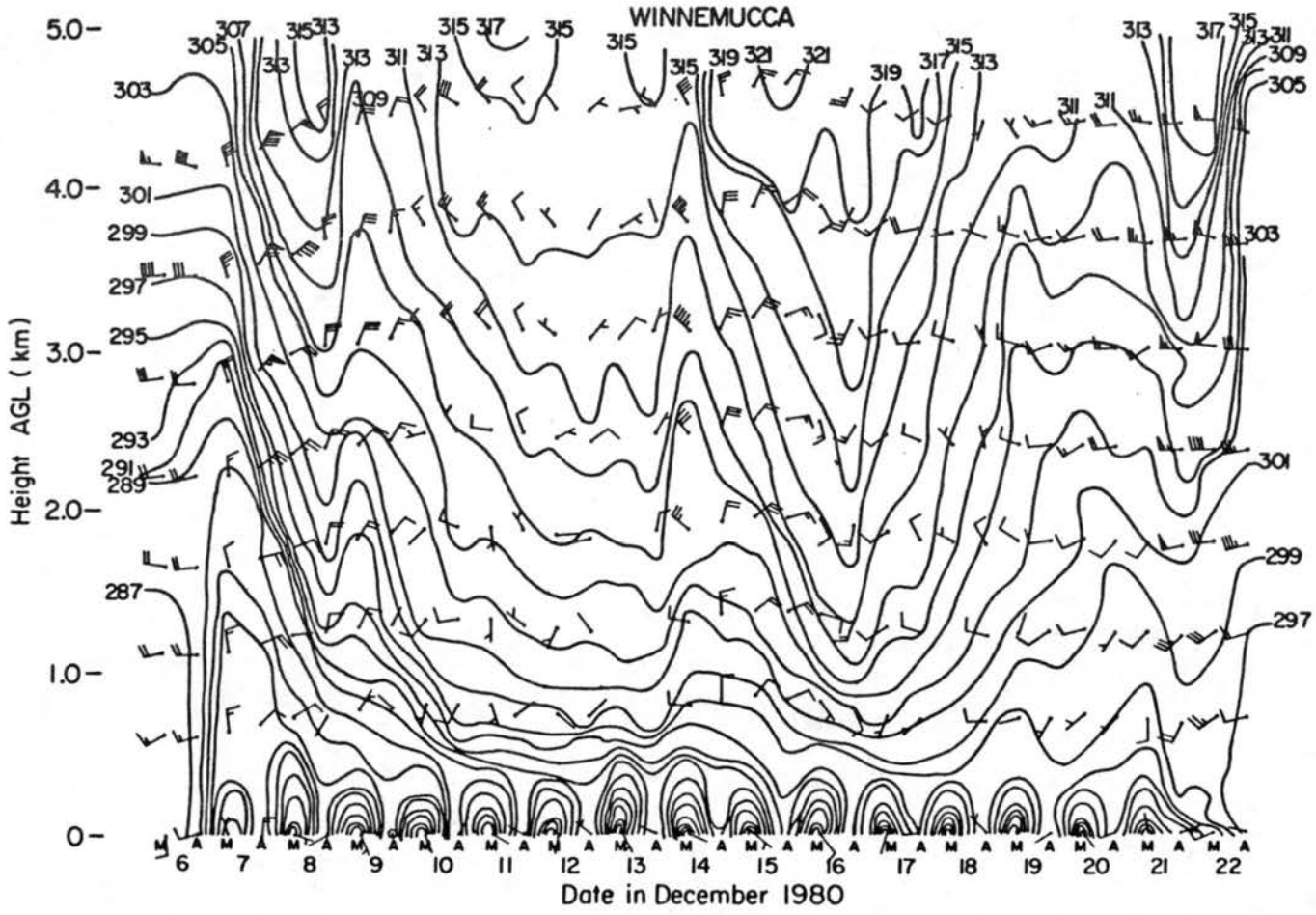

Figure 10. Same as Figure 9 but for Winnemucca.

The continuation phase of the episode began on the afternoon of the tenth when the adiabats between 0.5km and 1.0km became nearly horizontal and formed the capping stable layer. The vertical gradient of potential temperature across the capping stable layer is about $16Kkm^{-1}$. During the nighttime of the fourteenth cooling from 0.5km to 5.0km occurred resulting from the same system which affected Salt Lake City. The disturbance was able to noticeably weaken the capping stable layer but was not able to end the episode. By the morning of the fifteenth warming between 0.5km and 2.0km had begun.

The termination phase of the episode began on the sixteenth. Cooling aloft associated with the breakdown of the ridge over the western United States gradually weakened the capping stable layer. Between the morning sounding of the eighteenth and morning sounding of the nineteenth the capping stable layer appears to rise, and by the afternoon of the nineteenth the capping stable layer had weakened considerably. The afternoon sounding had a nearly adiabatic layer from the surface to at least 1.5km with lapse rates of around $-7°Ckm^{-1}$ capped by a moist layer.

Like Salt Lake City, the strongest synoptic-scale winds were associated with the descending regions of rapid warming. Winds were generally light during the termination of the episode and like Salt Lake City did not become stronger until the twenty-second.

Figures 11 and 12 show the height of the 298K and 304K adiabats for Grand Junction, Salt Lake City, Winnemucca, and Boise for December 6 to December 23, 1980. The figures indicate that like Salt Lake City and Winnemucca, at Grand Junction and Boise the initiation phase of the episode was associated with rapid warming aloft, the continuation phase

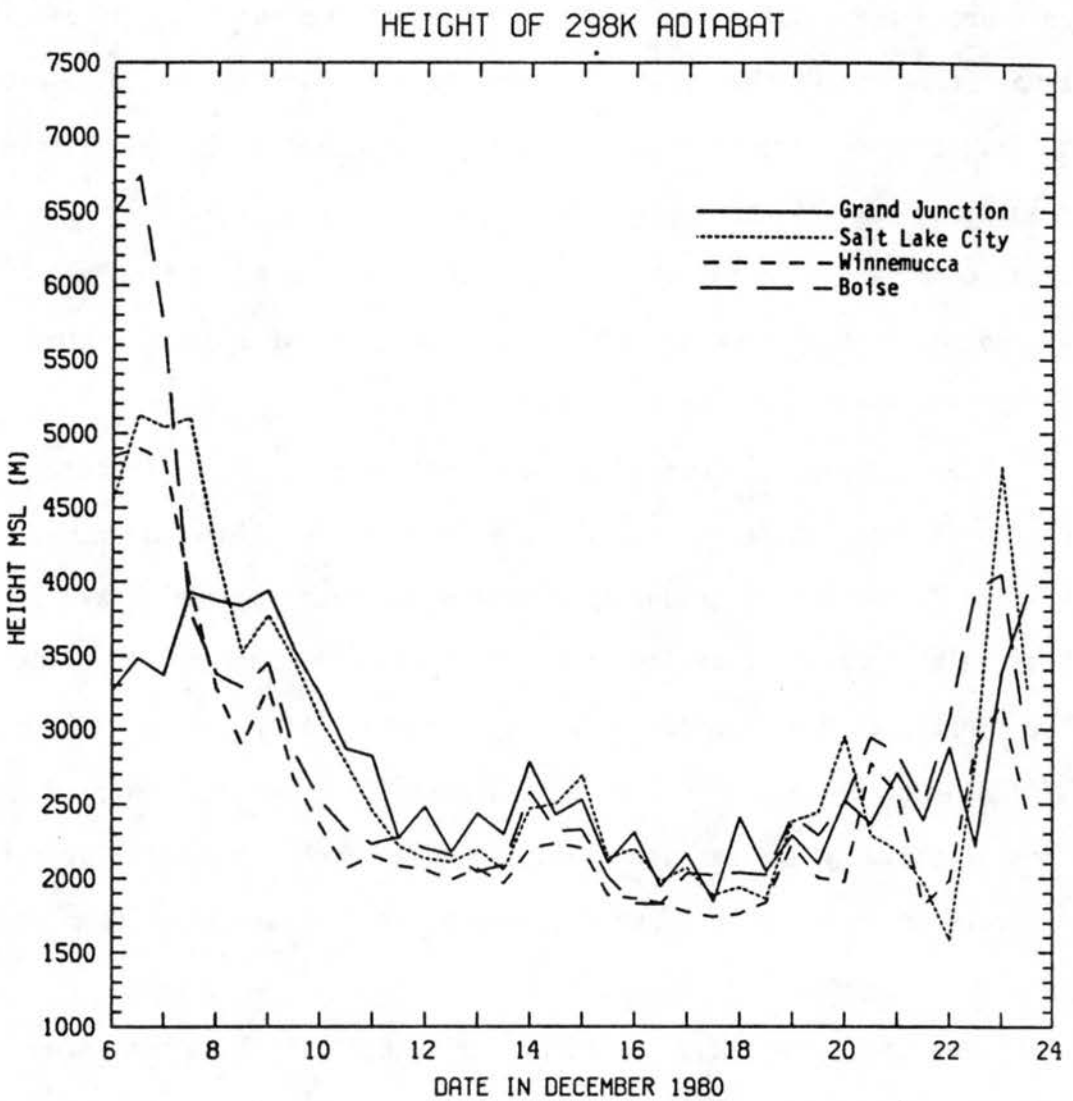

Figure 11. The height (MSL) of the 298K adiabat at Grand Junction, Salt Lake City, Winnemucca, and Boise from December 6-23, 1980. The values above the date numbers are for the morning soundings and values between the date numbers are for the afternoon soundings.

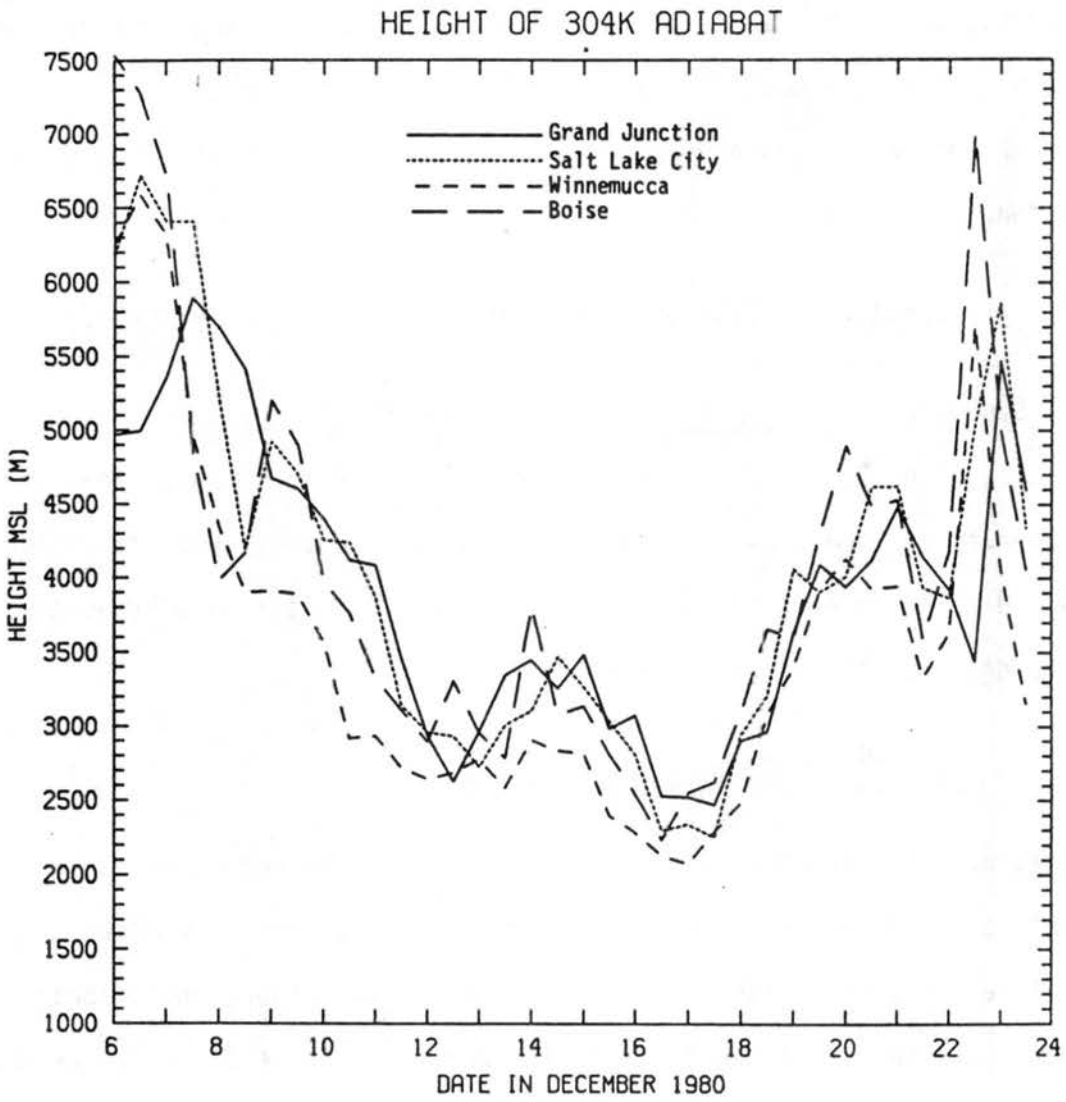

Figure 12. Same as Figure 11 but for the 304K adiabat.

had little temperature change, and the termination phase had cooling aloft. The adiabats at Winnemucca, Salt Lake City, and Boise show a progression of the region of rapid warming from west to east from the sixth through the twelfth. This indicates that the initiation phase of the episode was associated with a synoptic system moving into the region.

E. Analysis of Occurrence of Different Physical Processes

1. Synoptic-scale advection and vertical motion

Equation 3, the first law of thermodynamics in terms of potential temperature, shows that the local change in potential temperature can be caused by horizontal thermal advection, vertical motion, or diabatic heating. Equation 3 can be rewritten as:

$$\frac{\partial\theta}{\partial t} + \frac{\partial\theta}{\partial z}\left[w + \frac{\underset{\sim}{V}\cdot\nabla\theta}{\partial\theta/\partial z} - \frac{\theta}{c_p T}\ \frac{\dot{Q}}{\partial\theta/\partial z} \right] = 0 \quad . \qquad (4)$$

Equation 4 relates the local change in potential temperature to the vertical gradient of potential temperature and a term in brackets which includes vertical motion, horizontal thermal advection, and diabatic heating. The sum of the terms in the brackets can be described as the "effective" vertical motion necessary to cause the observed local change in potential temperature if horizontal thermal advection and diabatic heating are not present. Since the calculation is done in the eulerian reference frame, the sum of the terms in the brackets will be called the eulerian effective vertical motion (EEVM).

The EEVM is one way of discussing local changes in potential temperature in relative terms. It gives an objective indication of the maximum amount of vertical motion needed to cause a temperature change

at a given level. The product of the EEVM and vertical gradient of potential temperature equals the negative of the local heating rate. Since potential temperature very often increases with height, the EEVM and local heating rates usually have opposite signs. For the same vertical gradient of potential temperature, the magnitude of the EEVM is linearly related to the magnitude of the local heating rate. The EEVM is undefined if there is an adiabatic lapse. For superadiabatic lapse rates warming would result in effective rising motion which is opposite to the expected result for the normally stable atmosphere.

To calculate the EEVM only the vertical gradient of potential temperature and local change in potential temperature with time are needed. The vertical gradient in potential temperature can easily be obtained from each sounding. The local change in temperature with time was calculated by taking the slope of a second degree polynomial of potential temperature as a function of time. The data used to determine the second degree polynomial is the potential temperature at the previous sounding, the present sounding, and the next sounding. Averaged EEVM values were calculated for 500m increments from 1.0km to 4.5km. The averaging consisted of an integral average of EEVM values calculated at 10m increments in a 300m interval centered on the height.

Values of the averaged EEVM for Salt Lake City and Winnemucca appear in Tables 8 and 9. Data for other stations appear in Appendix D. From the eighth to the twelfth which is during the formation of the episode effective sinking motions of 0.5 to 1.5cms^{-1} were very common. On the thirteenth and fourteenth when the strength of the deep stable layers decreased the effective rising motions generally were from 0.0 to 1.0cms^{-1}. On the fifteenth and sixteenth when the deep stable layers

Table 8.
Eulerian effect vertical motion averaged over 300m (cms^{-1}) for Salt Lake City at 1.0km AGL, 1.5km AGL, 2.0km AGL, 2.5km AGL, 3.0km AGL, 3.5km AGL, 4.0km AGL, and 4.5 km AGL.

Date	1.0km	1.5km	2.0km	2.5km	3.0km	3.5km	4.0km	4.5km
6 M	0.22	1.03	-0.58	1.22	1.01	0.55	0.70	1.39
A	0.35	1.05	0.57	1.09	1.92	1.06	0.79	0.90
7 M	1.51	2.16	0.57	2.57	-4.00	-0.03	M	M
A	18.44	0.40	0.28	-0.84	-1.90	-2.11	M	M
8 M	0.41	-0.41	-6.79	-1.08	-2.32	-2.19	M	M
A	0.14	-0.11	-0.34	-0.36	-0.73	-0.21	-0.39	-0.28
9 M	-0.54	-0.54	-0.48	0.29	0.38	0.84	2.12	1.31
A	-0.91	-0.79	-0.80	-0.64	-1.55	-1.73	-1.01	-1.82
10 M	-0.76	-0.70	-0.71	-0.31	-0.40	-1.40	-2.70	-2.55
A	-2.39	-0.82	-0.89	-0.71	-0.39	-1.11	-1.86	-1.29
11 M	-0.65	-0.93	-1.33	-1.62	-0.56	-0.82	-0.75	-1.74
A	-0.55	-0.67	-2.83	-1.20	-0.53	-0.08	0.12	0.17
12 M	-0.23	-0.38	-0.24	-0.15	-0.18	-0.18	-0.13	0.45
A	0.12	-0.20	-0.26	0.38	0.12	-0.06	-0.50	-0.79
13 M	0.01	0.10	0.05	-0.03	0.19	0.56	0.59	1.94
A	0.58	0.94	0.60	0.04	0.11	0.30	0.57	0.66
14 M	0.44	0.34	2.03	-0.30	-0.48	-1.04	-1.60	-2.32
A	0.23	0.39	0.03	-0.33	-2.54	-0.51	-1.13	-0.64
15 M	-0.79	-0.32	-0.36	-2.66	-0.91	-0.36	-0.17	0.65
A	-1.75	-0.61	-0.38	-0.42	-1.05	-0.99	-1.26	-1.25
16 M	-0.51	-0.89	-0.45	-0.66	-0.55	-0.64	-0.81	-1.00
A	-0.56	-0.55	-0.46	-0.47	-0.26	0.13	0.50	0.86
17 M	-0.04	0.12	1.39	1.76	1.47	1.87	1.83	1.35
A	0.11	4.65	2.26	1.58	1.40	1.31	0.70	0.29
18 M	1.41	2.31	0.90	0.84	2.21	1.45	1.14	1.03
A	1.53	1.38	1.22	2.41	1.72	1.19	-0.84	28.93
19 M	0.68	0.60	1.28	1.26	0.68	1.12	0.72	0.89
A	0.49	0.66	0.76	0.04	0.02	-0.03	-1.12	-0.10
20 M	-0.14	-0.03	0.14	0.36	0.93	0.69	0.27	0.58
A	-0.93	-0.97	-0.42	8.11	1.31	0.45	0.90	1.77
21 M	-0.49	-0.90	-3.24	-10.19	-1.42	-1.17	-1.92	-1.07
A	-0.43	-1.77	-0.63	-1.14	-0.64	-0.43	-0.84	-1.01
22 M	1.39	1.96	3.13	1.10	2.53	2.80	3.07	1.21
A	5.43	6.87	4.25	-4.61	2.69	2.82	1.62	2.00
23 M	2.96	3.25	0.27	25.99	0.01	-0.43	-0.68	-0.19

Table 9.
Same as Table 8 but for Winnemucca.

Date	1.0km	1.5km	2.0km	2.5km	3.0km	3.5km	4.0km	4.5km
6 M	-0.03	-0.61	0.08	1.66	1.09	0.35	0.39	0.79
A	3.72	2.39	3.13	1.09	0.42	-0.02	0.05	0.16
7 M	3.22	0.50	0.44	-1.08	-1.07	-0.92	-1.81	-3.15
A	-3.14	-1.07	6.81	-0.96	-3.38	-3.40	-1.14	-12.96
8 M	-1.43	-2.26	-2.22	-1.57	-1.26	-0.79	-0.97	-2.34
A	-0.46	-0.87	-0.02	-0.11	-0.30	0.41	1.02	3.37
9 M	-0.61	-2.01	-0.18	-0.03	0.79	1.12	2.05	3.35
A	-0.42	-1.07	-1.42	-0.83	-0.42	-1.53	-2.11	-1.27
10 M	-0.47	-1.92	-1.53	-1.11	-0.88	-1.47	-3.36	-2.32
A	-0.39	-0.29	-1.47	-2.08	-1.07	-0.46	-1.92	-1.97
11 M	-0.06	-0.29	-0.34	-0.88	-0.96	-0.39	-0.26	-0.24
A	-0.23	-0.36	-0.42	-0.59	-0.64	-0.42	-0.14	0.44
12 M	-0.15	-0.06	-0.21	-0.21	-0.10	0.03	0.29	1.94
A	-0.08	0.09	0.00	0.06	0.22	0.18	0.24	0.27
13 M	-0.10	-0.18	-0.34	0.00	0.00	-0.04	-0.24	-0.26
A	0.46	0.30	0.43	1.43	1.18	1.00	1.07	0.17
14 M	0.57	0.20	3.50	1.27	0.23	-0.39	-1.65	-0.89
A	-0.06	-0.18	-0.15	-1.10	-1.05	-1.05	-1.02	-1.90
15 M	-0.49	-1.22	-0.80	-1.39	-1.42	-1.31	-0.79	-0.29
A	-0.58	-0.87	-1.51	-1.03	-1.01	-0.75	-0.39	0.12
16 M	-0.40	-0.76	-1.44	-0.63	-0.82	-0.58	0.15	0.87
A	-0.07	0.51	0.55	0.47	0.96	1.46	1.56	1.13
17 M	0.68	0.63	1.40	1.97	2.29	2.13	1.79	0.35
A	0.22	0.79	1.76	2.03	1.81	1.52	1.38	-11.87
18 M	0.64	1.27	2.09	2.14	2.22	2.54	2.56	7.45
A	1.01	1.26	0.83	2.61	2.38	-1.07	1.16	0.98
19 M	0.35	0.40	2.81	4.31	3.26	0.44	-0.03	-0.22
A	-0.17	0.48	1.93	0.71	0.05	-0.21	-0.25	1.00
20 M	0.73	1.23	-0.83	-0.01	0.22	0.17	0.24	1.31
A	1.97	0.51	-0.18	-0.35	0.53	-0.47	0.75	-0.72
21 M	-0.80	-0.36	-1.02	-0.96	-0.85	-1.10	-2.29	-5.50
A	-0.83	-1.47	0.07	-0.89	-0.13	-0.27	-0.75	-5.71
22 M	1.38	1.78	0.74	1.12	1.53	4.28	1.31	6.87
A	6.87	4.36	1.28	2.37	-9.89	-0.69	2.06	1.49
23 M	0.19	-0.82	-0.82	-1.18	-1.17	-2.77	-3.35	-2.03

strengthened the effective sinking motions were 0.5 to 1.5cms^{-1}. From the seventeenth to twentieth when the warm ridge aloft weakened, effective rising motions of 0.5 to 2.0cms^{-1} were calculated. The modest magnitudes of the EEVM values are typical values for synoptic-scale vertical motion and suggest that either vertical motion, horizontal temperature advection, or a combination of both are important for the warming or cooling aloft. On the twenty-first and twenty-second, when the fog layers at Salt Lake City and Boise were destroyed, the EEVM values show effective sinking motion. In this case the magnitude of the horizontal warm air advection was much larger than the rising motion causing effective sinking motion when actual rising motion was probably present.

The influences of diabatic heating on the amount of vertical motion or horizontal temperature advection needed to cause the observed warming/cooling can be important. The general IR cooling rate of the atmosphere is around 1°C(day)$^{-1}$. Calculations of IR heating rates in the next section will show that for clear skies the longwave cooling rate of the air above 1.0km (AGL) generally is 1.0 to 1.5°C(day)$^{-1}$. Tables 10 and 11 show for Salt Lake City and Winnemucca at 700mb and 500mb the observed heating rate without assuming an IR cooling rate and EEVM values averaged over 300m for an assumed IR cooling rate of 0°C(day)$^{-1}$, 1.0°C(day)$^{-1}$, and 1.5°C(day)$^{-1}$. The tables for Grand Junction and Boise are in Appendix D. The change in the averaged EEVM values caused by the diabatic cooling is large for weakly stable soundings. Except for a few instances, the averaged EEVM values with an assumed IR cooling rate of 1.5°C(day)$^{-1}$ have magnitudes of 2.5cms^{-1} or less. The addition of typical IR cooling rates does not alter the

Table 10.
The present warming rate (°C/12Hr) without any assumed diabatic heating, and EEVM values averaged over 300m (cms^{-1}) for assumed diabatic heating rates of 0.0°C/day, -1.0°C/day, and -1.5°C/day at 700mb and 500mb at Salt Lake City.

		700mb				500mb			
		Warming Rate	EEVM 0.0	EEVM -1.0	EEVM -1.5	Warming Rate	EEVM 0.0	EEVM -1.0	EEVM -1.5
12/ 6/80	M	-1.25	-3.94	-2.51	-1.80	-1.40	1.13	0.72	0.51
	A	-1.00	0.98	0.49	0.24	-0.98	0.99	0.47	0.22
12/ 7/80	M	-2.16	1.44	1.12	0.96	0.82	-0.43	-0.68	-0.80
	A	0.17	-0.08	-0.30	-0.41	2.74	-1.37	-1.62	-1.75
12/ 8/80	M	2.37	-3.26	-3.94	-4.28	5.60	-2.24	-2.44	-2.54
	A	1.67	-0.41	-0.54	-0.60	0.35	-0.56	-1.51	-1.98
12/ 9/80	M	2.14	-0.66	-0.82	-0.90	-2.70	1.80	1.46	1.30
	A	2.78	-1.06	-1.25	-1.34	1.25	-1.90	-2.66	-3.05
12/10/80	M	1.88	-0.70	-0.89	-0.98	3.94	-2.64	-2.98	-3.15
	A	1.33	-1.16	-1.59	-1.80	2.62	-1.33	-1.58	-1.71
12/11/80	M	2.26	-1.25	-1.53	-1.67	1.20	-1.81	-2.55	-2.93
	A	1.78	-1.92	-2.45	-2.71	-0.21	0.19	-0.27	-0.50
12/12/80	M	0.49	-0.22	-0.44	-0.56	-0.68	0.50	0.13	-0.05
	A	0.52	-0.28	-0.56	-0.70	0.76	-0.75	-1.25	-1.50
12/13/80	M	-0.08	0.04	-0.29	-0.45	-1.14	1.72	0.96	0.58
	A	-0.88	0.42	0.18	0.06	-0.74	0.65	0.22	0.00
12/14/80	M	-1.30	1.27	0.78	0.53	3.02	-2.43	-2.83	-3.03
	A	-0.51	0.22	0.02	-0.08	1.85	-0.70	-0.89	-0.98
12/15/80	M	2.51	-0.86	-1.08	-1.19	-0.79	0.63	0.23	0.02
	A	2.30	-0.37	-0.45	-0.49	1.02	-1.07	-1.60	-1.86
12/16/80	M	2.02	-0.49	-0.61	-0.67	1.41	-1.00	-1.35	-1.53
	A	1.57	-0.45	-0.60	-0.67	-1.05	1.05	0.55	0.30
12/17/80	M	-1.94	0.95	0.72	0.60	-1.44	1.37	0.90	0.66
	A	-3.23	4.83	4.07	3.69	-0.60	0.41	0.07	-0.10
12/18/80	M	-2.02	1.57	1.19	0.99	-1.70	1.04	0.74	0.58
	A	-1.56	0.85	0.58	0.44	-2.90	18.88	15.61	13.97
12/19/80	M	-1.21	0.83	0.49	0.32	-1.46	0.83	0.54	0.39
	A	-1.30	0.78	0.48	0.33	0.33	-0.13	-0.40	-0.53
12/20/80	M	-0.21	0.10	-0.15	-0.27	-0.64	0.13	0.11	0.11
	A	0.76	-0.78	-1.32	-1.59	-1.84	1.51	1.09	0.88
12/21/80	M	0.45	-1.57	-3.35	-4.24	2.08	-1.29	-1.60	-1.75
	A	0.78	-1.19	-1.96	-2.34	1.52	-1.00	-1.33	-1.49
12/22/80	M	-1.39	3.24	2.06	1.47	-2.69	1.27	1.03	0.91
	A	-4.25	3.90	3.44	3.21	-3.88	0.81	0.71	0.66
12/23/80	M	-1.18	1.24	0.77	0.54	0.63	-0.36	-0.66	-0.80
	A	3.82	-0.75	-0.84	-0.89	3.39	-1.62	-1.86	-1.98

Table 11.
Same as Table 10 but for Winnemucca.

		700mb				500mb			
		Warming Rate	EEVM 0.0	EEVM -1.0	EEVM -1.5	Warming Rate	EEVM 0.0	EEVM -1.0	EEVM -1.5
12/ 6/80	M	0.35	-0.62	-1.52	-1.97	-1.02	0.58	0.29	0.15
	A	-1.12	2.28	1.22	0.70	-0.21	0.15	-0.18	-0.34
12/ 7/80	M	-0.91	0.62	0.27	0.10	4.55	-2.68	-2.98	-3.12
	A	4.81	15.81	17.20	17.89	5.94	-4.39	-4.76	-4.94
12/ 8/80	M	6.60	-0.73	-0.79	-0.81	2.33	-1.80	-2.18	-2.37
	A	1.16	-0.34	-0.53	-0.63	-2.38	2.19	1.74	1.51
12/ 9/80	M	0.56	-1.73	-3.14	-3.84	-2.75	3.12	2.55	2.27
	A	2.89	-1.36	-1.59	-1.71	1.74	-1.42	-1.83	-2.03
12/10/80	M	2.38	-1.85	-2.24	-2.43	2.48	-2.51	-3.01	-3.26
	A	1.29	-1.02	-1.40	-1.60	1.63	-2.02	-2.65	-2.96
12/11/80	M	0.43	-0.22	-0.47	-0.60	0.38	-0.23	-0.51	-0.66
	A	0.96	-0.39	-0.59	-0.69	-0.23	0.62	-0.38	-0.88
12/12/80	M	0.15	-0.08	-0.33	-0.46	-0.38	2.03	-0.74	-2.12
	A	0.01	0.00	-0.19	-0.28	-0.25	0.30	-0.28	-0.57
12/13/80	M	0.63	-0.35	-0.62	-0.75	0.23	-0.35	-1.09	-1.46
	A	-0.72	0.29	0.09	0.00	-0.12	0.13	-0.42	-0.70
12/14/80	M	-1.34	2.06	1.31	0.94	2.81	-0.92	-1.09	-1.17
	A	0.27	-0.11	-0.41	-0.56	3.15	-2.39	-2.78	-2.97
12/15/80	M	3.05	-0.85	-0.99	-1.06	0.65	-0.47	-0.83	-1.01
	A	3.29	-1.33	-1.54	-1.65	-0.30	0.21	-0.14	-0.31
12/16/80	M	1.18	-1.12	-1.61	-1.85	-0.85	0.91	0.37	0.10
	A	-1.12	0.60	0.33	0.19	-0.77	1.01	0.37	0.05
12/17/80	M	-2.05	1.09	0.83	0.69	-0.54	0.43	0.03	-0.18
	A	-1.82	1.36	0.99	0.80	-1.73	-17.07	-11.87	-9.27
12/18/80	M	-2.84	1.84	1.51	1.35	-3.50	9.62	8.25	7.57
	A	-1.82	0.90	0.65	0.53	-1.39	1.53	1.00	0.73
12/19/80	M	-1.20	1.26	0.76	0.51	0.34	-0.17	-0.41	-0.53
	A	-1.25	1.25	0.76	0.52	-0.61	0.62	0.19	-0.03
12/20/80	M	-1.09	-0.21	-0.04	0.05	-1.73	0.52	0.37	0.29
	A	0.05	0.00	-0.27	-0.41	0.89	-0.17	-0.18	-0.19
12/21/80	M	1.20	-0.74	-1.05	-1.21	3.92	-3.98	-4.48	-4.74
	A	-0.36	0.12	-0.05	-0.13	2.89	-2.87	-3.37	-3.62
12/22/80	M	-1.29	1.17	0.72	0.50	-6.69	5.84	5.41	5.19
	A	-1.34	0.73	0.45	0.31	-3.15	4.18	3.53	3.20
12/23/80	M	2.28	-0.87	-1.07	-1.16	4.30	-2.72	-3.04	-3.19
	A	3.75	-1.78	-2.02	-2.13	1.76	-2.13	-2.73	-3.03

conclusion that vertical motion, horizontal temperature advection, or a combination of both are important for the warming or cooling aloft.

Tables 12 and 13 list for 500mb and 700mb at Salt Lake City and Winnemucca the EEVM values average over 300m, the observed warming in the previous 12 hours, the calculated warming rate, and the calculated warming rates due to synopotic-scale horizontal temperature advection. Tables for the other stations are listed in Appendix D. The local heating rate was used to determine the EEVM. The local heating rate and EEVM were calculated in the same manner as done for Tables 8-11. The horizontal advection is listed only when significant warming was observed. The horizontal advection was calculated by estimating from the National Weather Service 500mb and 700mb maps the horizontal temperature gradient along an estimated trajectory. The trajectory was assumed to be parallel to the contours and at the same speed as the observed wind at the station. Although this method is inexact, it still gives a good indication of the relative importance of horizontal advection to the total observed warming.

The data indicates that horizontal warm air advection provides a significant contribution to the total observed warming. Warm air advection, like subsidence, was important for providing the observed warming aloft. For example, at Salt Lake City at 500mb on the morning of the eighth the advective warming rate was $+4.8°C(12Hr)^{-1}$ and the calculated warming rate at that time was $+5.6°C(12Hr)^{-1}$. On the afternoon of the eighth the advective and present warming rate were $+0.3°C(12Hr)^{-1}$. At 700mb from the morning of the eighth to the afternoon of the ninth the advective warming rate was at least half as large as the observed warming rate. The analysis shows some examples

Table 12.
The EEVM averaged over 300m (cms^{-1}), the observed warming in the previous 12 hours (°C), the present warming rate (°C/12hr), and estimated warming from horizontal temperature advection (°C/12hr) at 500mb and 700mb for Salt Lake City.

		700mb				500mb			
		EEVM	Prev. 12Hr Warming	Present Rate	Adv. Rate	EEVM	Prev. 12Hr Warming	Present Rate	Adv. Rate
12/ 6/80	M	-3.94	-2.15	-1.25		1.13	0.68	-1.40	
	A	0.98	-0.40	-1.00		0.99	-3.53	-0.98	
12/ 7/80	M	1.44	-1.70	-2.16		-0.43	1.64	0.82	+9.8
	A	-0.08	-2.61	0.17	+0.7	-1.37	0.18	2.74	M
12/ 8/80	M	-3.26	3.11	2.37	+1.3	-2.24	5.64	5.60	+4.8
	A	-0.41	1.75	1.67	+1.7	-0.56	5.58	0.35	+0.3
12/ 9/80	M	-0.66	1.72	2.14	+3.9	1.80	-5.06	-2.70	-4.8
	A	-1.06	2.74	2.78	+2.1	-1.90	-0.27	1.25	+1.9
12/10/80	M	-0.70	2.93	1.88	M	-2.64	3.04	3.94	M
	A	-1.16	0.90	1.33	+3.0	-1.33	5.00	2.62	0.0
12/11/80	M	-1.25	1.90	2.26	+2.0	-1.81	0.31	1.20	-1.4
	A	-1.92	2.75	1.78	+1.1	0.19	2.08	-0.21	-0.5
12/12/80	M	-0.22	0.84	0.49	0.0	0.50	-2.55	-0.68	
	A	-0.28	0.16	0.52	-3.9	-0.75	1.24	0.76	
12/13/80	M	0.04	0.87	-0.08	M	1.72	0.20	-1.14	
	A	0.42	-1.09	-0.88		0.65	-2.52	-0.74	+2.4
12/14/80	M	1.27	-0.76	-1.30		-2.43	1.24	3.02	+1.6
	A	0.22	-1.81	-0.51		-0.70	4.91	1.85	-1.7
12/15/80	M	-0.86	0.98	2.51	M	0.63	-1.29	-0.79	
	A	-0.37	4.14	2.30	-0.8	-1.07	-0.23	1.02	
12/16/80	M	-0.49	0.57	2.02	0.0	-1.00	2.37	1.41	
	A	-0.45	3.55	1.57	-0.7	1.05	0.39	-1.05	
12/17/80	M	0.95	-0.56	-1.94		1.37	-2.57	-1.44	
	A	4.83	-3.54	-3.23		0.41	-0.34	-0.60	
12/18/80	M	1.57	-3.05	-2.02		1.04	-0.99	-1.70	
	A	0.85	-1.09	-1.56		18.88	-2.60	-2.90	
12/19/80	M	0.83	-2.11	-1.21		0.83	-3.28	-1.46	
	A	0.78	-0.37	-1.30		-0.13	0.38	0.33	
12/20/80	M	0.10	-2.24	-0.21		0.13	0.24	-0.64	
	A	-0.78	1.84	0.76		1.51	-1.62	-1.84	
12/21/80	M	-1.57	-0.30	0.45		-1.29	-1.93	2.08	
	A	-1.19	1.25	0.78		-1.00	6.19	1.52	
12/22/80	M	3.24	0.22	-1.39		1.27	-3.29	-2.69	
	A	3.90	-3.26	-4.25		0.81	-2.35	-3.88	
12/23/80	M	1.24	-5.26	-1.18		-0.36	-5.39	0.63	
	A	-0.75	3.17	3.82		-1.62	6.85	3.39	

Table 13.
Same as Table 10 but for Winnemucca.

		700mb				500mb			
		EEVM	Prev. 12Hr	Warming Present Rate	Adv. Rate	EEVM	Prev. 12Hr	Warming Present Rate	Adv. Rate
12/ 6/80	M	-0.62	-0.50	0.35		0.58	-1.87	-1.02	
	A	2.28	1.13	-1.12		0.15	-0.17	-0.21	
12/ 7/80	M	0.62	-3.43	-0.91		-2.68	0.06	4.55	+1.4
	A	15.81	2.00	4.81	+3.8	-4.39	9.42	5.94	0.0
12/ 8/80	M	-0.73	8.08	6.60	+3.2	-1.80	2.61	2.33	+3.0
	A	-0.34	5.13	1.16	-2.7	2.19	1.89	-2.38	-4.9
12/ 9/80	M	-1.73	-2.77	0.56	-2.3	3.12	-6.83	-2.75	-4.1
	A	-1.36	4.05	2.89	-2.6	-1.42	1.45	1.74	0.0
12/10/80	M	-1.85	1.87	2.38	M	-2.51	2.17	2.48	M
	A	-1.02	2.98	1.29	0.0	-2.02	2.91	1.63	0.0
12/11/80	M	-0.22	-0.36	0.43	0.0	-0.23	0.37	0.38	
	A	-0.39	1.27	0.96	0.0	0.62	0.35	-0.23	
12/12/80	M	-0.08	0.65	0.15	-0.6	2.03	-0.83	-0.38	
	A	0.00	-0.35	0.01		0.30	0.06	-0.25	
12/13/80	M	-0.35	0.40	0.63		-0.35	-0.55	0.23	
	A	0.29	0.81	-0.72		0.13	1.03	-0.12	
12/14/80	M	2.06	-2.35	-1.34		-0.92	-1.08	2.81	+5.3
	A	-0.11	-0.27	0.27	+1.4	-2.39	6.89	3.15	0.0
12/15/80	M	-0.85	1.00	3.05	M	-0.47	-0.55	0.65	0.0
	A	-1.33	5.27	3.29	+2.0	0.21	1.82	-0.30	+2.1
12/16/80	M	-1.12	1.37	1.18	0.0	0.91	-2.47	-0.85	
	A	0.60	0.92	-1.12	+1.4	1.01	0.73	-0.77	
12/17/80	M	1.09	-3.29	-2.05		0.43	-2.32	-0.54	
	A	1.36	-0.94	-1.82		17.07	1.11	-1.73	
12/18/80	M	1.84	-2.86	-2.84		9.62	-4.78	-3.50	
	A	0.90	-2.93	-1.82		1.53	-2.30	-1.39	
12/19/80	M	1.26	-0.81	-1.20		-0.17	-0.46	0.34	
	A	1.25	-1.69	-1.25		0.62	1.09	-0.61	
12/20/80	M	-0.21	-0.87	-1.09		0.52	-2.42	-1.73	
	A	0.00	-1.29	0.05		-0.17	-0.97	0.89	
12/21/80	M	-0.74	1.47	1.20		-3.98	3.01	3.92	
	A	0.12	0.90	-0.36		-2.87	5.02	2.89	
12/22/80	M	1.17	-1.71	-1.29		5.84	0.33	-6.69	
	A	0.73	-0.94	-1.34		4.18	13.90	-3.15	
12/23/80	M	-0.87	-1.59	2.28		-2.72	7.87	4.30	
	A	-1.78	6.38	3.75		-2.13	0.86	1.76	

where the warming from horizontal temperature advection is much larger than the observed warming. This descrepency may be the result of the methods used for assessing the horizontal temperature advection. When winds are nearly perpendicular to a strong temperature gradient, the results can potentially be inaccurate. To obtain a more exact value of the relative contribution of warm air advection and subsidence, the adiabatic method or omega equation, which requires gridded data for a significant portion of the western United States, would be preferable.

2. Longwave Radiation

a. Method for determining longwave fluxes and heating rates. As earlier hypothesized, longwave radiation properties of clouds, fog, and vertical temperature and moisture structure can aid in the initiation or termination of deep stable layer episodes because of their differences in emission or absorption of longwave radiation. To gain some insight into these effects, a computer program which calculates the upward and downward IR flux and heating rate for a layer will be used.

The model is described in Cox and Griffith (1979). Input to the model consists of a temperature and moisture profile, ozone concentration, carbon dioxide concentration, and liquid water content. The temperature and moisture profiles up to 100 mb from the NWS rawinsonde were used as input for the model. Above 100 mb the temperature and moisture profiles of temperature and moisture for mid-latitude winter soundings from McClatchey et al. (1972) were used. The ozone profiles in McClatchey et al. (1972) were also used. The concentration of carbon dioxide throughout the sounding was assumed to be $0.5 gkg^{-1}$.

Liquid water contents of clouds and fog can potentially be very important in this calculation. These values, unfortunately, are not routinely measured. For the IR calculation reasonable values of liquid water content had to used. Rauber (1985) measured liquid water contents in nonprecipitating wintertime stable clouds in western Colorado away from a large mountain barrier of around $0.05gm^{-3}$. Fukuta et al. (1984) measured the liquid water contents of 0.01 to $0.06gm^{-3}$ in non-precipitating wintertime stratus and stratoculumus near Salt Lake City at heights of 3.0 to 4.1km above sea level. For the IR calculations the liquid water contents of clouds will be $0.05gm^{-3}$.

The liquid water contents of fog layers have been measured by many authors. Pruppacher and Klett (1980) stated in a general survey of the literature that liquid water contents of fog are generally less than $0.1gm^{-3}$. Wallace and Hobbs (1977) shows measurements of another author who observed liquid water contents of of 0.05 to $0.10gm^{-3}$ in a fog layer which advected inland from the ocean. Garland (1971) studying fog layers in England observed liquid water contents as low as $0.023\ gm^{-3}$ in fog layers with low visual range (290m in this case). Given the inland locations of Boise and Salt Lake City a liquid content of $0.025gm^{-3}$ will be used for fog layer in the IR calculation. A general guideline for the presence of fog or clouds is a dew point depression of 3.0°C or less.

The upward and downward IR flux were calculated at 10mb increments below 500mb and at 50mb increments between 100mb and 500mb. Below 500mb the heating rate was calculated for 10mb thick layers. For all the IR calculations in this section the 500mb level was above 4.0km AGL. The calculations give an excellent indication of the potential importance of

longwave radiation in the initiation, continuation, and termination of an episode. Given that some of the parameters in the model, especially liquid water content, were estimated the model calculations do not give highly accurate values of the IR fluxes and heating rates for the time of the sounding. For very accurate calculations observed values of liquid water content, surface temperature, and other parameters will be needed.

b. Cool, moist air beneath warm, dry air. The morning soundings on the tenth at Grand Junction and the morning sounding on the twelfth at Salt Lake City both had moist layers near the surface with drier air at the same temperature or warmer above the moist layer. In both cases the skies were clear so no clouds were entered into the IR program. Figure 13 shows the sounding at Grand Junction. Figure 14 shows the calculated upward, downward, and net IR radiation and the calculated heating rates for the sounding. The patterns of the upward, downward, and net IR flux will not be discussed. The heating rate pattern shows a general cooling of 1.0 to 1.5°C(day)$^{-1}$ throughout the lowest 4.0km of the sounding. There is not a layer of significantly increased cooling below 1.0km.

Figure 15 shows the sounding at Salt Lake City and Figure 16 shows the calculated IR fluxes and heating rates from the model. The heating rate shows one layer near the surface with significant cooling and warming in the two layers immediately above the moist surface layer. The IR computations for Salt Lake City shows some indication of increased cooling near the surface. As with Grand Junction the model does not indicate that the difference in moisture with height is a major mechanism causing cooling of the air near the surface.

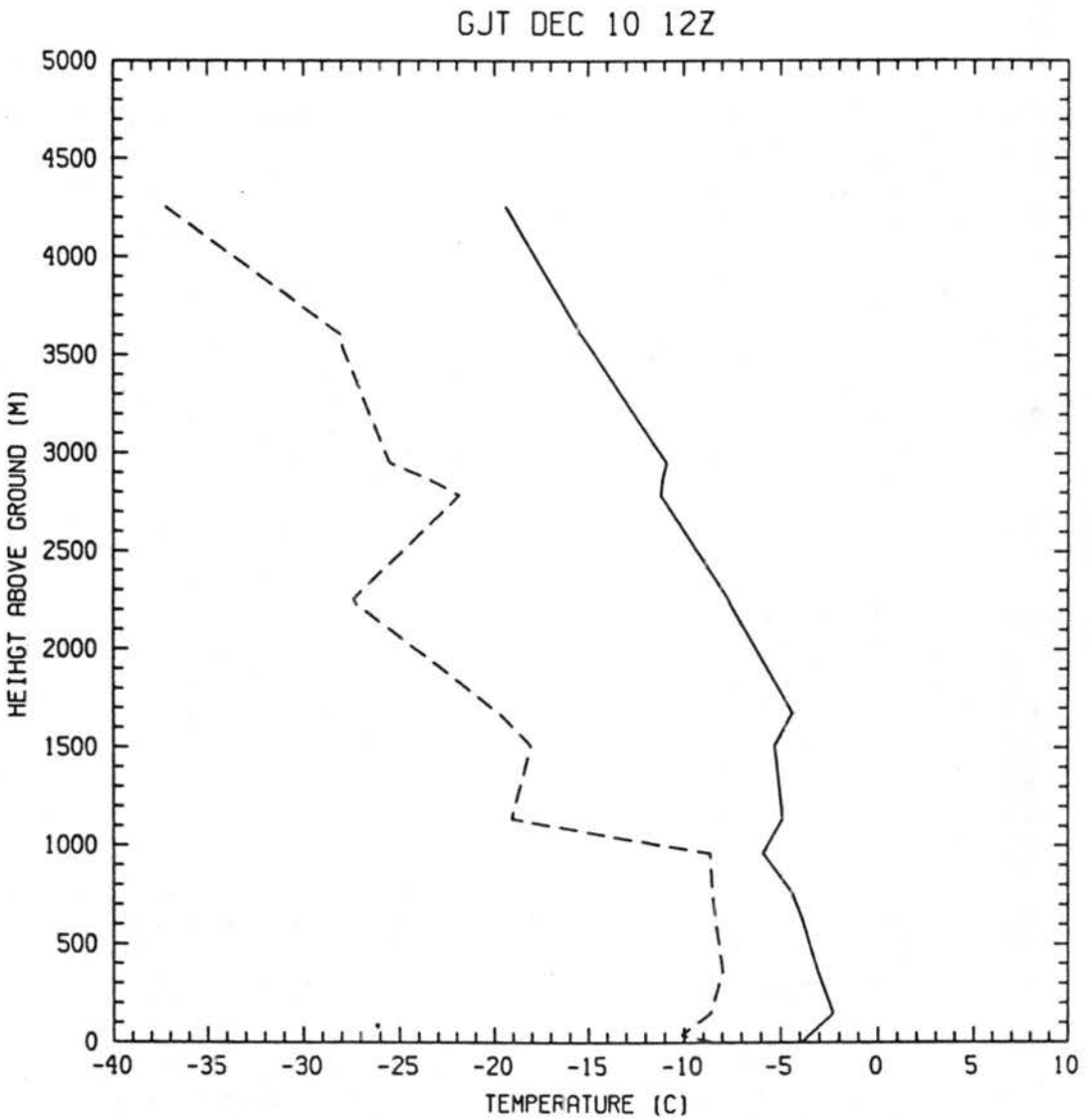

Figure 13. A temperature (solid line) and dew point (dashed line) versus height plot of the morning sounding on December 10, 1980 at Grand Junction.

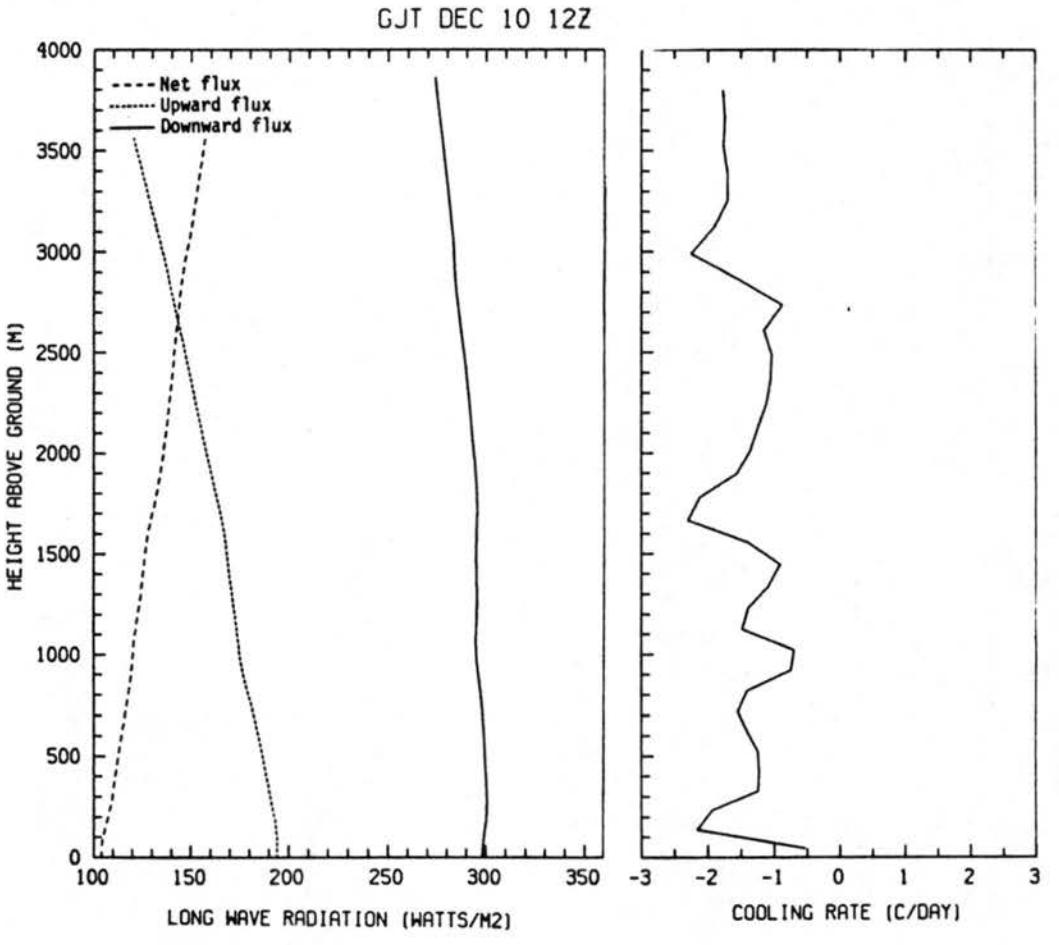

Figure 14. The calculated upward, downward, and net IR fluxes and the calculated IR heating rate for the morning sounding on December 10, 1980 at Grand Junction.

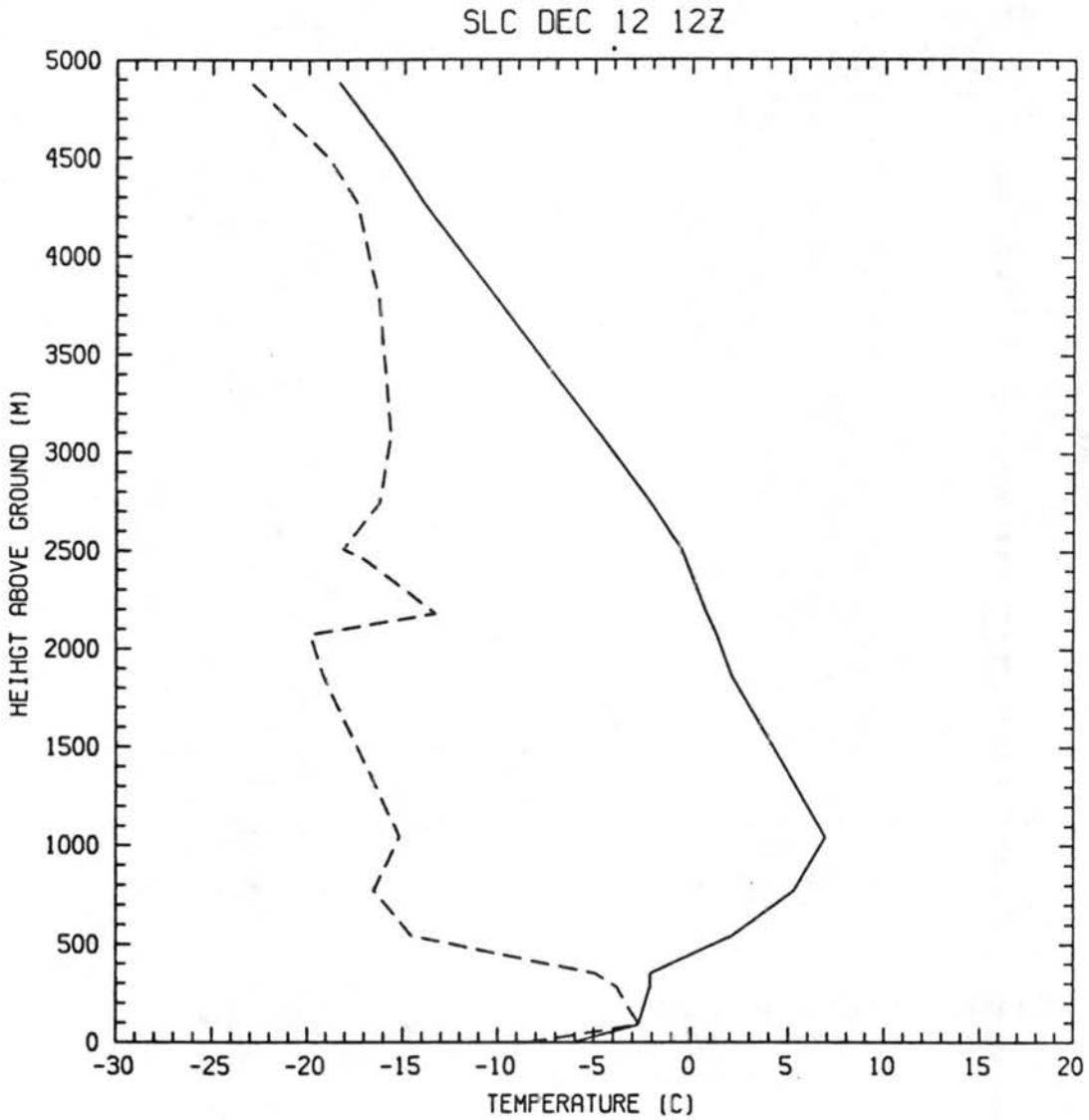

Figure 15. Same as Figure 13 but for the morning sounding on December 12, 1980 at Salt Lake City.

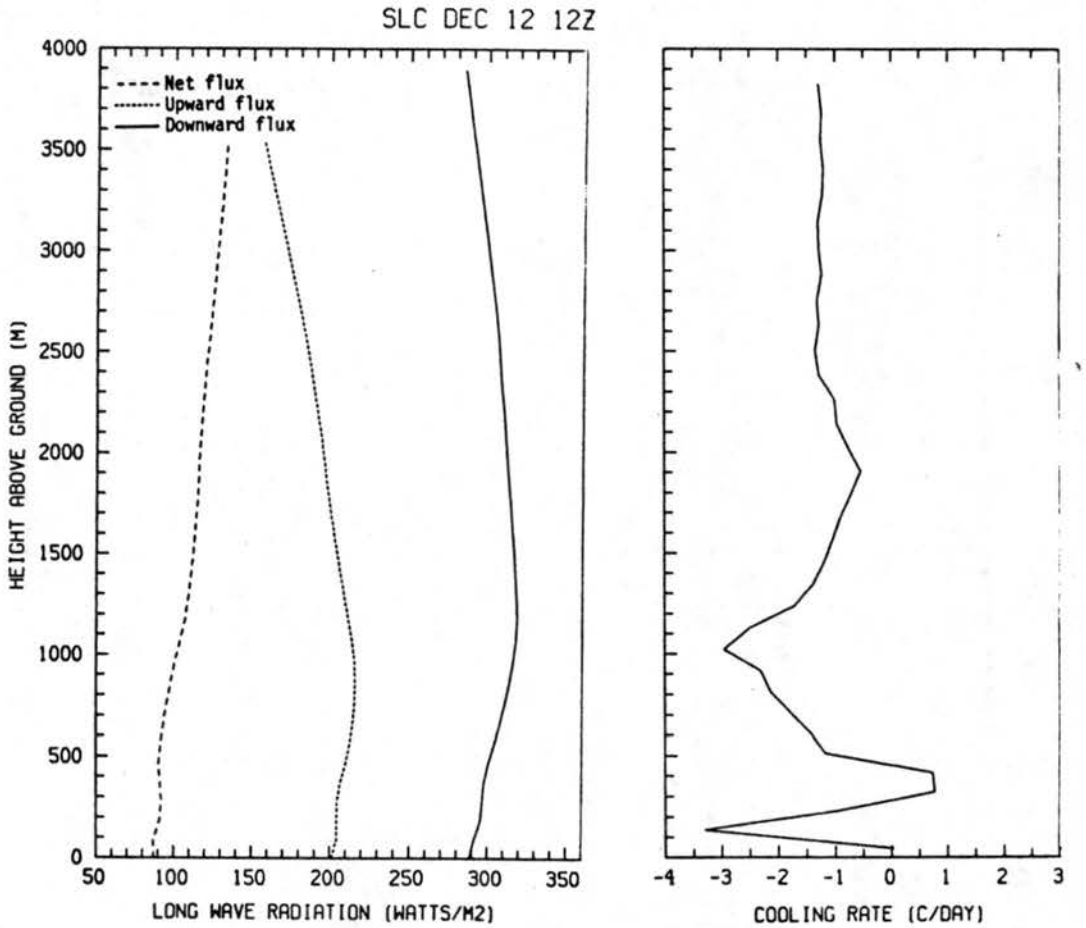

Figure 16. Same as Figure 14 but for the morning sounding on December 12, 1980 at Salt Lake City.

c. Deep fog layer. Figure 17 shows the morning sounding at Salt Lake City on the thirteenth and Figure 18 shows the calculated IR fluxes and heating rates from the program. The sounding had a fog layer up to 350m with warm, dry air above it. Cooling rates stronger than $10°C(day)^{-1}$ are present in the fog layer with slight warming above it. The IR calculation strongly suggests that the long wave emission from a cold fog layer with warm, dry air above it can significantly cool the fog layer. The cooling of the fog layer will increase the overall stability of the atmosphere and intensify the deep stable layer episode.

d. Low, warm cloud layer above fog. Figure 19 shows the afternoon sounding for Boise on the fourteenth and Figure 20 shows the calculated IR fluxes and heating rates from the model. Figure 21 shows the morning sounding on the fifteenth for Boise and Figure 22 shows the calculated IR fluxes and heating rates. In both cases the cloud layer was warmer than the fog layer. Figure 22 shows the effects the top of the cloud has on the heating rates. The heating rates for both cases show warming rates over $5°C(day)^{-1}$ in the fog layer which would cause a weakening of the overall stability of the lower atmosphere. The IR flux indicate that the cloud above the fog layer is the main cause of the warming of the fog layer. This may explain the warming which occurred at Boise on the fifteenth and the temporary dissipation of the fog.

e. Cloud or moist layer above clear air near the surface. Figure 23 shows the afternoon sounding on the fourteenth at Winnemucca and Figure 24 shows the morning sounding on the fifteenth at Winnemucca. For both cases a moist layer at least 1.0 km above the surface existed. The cloud data shows only 0.5 total coverage of clouds with 0.1 opaque at the afternoon sounding and 0.3 total and 0.1 opaque at the morning

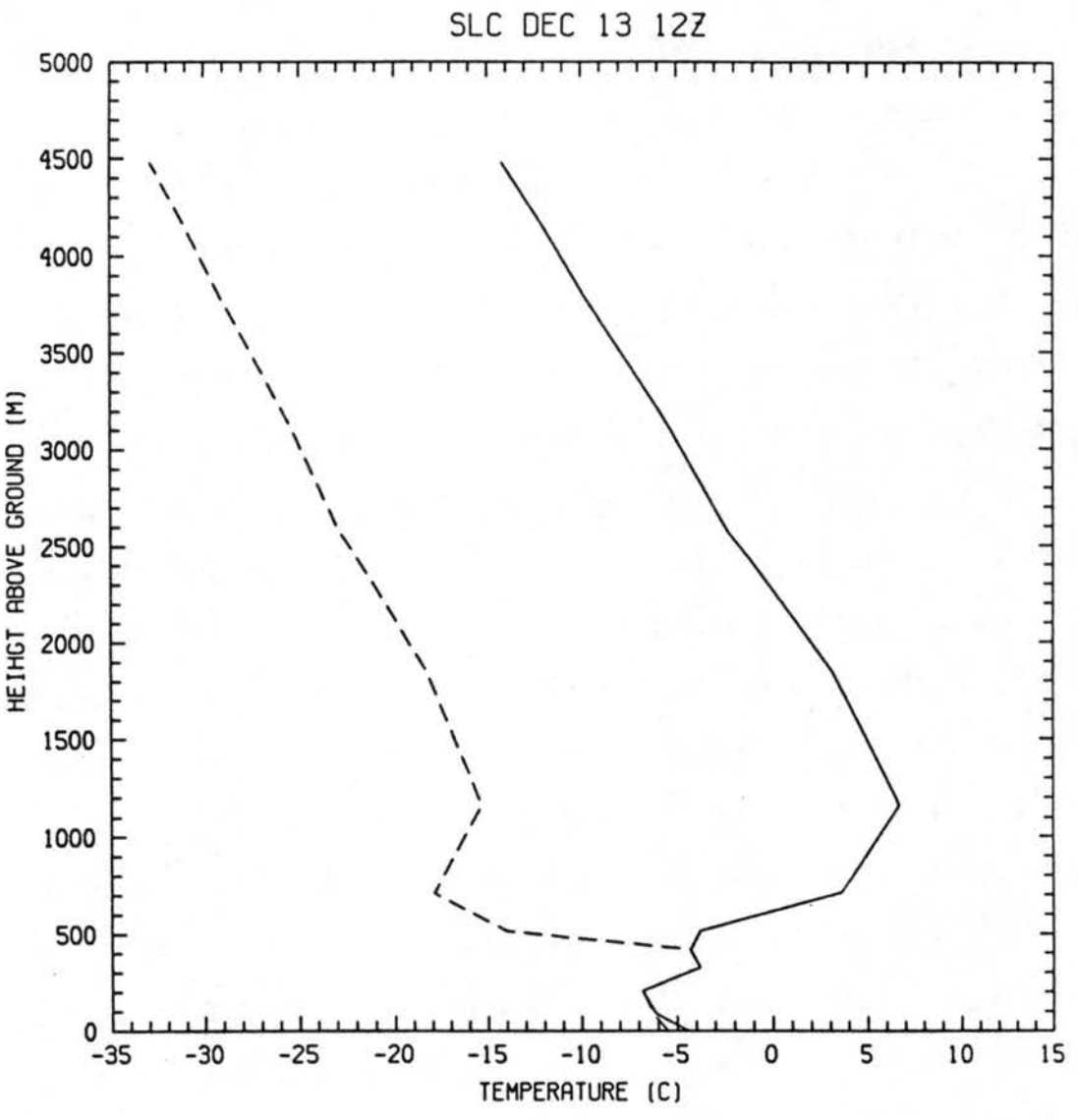

Figure 17. Same as Figure 13 but for the morning sounding on December 13, 1980 at Salt Lake City.

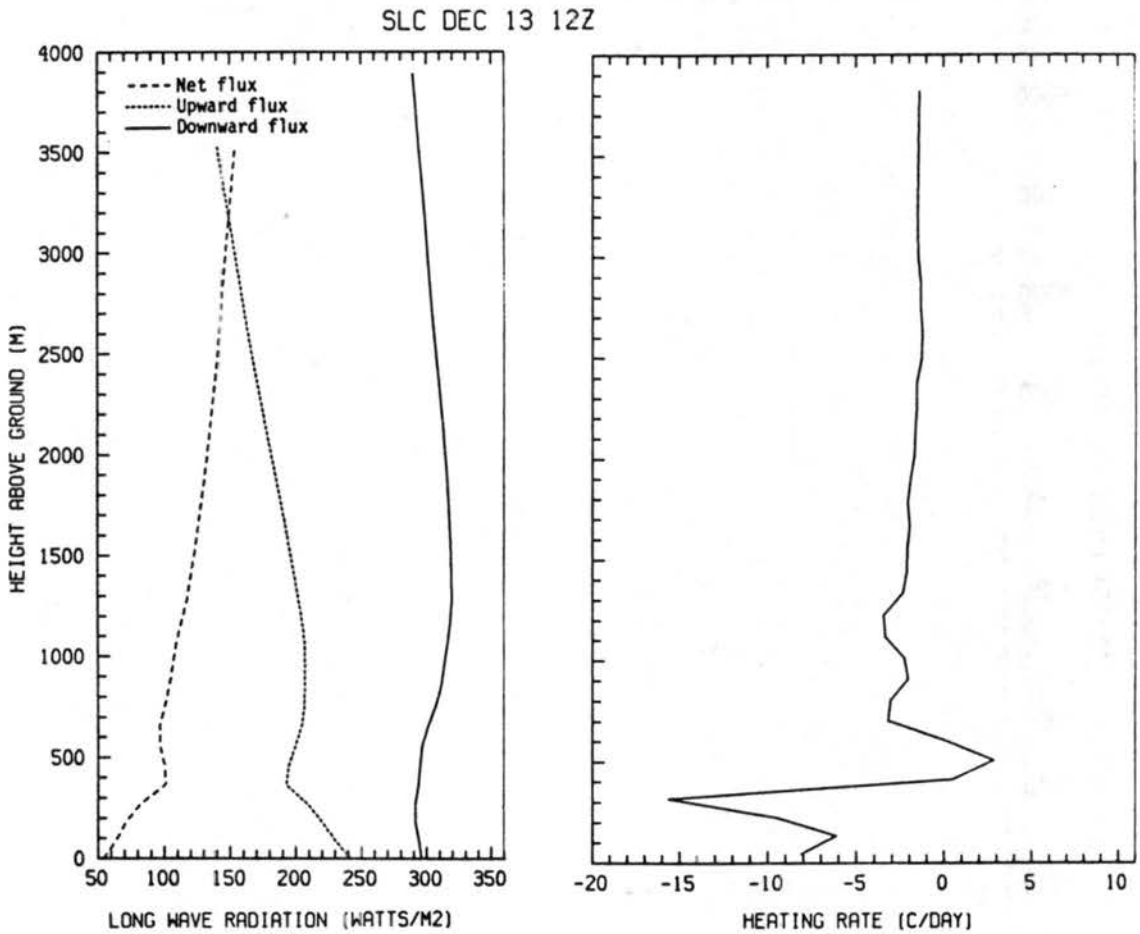

Figure 18. Same as Figure 14 but for the morning sounding on December 13, 1980 at Salt Lake City.

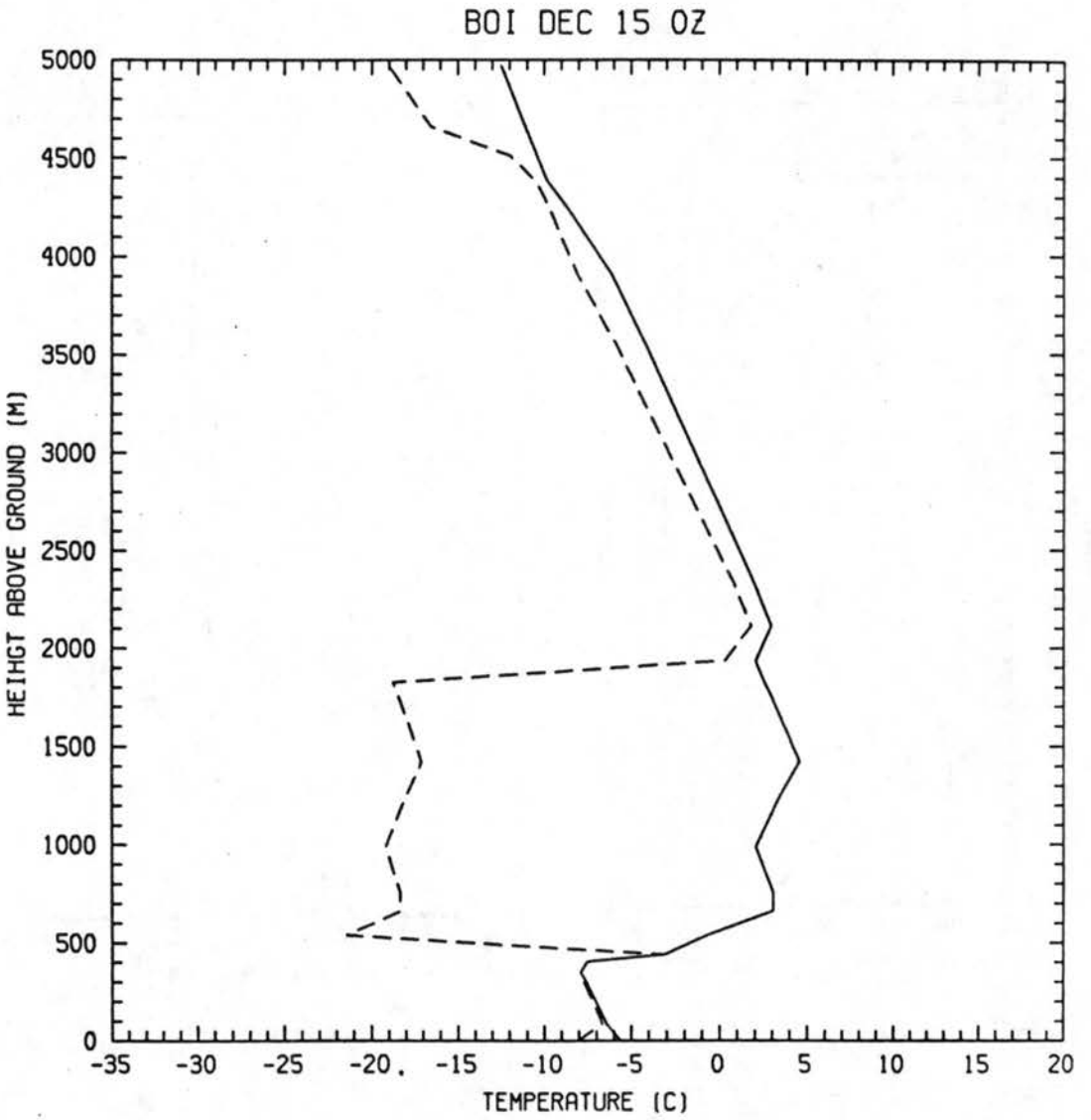

Figure 19. Same as Figure 13 but for the afternoon sounding on December 14, 1980 at Boise.

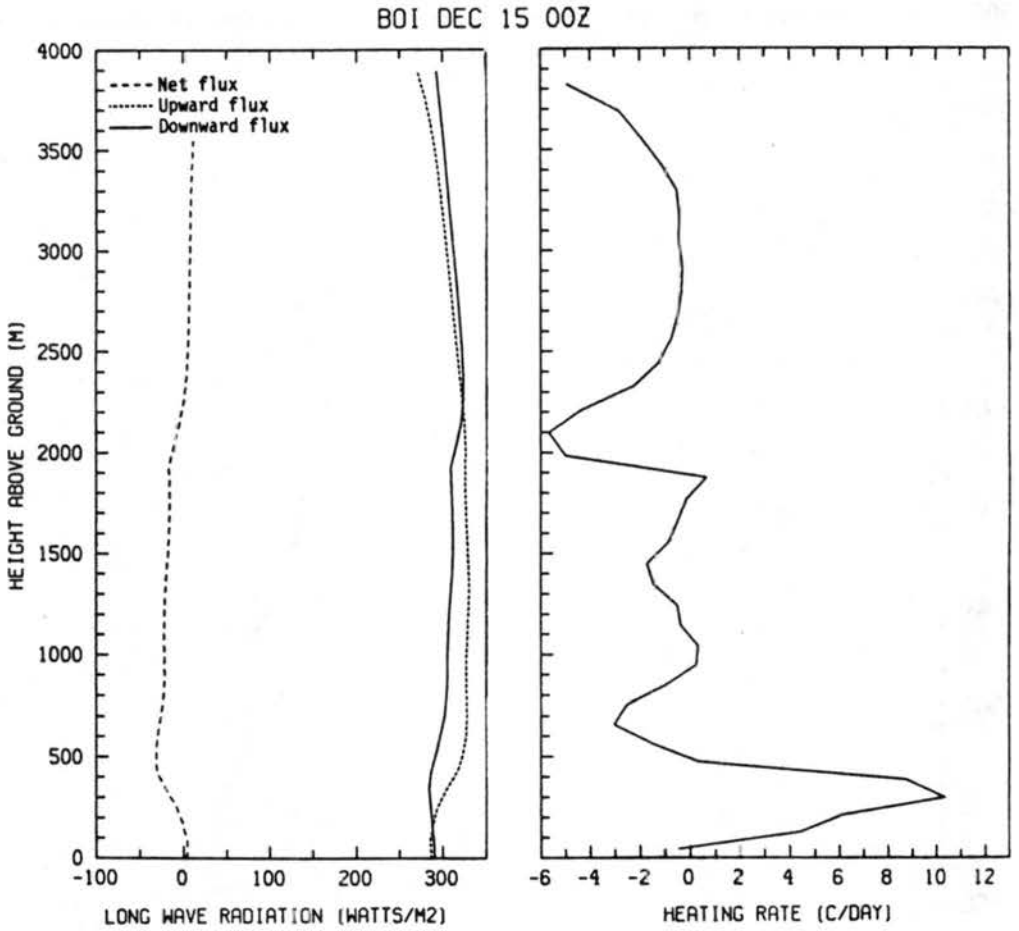

Figure 20. Same as Figure 14 but for the afternoon sounding on December 14, 1980 at Boise.

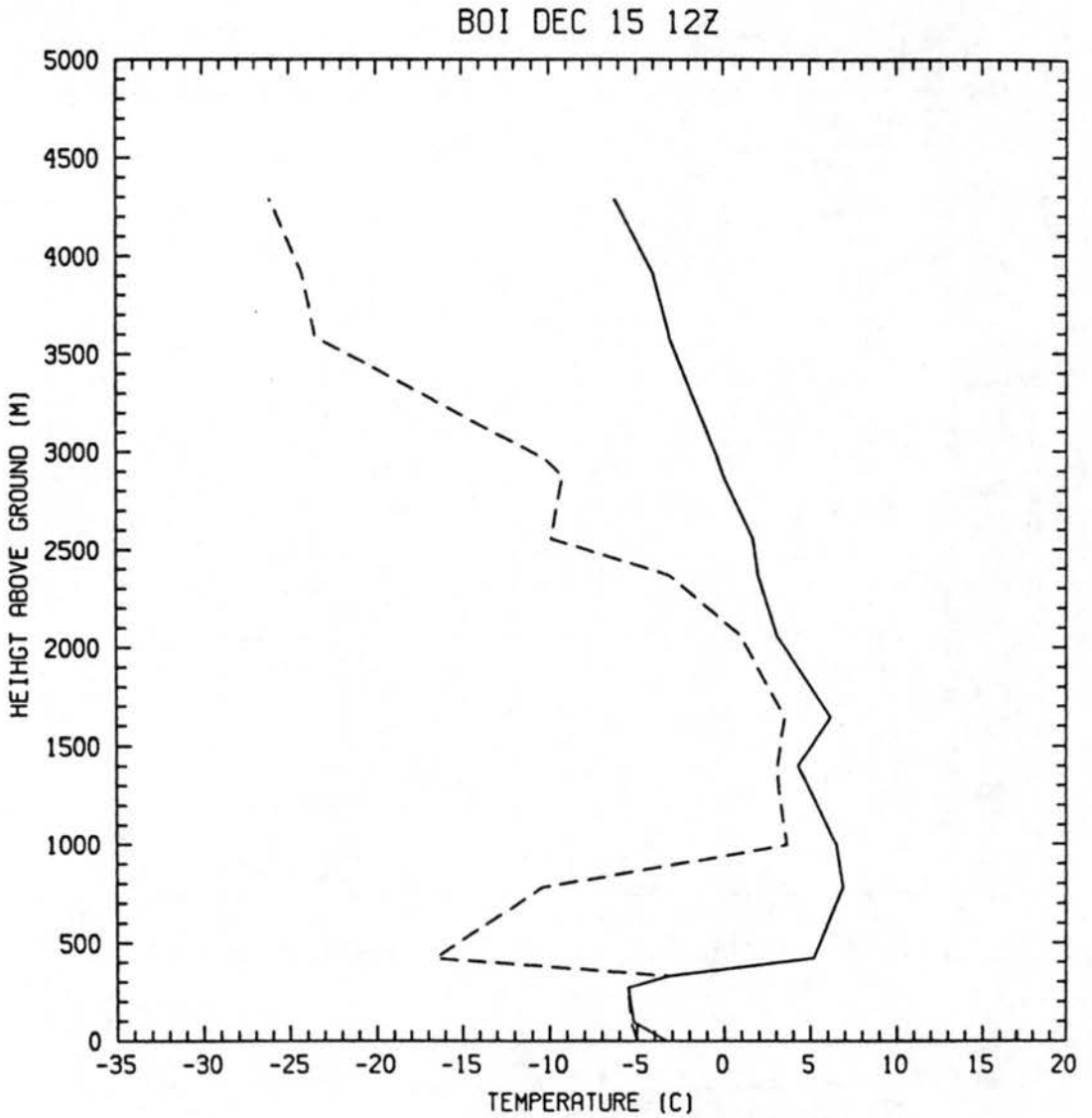

Figure 21. Same as Figure 13 but for the morning sounding on December 15, 1980 at Boise.

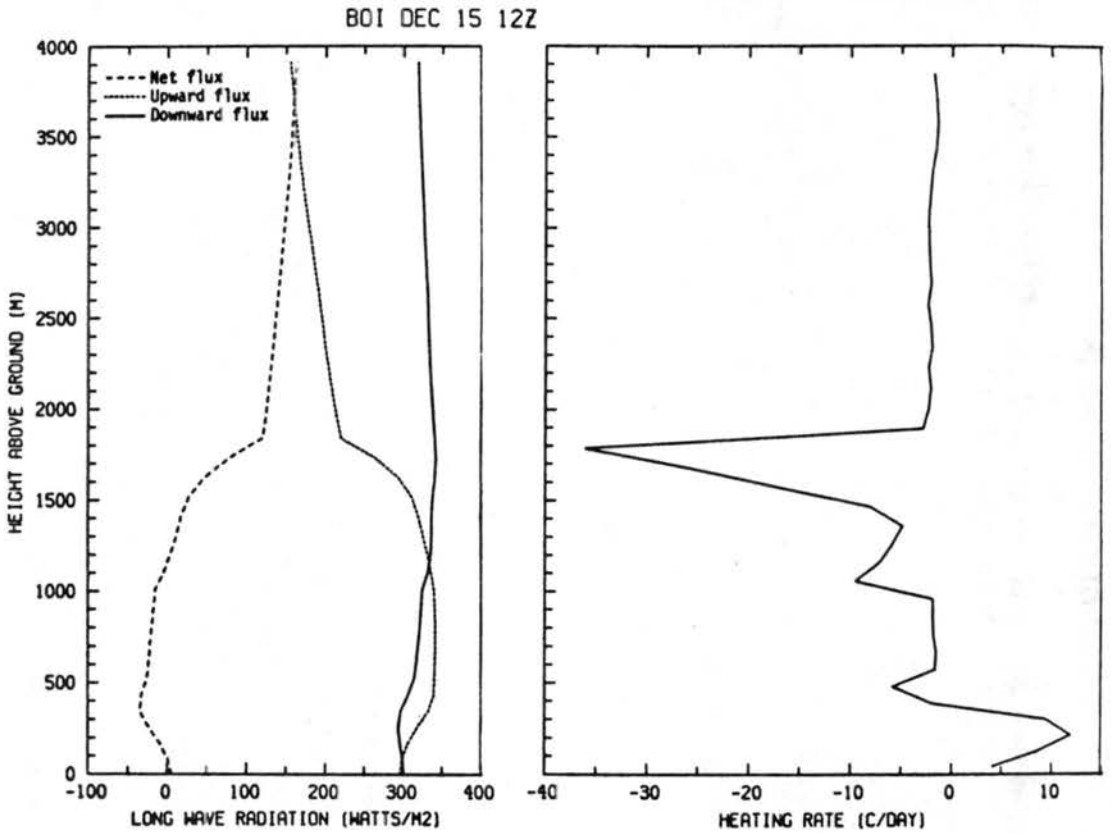

Figure 22. Same as Figure 14 but for the morning sounding on December 15, 1980 at Boise.

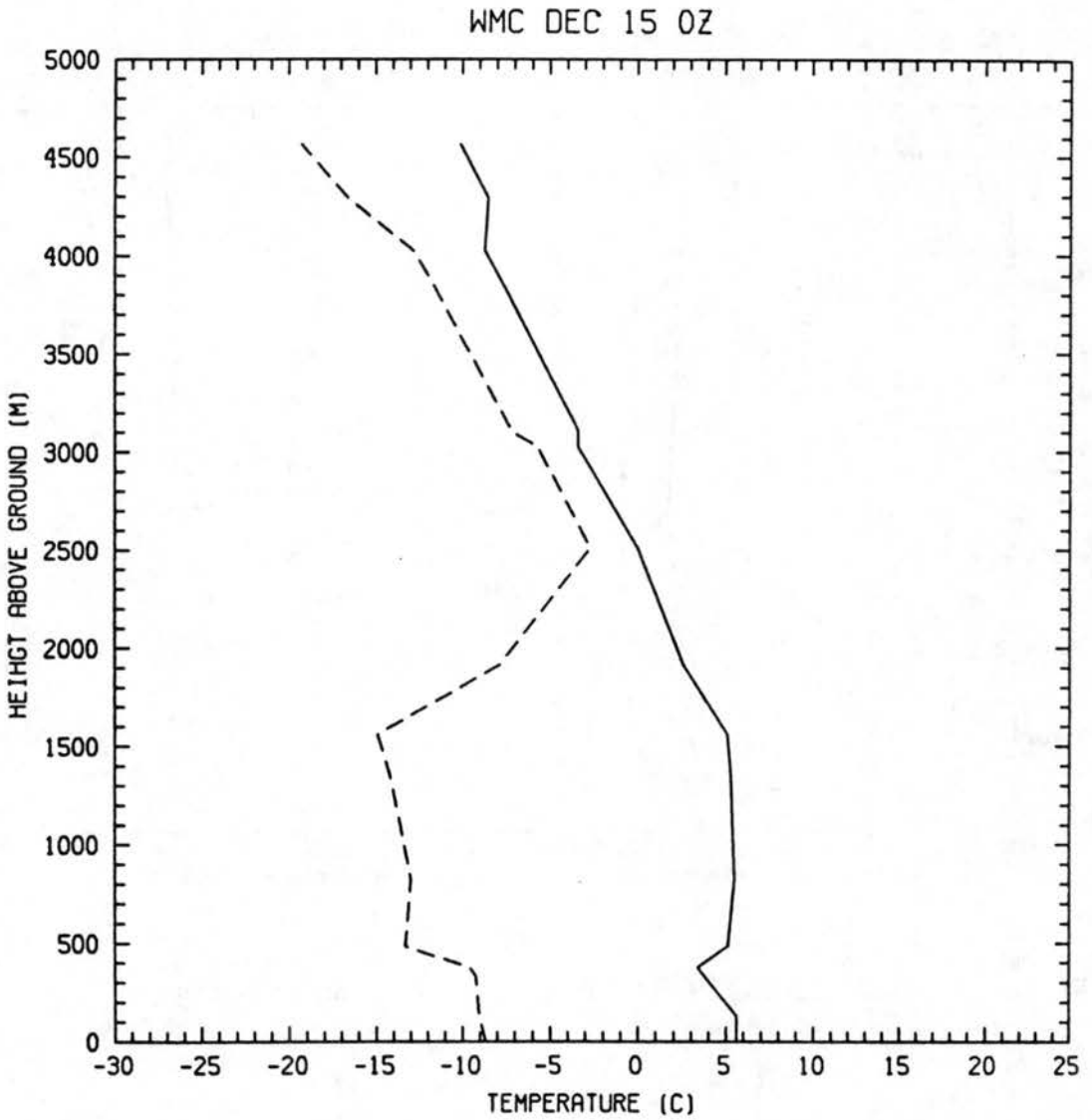

Figure 23. Same as Figure 13 but for the afternoon sounding on December 14, 1980 at Winnemucca.

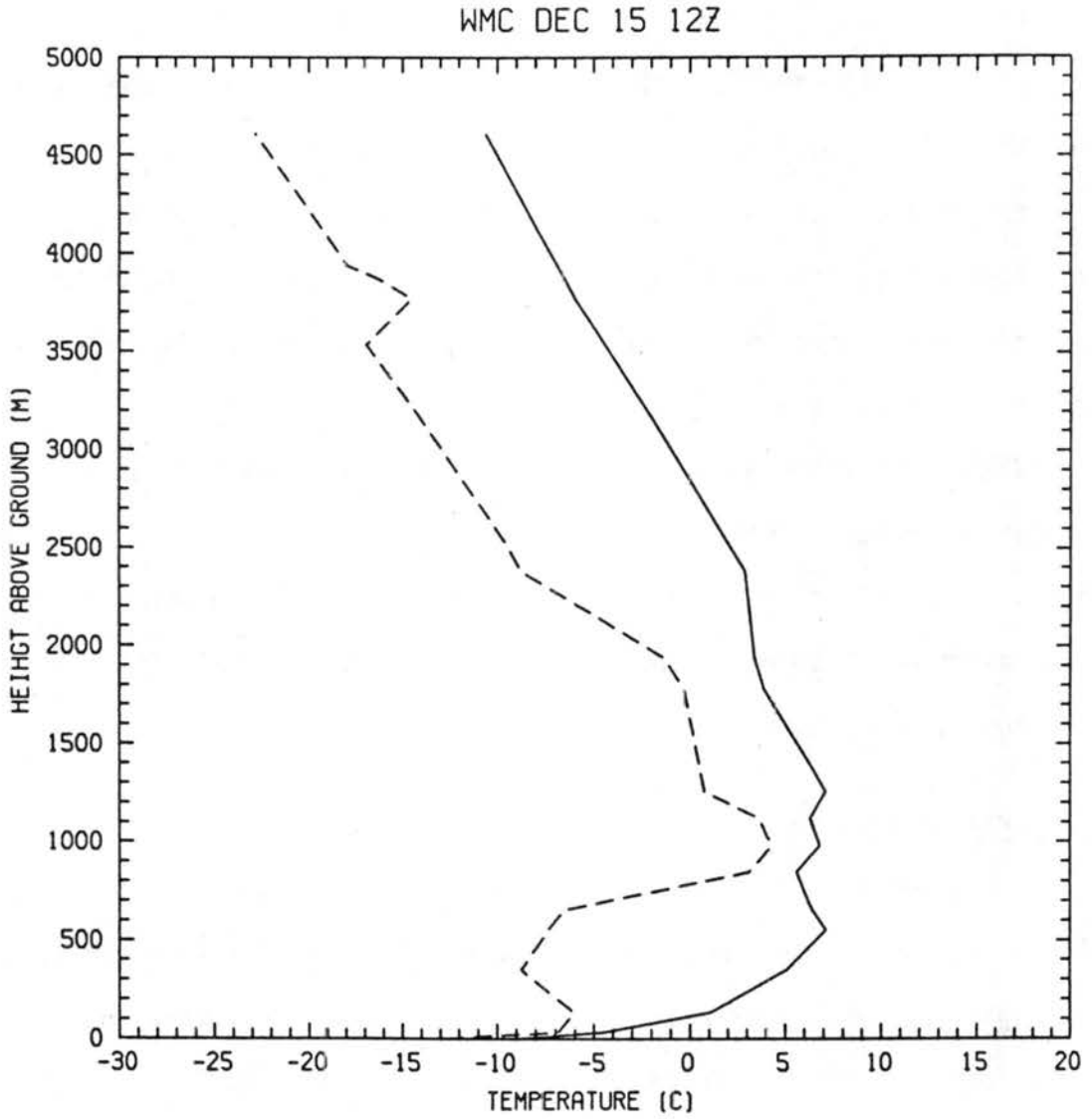

Figure 24. Same as Figure 13 but for the morning sounding on December 15, 1980 at Winnemucca.

sounding. Since a large percent of the sky was not covered by opaque clouds, IR calculations were run for the presence and absence of clouds to provide limits on the potential longwave effects. For the afternoon sounding Figure 25 shows the calculations without a cloud, Figure 26 shows the IR calculations with a cloud, and Figure 27 shows a comparison of heating rates with and without clouds. Figure 28, 29, and 30 are the same plots but for the morning sounding. The heating rates for both soundings show little indication of warming or reduced cooling near the surface. A comparison of heating rates for the cloud and no cloud cases show little difference except in and near the cloud layer. These IR calculations suggest that the clouds or moist layer did not significantly affect the IR induced heating rates near the surface. The cloud layers may have been too high or thin to greatly alter the heating rates near the surface.

3. Shortwave heating

a. Incoming solar radiation. Figure 31 shows 25% of the incoming solar radiation at the top of the atmosphere at Grand Junction and Boise from September 1985 to March 1986. The factor of 25% was used to roughly estimate the actual amount of solar radiation used to heat the air at the surface. Grand Junction has a latitude of 39.11° and is the furthest south of the stations. Boise's latitude is 43.56° and is the furthest north of the four stations.

Figure 31 shows that late November, December, and January is the time of the year with the weakest incoming solar radiation. The deep stable layer climatology showed that at the four intermountain region stations a large percentage of the days with deep stable layers occurred

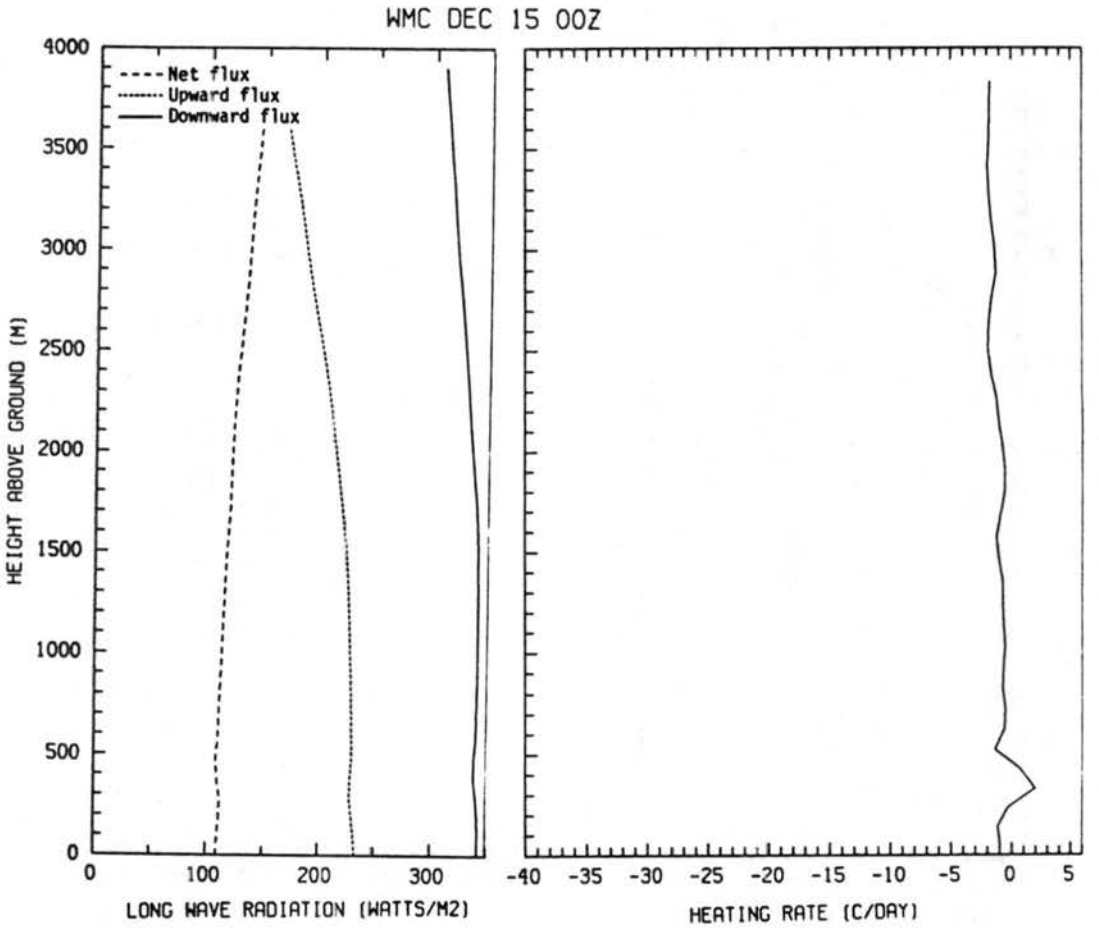

Figure 25. The calculated upward, downward, and net IR fluxes and the calculated IR heating rate for the afternoon sounding on December 14, 1980 at Winnemucca without clouds.

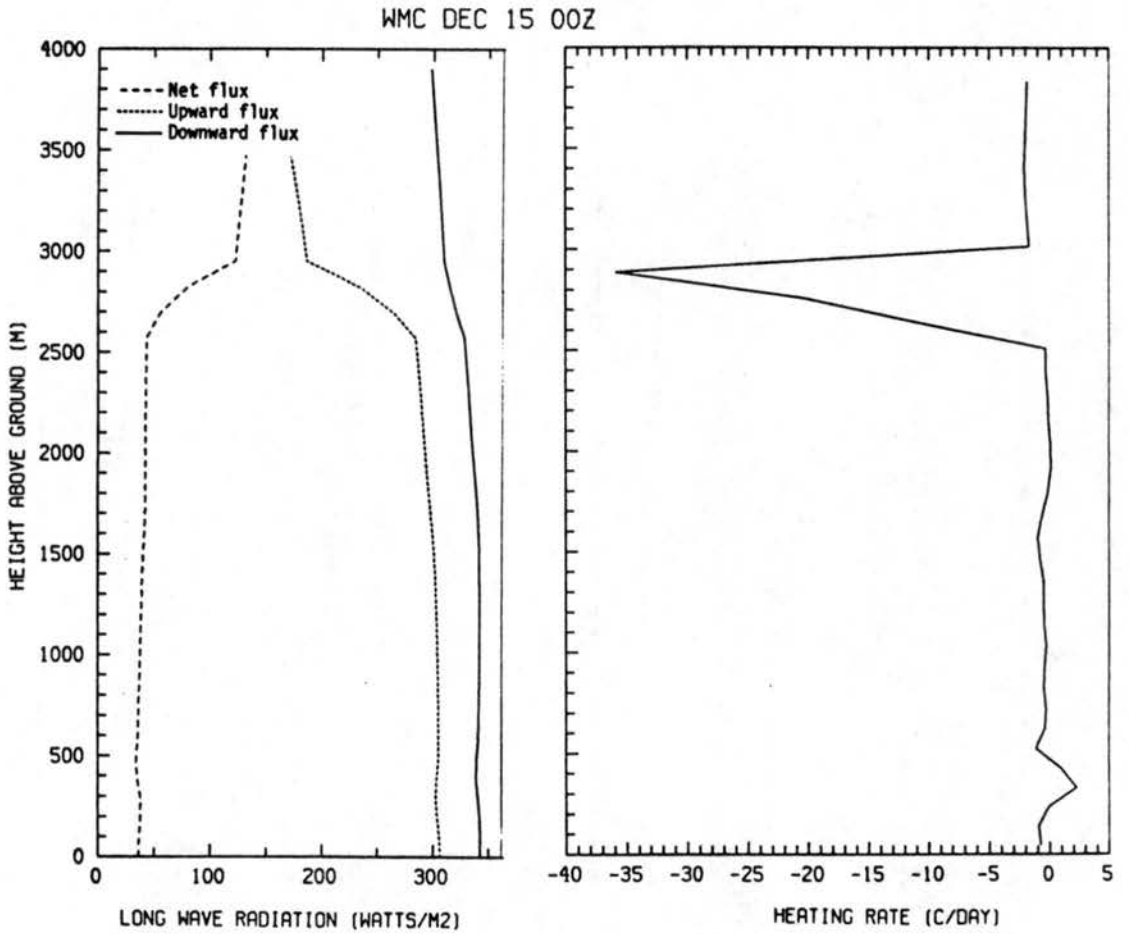

Figure 26. Same as Figure 25 but with clouds.

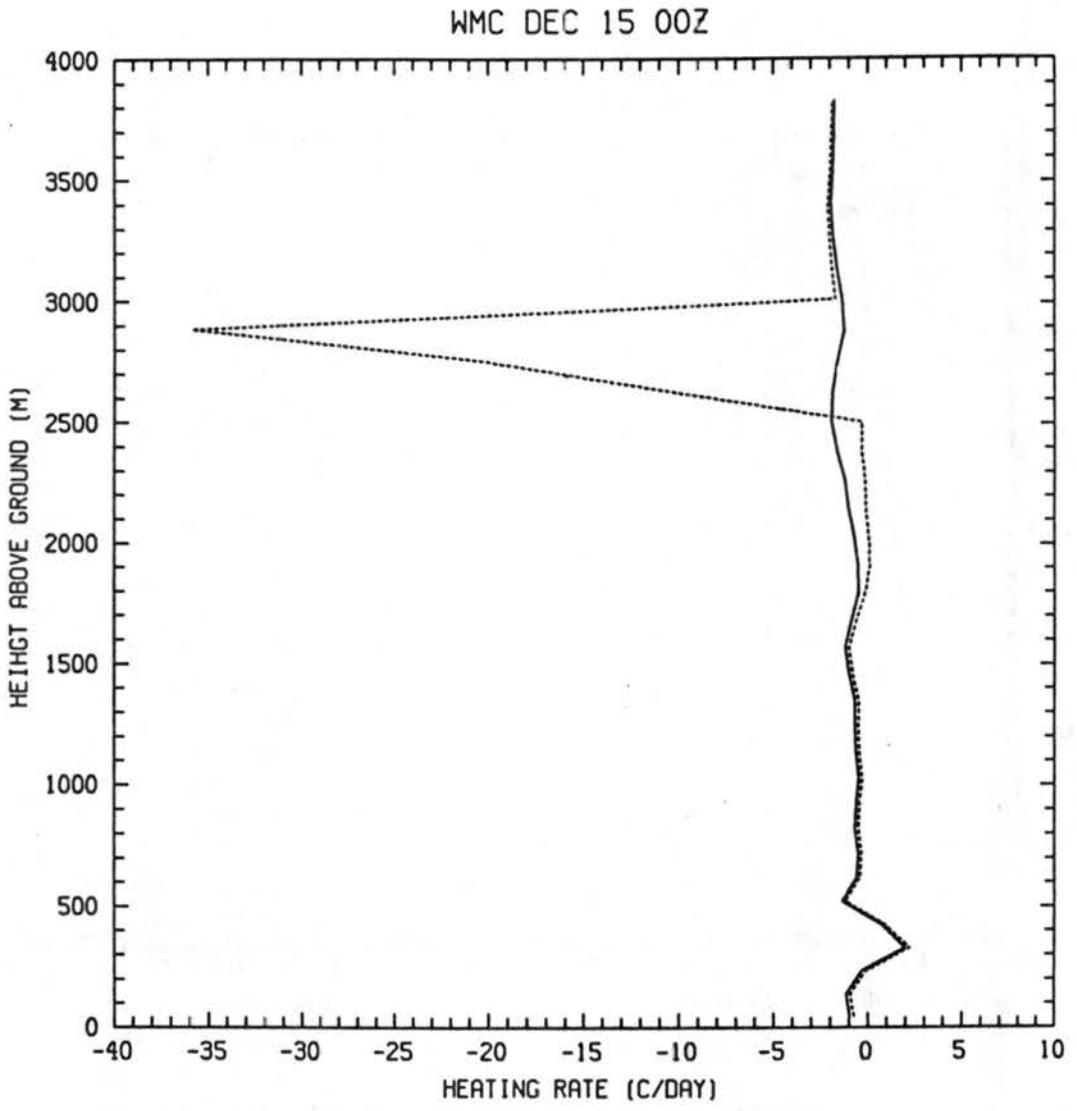

Figure 27. The calculated IR heating rates for the afternoon sounding on December 14, 1980 for cases with clouds (dashed line) and without clouds (solid line).

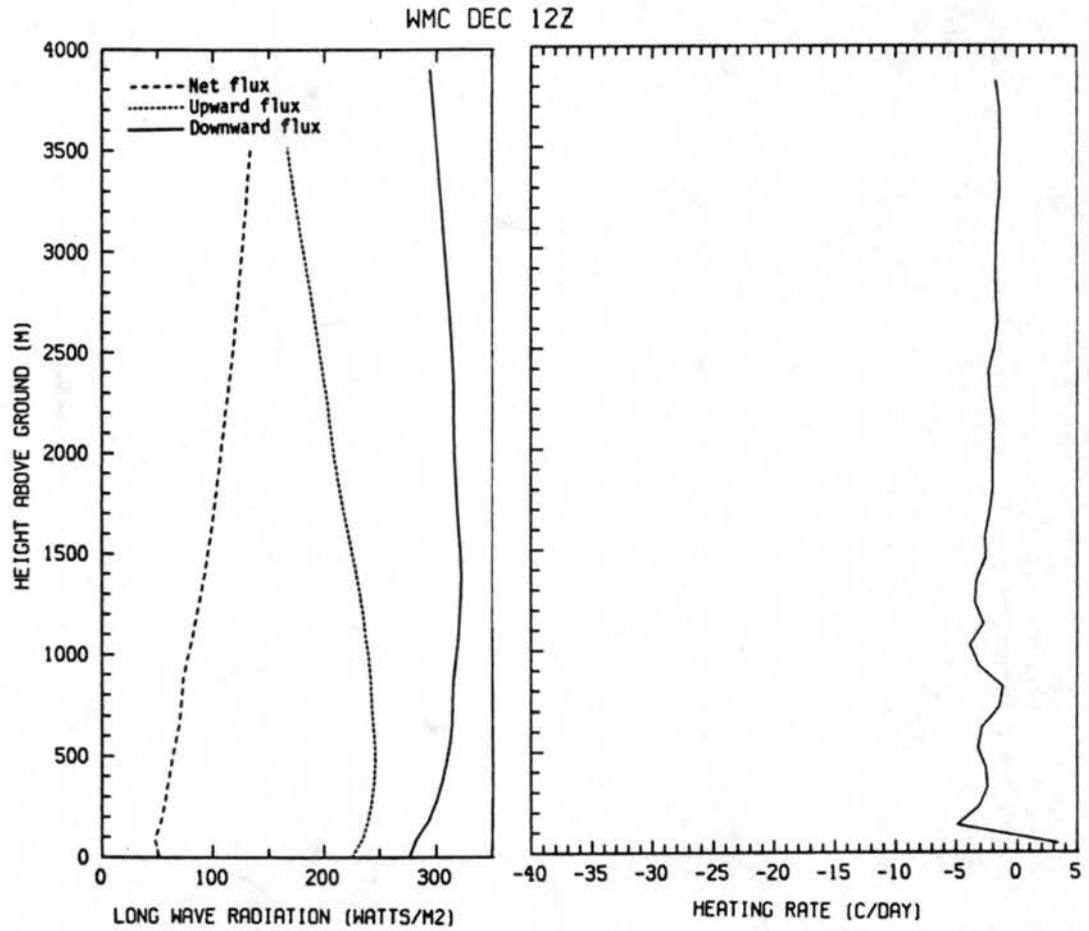

Figure 28. The calculated upward, downward, and net IR fluxes and the calculated IR heating rate for the morning sounding on December 14, 1980 at Winnemucca without clouds.

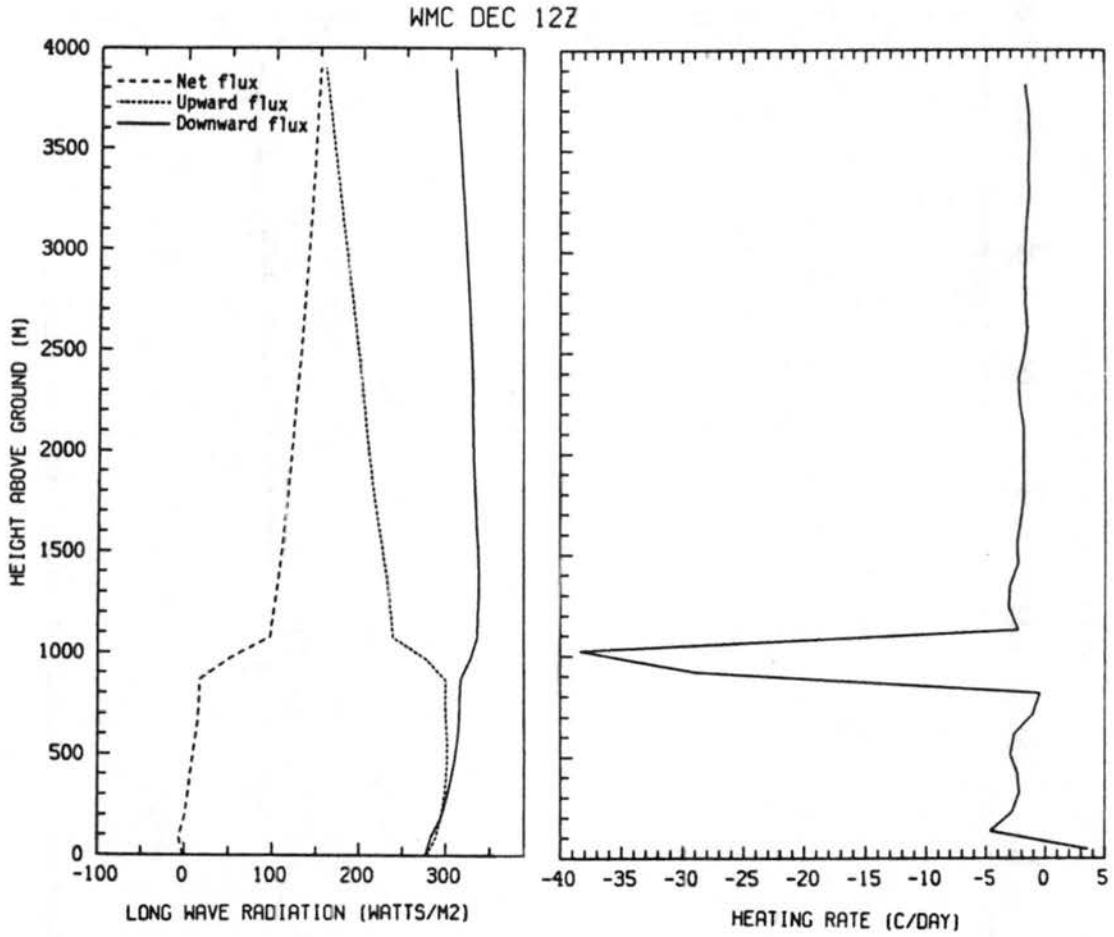

Figure 29. Same as Figure 28 but with clouds.

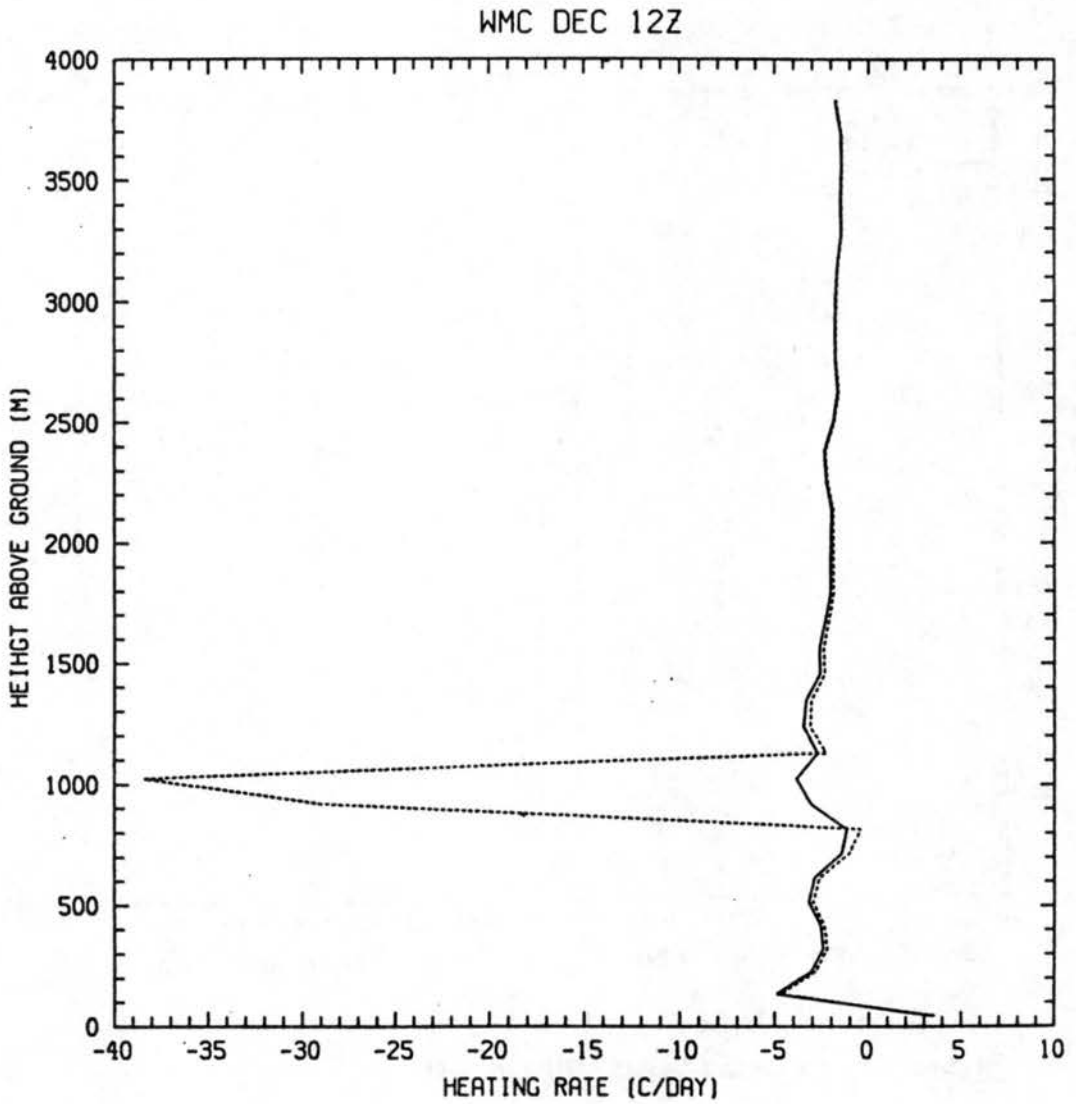

Figure 30. Same as Figure 27 but for the morning sounding on December 15, 1980 at Winnemucca.

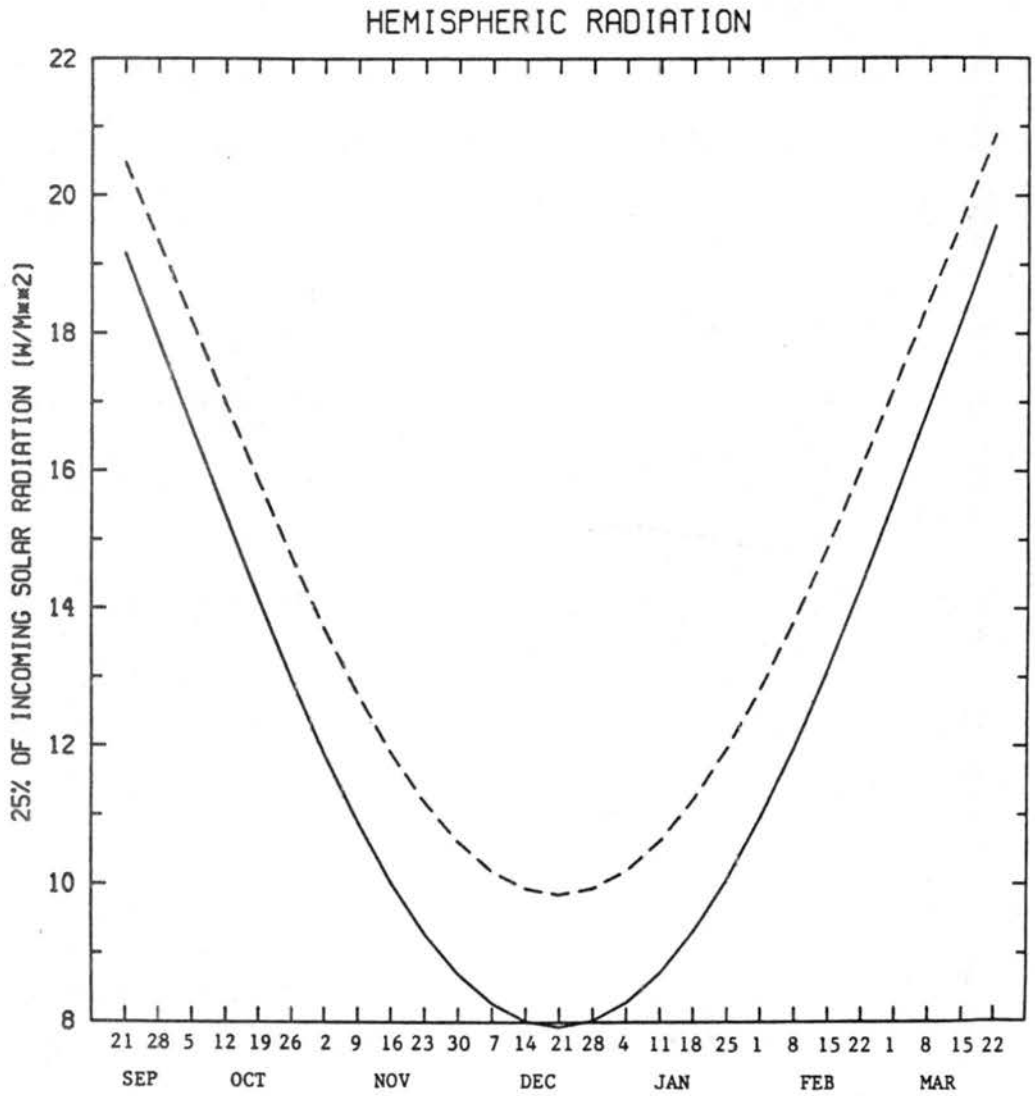

Figure 31. Twenty-five percent of the hemispheric solar radiation from September 21, 1985 to March 22, 1986 for Grand Junction (dashed line) and Boise (solid line).

in December and January. The coincidence of weak incoming solar radiation with the higher frequency of days with deep stable layers indicates that strong incoming solar radiation hampers the development of deep stable layers. Strong incoming solar radiation may allow for vigorous CBL growth which can break through the capping stable layer. Synoptic factors such as the frequency of stationary warm ridges aloft may also help cause the wintertime maximum in the number of deep stable layers.

The difference of incoming solar radiation between Boise and Grand Junction is the greatest on December 21, the winter solstice. The incoming solar radiation at Grand Junction is about $2*10^{-4}Wcm^{-2}$ or about 25% larger than Boise. At four weeks before and after the solstice the difference in the incoming solar radiation is still $1.8*10^{-4}Wcm^{-2}$ with Grand Junction receiving about 19% more radiation than Boise. With significantly less incoming solar radiation Boise may have a higher frequency of days with deep stable layers than Grand Junction.

b. Effects of cloud and snowcover. In this section snowcover and cloud cover will be examined to see if they have any noticeable effects on the CCBL height, daily surface temperature range, and the surface maximum temperature. The daily maximum and minimum temperature, the snowcover at 1200 GMT, and cloudcover data for December 6-23, 1980 at the four stations in this case study are listed in Appendix E. In Appendix B the CCBL heights are plotted on the adiabatic diagrams extending up to 2.5km.

At Salt Lake City a fog layer which lasts the entire day formed on the thirteenth and persists until the twenty-first. On the days with

persistent fog the daily surface temperature range was often very small indicating that slight surface heating occurred. On the tenth, eleventh, and twelfth there was significant cloud cover for at least part of each day. During the period 06-17 there was less opaque cloud cover on the twelfth than the tenth and eleventh. The CCBL height on this date, however, was the same as the eleventh and lower than the tenth and the surface temperature was the same or cooler than the previous two days.

Winnemucca did not have persistent fog layers so it is good for examining the effects of clouds other than fog on the surface heating. Between the eighth and nineteenth the days with significant coverage of thin clouds during 06-17 were the tenth and eleventh. On the eighteenth there was significant coverage of opaque clouds. On the tenth the CCBL height was lower than the ninth, but the CCBL heights on the tenth and eleventh were not significantly different than the heights throughout he episode. The CCBL height on the eighteenth, a day with significant dense cloud coverage, was not much different than the other days of the episode. The temperatures also show no noticeable changes on the days with cloudiness. The relationship of cloudcover to CCBL heights and surface maximum temperature for Grand Junction and Boise is given in Appendix E.

The analysis of the cloud data with the surface temperature data shows that in this episode no relationship between cloudiness and CCBL heights and temperature can be developed except for the case of fog. The amount of non-fog cloud cover appears to be of secondary importance in the episode. The analysis clearly shows that persistent fog layers do have a noticeable effect on surface temperatures and can be a major

influence in the deep stable layer episode. To more accurately determine the effects of cloudcover on the amount of solar radiation reaching the ground and surface heating, solar radiation measurements or more detailed sounding data is needed.

The effects of snowcover on surface heating are difficult to determine from this case study. Snowcover data is also listed in Appendix E. Boise was the only station with a measurable snowcover during the episode. The occurrence of a long episode with a lack of snowcover reveals that snowcover is not necessary for deep stable layer episodes of significant length. The lack of snowcover and mild surface maximum temperatures show that deep stable layers can occur with relatively mild weather.

F. Decoupling

As stated previously, a deep stable layer can possibly decouple the air near the surface from the air aloft even if the synoptic-scale winds have moderate to strong speeds. To briefly examine the nature of decoupling and to determine its influence on the winds near the surface, bulk Richardson numbers were calculated for 50mb thick layers. The bulk Richardson numbers for all the 50mb thick layers from near the surface to 500mb are given in Appendix F. Tables 14 and 15 show for Salt Lake City and Winnemucca the bulk Richardson number, the lapse rate, and the wind shear for the two lowest 50mb thick layers. Before the episode the bulk Richardson numbers in the two lowest layers generally were small. Values less than 2.0 are common. Panofsky and Dutton (1984) state that even though Richardson numbers calculated from rawinsondes are not very accurate, the probability of clear air turbulence is relatively high in

Table 14.
The bulk Richardson number, mean lapse rate ($^{\circ}Ckm^{-1}$), and wind shear ($ms^{-1}km^{-1}$) for the two lowest 50mb thick layers at Salt Lake City.

		850mb to 800mb 268m to 755m			800mb to 750mb 755m to 1274m		
		Ri Number	Lapse Rate	Wind Shear	Ri Number	Lapse Rate	Wind Shear
12/ 6/80	M	50.61	3.73	2.07	4.91	6.48	4.93
	A	0.86	7.48	9.79	1.74	3.95	11.06
12/ 7/80	M	8.16	7.10	3.44	34.90	5.15	2.20
	A	0.84	8.60	7.13	5.98	9.00	2.17
12/ 8/80	M	5.29	7.17	4.23	3.90	3.81	7.53
	A	0.90	9.32	4.24	5.98	-0.60	8.03
12/ 9/80	M	0.80	9.30	4.51	5.93	2.21	6.89
	A	2.27	9.30	2.71	8.01	-6.55	8.66
12/10/80	M	21.14	2.30	3.58	2.89	-5.10	13.67
	A	20.26	-12.60	6.29	0.50	5.95	16.48
12/11/80	M	56.75	-16.97	4.10	1.27	5.35	11.10
	A	81.97	-10.95	2.99	3.14	3.61	8.30
12/12/80	M	153.99	-15.16	2.40	87.18	-0.19	2.00
	A	43.89	-13.29	4.33	97.80	-0.38	1.91
12/13/80	M	240.10	-18.84	2.07	M	M	M
	A	247.56	-25.36	2.25	11.38	2.84	4.62
12/14/80	M	12.46	-12.71	8.09	9.49	-6.33	7.77
	A	47.23	-12.96	4.16	6.02	-2.50	8.52
12/15/80	M	8.25	-14.94	10.41	3.39	0.78	9.75
	A	215.53	-15.51	2.04	1.71	6.26	8.45
12/16/80	M	156.15	-8.59	2.04	7.36	-2.27	7.58
	A	189.34	-22.87	2.46	74.69	2.24	1.87
12/17/80	M	7.31	-11.59	10.17	6.67	-5.07	8.80
	A	215.72	-15.12	2.02	3.42	-2.81	11.30
12/18/80	M	16.34	-26.12	8.85	3.10	3.01	8.71
	A	M	M	M	M	M	M
12/19/80	M	45.05	-11.57	4.13	117.50	-2.49	1.93
	A	215.66	-15.61	2.05	62.86	3.25	1.91
12/20/80	M	10.54	-17.04	9.57	M	M	M
	A	52.55	-14.60	4.06	8.40	6.11	3.92
12/21/80	M	271.24	-15.07	1.81	7.51	4.00	5.20
	A	42.35	-19.80	4.99	0.55	4.93	17.57
12/22/80	M	1.19	5.77	10.75	0.37	7.94	12.99
	A	13.47	4.42	3.72	1.06	8.03	7.59
12/23/80	M	2.98	6.54	6.18	1.49	7.39	7.54
	A	7.08	7.76	3.17	2.93	8.17	4.42

Table 15.
Same as Table 12 but for Winnemucca.

		850mb to 800mb 242m to 734m			800mb to 750mb 734m to 1258m		
		Ri Number	Lapse Rate	Wind Shear	Ri Number	Lapse Rate	Wind Shear
12/ 6/80	M	0.50	8.11	10.92	1.29	8.53	5.90
	A	0.04	9.73	4.28	2.72	8.50	4.10
12/ 7/80	M	9.70	4.23	4.57	129.70	7.86	0.74
	A	0.20	9.73	2.79	1.39	7.06	8.55
12/ 8/80	M	49.31	-6.81	3.53	11.44	3.78	4.39
	A	848.25	1.88	0.58	3.80	-4.51	11.68
12/ 9/80	M	8.32	-3.77	7.69	3.67	-0.20	9.91
	A	44.42	0.83	2.69	114.63	-5.62	2.20
12/10/80	M	109.06	-10.29	2.57	73.90	-3.24	2.49
	A	11.03	-10.73	8.10	6.11	3.41	6.04
12/11/80	M	40.16	-11.97	4.38	380.75	1.14	0.89
	A	43.26	-6.07	3.59	24.44	0.38	3.67
12/12/80	M	99999.99	-13.39	0.04	24.70	-0.19	3.75
	A	145.39	-7.69	2.05	55.54	3.58	1.97
12/13/80	M	M	M	M	M	M	M
	A	M	M	M	M	M	M
12/14/80	M	32.25	-9.39	4.59	12.27	2.66	4.51
	A	10.81	-3.43	6.55	5.73	0.38	7.59
12/15/80	M	9.87	-1.01	6.18	2.97	-1.51	11.51
	A	7.66	-1.79	7.23	60.94	0.93	2.24
12/16/80	M	1154.78	-9.54	0.76	17.59	-2.97	5.00
	A	6.17	-3.58	8.65	9.95	-4.05	6.89
12/17/80	M	42.64	-12.95	4.30	5.49	3.35	6.35
	A	84.62	-0.40	2.04	5.66	-0.75	8.02
12/18/80	M	M	M	M	M	M	M
	A	4.02	4.99	6.41	10.89	4.15	4.24
12/19/80	M	28.60	-0.80	3.59	19.49	3.81	3.28
	A	18.62	6.39	2.50	3.00	6.45	6.22
12/20/80	M	17.34	-2.81	5.04	4.12	7.21	4.65
	A	40.69	4.42	2.14	7.63	8.59	2.31
12/21/80	M	7.04	-3.44	8.13	2.80	6.69	6.23
	A	0.34	6.77	17.40	0.36	6.83	16.75
12/22/80	M	1.07	7.78	7.99	2.47	7.79	5.27
	A	-0.44	10.42	7.27	1.01	8.81	5.75
12/23/80	M	3.52	7.54	4.71	6.31	6.99	3.97
	A	0.91	6.65	10.94	34.53	1.53	2.91

regions with relatively small Richardson numbers. When using rawinsondes they considered a Richardson number of 1.0 to be small. Once the deep stable layer became established the bulk Richardson numbers became much larger with values greater than 20.0 being commonplace. At the end of the episode the bulk Richardson numbers became much smaller with values often less than 2.0.

The lapse rates clearly show the increased stability associated with the continuation phase of the episode. The analysis of the wind shear in the 50mb thick layer shows generally small wind shears in the initiation and continuation phases of the episode. This suggests that winds near the surface during the continuation phase are light because the winds aloft are light. However, there are several cases where there are strong wind shears over a 50mb thick layer with bulk Richardson numbers greater than 5.0. This suggests that deep stable layers can decouple the air near the surface from the air aloft with moderate to strong winds aloft. The termination phase of the episode has a weakly stable thermal structure and has wind shears stronger than those generally seen in the continuation phase. This analysis indicates that deep stable layers can cause decoupling with moderate to strong synoptic-scale winds aloft. However, to better determine the conditions under which deep stable layers cause decoupling, analysis of more case studies is needed as well as further study of other phenomenon that can vertically transport momentum in a stable atmosphere.

G. Pollution Potential

Deep stable layers have been identified to be one group of days in the intermountain region of the western United States with which small

mixing volumes are associated. In this section the mixing volumes for the deep stable layer episode will briefly be examined and will show the behavior of the CCBL height, mean wind speed below the CCBL height, and mixing volume for December 6-23, 1980.

The CCBL heights, mean wind speeds, and mixing volumes for Salt Lake City and Winnemucca are shown in Figures 32 and 33, respectively. Figures for other stations are shown in Appendix F. The parameters were calculated in the same manner as in Chapter II. The mixing volumes are relatively large in the initiation phase of the episode because both wind speeds and CCBL heights are relatively large. In the continuation phase the mixing volumes are noticeably smaller with mixing volumes less than $500 m^2 s^{-1}$ being common. The small mixing volumes in this phase is related to both a decrease in CCBL height and wind speed. After the episode the mixing volumes are larger, but generally are not as large as the values in the initiation phase. The increase in mixing volumes were generally caused by a modest increase in CCBL heights and a significant increase in wind speed. These values show that the deep stable layer episode was accompanied by low mixing volumes, and that the changes in mixing volumes from the initiation phase to continuation phase were larger than the changes from the continuation phase to after the episode.

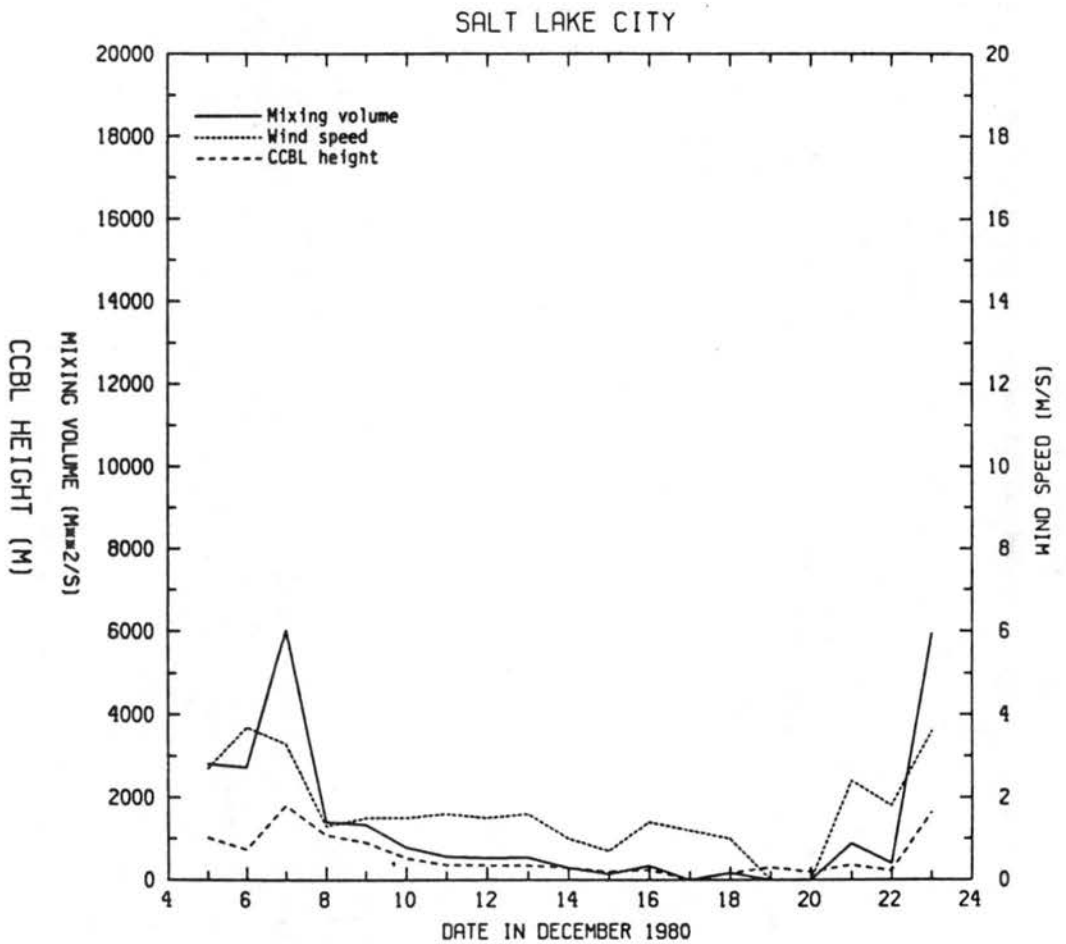

Figure 32. The CCBL height (m), mean wind speed below the CCBL height(ms^{-1}), and mixing volume (m^2s^{-1}) from December 5-23, 1980 for Salt Lake City.

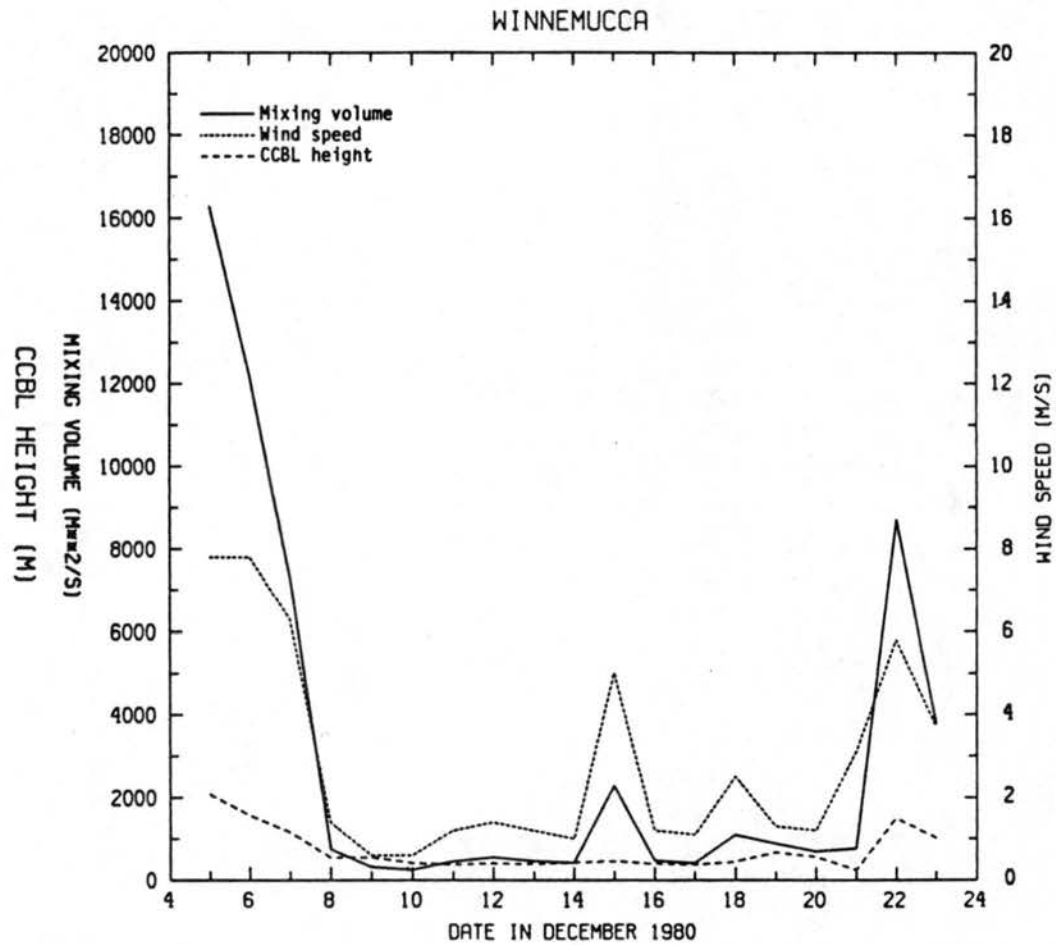

Figure 33. Same as Figure 32 but for Winnemucca.

CHAPTER V

CONCEPTUAL MODEL OF DEEP STABLE LAYER EPISODE

A. Introduction

In Chapter IV a deep stable layer episode in December 1980 at four stations in the intermountain region of the western United States was examined in-depth. The observations showed structure of the deep stable layer and the regions of warming and cooling in the atmosphere associated with the initiation, continuation, and termination of the episode. The analysis indicated the importance of the different physical process in the life cycle and determined which meteorological phenomenon are important for causing the physical processes to occur. In this chapter the results from throughout this thesis will be synthesized into a conceptual model of the initiation, continuation, and termination phases of the deep stable layer.

B. Initiation Phase

The initiation phase of the deep stable layer episode is the period of time in which processes which lead to the formation of deep stable layer occur. The end of the initiation phase occurs when a deep stable layer which does not change rapidly in structure or intensity forms. This phase is associated with a warm ridge aloft building into the area. The time versus height plots of potential temperature showed that the

main feature of the initiation phase is the descent of a layer of rapid warming. The end of the initiation phase occurred when the region of rapid warming descended to about 0.5 to 1.5km forming a capping stable layer.

The only process which can cause a large magnitude of diabatic heating away from the surface is condensation. The diagrams in Appendix B show that regions of rapid warming had dew point depressions larger than 3°C. Therefore, the only two mechanisms that can induce warming of the magnitude seen in the initiation phase are synoptic-scale subsidence and horizontal warm air advection. The EEVM values in the initiation phase were generally $-0.5 cms^{-1}$ to $-1.5 cms^{-1}$ and suggest that synoptic-scale subsidence or warm air advection could cause the warming. The estimate of warm air advection at 500mb and 700mb shows that warm air advection, like subsidence, is important for causing the warming aloft. As seen in Figures 11 and 12 the progression of the 298K and 304K adiabats from west to east indicates that the initiation of the episode was associated with synoptic systems moving through or into the region.

Figures 34 to 37 are plots of the potential temperature at the surface, 300m, 600m, 900m, 1200m, 1500m, 3000m, and 4500m AGL for each of the four stations. At all the stations there is some cooling in the lowest 1500m of the atmosphere from the sixth to the ninth. During this time a cold 700mb trough passed over the region. The cooling of the air near the surface could be caused by the advection of cold air into the basin by winds above the top of the elevated terrain. The cold air in the basin cannot horizontally advect out of the area. Once warming near the top of the surrounding elevated terrain beings, the stability of the

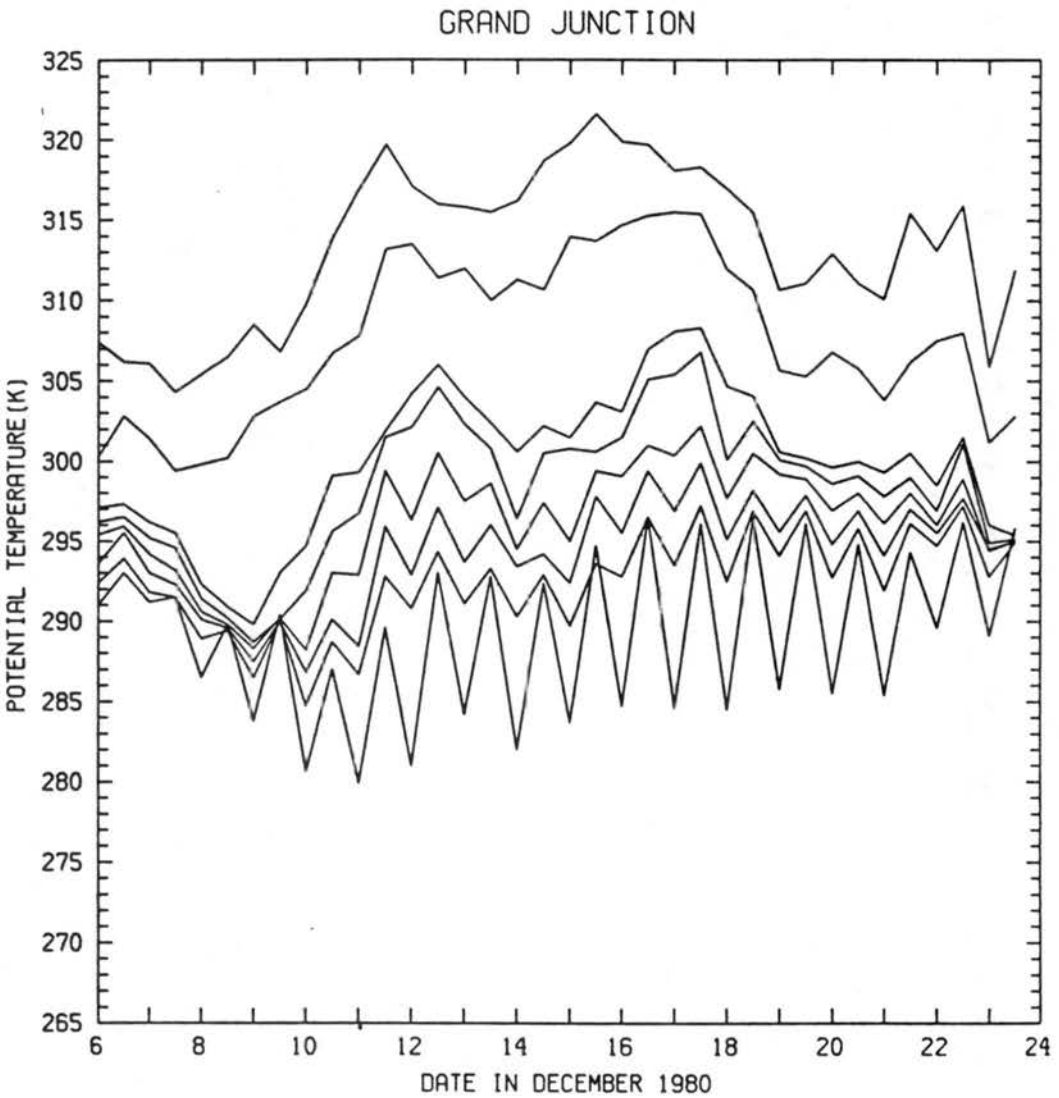

Figure 34. The potential temperature at the surface, 300m AGL, 600m AGL, 900m AGL, 1200m AGL, 1500m AGL, 3000m AGL, and 4500m AGL (from bottom to top) from December 6-23, 1980 at Grand Junction.

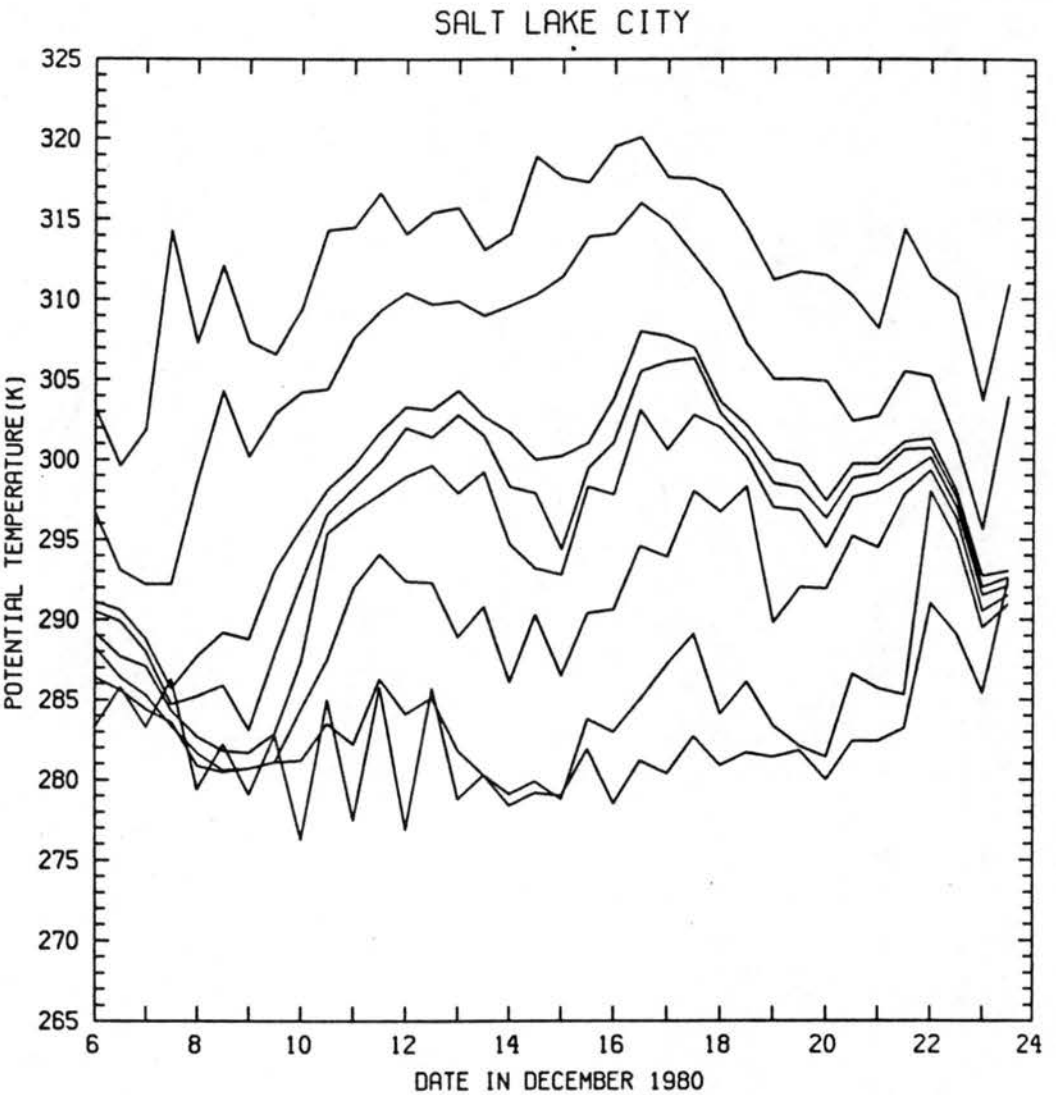

Figure 35. Same as Figure 34 but for Salt Lake City.

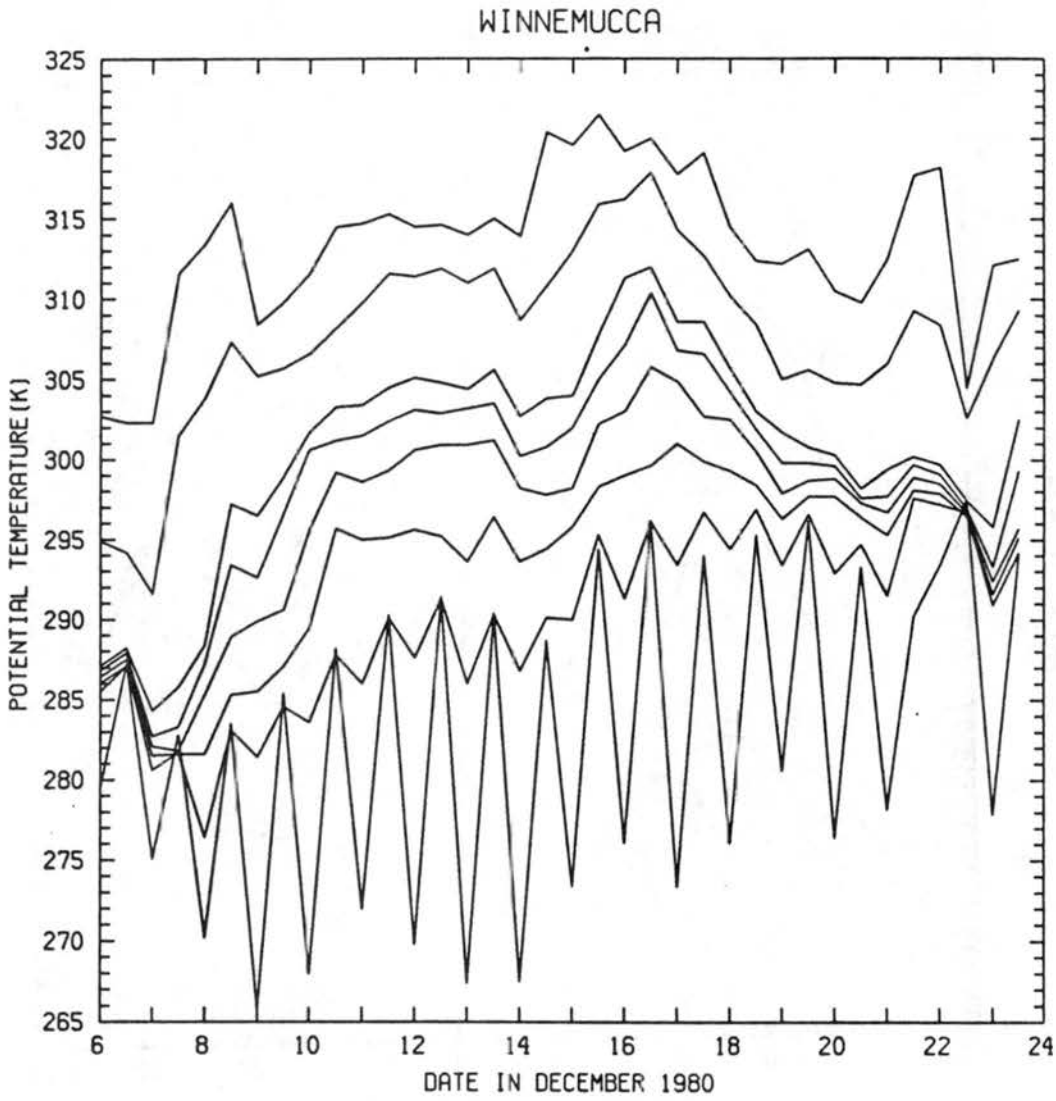

Figure 36. Same as Figure 34 but for Winnemucca.

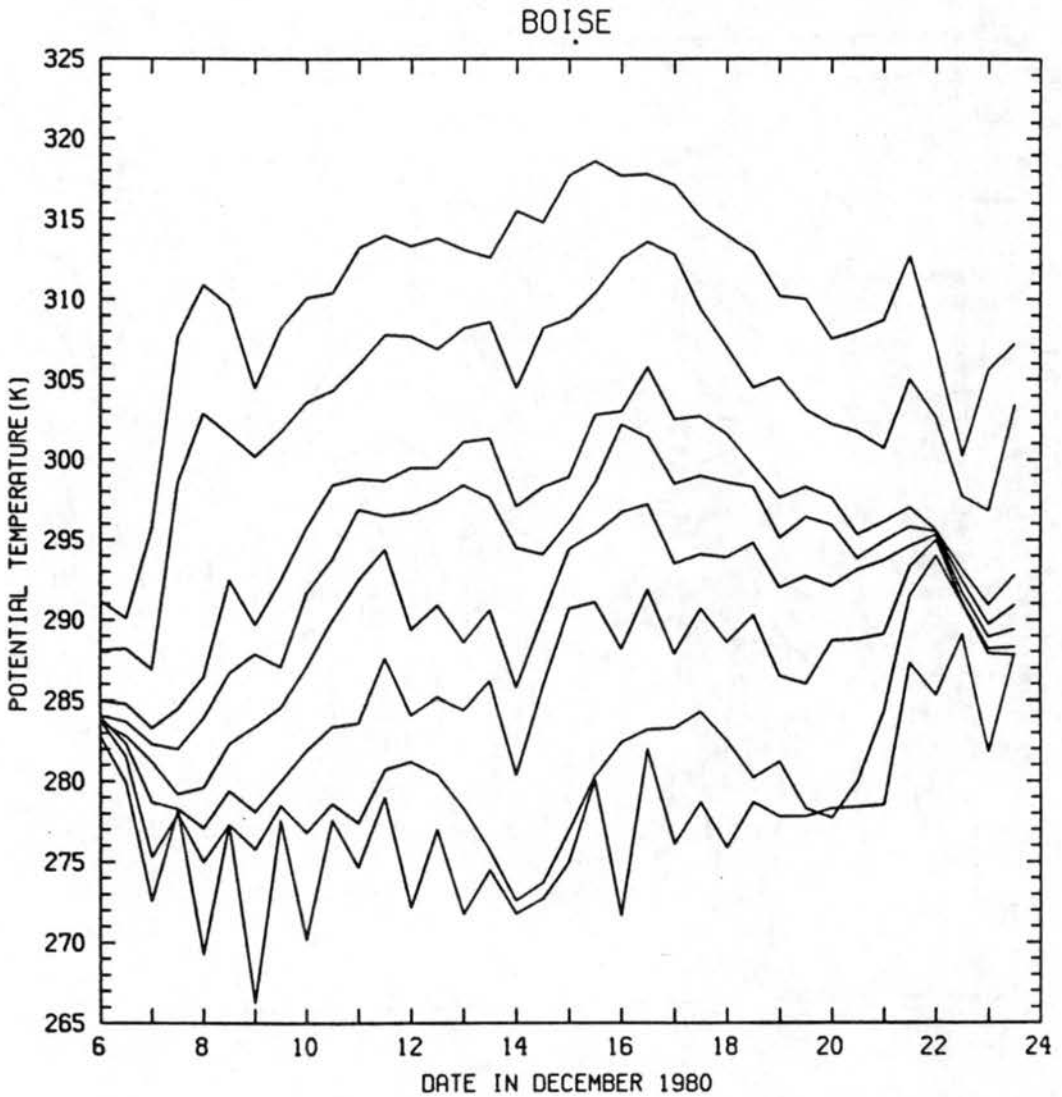

Figure 37. Same as Figure 34 but for Boise.

air increases. Since the cold, stable air needs strong winds to rise over the surrounding elevated terrain or to mix out of the basin, the cold air can easily become trapped in the basin. Cold air near the surface increases the stability of the atmosphere and would increase the intensity of the deep stable layer.

Weak incoming solar radiation or surface heating appears to be very important for the initiation of the deep stable layer episode. The analysis showed no clear relationship of snowcover or cloudcover to the CCBL height. The climatology, however, showed that most of the deep stable layers occurred during the months with weak incoming solar radiation. Moderate or strong surface heating can cause the daytime CBL to mix through a significant portion of the descending stable layer greatly weakening it. With weak surface heating the daytime CBL cannot mix through a significant portion of the descending stable layer, and the resulting small diabatic heating near the surface will allow for the continued existence of cold air near the surface.

The analysis of the potential influence of longwave induced heating or cooling on the episode indicated that the effects are significant only when fog is present. A deep, persistent fog layer was not observed at any of the stations during the initiation phase of the episode. As indicated in the studies of high inversion fog, the deep fog often forms several days after the stagnation begins. The influences of longwave cooling are not important to the initiation of the episode, but the longwave cooling may be important to the formation of fog which can result in strengthening of the episode.

C. Continuation Phase

The continuation phase of the deep stable layer episode is associated with the existence of a deep stable layer which does not greatly strengthen or weaken. The time versus height plots showed that this portion of the episode is accompanied by the continuous presence of a capping stable layer. On the fourteenth and fifteenth a disturbance moving over the region was able to temporarily weaken the deep stable layer at the four stations but was not able to destroy it. The EEVM analysis showed that the effective rising motion from the disturbance had the same magnitude as the sinking motion in the initiation phase, but the duration was shorter. Another factor which may have aided in preventing the disturbance from terminating the episode is that warming aloft which immediately followed the passage of the disturbance strengthened the deep stable layer.

In the continuation phase of the episode there cannot be significant surface heating by solar radiation. As stated in the initiation phase section, strong incoming solar radiation can lead to large surface heating that can form a daytime CBL that can mix through the descending stable layer. In the continuation phase strong surface heating can mix through the capping stable layer terminating the episode. The surface heating analysis suggests that the amount of clouds or the presence of snowcover are secondary effects throughout the episode. Fog, however, can be very important to surface heating by greatly reducing the intensity of the incoming solar radiation reaching the surface.

Longwave radiation can have a more important role in the continuation phase than the initiation phase. A brief summarization of

the results of the longwave radiation calculations shows that cool, moist air beneath warm, dry air will not cause significantly increased IR induced cooling near the surface. A fog layer can cause significant longwave cooling near the surface which could increase the strength of the deep stable layer. A cloud layer which is warmer than the fog layer can lead to longwave heating of the fog layer. This could cause the fog layer to temporarily dissipate and weaken the deep stable layer. Beside the longwave heating decreasing the stability of the deep stable layer, with the absence of a fog layer the intensity of solar radiation reaching the surface will be larger and can cause increased surface heating. Elevated moist layers can only have a minor influence on the IR heating rates near the surface.

These calculations show that when fog is present there can be significant longwave induced heating or cooling in the fog layer. As previously indicated, the cooling near the surface can strengthen the deep stable layer while the IR induced warming can weaken the deep stable layer. The IR calculations of the cloud above the fogless surface indicate that the cloud layer will cause little additional warming of the air near the surface. If the IR induced heating is able to dissipate the fog layer, it is highly unlikely that the cloud layer can cause additional IR warming resulting in the further weakening of the episode.

D. Termination Phase

The termination phase is associated with processes which cause the destruction of a deep stable layer episode. There are two different scenarios for destruction. One is with the presence of a persistent fog

layer which occurred at Salt Lake City and Boise. The other scenario is without a fog layer and it occurred at Grand Junction and Winnemucca.

In the case without fog cooling occurs above the deep stable layer. This cooling may be caused by synoptic-scale cold air advection or rising motion. It is accompanied by the breaking down of the warm ridge aloft and a passage of a disturbance over the region. The time versus height plots of potential temperature show an apparent lifting of the capping stable layer associated with the cooling aloft. With the significant reduction in stability in the lowest 1.5km of the atmosphere, the air near the surface can likely become coupled with the synoptic-scale atmosphere. With the weak stability the daytime CBL can easily grow to great depths. The EEVM values are generally $1.0 cms^{-1}$ to $2.5 cms^{-1}$ which are common values for synoptic-scale rising motion.

The case with persistent fog has synoptic-scale cooling above the deep stable layer at the start of the termination phase. The cooling is able to weaken the deep stable layer, but unlike the case without fog, the cooling was not able to end the episode. The high albedo of the fog layer may help prolong the episode by preventing significant heating of the surface by shortwave radiation. The longwave properties of fog may also be very important for preventing the destruction of the episode. The significant longwave cooling of the fog layer may have allowed for a stronger deep stable layer so the disturbance, while being able to terminate the episode if fog was not present, may not have been sufficiently strong to end the episode. The fog layer can also provide a cooling region in the lower atmosphere that can help maintain the deep stable layer despite the weakening of the warm ridge aloft. The termination of the deep stable layer with fog had a rapid destruction of

the fog layer with significant warming near the surface. The termination is associated with warming aloft and is probably accompanied by synoptic-scale rising motion.

CHAPTER VI

CONCLUSIONS

Deep stable layers are fairly common occurrences at Grand Junction, Salt Lake City, Winnemucca, and Boise which are stations in the intermountain region in the western United States. They occur most commonly in December and January with episodes of three days or longer happening at least once every two years at Salt Lake City and Winnemucca and at least once every year at Grand Junction and Boise. An analysis of mixing volumes for the month of December from 1976 to 1980 showed that all the deep stable layer days had low mixing volumes. Deep stable layers are one group of days which cause low mixing volumes at stations in the intermountain region of the western United States. Since they are associated with low mixing volumes and can have episodes of three days or longer occur at least once every two years, deep stable layers are important for regional air quality in the intermountain region.

A deep stable layer episode which happened in December 1980 was examined in-depth. Using this case study a conceptual model of a life cycle of a deep stable layer episode was formulated. The deep stable layer episode was divided into three phases: the initiation phase, the continuation phase, and the termination phase. The initiation phase of the episode was synoptically dominated. It was associated with a warm ridge aloft building into the area and was accompanied by a descending layer of rapid warming which may be due to synoptic-scale horizontal

warm air advection or synoptic-scale subsidence. About 24 to 48 hours after the descending warming layer appeared at 5000m it reached 0.5km to 1.5km forming a stable layer which acted as a cap isolating the air near the surface from the free air above it. Throughout the initiation phase cold air remained in the basin. Without strong winds the cold air cannot mix out of the basin or rise over the surrounding elevated terrain. Weak surface heating prevented the daytime CBL from being able to mix through the descending stable layer and to warm the air in the basin. Because of the absence of persistent fog in this phase of the episode, longwave cooling was not an important physical process for this phase of the episode.

The continuation phase of the deep stable layer episode was accompanied by changes in the deep stable layer strength which did not lead to the termination of the episode. Synoptic-scale influences in this phase were less noticeable than the initiation phase because the synoptic situation did not drastically change. Weak incoming solar radiation prevents the development of a daytime CBL which can mix through the capping stable layer. The longwave radiation effects are more important in the continuation phase than in the initiation phase. Fog layers can cause significant longwave cooling near the surface which can stregnthen the deep stable layer. Cloud layers warmer than fog layers can cause longwave induced warming in the fog layer and a temporary dissipation of the fog layer. Another important consequence of the fog layer is to reduce the diabatic heating of the air near the surface because of its high albedo.

The termination phase of the episode was synoptically dominated. The destruction of the warm ridge aloft and the movement of disturbances

over the region accompanied the termination of the episode. In cases without fog surface heating can aid in the termination of the episode by being able to form a CBL which assists in the destruction of the capping stable layer. A significantly stronger disturbance was needed to destroy the deep stable layer when a layer of persistent fog was present. The fog layer can help prolong the episode by hampering surface heating, by causing a stronger deep stable layer, or by providing a cooling mechanism near the surface which can help maintain the stability of the lower atmosphere.

REFERENCES

Bader, D. C. and T. B. McKee, 1985: Effects of Shear, Stability, and Valley Characteristics on the Destruction of Temperature Inversions. Journal of Climate and Applied Meteorology, 24, pp. 822-832.

Boettger, C. M., 1961: Air Pollution Potential East of the Rocky Mountains: Fall 1959. Bulletin of the American Meteorological Society, 42, pp. 615-620.

Cox, S. K. and K. T. Griffith, 1979: Estimates of Radiative Divergence During Phase III of the GARP Atlantic Tropical Experiment: Part I, Methodology. Journal of Atmopsheric Sciences, 36, pp. 576-585.

Fukuta, N. M., H. S. Chang, J. L. Sutherland, and D. A. Griffith, 1984: Comparative Airborne Tests of Vapor-Activated Methaldehyde and Silver Iodide Particles in Supercooled Stratus Clouds. Preceedings of the Ninth Weather Conference on Weather Modification, May 21-23, 1984, pp. 6-7.

Garland, J. A., 1971: Some Fog Droplet Size Distributions Obtained by an Impaction Method. Quarterly Journal of the Royal Meteorological Society, 97, pp. 483-494.

Hanson, K. R. and T. B. McKee, 1983: Potential for Regional Air Pollution Episodes in Colorado. Atmospheric Science Paper No. 375. Department of Atmospheric Science, Colorado State University, Fort Collins, CO, 51 p.

Holets, S. and R. N. Swanson, 1981: High-Inversion Fog Episodes in Central California. Journal of Applied Meteorology, 20, pp. 890-899.

Holton, J. R., 1979: An Introduction to Dynamic Meteorology, second edition, Academic Press, 391 p.

Holzworth, G. C., 1962: A Study of Air Pollution Potential for the Western United States. Journal of Applied Meteorology, 1, pp. 366-382.

Holzworth, G. C., 1967: Mixing Depths, Wind Speeds, and Air Pollution Potential for Selected Locations in the United States. Journal of Applied Meteorology, 6, pp. 1039-1044.

Holzworth, G. C. and R. W. Fisher, 1979: Climatological Summaries of the Lower Few Kilometers of Rawinsonde Observations. EPA-600-/4-79-026. Enviromental Sciences Research Laboratory, Research Triangle Park, NC, p. 141.

Hosler, C. E., 1961: Low-Level Inversion Frequency in the Contiguous United States. Monthly Weather Review, 89, pp. 319-339.

Lockhart, W. M., 1943: A Winter Fog in the Interior. Chapter II in Characteristic Weather Phenomena of California (by H. R. Byers). Massachusetts Institute of Technology Meteorological Papers, Vol. 1, No. 2, Cambridge, MA, pp. 11-20.

McClatchey, R. A., R. W. Fenn, S. E. A. Selby, F. E. Volz, and V. S. Garing, 1972: Optical Properties of the Atmosphere, third edition. Environmental Research Paper No. 411, Air Force Cambridge Research Laboratories, Bedford, MA, 108 p.

National Oceanic and Atmsopheric Administration, 1981: Local Climatological Data for Grand Junction, Annual Summary. NCDC, Asheville, NC.

National Weather Service, 1968: Manual for Radiosonde Coding, third edition. United States Printing Office, Washington, D.C.

Niemeyer, L. E., 1960: Forecasting Air Pollution Potential. Monthly Weather Review, 88, pp. 88-96.

Orgill, M. M., 1971: A Planning Guide for Future Studies. PNL-3656, Pacific Northwest Laboratory, Richland WA, ASCOT/80/4.

Panofsky, H. A. and J. A. Dutton, 1984: Atmospheric Turbulence. John Wiley and Sons, Inc., 397 p.

Parish, T. R., 1982: Barrier Winds Along the Sierra Nevada Mountains. Journal of Applied Meteorology, 21, pp. 925-930.

Pruppacher, H. R. and J. D. Klett, 1980: Microphysics of Clouds and Precipitation, D. Reidel Publishing Company, 714 p.

Rauber, R. M., 1985: Physical Structure of Nothern Colorado River Basin Cloud Systems. Atmospheric Science Paper No. 390, Department of Atmospheric Science, Colorado State University, Fort Collins, CO, 360 p.

Wallace, J. M. and P. V. Hobbs, 1977: Atmospheric Science An Introductory Survey, Academic Press, 467 p.

Willett, H. C., 1928: Fog and Haze, Their Cases, Distribution, and Forecasting. Monthly Weather Review, 56, pp. 435-468.

Yu, C. and R. A. Pielke, 1985: Mesoscale Air Quality Under Stagnant Synoptic Cold Season Conditions in the Lake Powell Area. National Park Service, Department of the Interior, Denver, CO, 119 p.

APPENDIX A

WEATHER MAPS FOR THE DEEP STABLE LAYER EPISODE

In this appendix the National Weather Service surface, 700mb, and 500mb weather maps from December 6 to December 23, 1980 will be listed. For the surface chart the interval at which the isobars is plotted is 4mb. For the 700mb maps the contour interval is 30m and for the 500mb map the contour interval is 60m.

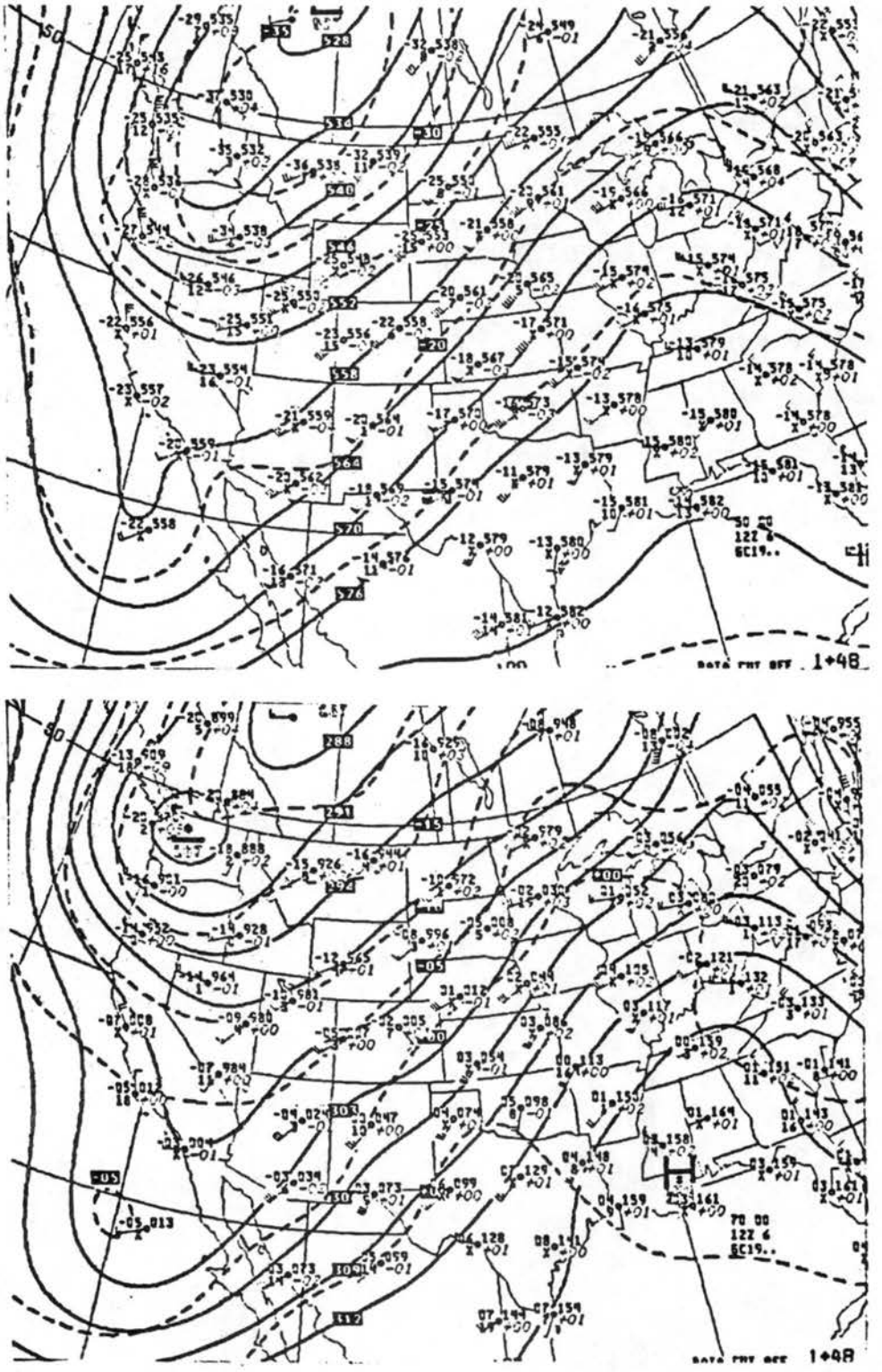

Figure A1. The 500mb (top) and 700mb (bottom) National Weather Service maps for 12Z December 6, 1980.

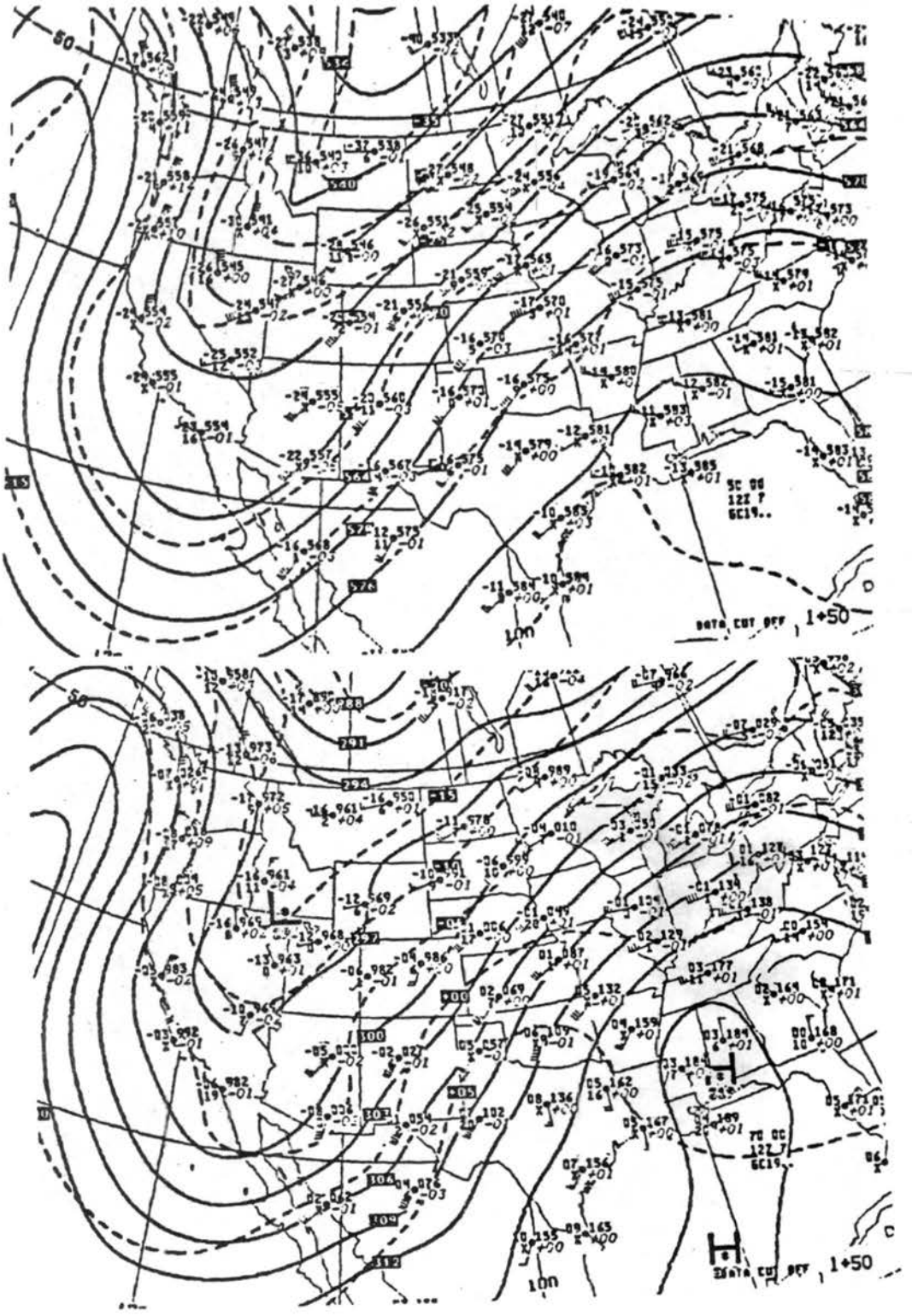

Figure A2. The 500mb (top) and 700mb (bottom) National Weather Service maps for 12Z December 7, 1980.

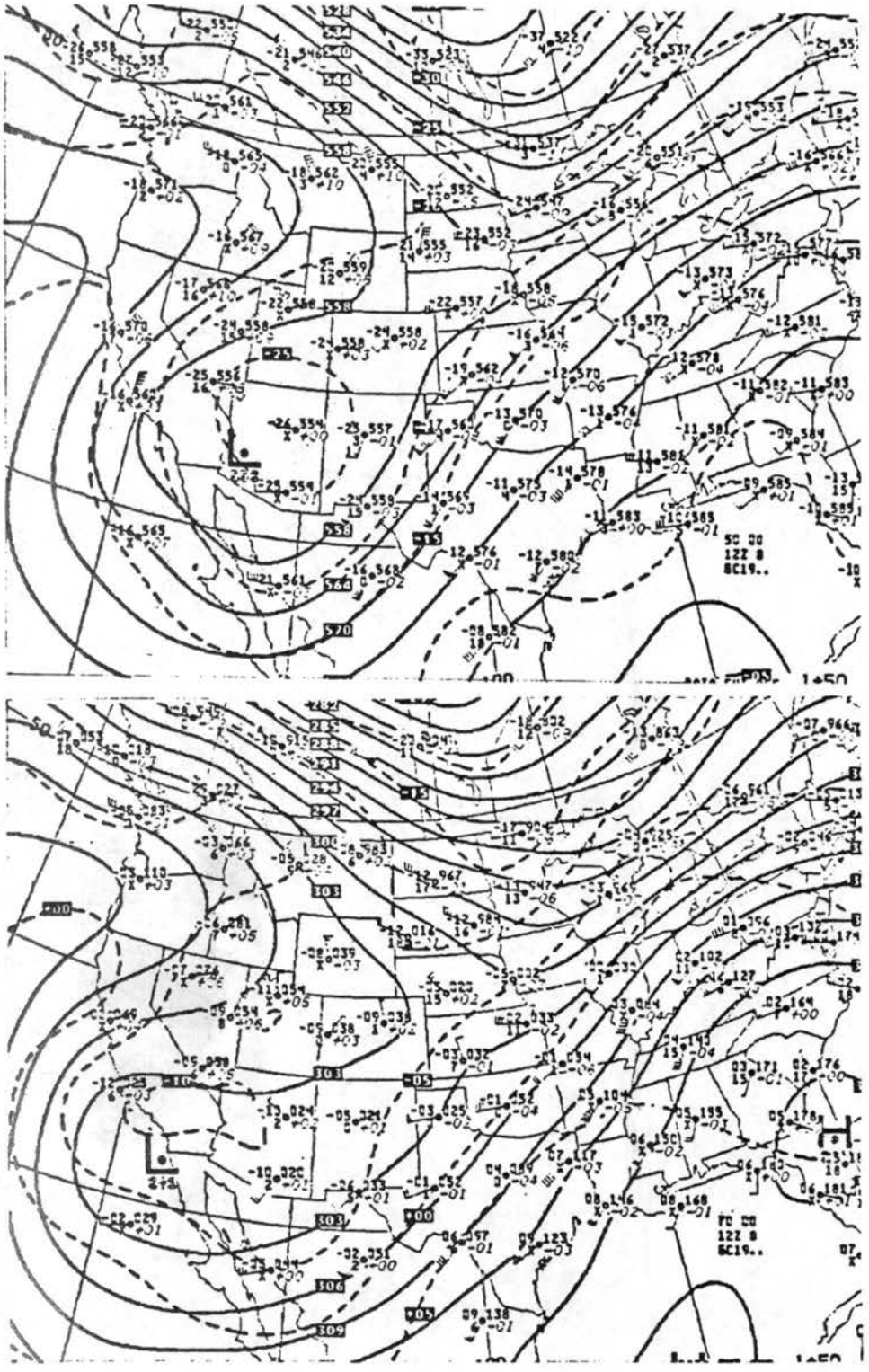

Figure A3. The 500mb (top) and 700mb (bottom) National Weather Service maps for 12Z December 8, 1980.

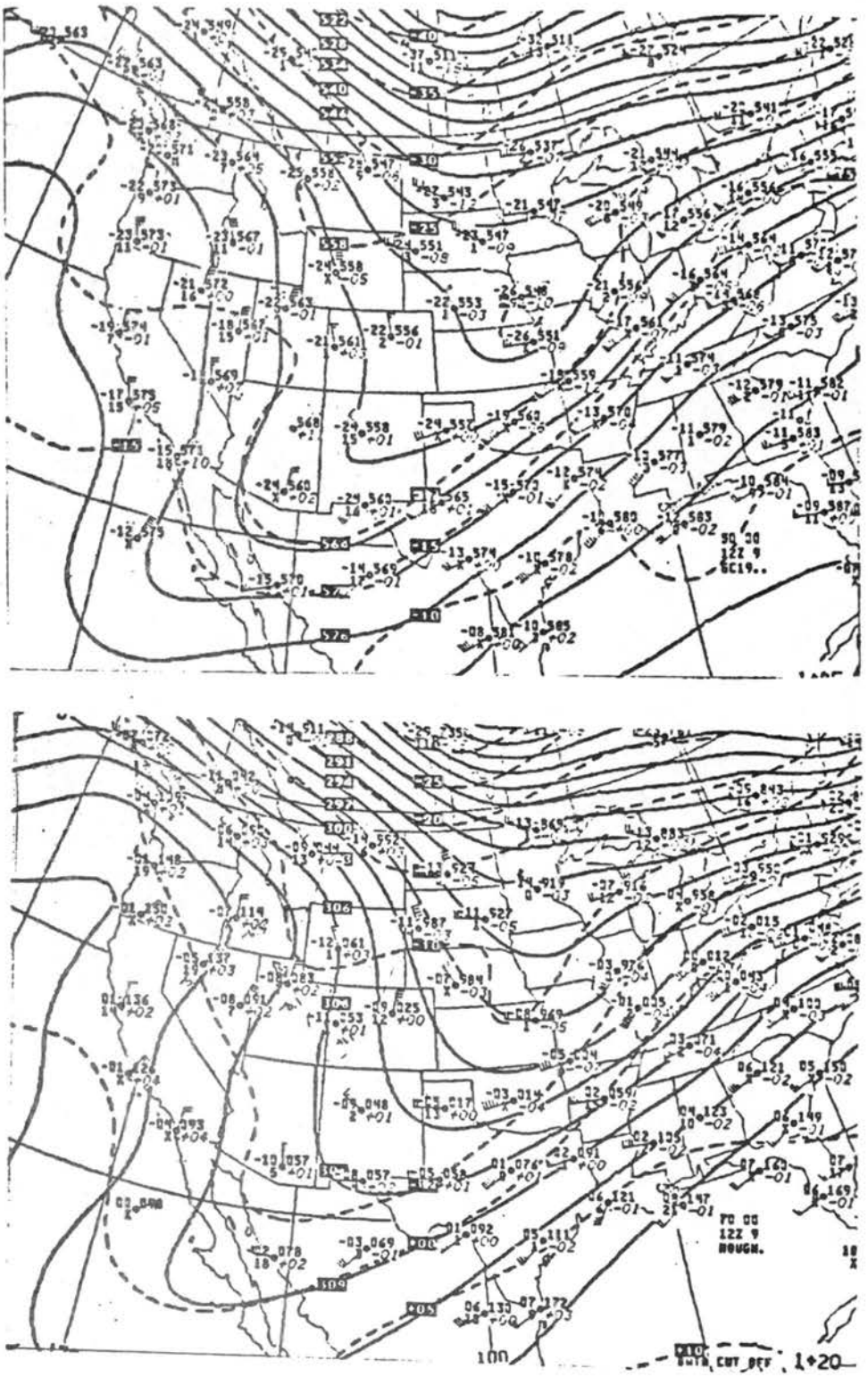

Figure A4. The 500mb (top) and 700mb (bottom) National Weather Service maps for 12Z December 9, 1980.

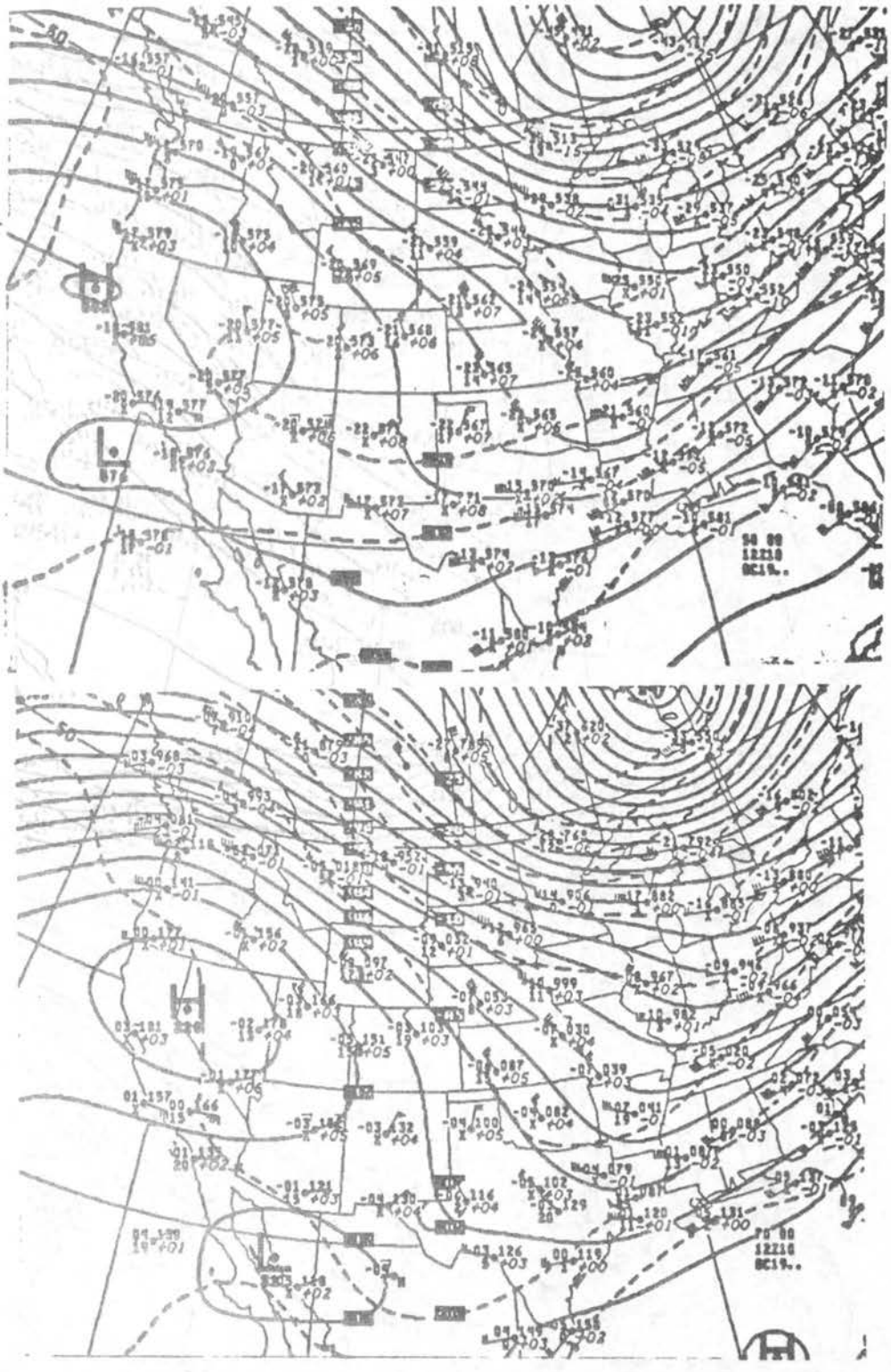

Figure A5. The 500mb (top) and 700mb (bottom) National Weather Service maps for 12Z December 10, 1980.

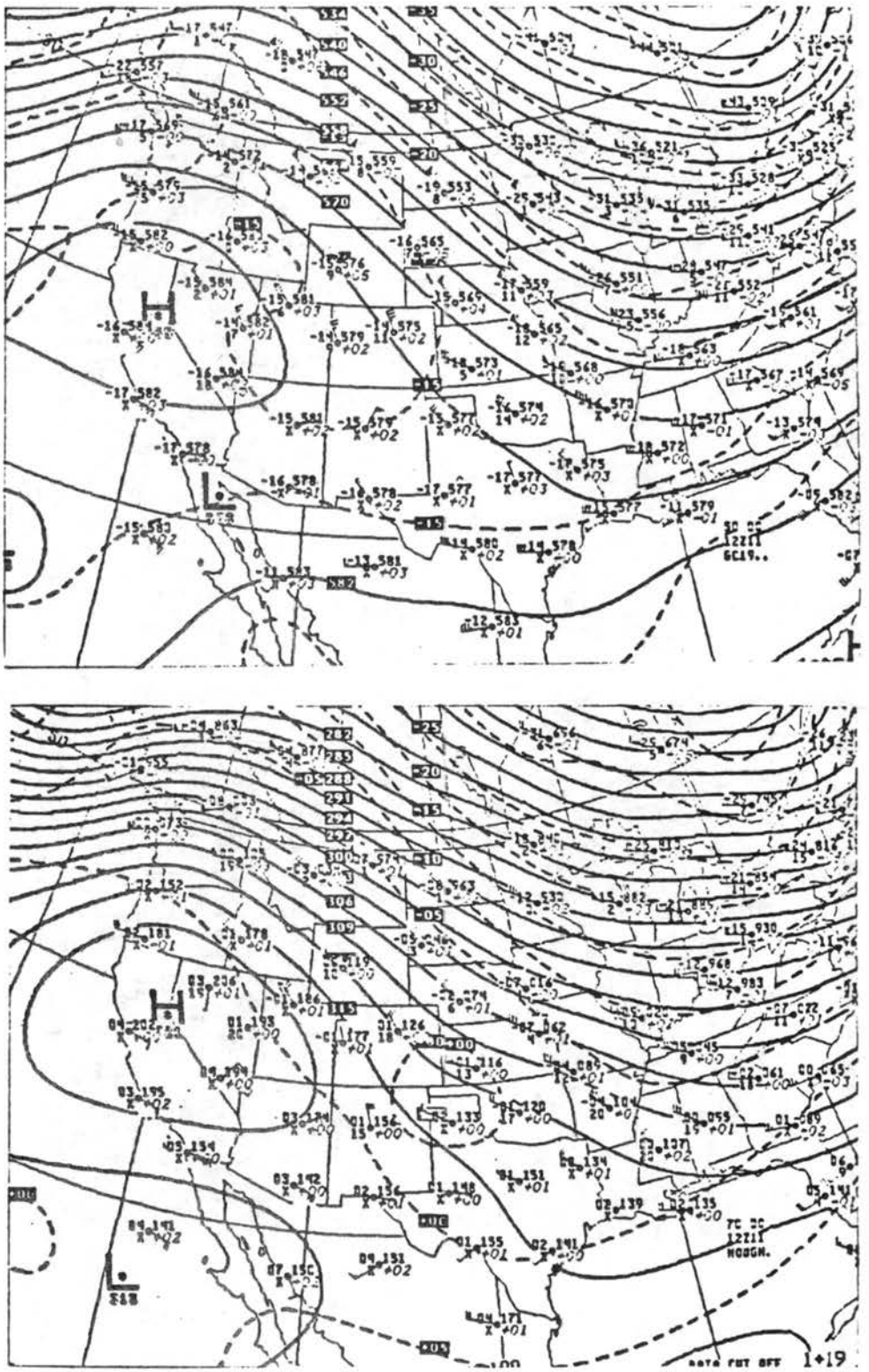

Figure A6. The 500mb (top) and 700mb (bottom) National Weather Service maps for 12Z December 11, 1980.

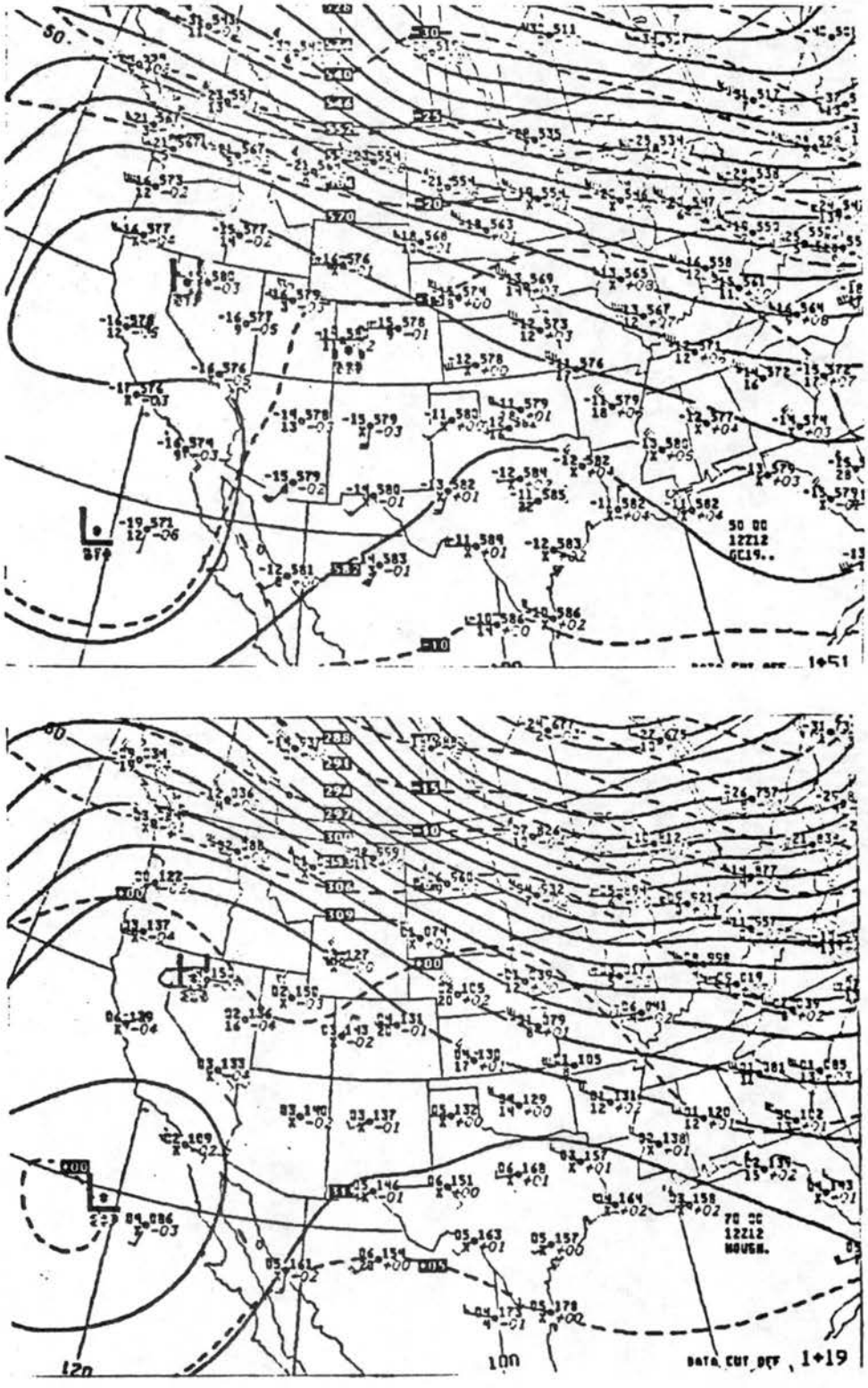

Figure A7. The 500mb (top) and 700mb (bottom) National Weather Service maps for 12Z December 12, 1980.

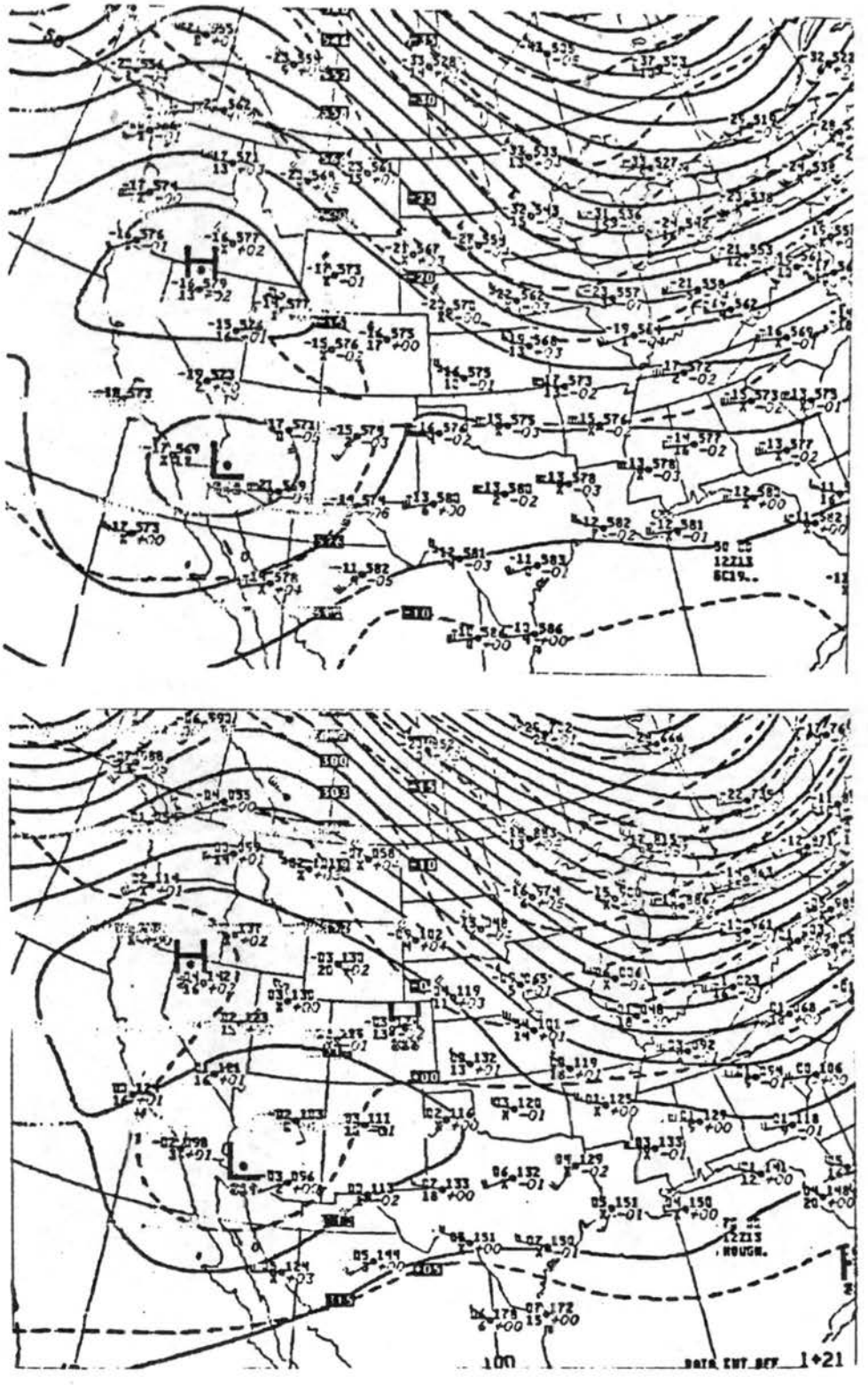

Figure A8. The 500mb (top) and 700mb (bottom) National Weather Service maps for 12Z December 13, 1980.

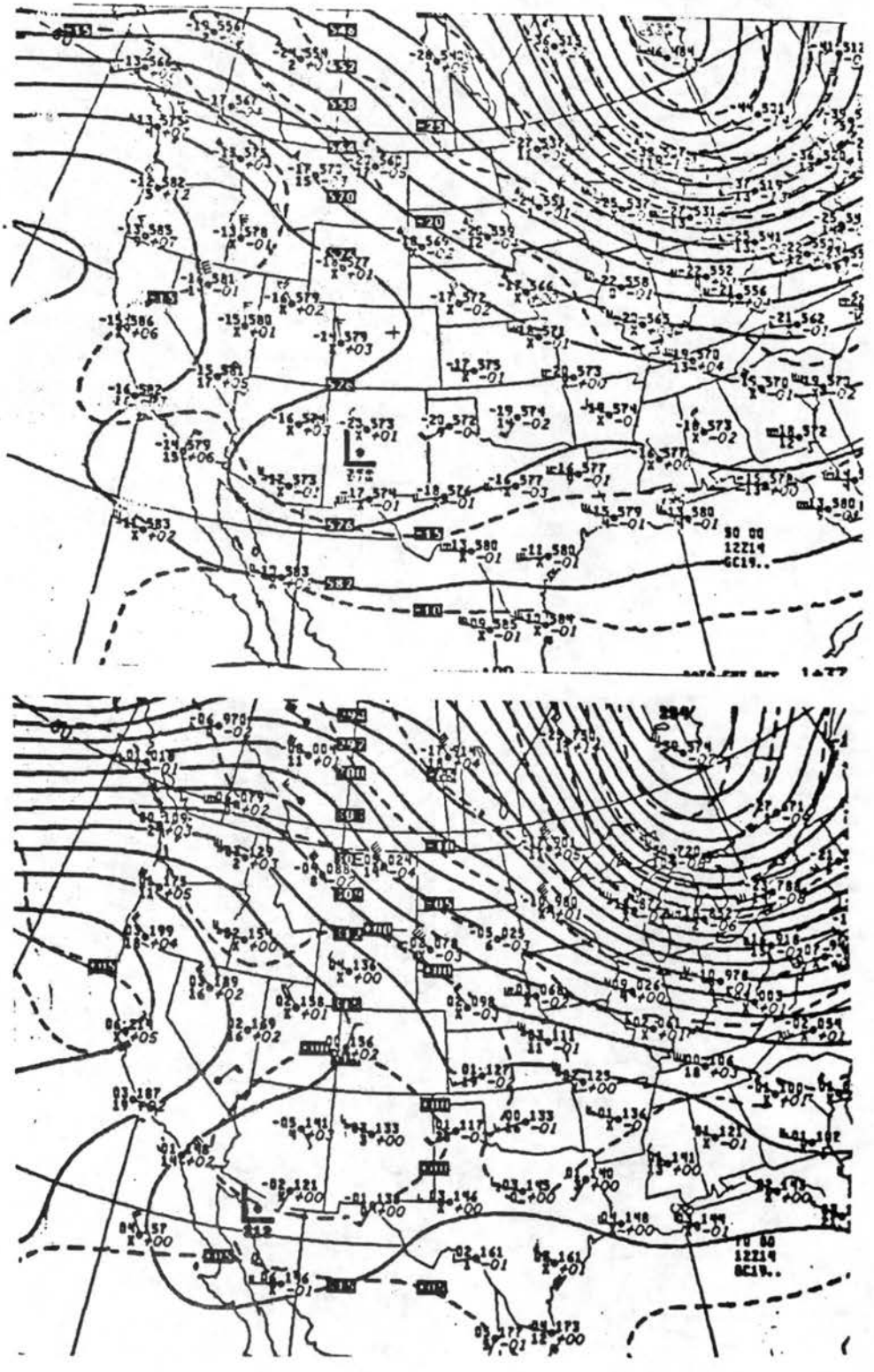

Figure A9. The 500mb (top) and 700mb (bottom) National Weather Service maps for 12Z December 14, 1980.

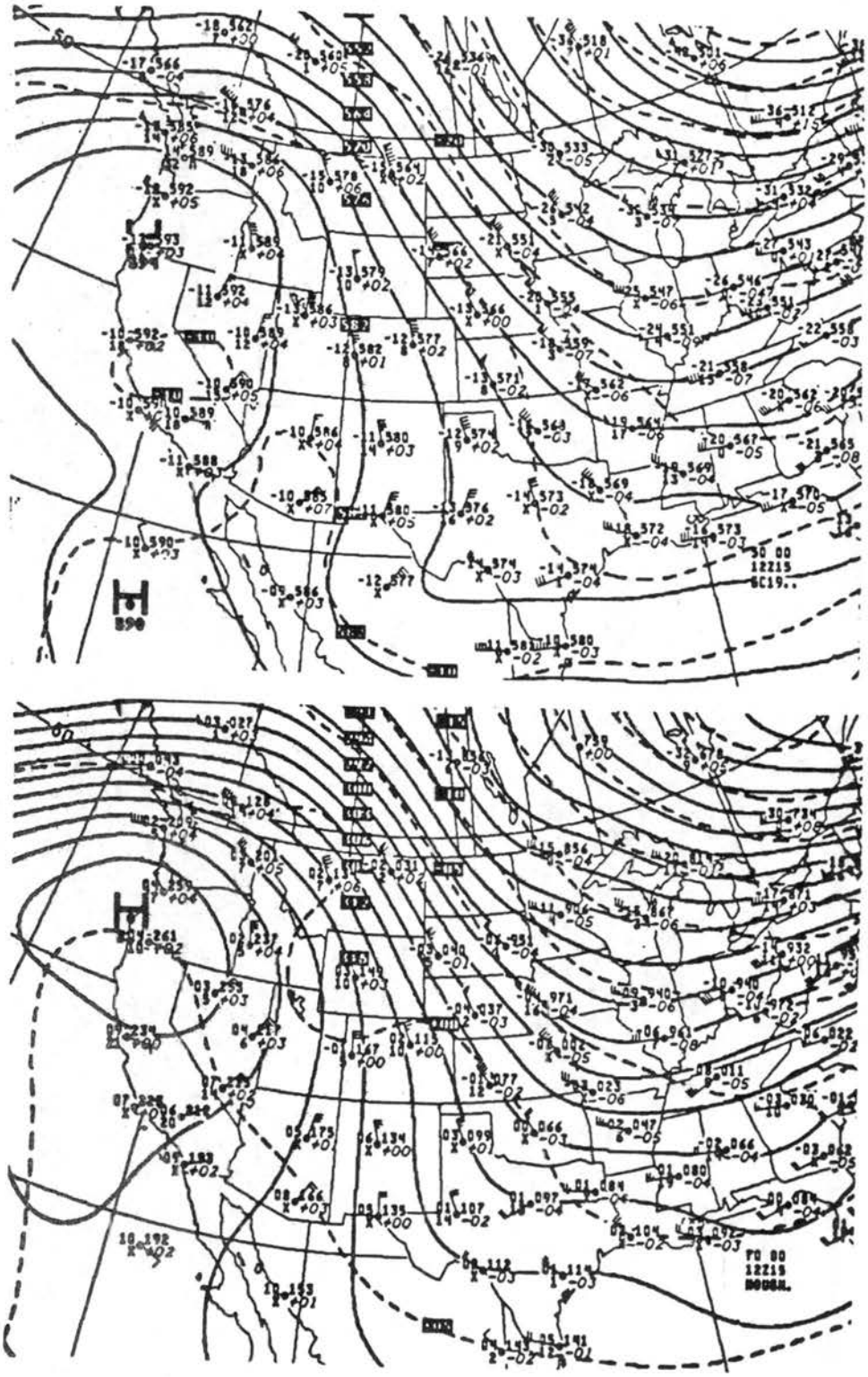

Figure A10. The 500mb (top) and 700mb (bottom) National Weather Service maps for 12Z December 15, 1980.

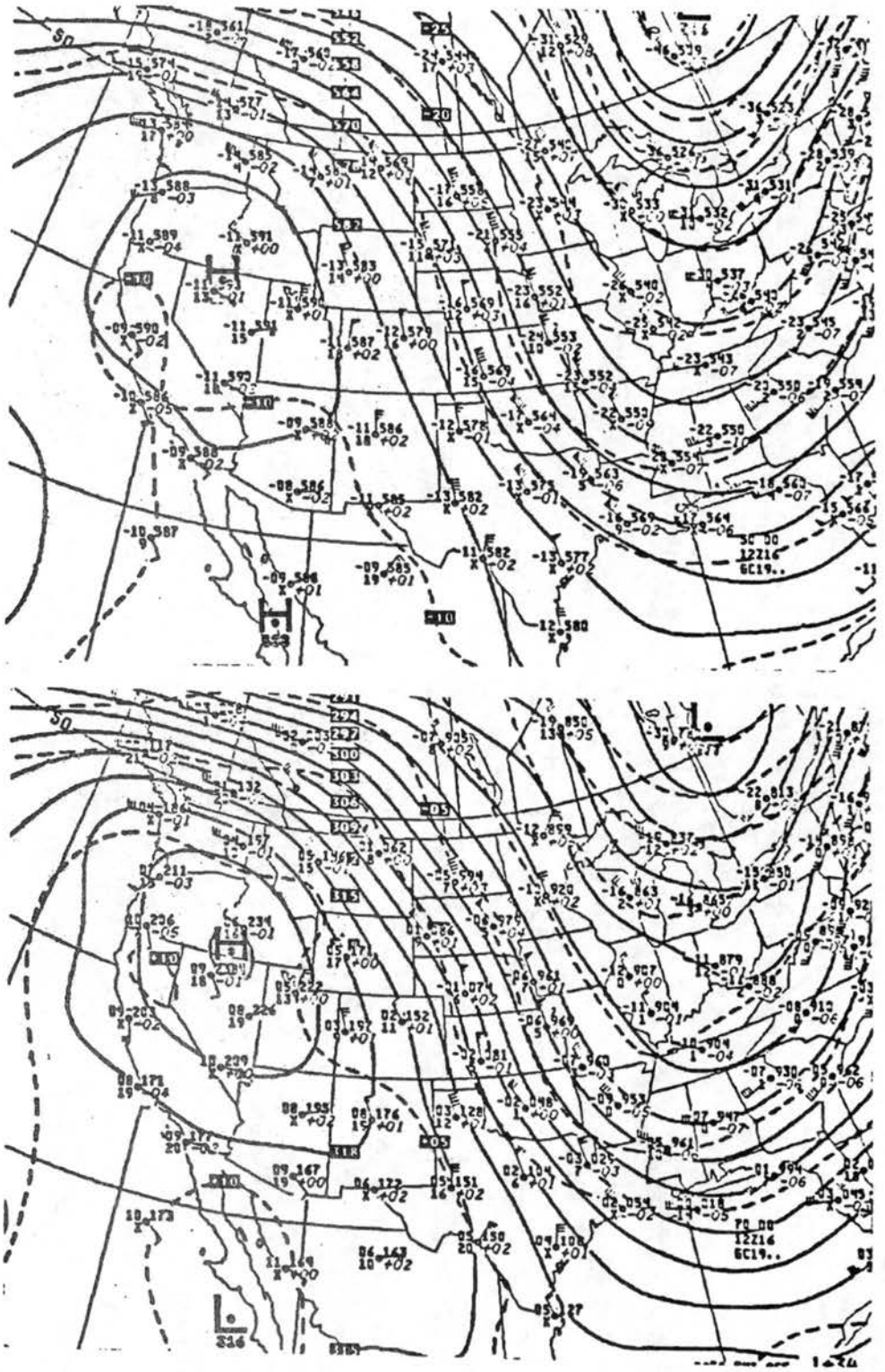

Figure A11. The 500mb (top) and 700mb (bottom) National Weather Service maps for 12Z December 16, 1980.

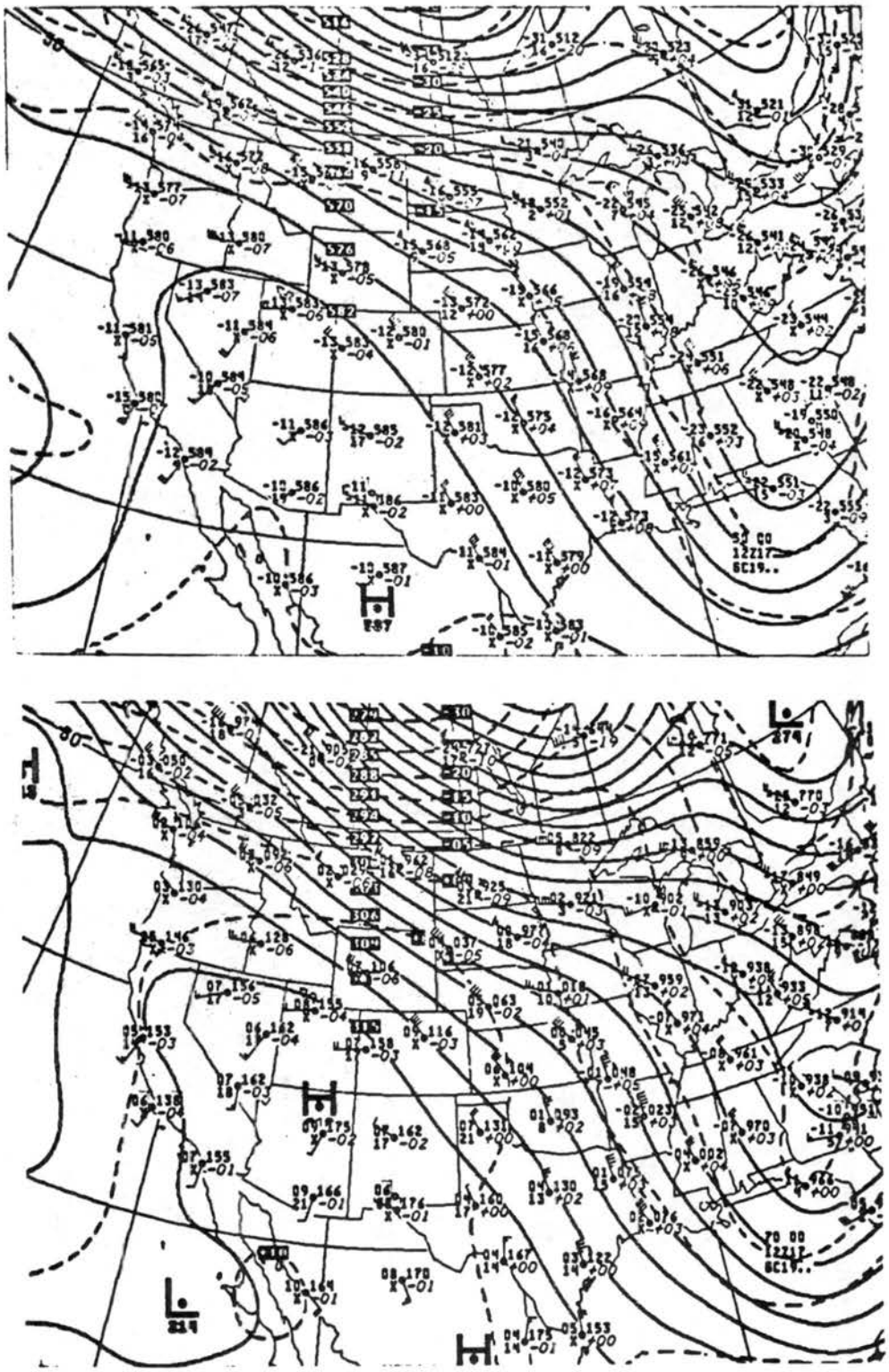

Figure A12. The 500mb (top) and 700mb (bottom) National Weather Service maps for 12Z December 17, 1980.

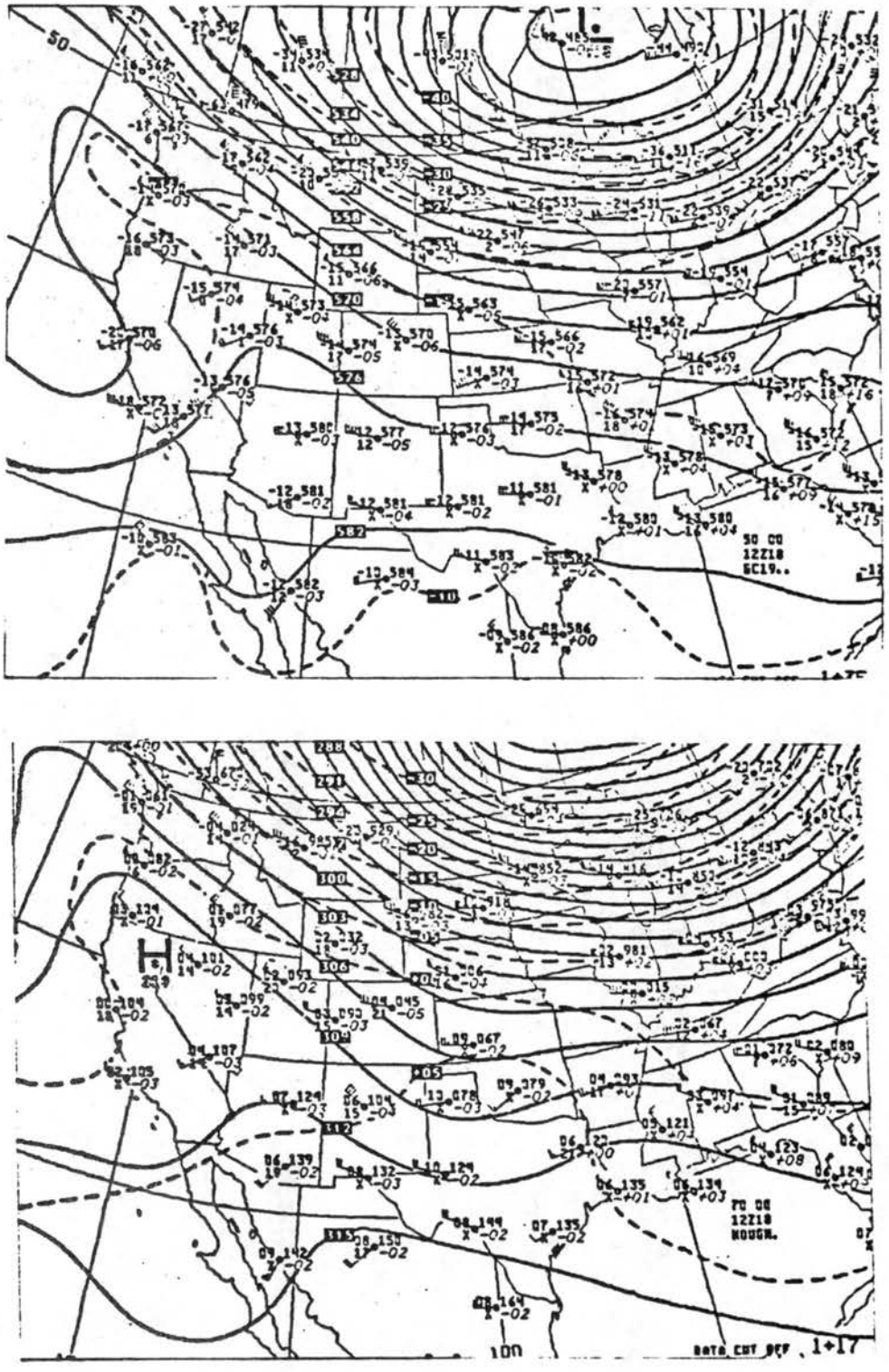

Figure A13. The 500mb (top) and 700mb (bottom) National Weather Service maps for 12Z December 18, 1980.

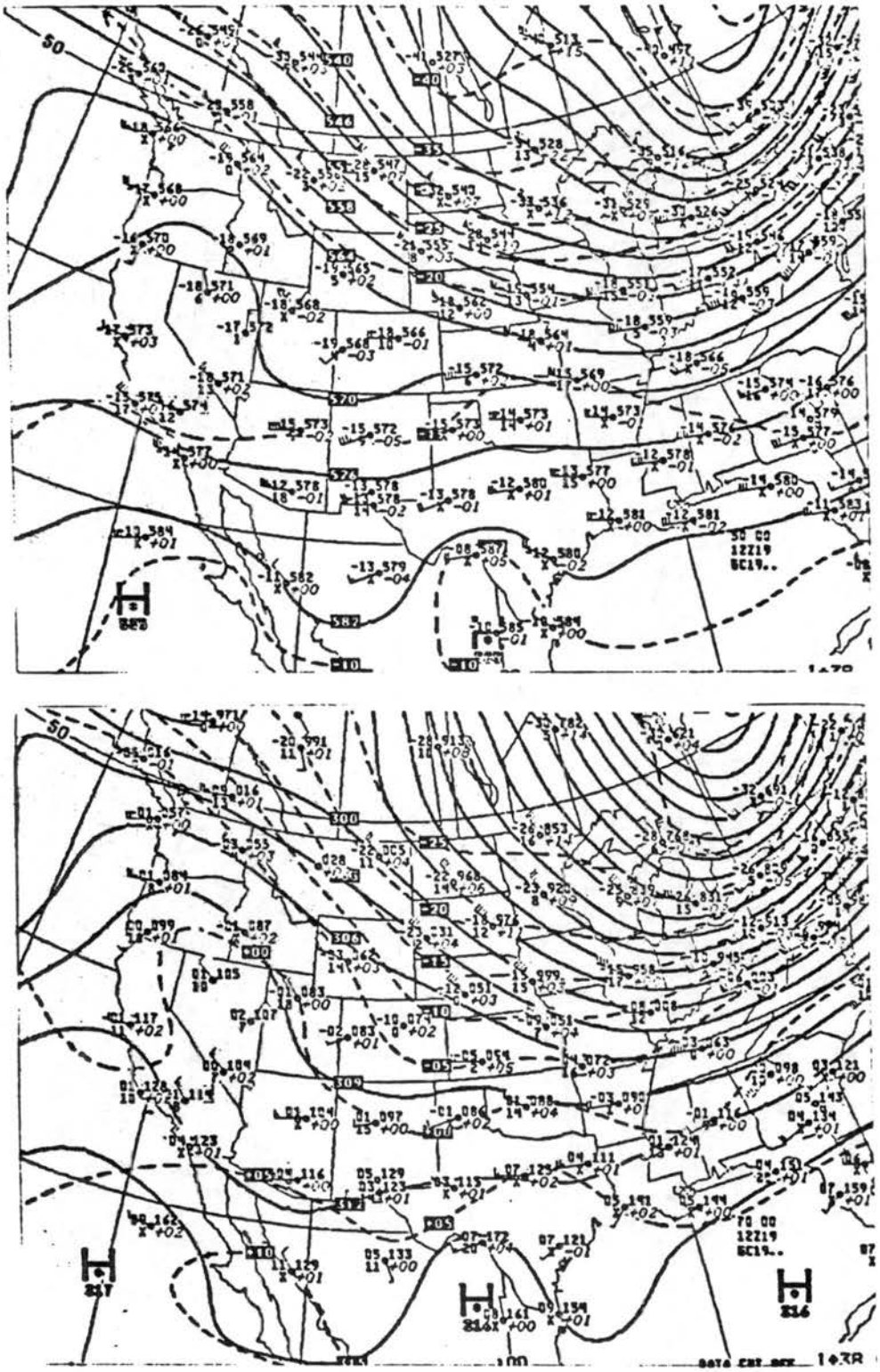

Figure A14. The 500mb (top) and 700mb (bottom) National Weather Service maps for 12Z December 19, 1980.

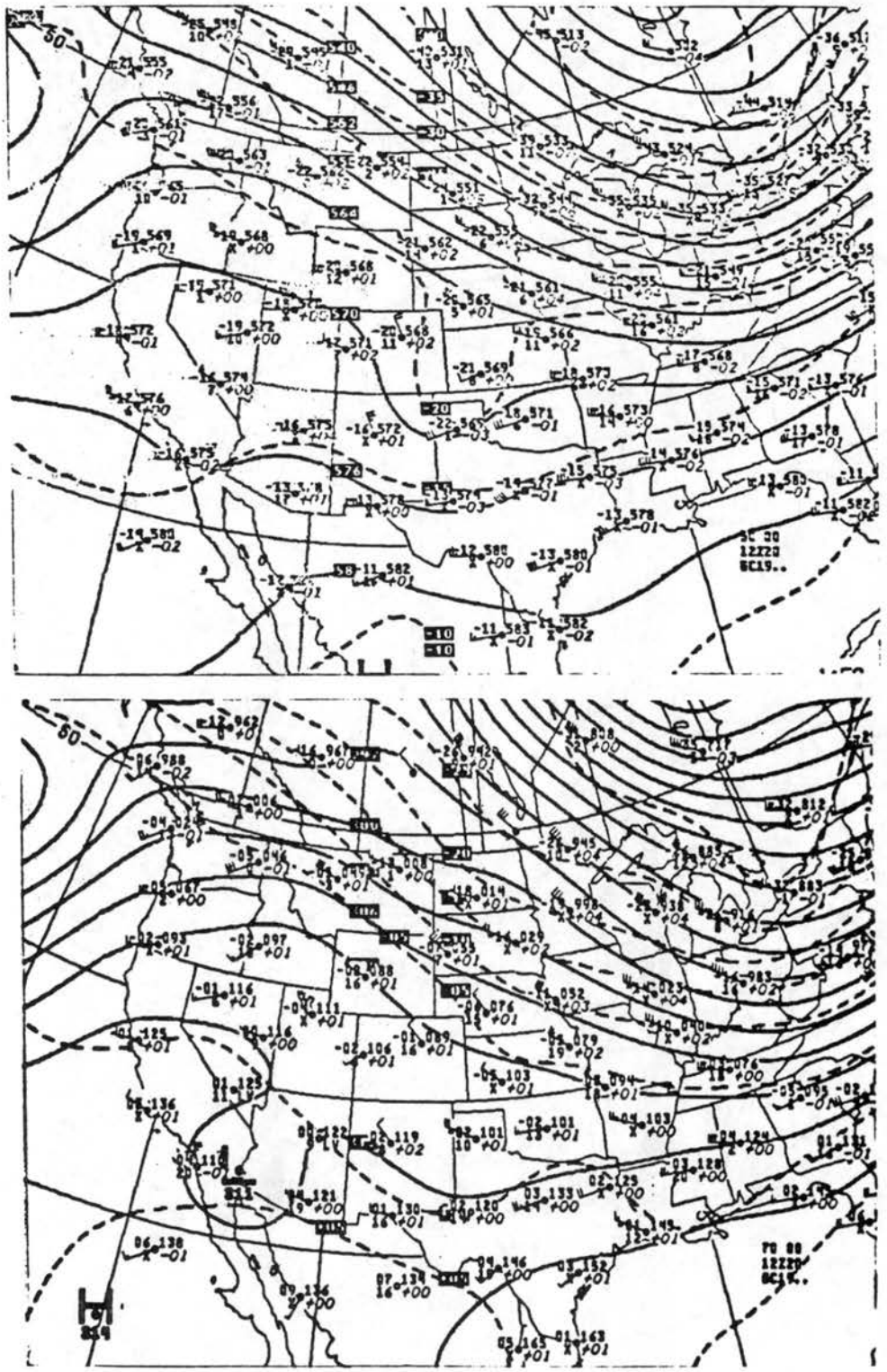

Figure A15. The 500mb (top) and 700mb (bottom) National Weather Service maps for 12Z December 20, 1980.

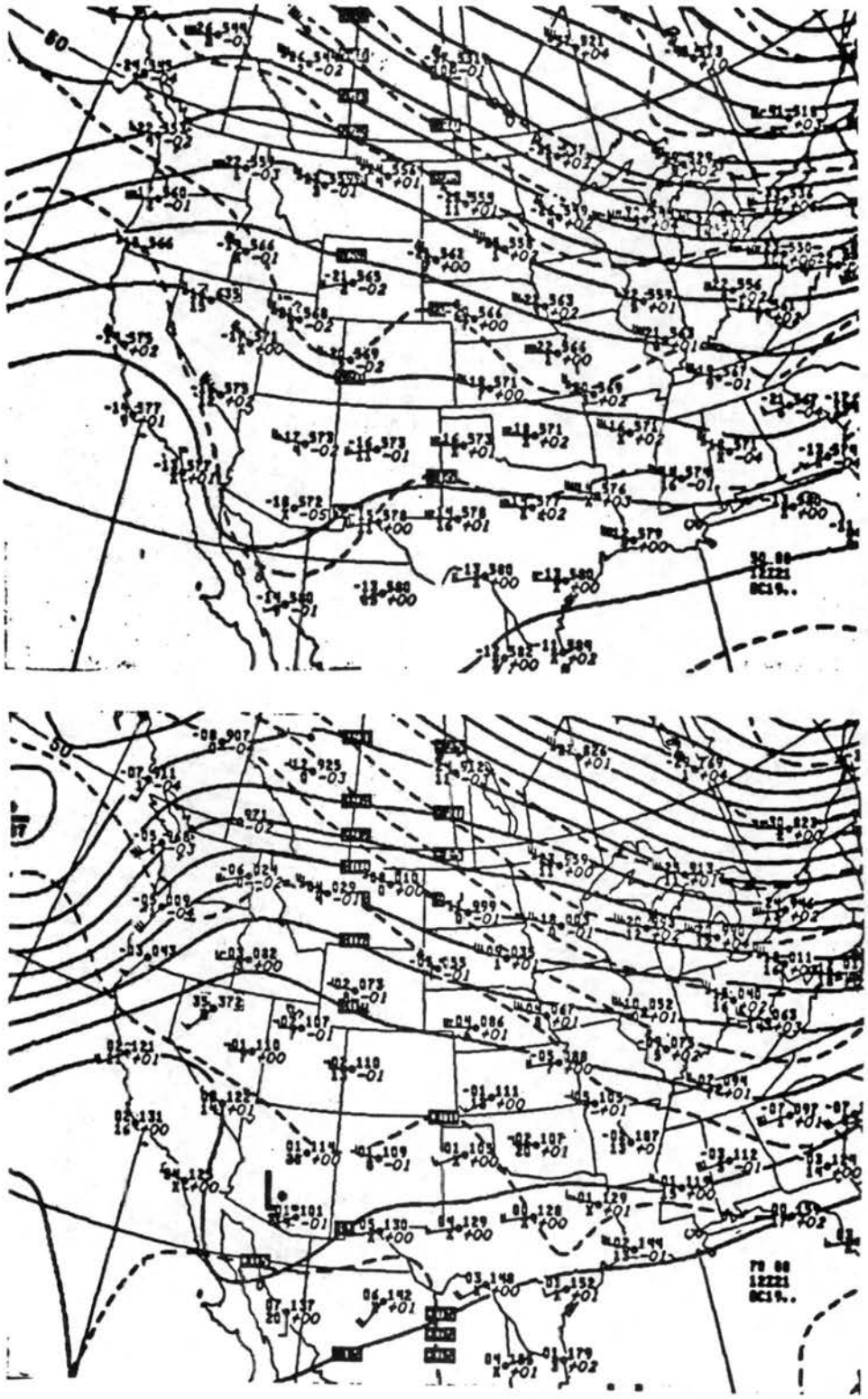

Figure A16. The 500mb (top) and 700mb (bottom) National Weather Service maps for 12Z December 21, 1980.

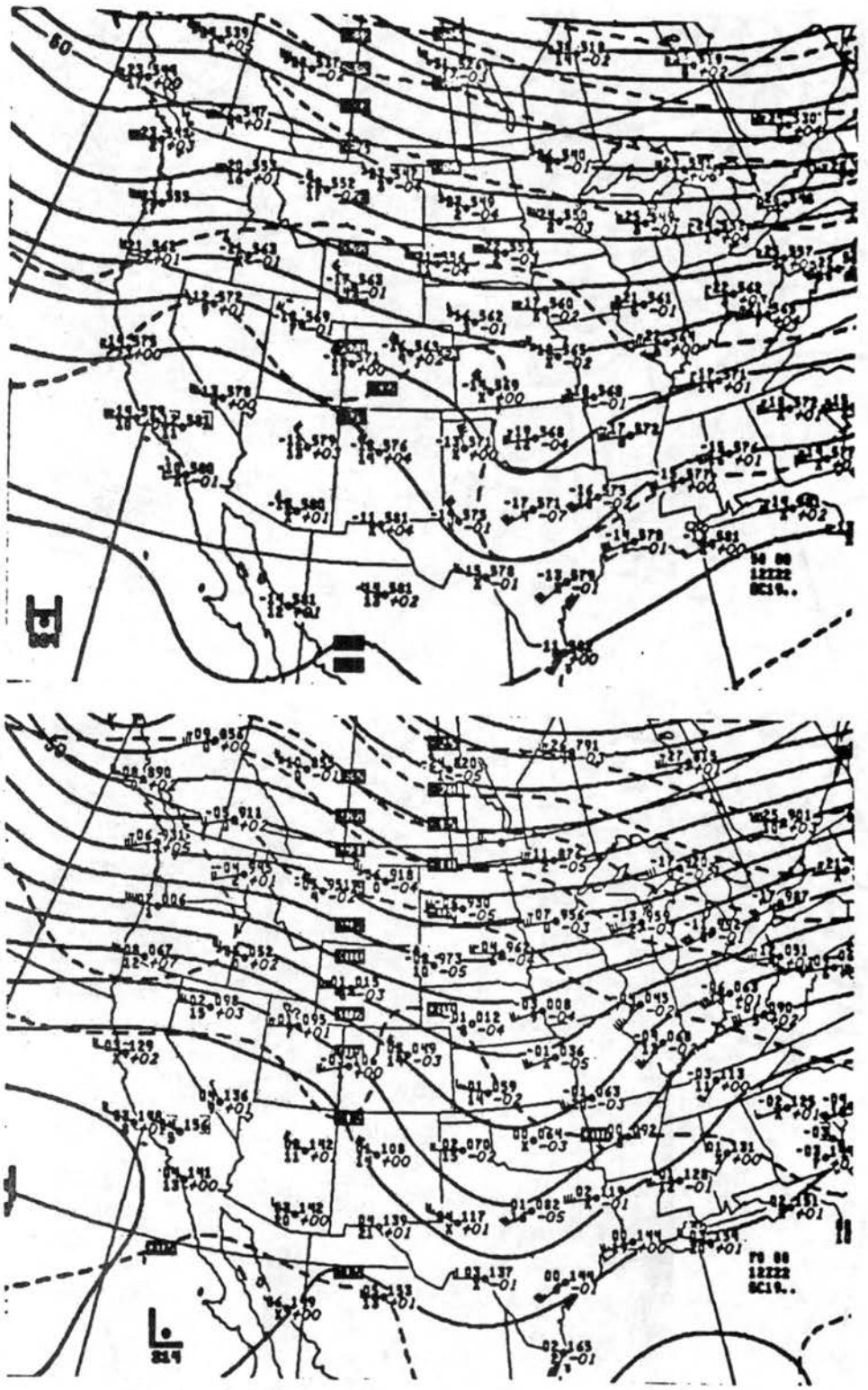

Figure A17. The 500mb (top) and 700mb (bottom) National Weather Service maps for 12Z December 22, 1980.

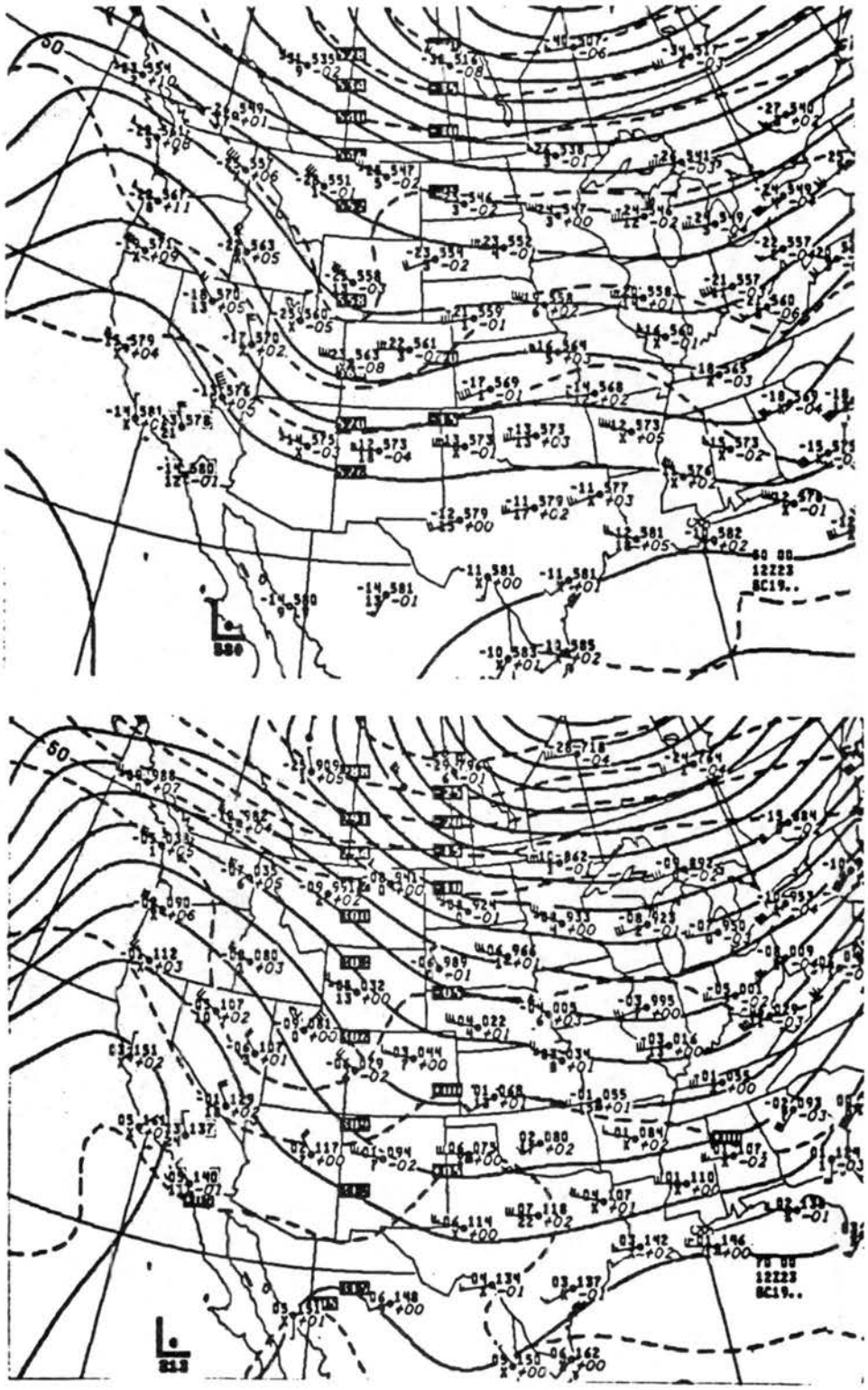

Figure A18. The 500mb (top) and 700mb (bottom) National Weather Service maps for 12Z December 23, 1980.

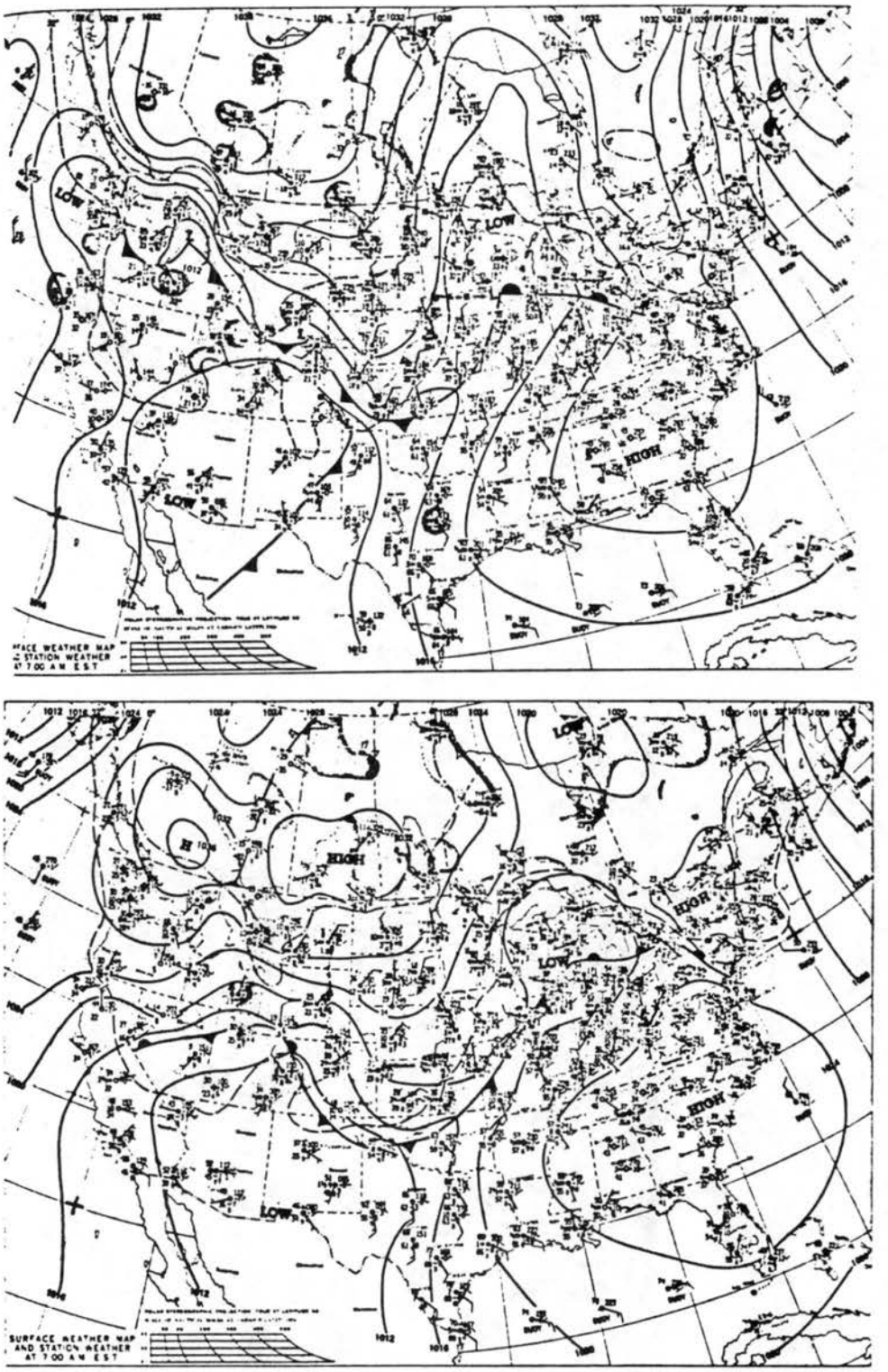

Figure A19. The surface weather map for 12Z December 6 (top) and 12Z December 7, 1980 (bottom) from the Daily Weather Maps Series.

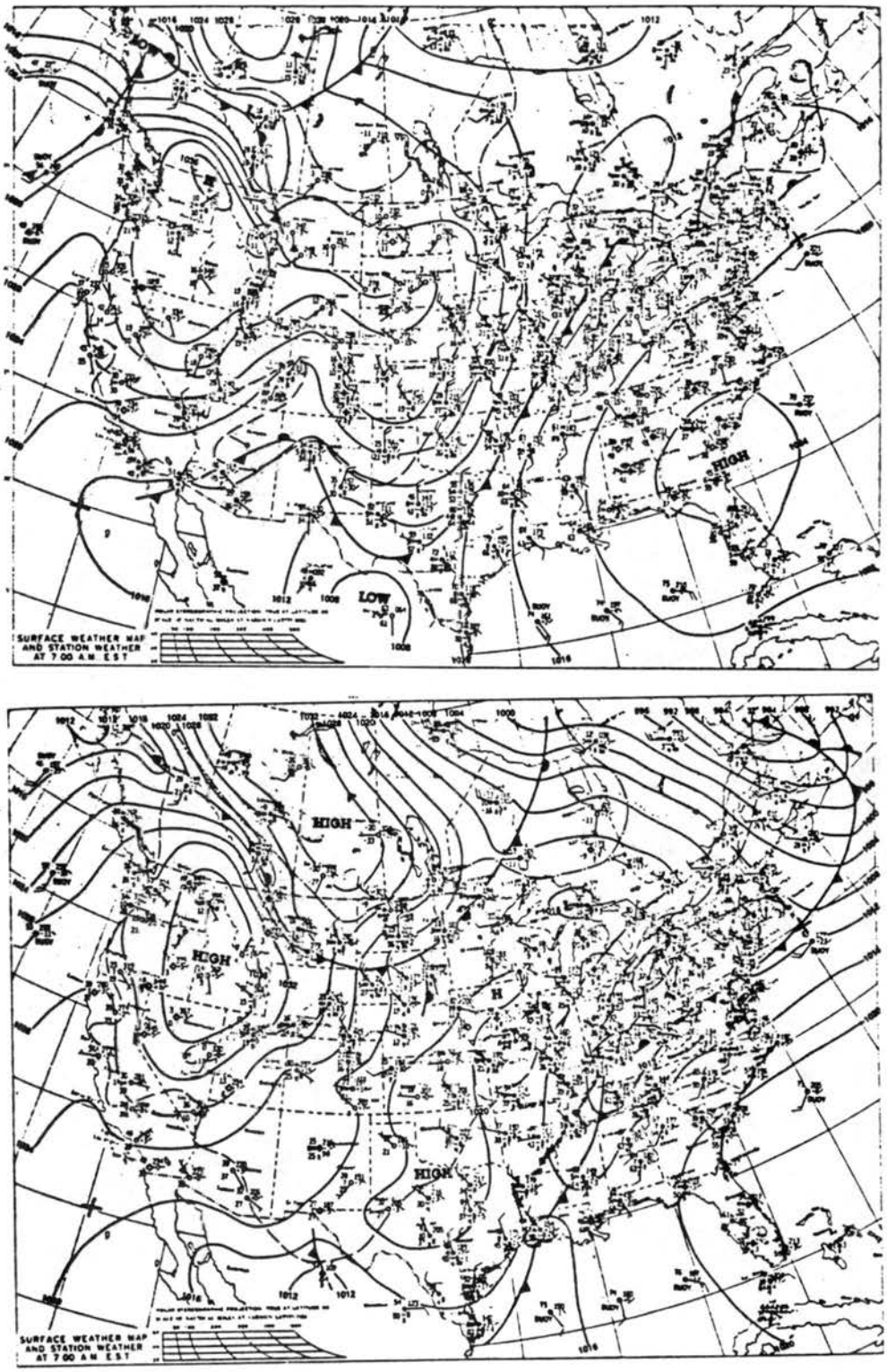

Figure A20. The surface weather map for 12Z December 8 (top) and 12Z December 9, 1980 (bottom) from the Daily Weather Maps Series.

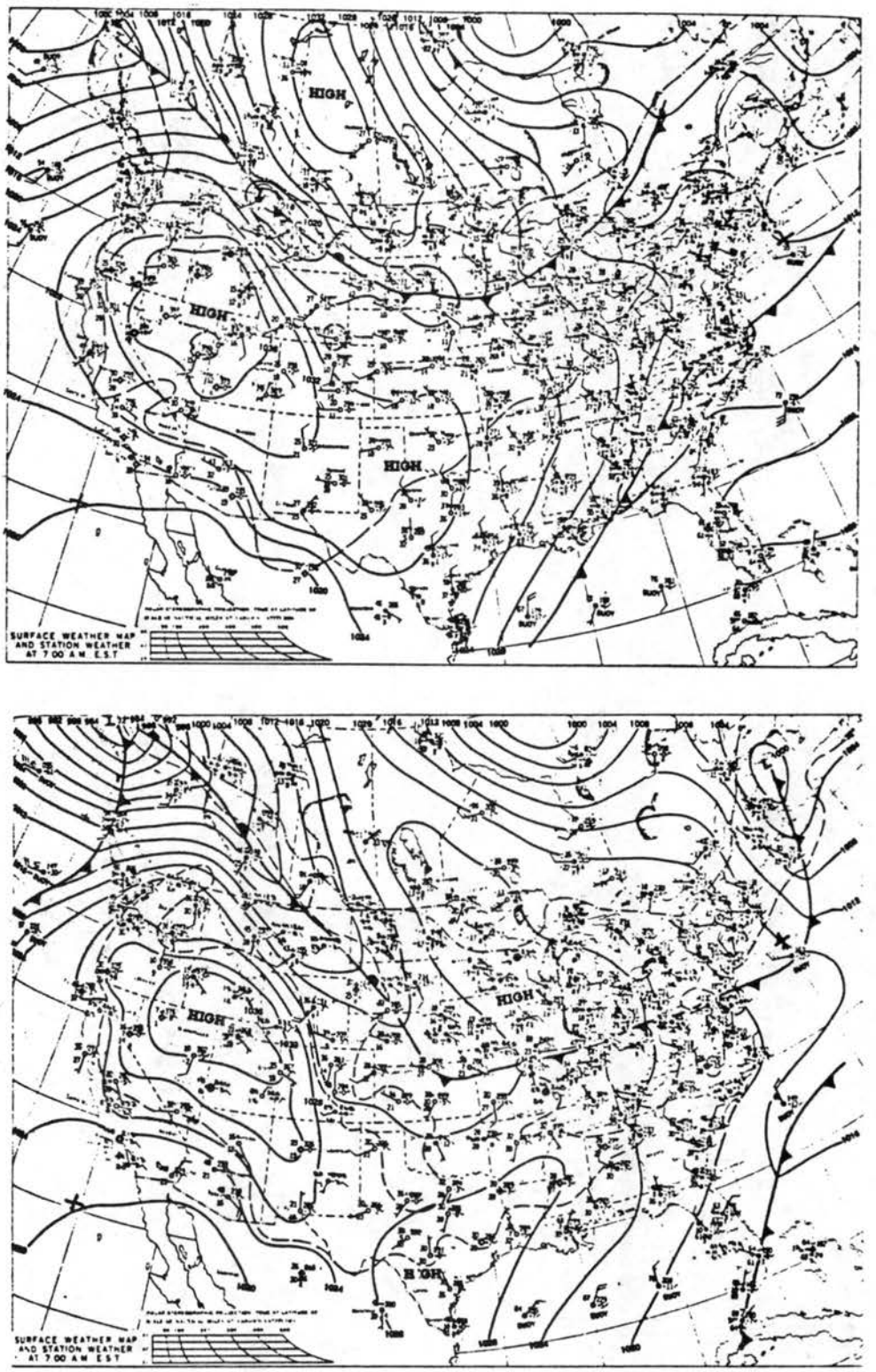

Figure A21. The surface weather map for 12Z December 10 (top) and 12Z December 11, 1980 (bottom) from the Daily Weather Maps Series.

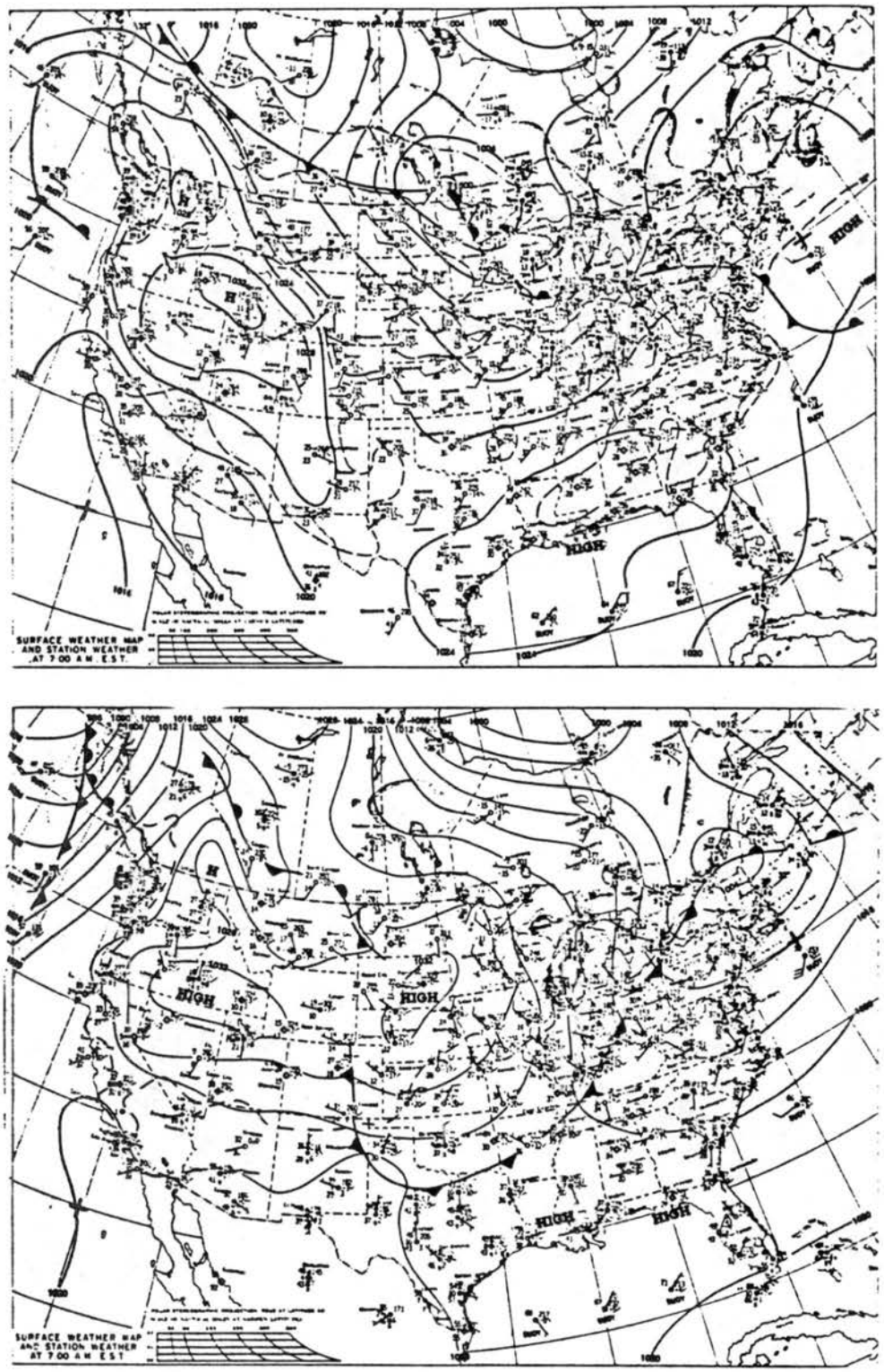

Figure A22. The surface weather map for 12Z December 12 (top) and 12Z December 13, 1980 (bottom) from the Daily Weather Maps Series.

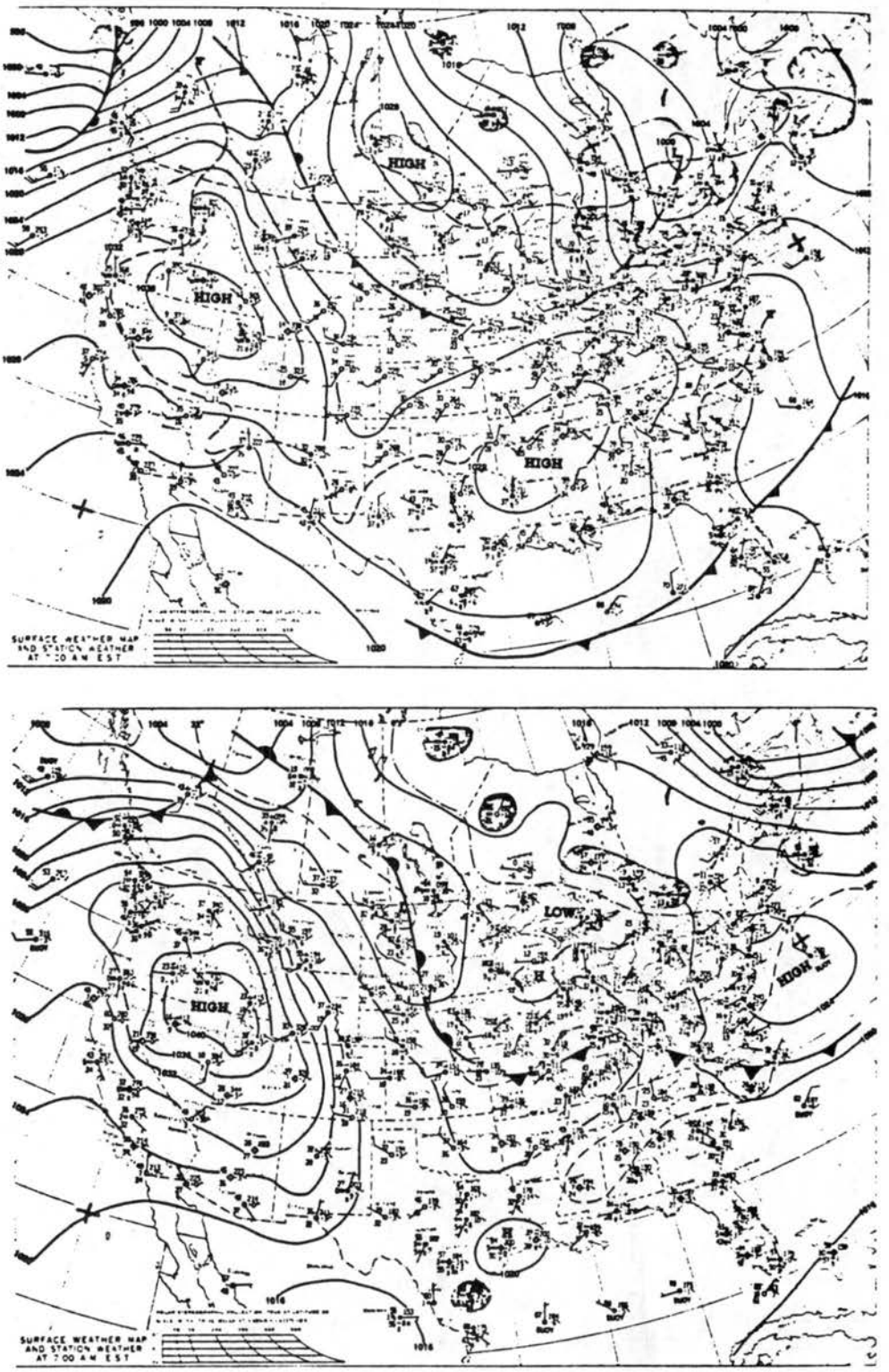

Figure A23. The surface weather map for 12Z December 14 (top) and 12Z December 15, 1980 (bottom) from the Daily Weather Maps Series.

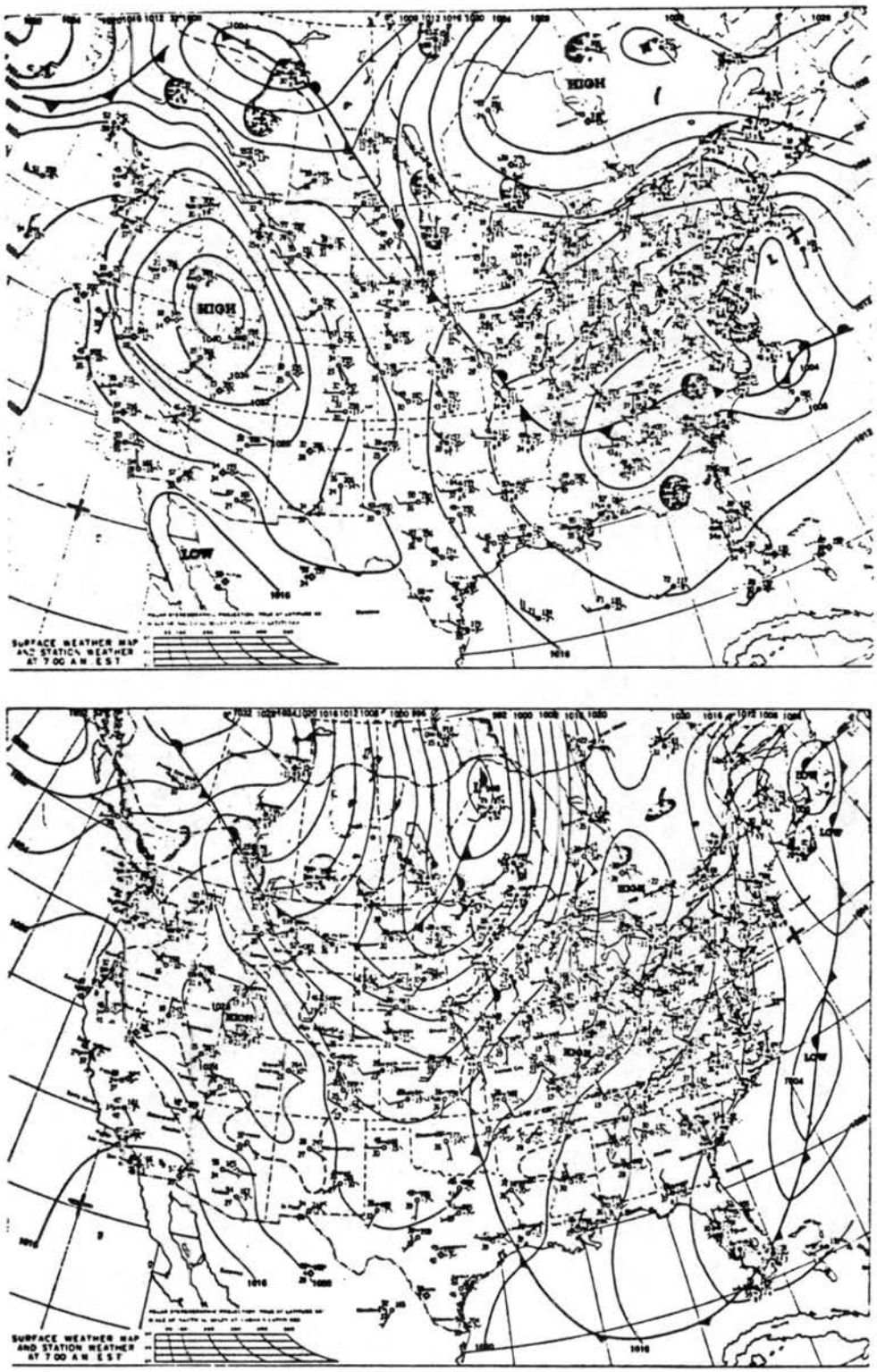

Figure A24. The surface weather map for 12Z December 16 (top) and 12Z December 17, 1980 (bottom) from the Daily Weather Maps Series.

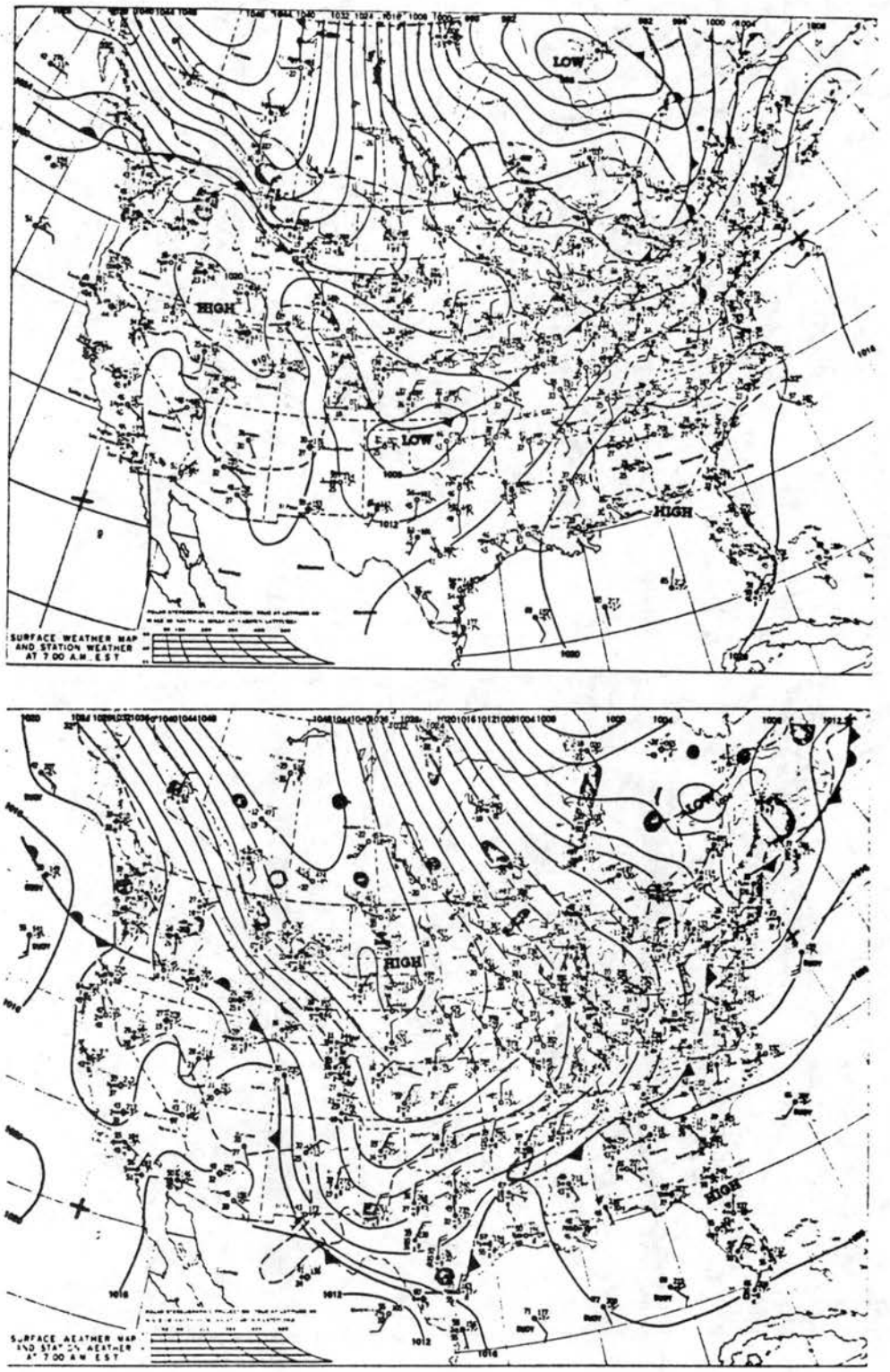

Figure A25. The surface weather map for 12Z December 18 (top) and 12Z December 19, 1980 (bottom) from the Daily Weather Maps Series.

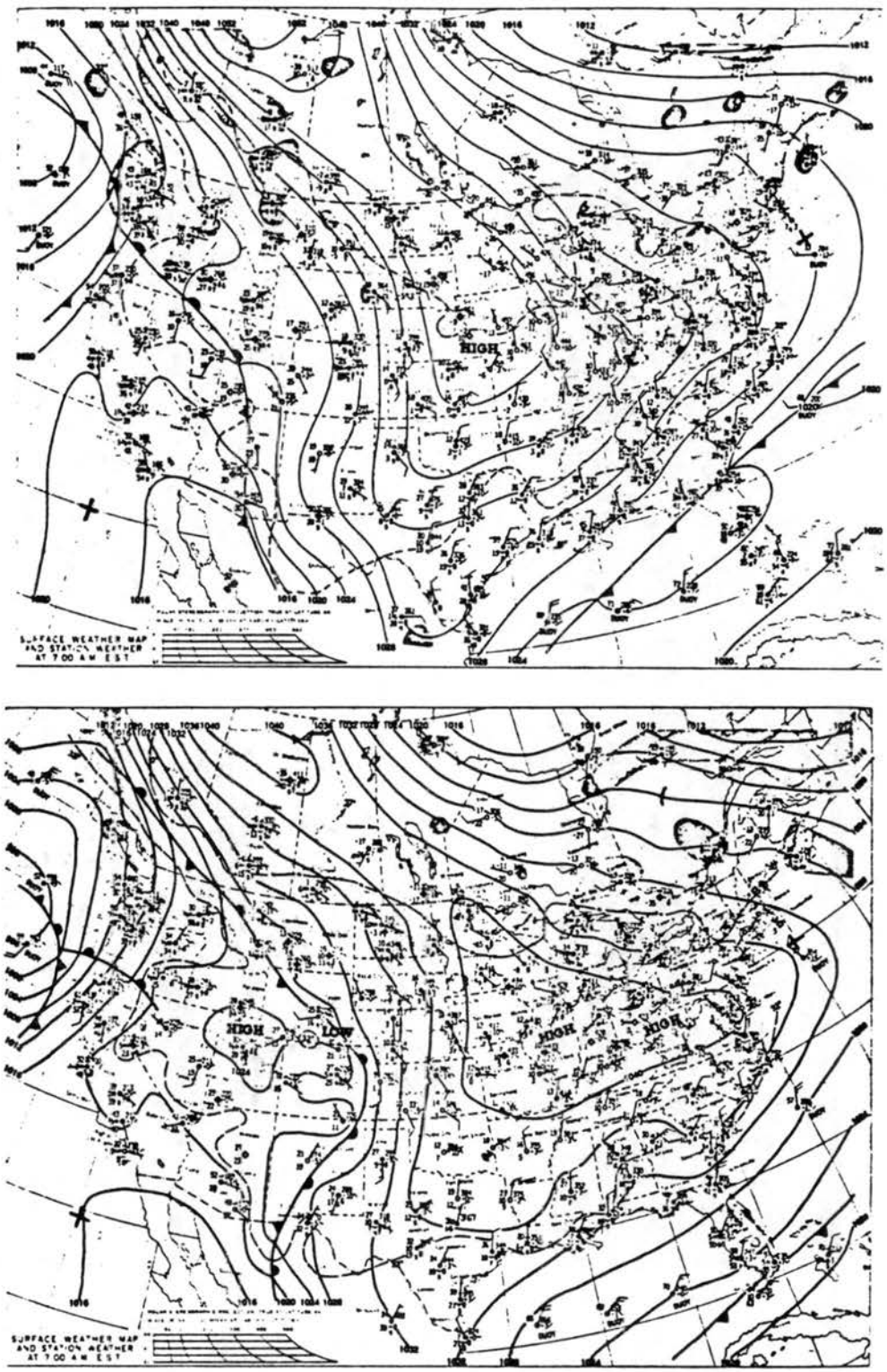

Figure A26. The surface weather map for 12Z December 20 (top) and 12Z December 21, 1980 (bottom) from the Daily Weather Maps Series.

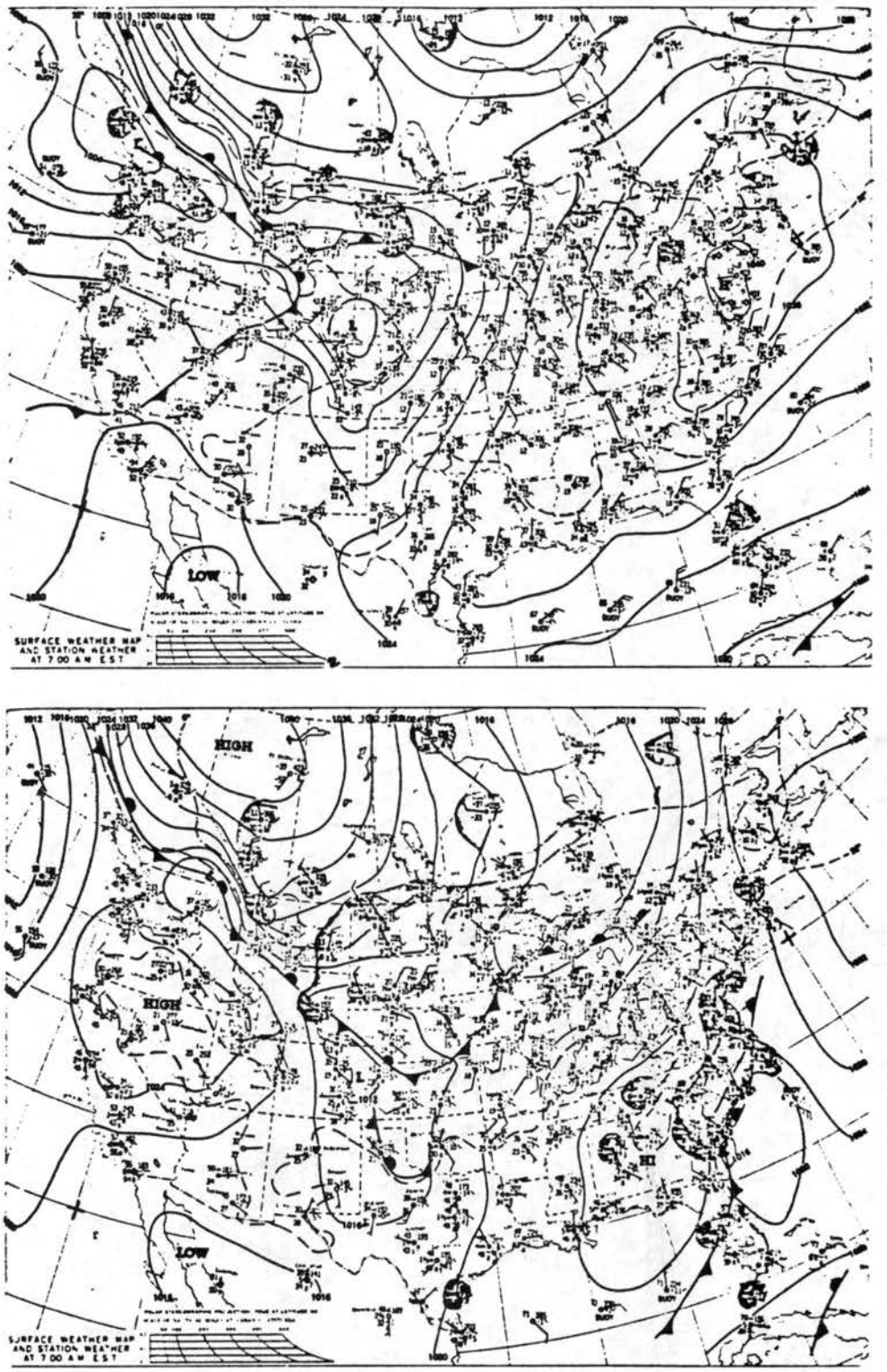

Figure A27. The surface weather map for 12Z December 22 (top) and 12Z December 23, 1980 (bottom) from the Daily Weather Maps Series.

APPENDIX B.

ADIABATIC DIAGRAMS FOR THE DEEP STABLE LAYER EPISODE

The adiabatic diagrams give the potential temperature and winds for the deep stable layer episode which occurred in December 1980. The adiabats are drawn at 2K intervals. The wind barbs shows the direction from which the wind is blowing. Each small barb represents a speed of 2-3ms^{-1}. Each full barb represents a speed of 4-6ms^{-1}, and a flag respresents a speed of 24-26ms^{-1}. Figures B1 and B2 are the adiabatic diagrams extending up to 5.0km AGL for Grand Junction and Boise, respectively. Figures B3 to B6 are the adiabatic diagrams extending up to 2.5km AGL for Grand Junction, Salt Lake City, Winnemucca, and Boise, respectively. Figures B7 to B10 are the adiabatic diagrams extending up to 5.0km AGL for Grand Junction, Salt Lake City, Winnemucca, and Boise with regions of dew point depressions 3.0°C or less shaded.

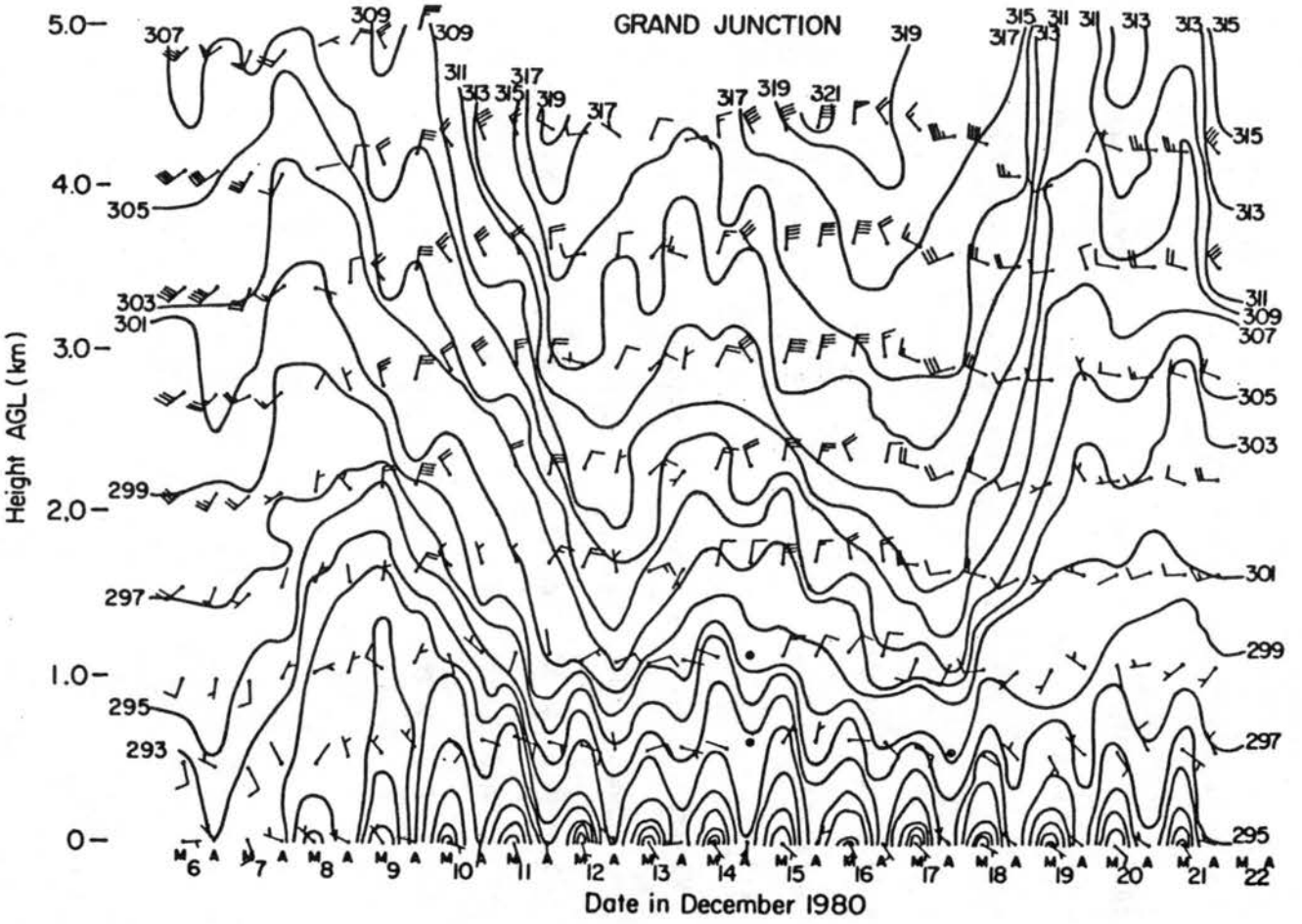

Figure B1. A time versus height plot of potential temperature and winds from December 6-22, 1980 for Grand Junction. Adiabats are plotted at 2K intervals and the figure extends to 5.0km AGL.

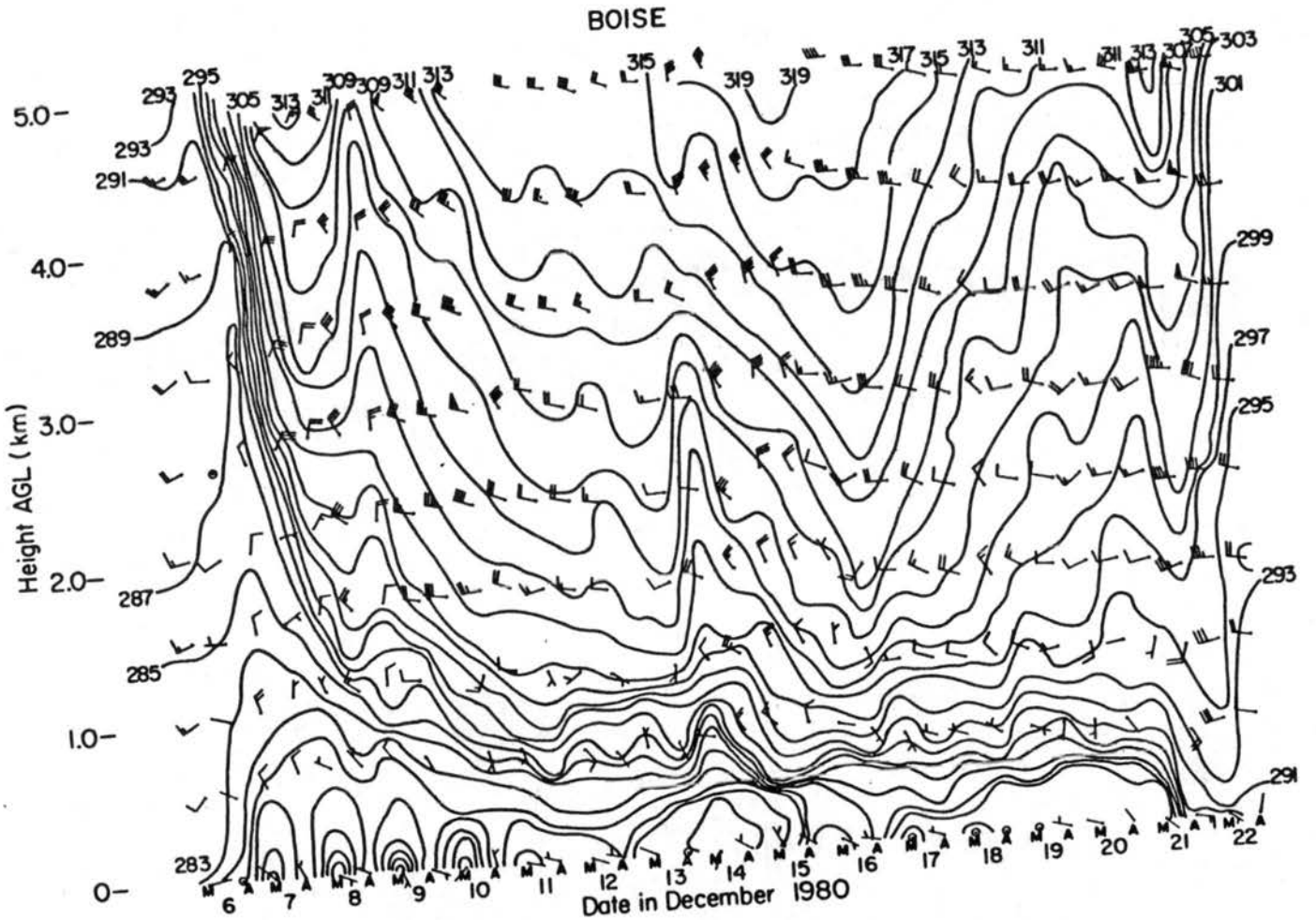

Figure B2. Same as Figure B1 but for Boise.

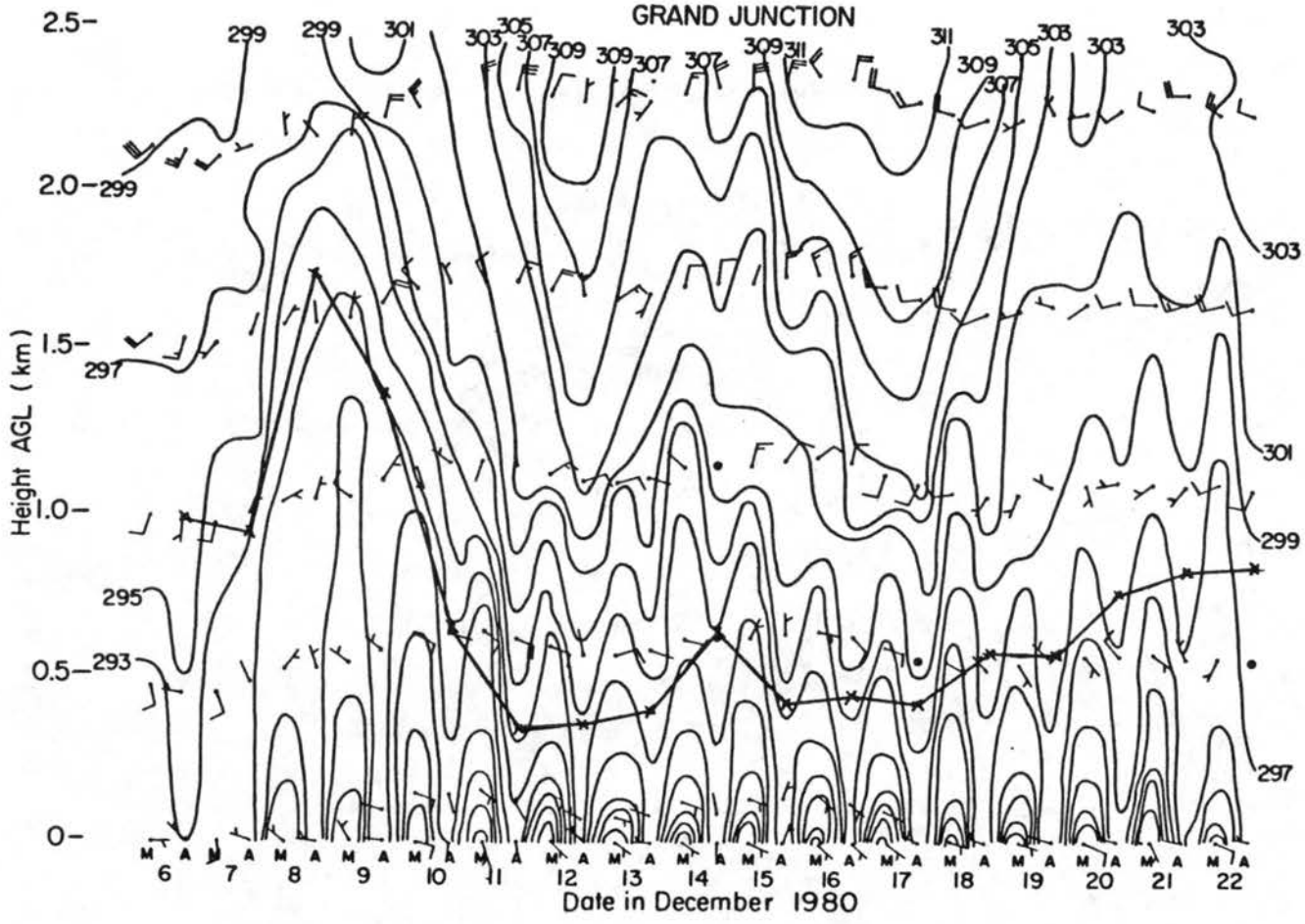

Figure B3. Same as Figure B1 but the figure extends to 2.5km AGL. The line connecting the X's give the CCBL heights.

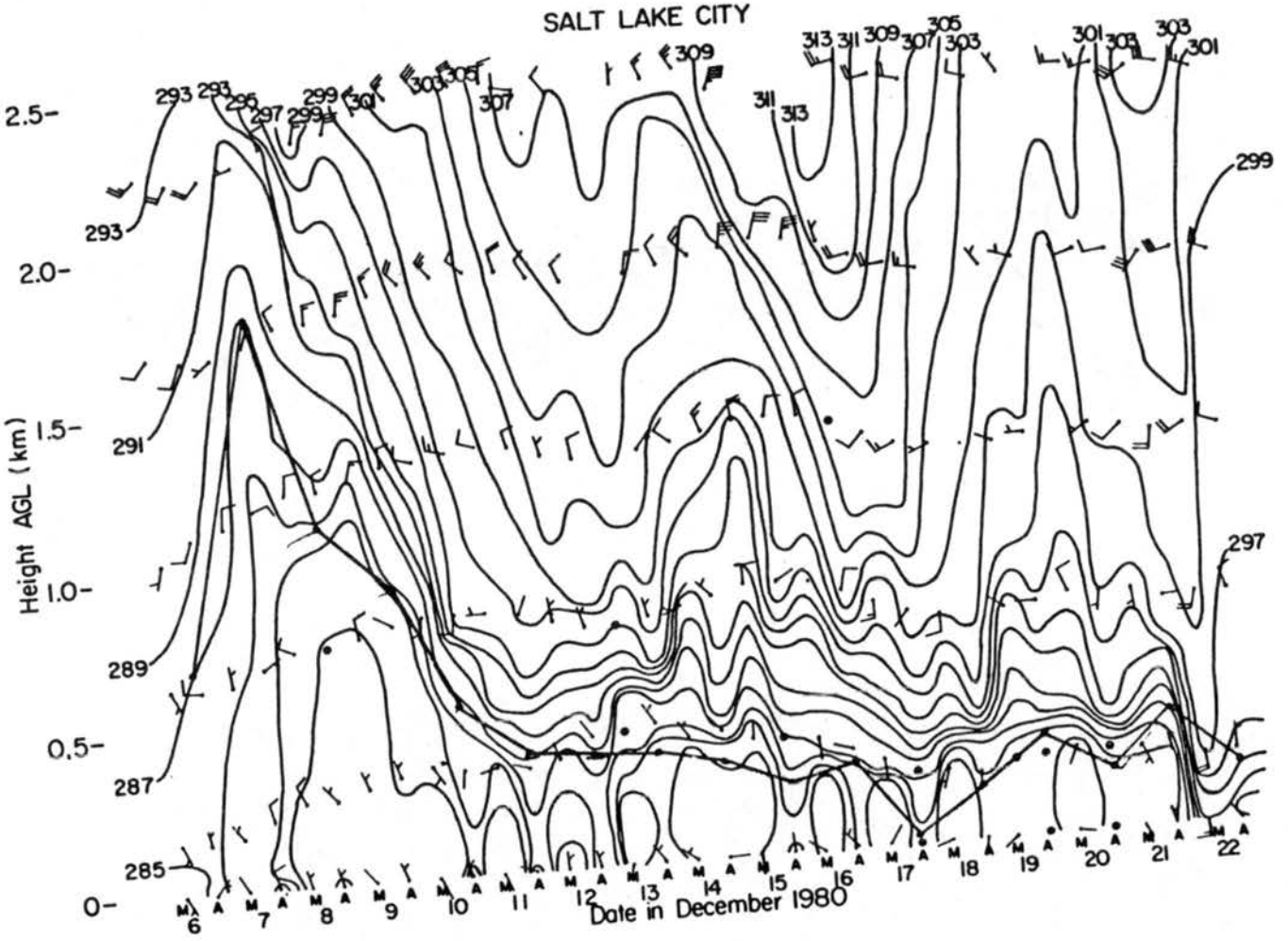

Figure B4. Same as Figure B3 but for Salt Lake City.

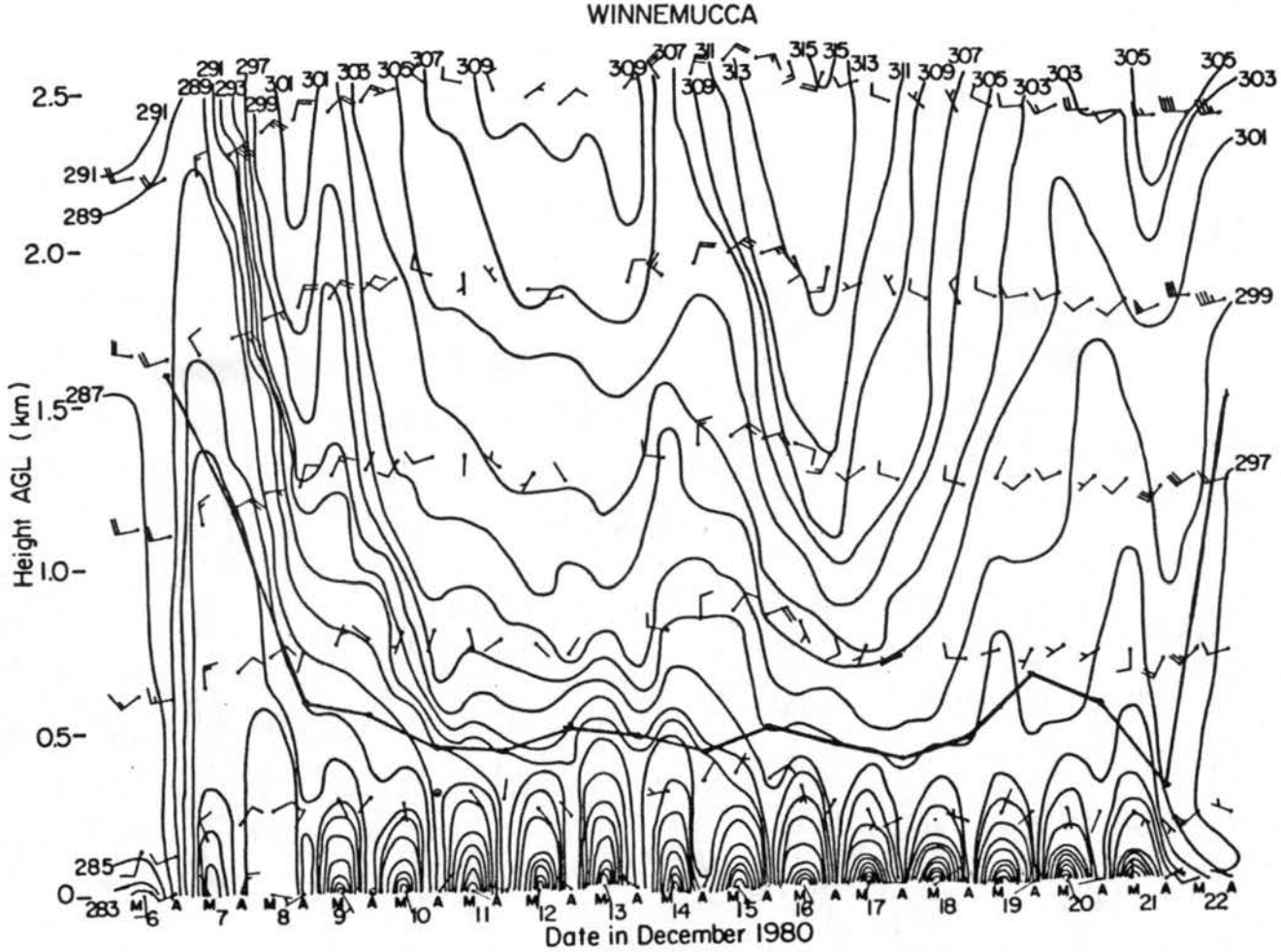

Figure B5. Same as Figure B3 but for Winnemucca.

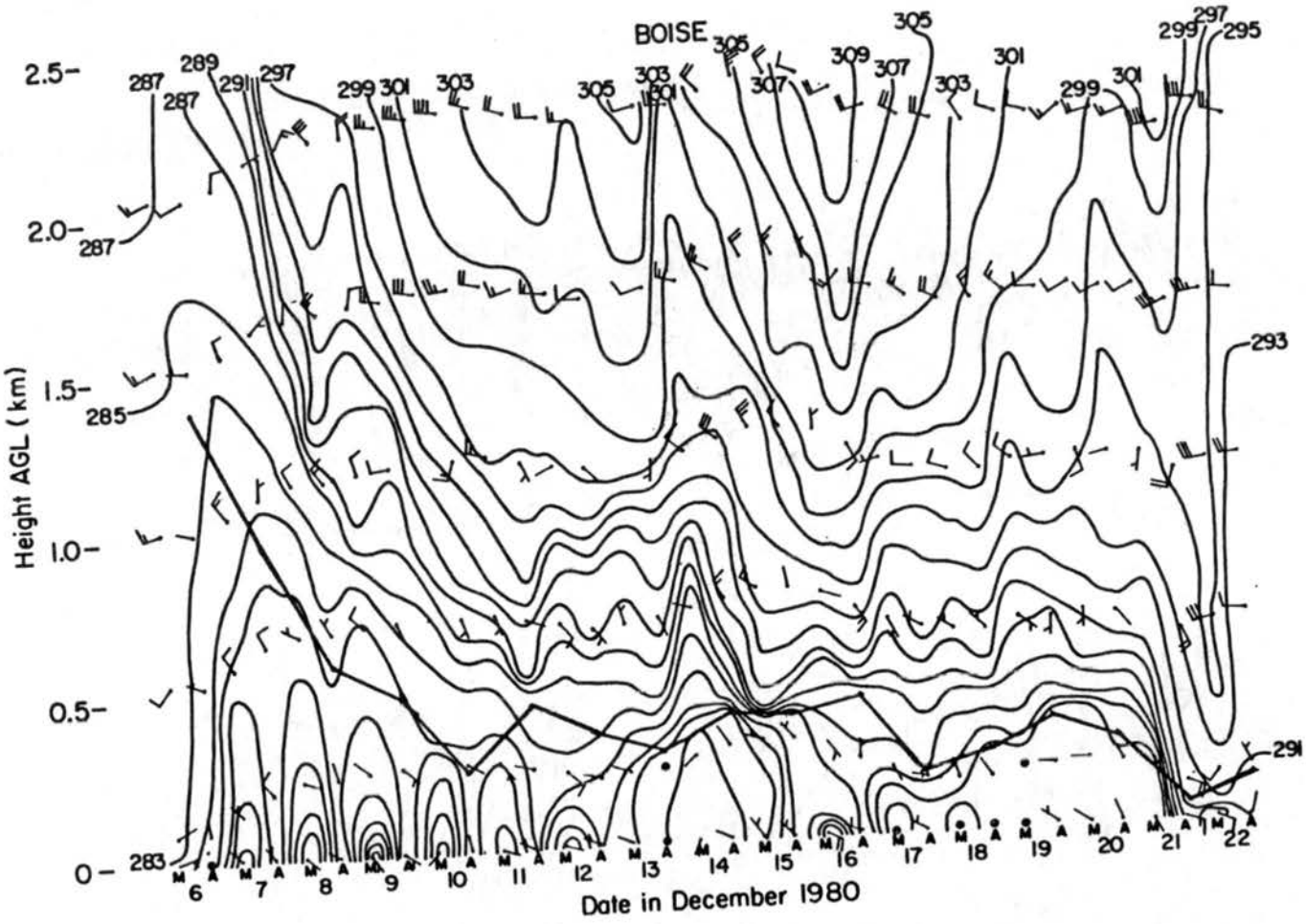

Figure B6. Same as Figure B3 but for Boise.

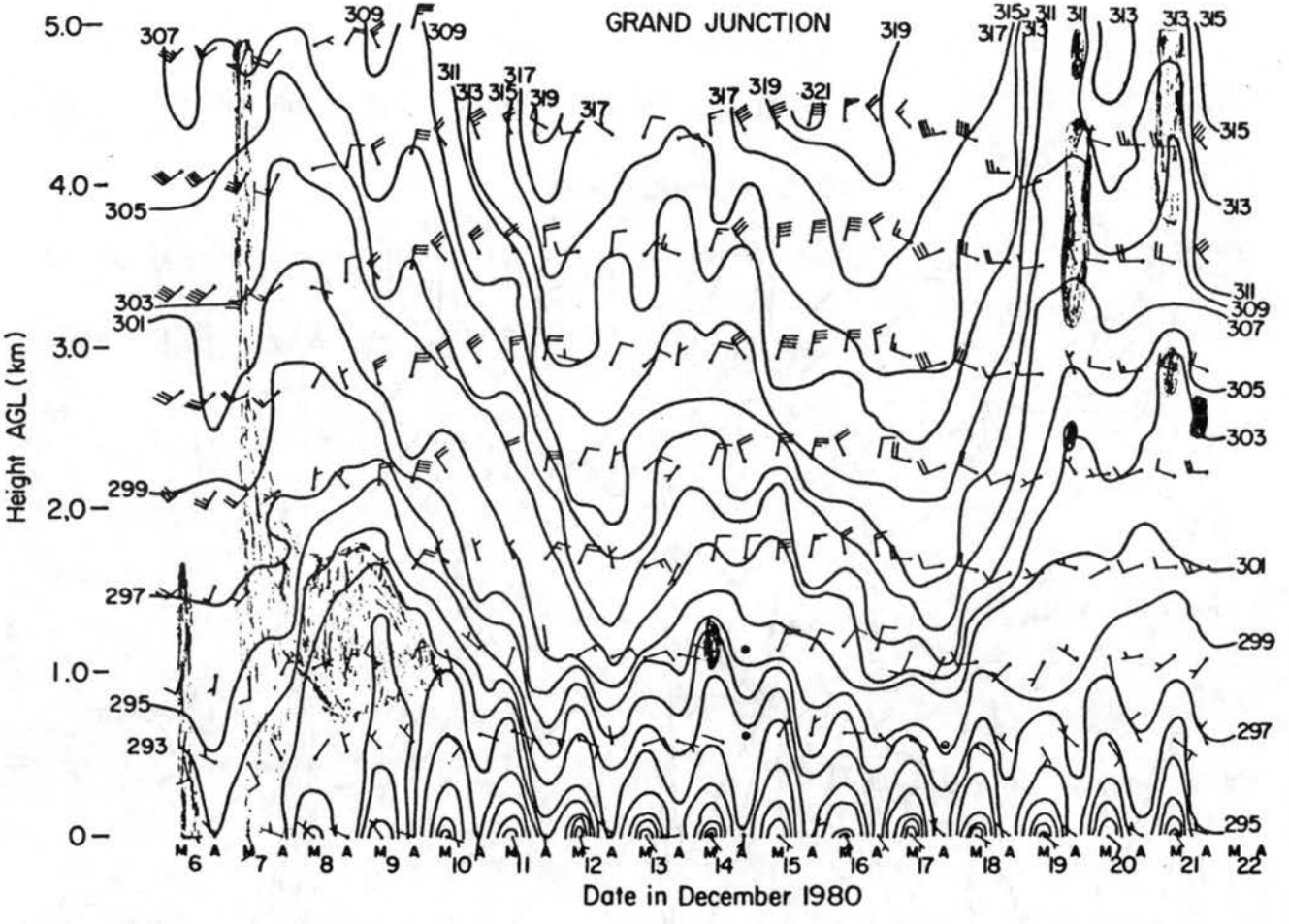

Figure B7. The adiabatic diagram for Grand Junction which extends to 5.0km with regions of dew point depression of 3.0°C or less shaded.

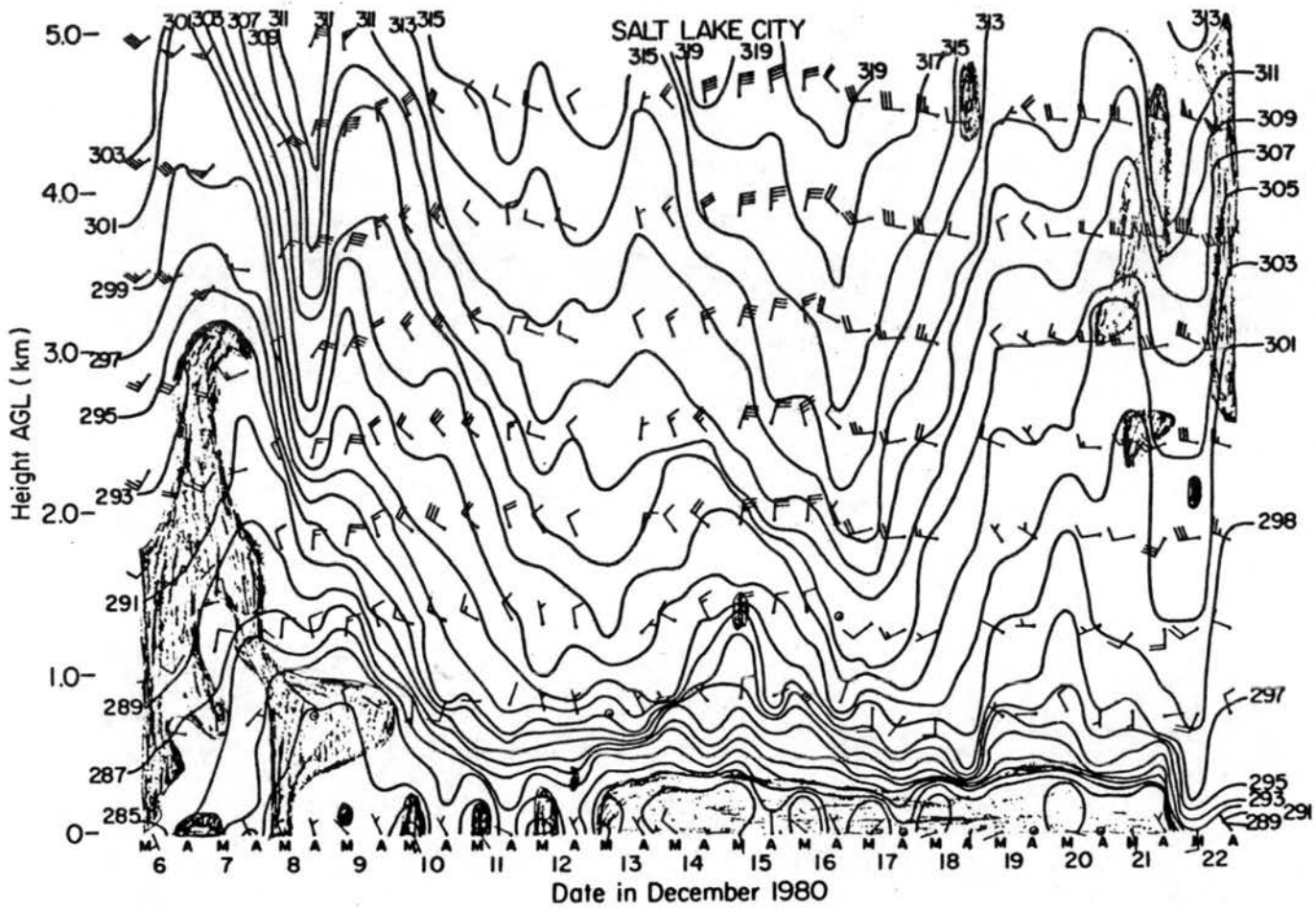

Figure B8. Same as Figure B7 but for Salt Lake City.

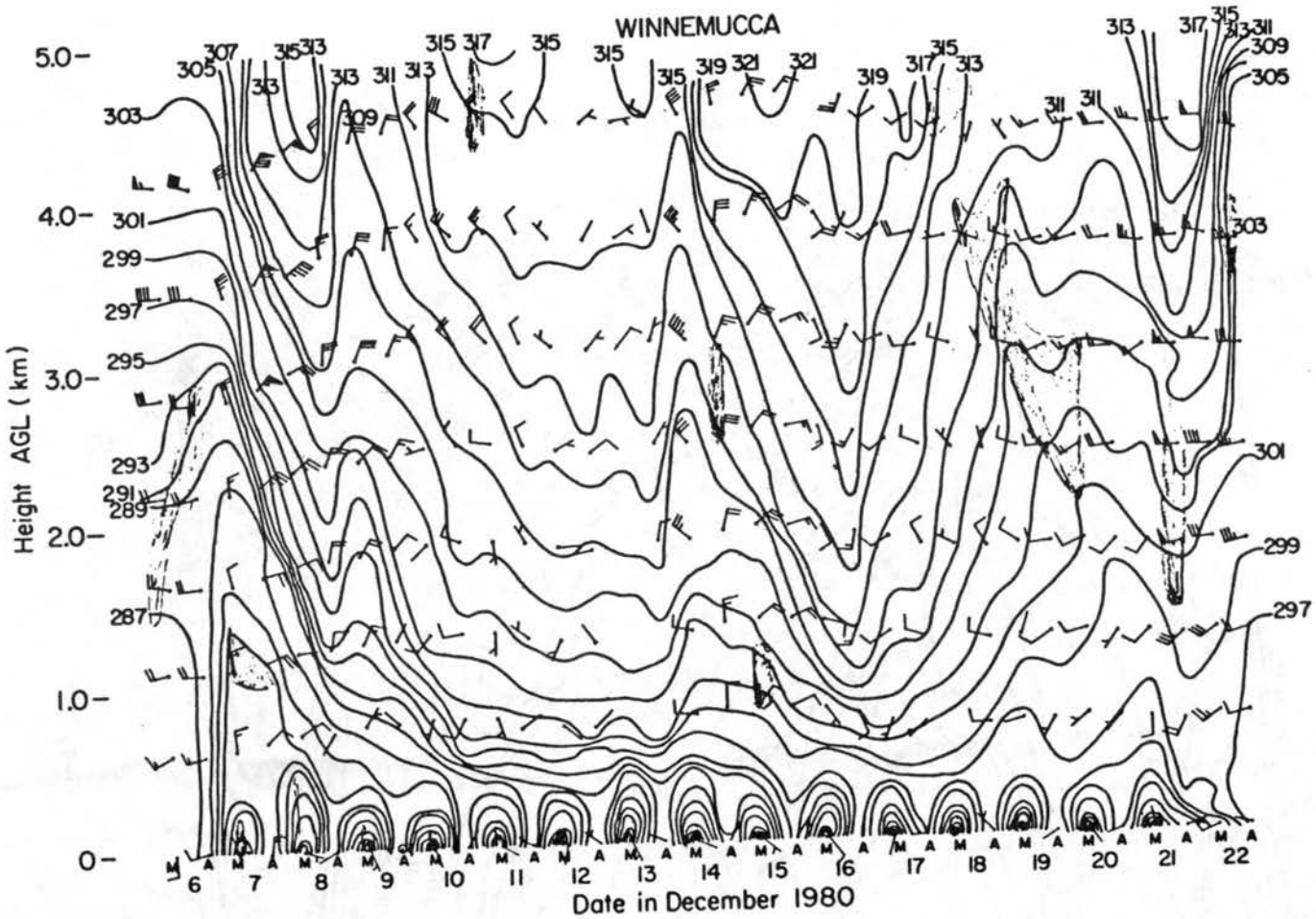

Figure B9. Same as Figure B7 but for Winnemucca.

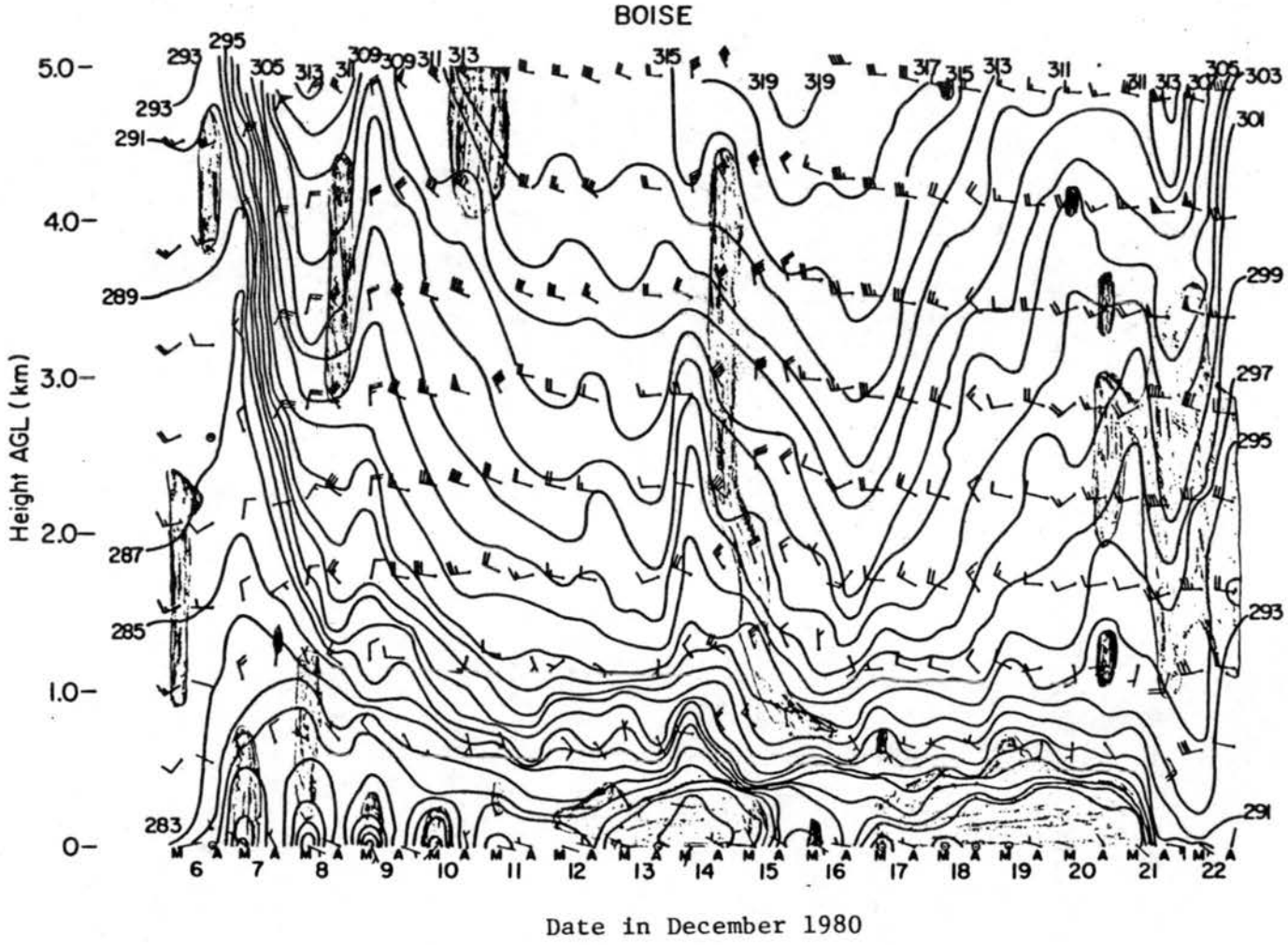

Figure B10. Same as Figure B7 but for Boise.

APPENDIX C

DESCRIPTION OF TOPOGRAPHY AROUND THE STATIONS

Grand Junction, Salt Lake City, and Boise are located in clearly defined large valleys or basins. Grand Junction is located at latitude of 39.11° and longitude 108.53°. The elevation at the launching point of the soundings is 1474m MSL. The city is situated in a wide valley in western Colorado formed by the Colorado River. The valley is orientated southeast to northwest near Grand Junction and has a northeast to southwest orientation further west of Grand Junction. The Local Climatological Data (LCD) for Grand Junction (1981) states that the valley has an elevation 4400 to 4800 feet (1341m to 1463m) MSL with terrain of 9000 to 12000 feet (2743m to 3658m) MSL 10 to 60 miles in all directions. Closer examination of the local terrain shows that the terrain at about 25 miles to the north of the valley rises to around 7500 feet (2286m) MSL and at about 15 miles to the southwest the terrain rises to above 7500 feet (2286m) MSL.

Salt Lake City is located at latitude of 40.76° and longitude 111.96°. The elevation at the launching point of the sounding is 1288m MSL. The Wasatch Mountains form an extensive barrier at an elevation of at least 8500 feet (2591m) MSL just to the east of the city. About 20 miles to the southwest the Oquirrh Mountains rise to around 7500 feet (2286m) MSL. A ridge of around 6000 feet (1829m) MSL extends between the two mountain ranges about 25 miles to the south of the city and north of

Utah Lake. These terrain features enclose Salt Lake City on three sides with the Great Salt Lake being to the west to north of the city.

Boise is located at latitude 43.56° and longitude 116.21°. The elevation of the launching point of the soundings is 871m MSL. The city is in a wide valley containing to Snake River and the Boise River. At Boise the valley is orientated northwest to southeast. The mountains to the north and east of the city rise to over 5000 feet (1524m) MSL. To the west and south of the valley there is a mountain range which rises to over 6000 feet (1829m) MSL.

Winnemucca is located at latitude 40.90° and longitude 117.80°. The elevation of the launching point of the soundings is 1312m MSL. Unlike the other stations, Winnemucca is not in a clearly defined valley or local basin. It is located between two ridges which extend up to at least 7000 feet MSL. To the northeast and southwest the terrain opens into broad, gently sloping basins with mountain ridges which do not connect into a continuous barrier.

APPENDIX D

TABLES GIVING MORE INFORMATION ON EULERIAN EFFECTIVE VERTICAL MOTION

Tables D1 and D2 give the eulerian effective vertical motion (EEVM) averaged over 300m for layers at 500m intervals between 1.0km AGL and 4.5km AGL for Grand Junction and Boise. Tables D3 and D4 give for Grand Junction and Boise at 700mb and 500mb the observed warming rate and the EEVM for assumed diabatic heating of $0.0°C(day)^{-1}$, $-1.0°C(day)^{-1}$, and $-1.5°C(day)^{-1}$. Tables D5 and D6 give for 700mb and 500mb at Grand Junction and Boise the EEVM averaged over 300m, observed warming in the previous 12 hours, the calculated warming rate, and calculated warming due to horizontal temperature advection.

Table D1.
EEVM values averaged over 300m (cms^{-1}) for Grand Junction at 1.0km AGL, 1.5km AGL, 2.0km AGL, 2.5km AGL, 3.0km AGL, 3.5km AGL, 4.0km AGL, and 4.5km AGL.

Date	1.0km	1.5km	2.0km	2.5km	3.0km	3.5km	4.0km	4.5km
6 M	0.63	0.46	0.65	-0.15	0.02	0.36	0.46	0.85
A	1.31	0.83	0.23	-0.20	-0.49	0.25	0.70	0.67
7 M	0.81	0.48	0.32	1.49	1.40	2.26	2.99	0.48
A	1.11	76.28	0.55	1.03	0.70	0.91	0.36	0.20
8 M	2.08	1.40	0.32	-0.20	-0.63	-0.36	-0.80	-0.51
A	2.68	1.26	0.27	-0.07	-0.99	-1.72	-0.88	-0.98
9 M	0.67	-0.37	-0.61	-0.42	-0.66	-0.66	-0.62	-0.28
A	-0.17	-0.48	-0.83	-1.03	-0.75	-0.25	-0.34	-1.21
10 M	-0.70	-0.59	-0.87	-0.12	-0.78	-1.58	-1.58	-4.45
A	-0.75	-0.94	-0.99	-0.60	-0.76	-0.81	-1.40	-2.22
11 M	-0.55	-0.42	-1.13	-3.95	-2.02	-1.09	-0.88	-1.41
A	-0.86	-3.50	-1.09	-0.81	-1.38	-1.25	-0.57	-0.04
12 M	-0.13	-0.66	-1.00	-0.56	0.74	1.19	1.36	2.06
A	-0.02	0.05	0.53	1.04	0.91	0.42	2.05	0.37
13 M	0.30	0.71	1.15	0.95	0.32	0.64	1.01	0.35
A	0.57	0.74	0.80	0.31	0.16	-0.16	-0.49	-0.12
14 M	0.20	0.03	-0.27	-0.37	-0.17	-0.15	-1.54	-1.93
A	-0.19	-0.19	0.03	-1.00	-0.81	-0.61	-0.63	-0.87
15 M	-0.11	-0.74	-0.59	-0.32	-0.92	-0.86	-0.95	-0.56
A	-1.17	-0.21	-0.65	-0.26	-0.23	-0.41	-0.20	-0.03
16 M	-1.68	-0.61	-0.11	-0.61	-0.33	-0.50	-0.67	0.57
A	-0.42	-0.91	-0.52	-0.36	-0.23	0.11	0.92	1.01
17 M	-0.11	-0.18	-0.19	-0.08	-0.02	0.65	1.60	0.86
A	0.48	0.80	0.81	0.80	1.69	1.89	1.35	0.40
18 M	0.41	0.58	0.80	1.49	1.53	1.16	0.82	1.18
A	-0.16	0.88	1.28	1.42	1.64	1.57	2.67	14.00
19 M	0.83	2.33	0.76	3.44	4.08	1.84	-2.99	12.33
A	0.83	0.65	0.25	0.33	-0.39	-0.08	2.11	-0.54
20 M	0.17	0.05	0.26	0.11	-0.18	-0.25	-0.45	-0.05
A	0.28	0.14	0.25	0.60	0.66	0.70	0.97	-0.23
21 M	0.03	-0.07	-0.41	0.09	-0.05	-0.89	-6.10	-1.10
A	0.16	0.26	-0.14	-1.59	-3.59	-1.13	-1.07	-1.20
22 M	-0.64	-0.25	-0.40	-0.80	-0.26	0.81	0.08	-0.09
A	0.32	-9.83	0.52	1.37	2.42	2.29	1.52	2.33
23 M	-3.74	28.06	2.14	3.35	4.28	0.88	0.90	1.37

Table D2.
Same as Table D1 but for Boise.

Date	1.0km	1.5km	2.0km	2.5km	3.0km	3.5km	4.0km	4.5km
6 M	1.10	0.43	-3.23	0.84	1.21	1.90	1.97	0.96
A	1.07	0.63	2.35	0.54	0.63	4.79	0.07	-2.58
7 M	0.89	0.12	-0.61	-1.63	-27.76	-34.10	-3.20	-2.41
A	0.19	-0.68	-1.65	-1.48	-2.72	-4.10	-3.99	-1.73
8 M	-0.31	-0.91	-1.01	-1.00	-0.39	-1.17	-1.36	-0.28
A	-0.57	-0.47	-0.19	0.12	0.49	6.68	1.28	1.22
9 M	-0.22	0.08	-0.91	-0.20	0.01	1.00	1.12	0.56
A	-0.44	-0.43	-2.30	-1.43	-1.18	-2.56	2.95	-2.01
10 M	-0.41	-0.52	-0.87	-0.93	-0.87	-0.82	-0.62	-1.55
A	-0.56	-0.32	-0.73	-0.92	-1.00	-1.42	-3.30	-0.43
11 M	-0.32	-0.10	-0.18	-0.82	-1.31	-0.79	-1.55	-1.56
A	0.16	-0.11	-0.33	-0.37	-0.44	-0.26	-0.06	-0.08
12 M	0.05	-0.10	0.04	0.31	0.26	0.17	0.04	0.08
A	0.04	-0.26	0.05	-0.16	-0.11	-0.22	-0.16	0.13
13 M	0.03	-0.29	-0.58	-0.56	-1.20	-0.12	0.52	1.05
A	0.14	0.67	0.82	1.86	1.36	0.56	-0.77	-1.21
14 M	0.07	0.86	0.86	0.34	0.05	-0.09	-0.45	-1.48
A	-0.90	-0.39	-0.43	-1.01	-0.92	-0.56	-0.54	-0.53
15 M	-1.03	-0.46	-1.12	-0.18	-0.40	-0.54	-0.75	-1.00
A	-0.39	0.50	-1.43	-1.77	-0.57	-0.43	-0.20	-0.01
16 M	-0.13	-1.22	-0.70	-1.02	-0.73	-0.65	-0.15	0.31
A	0.28	0.06	-0.03	-0.02	-0.06	-0.17	0.02	0.48
17 M	0.21	0.39	0.54	0.80	0.92	2.14	1.49	1.58
A	-0.02	0.17	0.64	1.47	1.68	1.41	1.59	1.70
18 M	-0.05	0.51	5.82	0.87	1.31	0.93	0.98	0.55
A	0.20	1.09	0.84	0.87	0.73	0.47	0.61	1.07
19 M	0.20	0.17	0.46	0.65	0.45	0.95	2.11	1.21
A	-0.03	0.03	-0.32	0.58	1.96	1.44	1.10	0.36
20 M	0.08	1.23	0.53	0.55	0.85	0.62	0.11	0.31
A	-0.31	0.29	0.27	0.70	-2.13	0.00	-0.83	-0.30
21 M	-0.41	-0.51	-0.94	-13.21	-1.04	-0.77	-0.80	-1.61
A	-0.39	0.10	0.33	-0.40	-0.59	1.23	0.20	0.47
22 M	6.03	31.02	0.69	2.18	1.91	0.45	2.54	3.85
A	3.12	1.03	5.57	1.28	1.32	2.83	0.87	0.03
23 M	0.92	0.01	-1.19	-2.31	-0.96	-1.74	-1.69	-1.66
A	-1.20	-1.21	-0.87	-1.75	-2.61	-1.99	-3.44	-15.74

Table D3.
The present heating rate (°C/12Hr) without any assumed diabatic heating, and EEVM values averaged over 300m (cms^{-1}) for assumed diabatic heating rates of 0.0°C/day, -1.0°C/day, and -1.5°C/day at 700mb and 500mb at Grand Junction.

		700mb				500mb			
		Warming	EEVM			Warming	EEVM		
		Rate	0.0	-1.0	-1.5	Rate	0.0	-1.0	-1.5
12/ 6/80	M	-0.62	0.47	0.09	-0.10	-0.65	0.43	0.10	-0.07
	A	-0.48	0.99	-0.09	-0.54	-0.75	0.79	0.27	0.01
12/ 7/80	M	-0.70	0.45	0.14	-0.01	-1.26	2.31	1.42	0.97
	A	-1.72	60.91	44.22	35.87	-0.39	0.27	-0.07	-0.25
12/ 8/80	M	-2.41	1.15	0.90	0.78	1.15	-0.78	-1.12	-1.29
	A	-1.20	1.12	0.65	0.42	2.23	-1.08	-1.32	-1.44
12/ 9/80	M	1.71	-0.52	-0.68	-0.76	0.71	-0.87	-1.55	-1.88
	A	3.37	-0.82	-0.94	-1.00	0.66	-0.96	-1.67	-2.03
12/10/80	M	2.65	-0.80	-0.96	-1.04	3.36	-3.01	-3.45	-3.67
	A	1.85	-1.23	-1.56	-1.73	3.34	-1.92	-2.20	-2.34
12/11/80	M	1.31	-0.63	-0.87	-0.99	3.03	-1.18	-1.38	-1.47
	A	2.29	-2.09	-2.54	-2.77	0.35	-0.21	-0.53	-0.70
12/12/80	M	2.23	-0.82	-1.00	-1.09	-1.92	1.82	1.35	1.11
	A	-0.27	0.11	-0.09	-0.20	-0.66	1.93	0.52	-0.19
12/13/80	M	-1.85	0.81	0.59	0.48	-0.34	0.28	-0.20	-0.44
	A	-1.36	0.73	0.46	0.32	0.27	-0.14	-0.40	-0.54
12/14/80	M	0.09	-0.04	-0.20	-0.28	1.41	-2.53	-3.47	-3.94
	A	0.03	-0.02	-0.19	-0.28	1.55	-0.51	-0.66	-0.74
12/15/80	M	1.59	-0.99	-1.30	-1.45	1.58	-0.82	-1.08	-1.21
	A	1.62	-0.54	-0.70	-0.78	0.28	-0.09	-0.26	-0.35
12/16/80	M	0.89	-0.17	-0.27	-0.32	-0.57	0.39	0.01	-0.18
	A	2.09	-0.80	-0.99	-1.08	-0.87	1.14	0.47	0.14
12/17/80	M	0.39	-0.14	-0.32	-0.41	-0.90	1.34	0.60	0.23
	A	-2.09	0.96	0.73	0.62	-0.76	0.85	0.30	0.03
12/18/80	M	-2.27	0.81	0.63	0.54	-1.21	0.94	0.55	0.36
	A	-2.28	1.09	0.86	0.74	-3.32	11.79	9.98	9.07
12/19/80	M	-2.02	1.89	1.42	1.18	-3.02	1.50	1.26	1.15
	A	-0.14	0.23	-0.26	-0.51	1.31	0.28	0.38	0.42
12/20/80	M	-0.09	0.04	-0.13	-0.21	0.79	-0.48	-0.87	-1.07
	A	-0.14	-0.19	0.21	0.41	-1.84	-7.66	-5.60	-4.56
12/21/80	M	0.32	-0.18	-0.43	-0.56	1.81	-3.69	-4.75	-5.28
	A	-0.55	0.49	0.05	-0.17	1.75	-1.06	-1.36	-1.51
12/22/80	M	0.40	-0.15	-0.35	-0.45	0.16	-0.04	-0.07	-0.08
	A	-1.52	-5.98	-3.79	-2.69	-3.72	1.78	1.54	1.41
12/23/80	M	-3.15	28.85	24.12	21.75	-1.98	1.17	0.88	0.73
	A	1.51	-6.85	-8.81	-9.79	3.13	-1.76	-2.04	-2.18

Table D4.
Same as Table D3 but for Boise.

		700mb				500mb			
		Warming	EEVM			Warming	EEVM		
		Rate	0.0	-1.0	-1.5	Rate	0.0	-1.0	-1.5
12/ 6/80	M	-1.14	-5.30	-3.14	-2.06	-2.16	0.97	0.75	0.64
	A	-0.88	1.29	0.65	0.33	2.46	-2.76	-3.33	-3.62
12/ 7/80	M	1.25	-1.04	-1.44	-1.65	9.73	-2.73	-2.87	-2.94
	A	5.08	-2.19	-2.41	-2.51	8.49	-3.59	-3.80	-3.91
12/ 8/80	M	4.44	-1.18	-1.31	-1.38	0.87	-0.45	-0.72	-0.86
	A	0.02	0.00	-0.20	-0.30	-3.84	2.11	1.84	1.70
12/ 9/80	M	1.05	-0.55	-0.81	-0.94	-1.09	1.25	0.69	0.41
	A	2.77	-1.64	-1.94	-2.09	2.77	-4.80	-5.66	-6.09
12/10/80	M	1.62	-0.94	-1.22	-1.37	2.23	-2.14	-2.64	-2.89
	A	1.19	-0.93	-1.32	-1.52	1.72	-0.64	-0.83	-0.92
12/11/80	M	1.01	-0.54	-0.80	-0.93	0.79	-0.61	-0.96	-1.14
	A	0.74	-0.29	-0.49	-0.59	0.06	-0.05	-0.47	-0.67
12/12/80	M	-0.57	0.46	0.04	-0.16	-0.38	1.00	-0.20	-0.79
	A	0.02	0.01	-0.31	-0.47	-0.33	0.67	-0.39	-0.92
12/13/80	M	1.55	-0.67	-0.88	-0.99	-0.45	0.56	-0.03	-0.33
	A	-2.35	1.26	1.00	0.86	1.56	-1.36	-1.80	-2.02
12/14/80	M	-0.78	0.42	0.15	0.02	2.19	-1.25	-1.54	-1.69
	A	2.29	-0.98	-1.19	-1.29	1.54	-0.46	-0.61	-0.68
12/15/80	M	0.79	-0.24	-0.39	-0.47	1.20	-0.71	-1.02	-1.17
	A	2.18	-1.87	-2.30	-2.52	-0.31	0.28	-0.17	-0.39
12/16/80	M	2.10	-0.79	-0.98	-1.07	-0.91	0.83	0.38	0.15
	A	-0.29	0.15	-0.11	-0.24	-0.67	1.26	0.32	-0.14
12/17/80	M	-2.08	0.72	0.55	0.46	-0.68	0.66	0.20	-0.02
	A	-2.25	1.18	0.92	0.79	-1.16	0.55	0.31	0.19
12/18/80	M	-1.95	3.66	2.71	2.23	-1.52	0.80	0.54	0.41
	A	-1.15	0.82	0.45	0.27	-2.14	1.26	0.97	0.82
12/19/80	M	-1.23	0.62	0.37	0.24	-0.75	0.49	0.19	0.04
	A	-0.63	-0.06	-0.01	0.01	-0.84	0.25	0.10	0.02
12/20/80	M	-0.57	0.43	0.05	-0.15	-1.71	0.77	0.55	0.44
	A	-0.87	0.44	0.19	0.07	0.00	0.01	-0.33	-0.50
12/21/80	M	1.48	-8.94	-11.93	-13.42	2.29	-1.26	-1.53	-1.67
	A	-0.59	0.18	-0.05	-0.16	-0.87	0.46	0.20	0.06
12/22/80	M	-3.82	1.96	1.71	1.58	-5.92	3.24	2.97	2.83
	A	-2.01	3.78	2.66	2.10	-0.56	0.28	0.02	-0.11
12/23/80	M	2.86	-1.88	-2.21	-2.38	2.70	-1.24	-1.47	-1.59
	A	3.95	-1.51	-1.70	-1.79	3.13	-11.33	-13.13	-14.02

APPENDIX E

SURFACE CLIMATOLOGICAL DATA, CLOUDCOVER DATA, AND INFLUENCES OF CLOUDCOVER FOR THE DEEP STABLE LAYER EPISODE

Tables E1 and E2 give surface temperature, precipitation, and snowcover data for Grand Junction, Salt Lake City, Winnemucca, and Boise. Tables E3 to E5 give six-hour averages of total and opaque cloudcover for Grand Junction, Salt Lake City, and Boise while Table E6 gives observed cloudcover data for Winnemucca. In the next two paragraphs a discussion of the relationship of cloudcover to CCBL heights and surface temperatures for Grand Junction and Boise will be given.

The surface climatological data for Boise is given in Table E2 and cloud data is given in Table E5. At Boise a persistent fog layer lasting the entire day occurs from the thirteenth to fourteenth and from the seventeenth to twenty-first. Like at Salt Lake City, the surface diurnal temperature range on persistent fog days often are small. On the days from the eighth to twelfth, the eighth and eleventh have significant amounts of thin clouds during 06-17, the ninth is almost clear during the period, and the tenth and twelfth have significant opaque cloudiness. The CCBL heights on the tenth and twelfth are lower than the other days. The surface temperature tables show little cooling from the ninth to tenth but shows significant warming from the tenth to eleventh.

At Grand Junction fog layers did not form in this episode so it is better at assessing the effects of clouds other than fog on surface heating. The surface climatological data is given in Table E1 and cloud data is given in Table E3. From the tenth to the nineteenth the days with significant thin cloudiness during 06-17 are the tenth, twelfth, thirteenth, fourteenth, fifteenth, sixteenth, and eighteenth. No days with significant coverage of opaque cloudiness occurred during this period. Interestingly, the CCBL height is lowest on the eleventh, a clear day, and the surface maximum temperature is cooler than the surrounding days. On the sixteenth and seventeenth the CCBL heights and surface temperatures are nearly the same. The CCBL heights show noticeable increases from the previous day on the fourteenth and eighteenth, two of the days with significant thin clouds.

Table E1.
The surface climatological data for Grand Junction and Salt Lake City from December 6-23, 1980. The temperatures are in °F and precipitation and snowcover are in inches.

Surface Climatological Data for Grand Junction, December 1980

Day	Maximum	Minimum	Mean	Range	Precipitation	Snowcover
6	48	32	40.0	16	0.01	0
7	44	34	39.0	10	0.17	0
8	42	32	37.0	10	0.00	0
9	43	28	35.5	15	0.00	0
10	42	22	32.0	20	0.00	0
11	46	24	35.0	22	0.00	0
12	48	25	36.5	23	0.00	0
13	47	24	35.5	23	0.00	0
14	49	23	36.0	26	0.00	0
15	51	24	37.5	27	0.00	0
16	54	27	40.5	27	0.00	0
17	54	27	40.5	27	0.00	0
18	53	25	39.0	28	0.00	0
19	53	26	39.5	27	0.00	0
20	53	26	39.5	27	0.00	0
21	53	29	41.0	24	0.00	0
22	54	32	43.0	22	0.03	0
23	52	34	43.0	18	0.01	0

Surface Climatological Data for Salt Lake City, Decmber 1980

Day	Maximum	Minimum	Mean	Range	Precipitation	Snowcover
6	36	27	31.5	9	0.01	0
7	38	24	31.0	14	T	0
8	33	22	27.5	11	0.00	0
9	33	19	26.0	14	0.00	0
10	37	20	28.5	17	0.00	0
11	40	21	30.5	19	0.00	0
12	37	20	28.5	17	0.00	0
13	28	23	25.5	5	T	0
14	27	22	24.5	5	T	0
15	31	24	27.5	7	T	0
16	32	25	28.5	7	T	T
17	30	25	27.5	5	T	T
18	29	25	27.0	4	T	T
19	30	27	28.5	3	T	T
20	30	26	28.0	4	T	T
21	38	29	33.5	9	0.06	T
22	49	33	41.0	16	T	0
23	50	30	40.0	20	0.01	0

Table E2.
Same as Table E1 but for Winnemucca and Boise.

Surface Climatological Data for Winnemucca, Decmber 1980

Day	Maximum	Minimum	Mean	Range	Precipitation	Snowcover
6	38	21	29.5	17	T	0
7	30	12	21.0	18	0.00	T
8	34	2	18.0	32	0.00	0
9	38	-1	18.5	39	0.00	0
10	42	-1	20.5	43	0.00	0
11	46	2	24.0	44	0.00	0
12	47	1	24.0	46	0.00	0
13	46	-1	22.5	47	0.00	0
14	47	0	23.5	47	0.00	0
15	56	14	35.0	42	0.00	0
16	55	13	34.0	42	0.00	0
17	55	12	33.5	43	0.00	0
18	55	14	34.5	41	0.00	0
19	56	19	37.5	37	0.00	0
20	53	15	34.0	38	0.00	0
21	54	18	36.0	36	0.02	0
22	55	24	39.5	31	0.00	0
23	53	14	33.5	39	0.00	0

Surface Climatological Data for Boise, December 1980

Day	Maximum	Minimum	Mean	Range	Precipitation	Snowcover
6	38	23	30.5	15	0.13	1
7	32	7	19.5	25	0.00	1
8	32	9	20.5	23	0.00	1
9	32	8	20.0	24	0.00	1
10	31	10	20.5	21	0.00	1
11	36	13	24.5	23	0.00	1
12	35	11	23.0	24	0.00	1
13	25	11	18.0	14	T	1
14	26	20	23.0	6	T	1
15	38	22	30.0	16	0.00	1
16	42	19	30.5	23	0.00	T
17	37	20	28.5	17	T	T
18	30	22	26.0	8	T	T
19	31	27	29.0	4	0.03	T
20	32	27	29.5	5	T	T
21	47	27	37.0	20	0.09	T
22	51	35	43.0	16	0.11	0
23	48	31	39.5	17	0.00	0

Table E3.
Six hour averages of total and opaque cloud cover for Grand Junction from December 6-23, 1980. Values of 1.00 indicate total coverage.

	Time period (MST)			
Date	0000-0500	0600-1100	1200-1700	1800-2300
6	0 55/0.55	0.55/0.53	0.75/0.75	0.75/0 67
7	1.00/1.00	0.98/0.98	0.90/0 90	0.90/0.90
8	0.42/0.40	0.98/0.98	0.92/0.92	0.90/0.90
9	0.49/0.49	0.68/0.68	0 03/0.03	0.00/0.00
10	0 00/0.00	0.22/0.02	0.53/0.08	0.42/0 08
11	0.00/0.00	0.23/0.05	0.02/0.00	0 00/0.00
12	0.00/0.00	0.55/0.12	0.68/0.15	0.68/0.23
13	0.28/0.10	0.67/0.25	0.38/0.13	0.00/0.00
14	0.00/0.00	0.00/0.00	0.48/0.05	0.63/0.07
15	0.03/0.00	0.60/0.07	0.98/0.27	0.52/0.12
16	0.03/0.00	0.68/0.22	0.68/0.10	0.22/0 05
17	0.00/0.00	0.28/0.00	0.02/0.00	0.00/0.00
18	0.42/0.15	0.15/0 05	0.78/0.25	0.68/0.32
19	0 30/0.10	0.20/0.05	0.42/0.32	0.22/0.17
20	0.00/0.00	0.02/0.02	0.52/0.52	0.20/0.03
21	0.77/0.02	0.70/0.32	0.40/0.08	0.67/0.20
22	1.00/0.83	1.00/0.55	0.93/0.28	0.98/0.87
23	0 80/0.80	0 72/0.68	0.23/0.20	0.22/0.03

Table E4.
Sames as Table E3 but for Salt Lake City.

	Time period (MST)			
Date	0000-0500	0600-1100	1200-1700	1800-2300
6	0.50/0.37	0.83/0.82	1.00/0.97	1.00/0.98
7	0.95/0.92	0.90/0.77	0.55/0.50	0.03/0.03
8	0.42/0.38	0.75/0.63	0.75/0.55	0.63/0.27
9	0.85/0.75	0.45/0 28	0.55/0.33	0.38/0.02
10	0.12/0.08	0.55/0.23	1.00/0.42	0.48/0.17
11	0.48/0.35	0.45/0.40	0.22/0.20	0.10/0.10
12	0.10/0.10	0.27/0.25	0.52/0.22	0.80/0.45
13	1.00/1.00	1.00/1.00	1.00/1.00	1.00/1.00
14	1.00/1.00	1.00/1.00	1.00/1.00	1.00/1.00
15	1.00/1.00	1.00/1.00	0.82/0.77	0.88/0.88
16	1.00/1.00	0.98/0.98	1.00/0.95	1.00/1.00
17	1.00/1.00	1.00/1.00	0.95/0.95	1.00/1.00
18	1.00/1.00	1.00/1.00	1.00/1.00	1.00/1.00
19	1.00/1.00	1.00/1.00	1.00/1.00	1.00/1.00
20	1.00/1.00	1.00/1.00	1.00/1.00	1.00/1.00
21	1.00/1.00	0.97/0.97	1.00/1.00	1.00/1.00
22	1.00/1.00	1.00/0.75	1.00/0.90	0.95/0.95
23	0.83/0.82	0.35/0.35	0.52/0.05	0.68/0.32

Table E5.
Same as Table E3 but for Boise.

	Time Period (MST)			
Date	0000-0500	0600-1100	1200-1700	1800-2300
6	0.93/0.93	1.00/0.93	0.98/0.98	0.92/0.90
7	0.63/0.58	0.10/0.10	0.00/0.00	0.00/0.00
8	0.23/0.07	0.63/0.23	0.63/0.18	0.20/0.12
9	0.07/0.02	0.17/0.05	0.18/0.00	0.15/0.02
10	0.62/0.35	0.85/0.47	0.93/0.47	0.93/0.78
11	0.87/0.85	0.40/0.15	0.27/0.08	0.28/0.07
12	0.10/0.10	0.58/0.48	0.90/0.48	0.67/0.27
13	0.70/0.63	1.00/1.00	0.98/0.90	1.00/1.00
14	1.00/1.00	1.00/1.00	1.00/1.00	1.00/1.00
15	1.00/1.00	0.98/0.87	0.38/0.12	0.00/0.00
16	0.00/0.00	0.45/0.08	0.55/0.12	0.67/0.63
17	1.00/1.00	0.90/0.87	0.48/0.48	0.87/0.87
18	1.00/1.00	0.98/0.98	0.95/0.95	1.00/1.00
19	1.00/1.00	1.00/1.00	1.00/1.00	1.00/1.00
20	1.00/1.00	1.00/1.00	1.00/1.00	1.00/1.00
21	1.00/1.00	1.00/1.00	1.00/1.00	0.93/0.93
22	1.00/1.00	1.00/1.00	0.95/0.92	0.92/0.88
23	0.87/0.85	0.38/0.22	1.00/0.57	0.95/0.92

Table E6.
The observed total and opaque cloud coverage (tenths) for Winnemucca from December 6-23, 1980.

	Time (PST)							
Date	0100	0400	0700	1000	1300	1600	1900	2200
6	6/4	2/2	6/6	6/6	10/10	9/9	10/10	10/10
7	6/6	0/0	6/6	4/4	4/4	1/1	0/0	0/0
8	0/0	0/0	0/0	0/0	2/0	3/1	0/0	0/0
9	0/0	0/0	0/0	0/0	0/0	0/0	0/0	0/0
10	0/0	0/0	0/0	8/3	10/4	10/3	10/3	10/7
11	9/7	3/1	1/0	9/2	4/1	6/3	10/7	7/3
12	5/2	4/1	0/0	0/0	7/1	8/1	0/0	0/0
13	0/0	0/0	0/0	0/0	1/0	0/0	0/0	0/0
14	0/0	0/0	0/0	0/0	6/2	5/1	3/0	2/0
15	2/0	3/1	8/3	3/1	4/2	3/1	2/1	0/0
16	0/0	0/0	3/1	3/0	4/1	1/0	0/0	0/0
17	0/0	0/0	0/0	0/0	0/0	5/4	4/1	2/2
18	0/0	2/2	7/6	3/3	9/9	10/8	10/7	7/5
19	6/2	7/6	7/2	2/0	0/0	8/3	10/4	2/0
20	0/0	1/0	7/3	7/4	9/6	2/2	1/1	1/0
21	6/2	8/6	10/9	10/10	10/10	10/10	10/10	10/7
22	8/4	10/7	10/9	10/8	9/8	2/2	1/1	0/0
23	0/0	0/0	3/1	10/2	10/4	10/8	10/8	8/7

APPENDIX F

DATA ON DECOUPLING AND POLLUTION POTENTIAL

Tables F1 to F4 give the bulk Richardson number for 50mb thick layers at Grand Junction, Salt Lake City, Winnemucca, and Boise during the deep stable layer episode. Tables F5 and F6 give the bulk Richardson number, lapse rate, and wind shear for the two lowest 50mb thick layers at Grand Junction and Boise. Figures F1 and F2 give the CCBL height, mean wind speed below the CCBL height, and mixing volumes for Grand Junction and Boise during the deep stable layer episode.

Table F1.
The bulk Richardson numbers for 50mb thick layers at Grand Junction from December 6-23, 1980. The numbers in the heading show the pressure levels which define the boundaries of the layers and the mean height AGL of the pressure levels.

		850MB 85M	800MB 563M	750MB 1084M	700MB 1636M	650MB 2223M	600MB 2849M	550MB 3520M	500MB 4242M
12/ 6/80	M	0.82	10.08	0.55	1.40	10.53	8.61	41.87	
	A	5.20	1.33	1.56	0.79	2.22	8.34	8.63	
12/ 7/80	M	4.21	4.00	3.09	1.44	2.00	1.06	6.04	
	A	1.17	4.66	8.92	2.03	1.79	32.70	8.90	
12/ 8/80	M	8.09	8.78	16.85	30.37	5.50	8.33	34.88	
	A	0.15	1.53	4.90	16.94	34.67	22.77	18.02	
12/ 9/80	M	22.00	18.25	2.03	1.31	10.25	6.44	10.41	
	A	-0.44	0.50	2.23	6.95	3.76	30.96	3.16	
12/10/80	M	19.34	3.77	2.43	2.58	48.58	4.27	16.96	
	A	45.93	8.71	43.34	M	0.00	9.65	M	
12/11/80	M	62.00	7.93	2.61	1.46	7.58	4.83	31.84	
	A	13.31	7.78	0.32	0.94	3.38	7.56	1.79	
12/12/80	M	47.13	3.55	5.87	5.20	1.54	3.22	20.89	
	A	29.71	7.43	3.80	41.31	5.46	6.77	2.43	
12/13/80	M	11.14	31.04	8.49	15.46	65.27	5.56	4.76	
	A	15.33	64102.97	8.78	36.42	2.46	1.23	0.50	
12/14/80	M	22.97	11.95	4.68	7.47	20.56	9.79	4.73	
	A	33.35	99999.99	3.51	2.16	1.27	16.53	2.19	
12/15/80	M	9.08	5.46	0.34	71.92	7.48	4.99	6.39	
	A	67.01	3.00	12.66	3.24	2.06	2.49	54.82	
12/16/80	M	26.03	9.00	0.93	21.55	0.88	1.84	3.56	
	A	13.64	1.72	3.28	9.73	11.09	6.56	8.41	
12/17/80	M	40.21	3.93	1.31	3.22	5.19	18.14	123.57	
	A	13.85	7.17	2.82	3.34	2.42	19.13	2.80	
12/18/80	M	101.31	3.55	2.76	36.34	11.46	7.83	1.14	
	A	42.92	4.80	8.79	267.90	19.63	2.48	6.14	
12/19/80	M	35.25	10.89	3.40	367.99	7.79	49.56	4.43	
	A	16.91	136.07	8.69	8.52	39.72	32.47	5.70	
12/20/80	M	95.53	19.83	13.12	12.36	11.60	436.73	23.74	
	A	7.27	2.40	7.82	14.48	5.70	16.12	6.82	
12/21/80	M	219.19	3.68	10.12	4.00	3.10	9.30	6.95	
	A	6.66	1.58	1.47	1.70	5.34	1.79	60.46	
12/22/80	M	2.66	1.33	1.29	1.35	4.43	2.84	1.10	
	A	1.89	1.50	1.83	1.61	2.39	2.04	4.80	
12/23/80	M	2.81	0.14	1.42	14.45	5.63	1.09	1.65	
	A	2.43	-0.27	1.81	4.28	1.43	2.60	2.98	

Table F2.
Same as Table F1 but for Salt Lake City.

		850MB 268M	800MB 766M	750MB 1274M	700MB 1826M	650MB 2410M	600MB 3034M	550MB 3702M	500MB 4427M
12/ 6/86	M	50.61	4.91	2.07	1.01	48.19	21.41	3.08	
	A	6.86	1.74	5.58	2.64	6.54	2.72	9.82	
12/ 7/86	M	8.16	34.90	6.62	1.57	-6.23	1.87	2.22	
	A	6.84	5.98	6.99	3.27	1.49	15.30	M	
12/ 8/86	M	5.29	3.90	40.77	9.58	28.91	2.37	6.58	
	A	6.90	5.98	8.74	33.10	3.63	3.55	3.88	
12/ 9/86	M	6.80	5.93	9.62	8.61	3.15	20.12	2.35	
	A	2.27	8.61	24.13	7.71	65.07	8.54	27.36	
12/10/86	M	21.14	2.89	2.66	32.22	21.74	9.24	10.17	
	A	20.26	6.56	1.23	2.88	8.78	77.28	6.74	
12/11/86	M	56.75	1.27	3.38	2.95	6.28	4.33	8.11	
	A	81.97	3.14	3.80	16.00	6.80	5.35	3.26	
12/12/86	M	153.99	87.18	16.17	6.96	10.30	421.56	45.99	
	A	43.89	97.80	188.22	7.61	20.79	17.48	2.71	
12/13/86	M	240.10	M	M	M	M	M	M	
	A	247.56	11.38	2.28	2.51	17.54	32.58	15.48	
12/14/86	M	12.46	9.49	42.49	4.59	58.32	16.12	7.07	
	A	47.23	6.02	1.70	35.57	2.62	10.39	82.16	
12/15/86	M	8.25	3.39	2.40	3.70	2.75	10.53	35.15	
	A	215.53	1.71	1.70	29.72	15.51	1.13	13.16	
12/16/86	M	156.15	7.36	1.10	7.27	31.00	4.13	3.20	
	A	189.34	74.69	9.38	4.56	2.54	4.63	24.42	
12/17/86	M	7.31	6.67	3.31	3.63	5.57	1.14	27.94	
	A	215.72	3.42	6.34	5.83	6.47	2.14	11.17	
12/18/86	M	16.34	3.10	6.64	13.38	4.82	6.10	14.80	
	A	M	M	M	M	M	M	M	
12/19/86	M	45.65	117.50	43.78	2.48	9.72	13.77	7.99	
	A	215.66	62.86	11.92	25.57	22.79	15.34	4.96	
12/20/86	M	10.54	M	M	M	M	M	M	
	A	52.55	8.46	10.66	1.88	4.25	27.73	18.66	
12/21/86	M	271.24	7.51	3.24	6.39	2.66	9.85	26.81	
	A	42.35	6.55	6.20	6.53	78.03	2.87	1.58	
12/22/86	M	1.19	6.37	6.52	6.96	6.53	1.74	1.60	
	A	13.47	1.66	6.53	5.81	1.17	1.30	6.93	
12/23/86	M	2.90	1.49	6.84	7.73	6.69	20.12	3.34	
	A	7.60	2.93	2.48	1.43	15.94	3.16	4.37	

Table F3.
Same as Table F1 but for Winnemucca.

		850MB 242M	800MB 734M	750MB 1268M	700MB 1812M	650MB 2401M	600MB 3029M	550MB 3702M	500MB 4427M
12/ 6/88	M	0.50	1.29	0.48	5.34	5.04	1.89	1.52	
	A	0.04	2.72	2.48	1.22	7.19	3.83	4.18	
12/ 7/88	M	9.70	129.70	31.29	6.63	2.51	6.29	3.77	
	A	0.20	1.39	14.18	0.86	1.23	1.68	7.96	
12/ 8/88	M	49.31	11.44	5.02	2.66	7.55	2.48	33.27	
	A	848.25	3.80	6.01	44.26	7.73	8.26	7.01	
12/ 9/88	M	8.32	3.67	10.74	29.44	5.79	4.40	12.97	
	A	44.42	114.63	3.67	4.63	9.02	7.02	2.59	
12/10/88	M	109.06	73.90	2.83	29.32	2.05	7.82	6.22	
	A	11.03	6.11	9.65	11.08	1.69	3.46	5.75	
12/11/88	M	40.16	388.75	49.43	2.09	1.04	9.59	3.72	
	A	43.26	24.44	48.37	6.22	8.74	7910.09	8.17	
12/12/88	M	99999.99	24.70	9.39	23.28	2.70	91.34	26.23	
	A	145.39	55.54	48.64	2.85	25.87	6.69	6.41	
12/13/88	M	M	M	M	M	M	M	M	
	A	M	M	0.00	19.94	M	M	M	
12/14/88	M	32.25	12.27	2.41	0.54	0.84	4.09	1.69	
	A	10.81	5.73	9.30	2.74	29.70	28.00	5.93	
12/15/88	M	9.87	2.97	4.11	5.74	425.64	4.15	38.95	
	A	7.66	60.94	23.59	10.39	6.03	8.97	19.44	
12/16/88	M	1154.78	17.59	10.78	1.38	2.59	29.98	4.13	
	A	6.17	9.95	14.21	7.55	4.44	4.49	14.28	
12/17/88	M	42.64	5.49	48.94	22.13	11.16	3.22	12.01	
	A	84.62	5.66	6.51	2.58	9.30	1.83	3.49	
12/18/88	M	M	M	0.00	38.77	M	M	M	
	A	4.02	10.89	4.47	54.93	659.54	5.32	7.47	
12/19/88	M	28.60	19.49	4.08	3.52	8.66	3013.33	3.70	
	A	18.62	3.00	7.86	18.07	1.77	5.11	15.06	
12/20/88	M	17.34	4.12	19.45	6.08	58.19	12.34	41.34	
	A	40.69	7.63	7.00	2.12	7.32	16.04	20.88	
12/21/88	M	7.04	2.80	153.53	15.86	1.13	9.16	1400.35	
	A	0.34	0.36	0.36	1.64	43.83	50.24	3.34	
12/22/88	M	1.07	2.47	0.56	3.47	1.40	4.75	2.20	
	A	-0.44	1.01	0.41	7.88	265.77	-0.65	1.97	
12/23/88	M	3.52	6.31	1.95	1.62	4.07	1.80	0.86	
	A	0.91	34.53	2.20	1.53	1.13	36.22	1.89	

Table F4.
Same as Table F1 but for Boise.

		900MB 215M	850MB 673M	800MB 1162M	750MB 1682M	700MB 2232M	650MB 2817M	600MB 3340M	550MB 4107M	500MB 4826M
12/ 6/88	M	0.21	-0.48	0.11	38.44	1.55	2.72	5.17	4.83	
	A	14.58	99999.99	23.92	2.84	2.17	0.74	0.36	0.91	
12/ 7/88	M	6.28	49.75	9.12	17.36	7.15	1.89	2.66	1.43	
	A	1.58	3.51	18.52	65.11	0.65	4.36	2.62	18.46	
12/ 8/88	M	5.48	16.45	13.24	5.55	4.89	25.54	36.62	5.18	
	A	18.81	3.72	7.72	5.44	62.84	16.76	5.66	4.15	
12/ 9/88	M	3.33	24.54	19.84	1.37	8.84	4.62	4.47	36.96	
	A	9.91	4.86	5.46	5.35	1.58	0.63	0.72	0.78	
12/10/88	M	M	M	0.00	5.64	464.34	M	M	M	
	A	19.48	3.58	1.15	0.24	1.77	5.76	5.12	5.78	
12/11/88	M	135.29	2.38	3.22	5.31	0.41	M	M	M	
	A	34.64	70.13	1.15	1.66	20.91	3.65	0.94	46.78	
12/12/88	M	79.23	6.58	2.16	11.96	8.77	5.55	36.49	7.15	
	A	8.91	159.11	1.94	4.33	3.72	5.38	2.12	2.58	
12/13/88	M	84.54	M	M	M	M	M	M	M	
	A	25.26	53.25	7.49	12.88	9.16	8.27	14.28	61.57	
12/14/88	M	46.82	16.62	8.38	1.34	9.45	1.91	0.88	10.96	
	A	6.92	1.75	25.43	2.88	16.39	8.68	36.45	3.55	
12/15/88	M	9.66	1.19	22.16	1.29	8.24	13.21	6.68	9.69	
	A	139.76	5.36	7.42	6.57	16.98	518.16	3.58	9.44	
12/16/88	M	33.51	21.89	18.56	8.83	7.22	11.16	1.97	2.89	
	A	1.83	12.77	2.21	2.29	6.84	4.59	3.82	6.21	
12/17/88	M	122.75	15.06	5.82	2.94	3.16	2.36	336.44	3.39	
	A	38.46	18.28	16.63	11.92	6.34	2.46	4.21	6.25	
12/18/88	M	66.63	8.28	16.26	7.14	9.18	57.24	5.26	13.33	
	A	51.66	11.91	44.48	28.82	7.39	59.61	21.69	2.71	
12/19/88	M	38.49	3.39	7.27	5.14	7.21	16.96	21.32	2.63	
	A	31.86	16.69	4.83	44.63	4.38	5.11	36.84	18.93	
12/20/88	M	19.16	44.54	1.57	3.91	26.96	2.82	5.31	17.98	
	A	45.42	26.45	1.82	38.84	37.54	7.62	72.98	4.96	
12/21/88	M	M	0.66	4.46	4.67	3.96	22.82	5.94	M	
	A	1.25	0.37	0.35	1.18	0.52	31.39	4.76	6.58	
12/22/88	M	0.45	1.67	0.21	0.76	1.28	5.45	0.23	5.94	
	A	0.87	1.89	0.78	3.27	3.87	3.18	0.96	6.62	
12/23/88	M	0.24	5.28	23.56	0.52	1.18	0.75	1.19	2.88	
	A	1.33	1.63	2.43	7.45	1.59	5.61	0.86	0.78	

Table F5.
The bulk Richardson number, mean lapse rate ($°Ckm^{-1}$), and wind shear ($ms^{-1}km^{-1}$) for the two lowest 50mb thick layers at Grand Junction.

		850mb to 800mb 85m to 563m			800mb to 750mb 563m to 1084m		
		Ri Number	Lapse Rate	Wind Shear	Ri Number	Lapse Rate	Wind Shear
12/ 6/80	M	0.82	6.40	12.04	10.08	4.44	4.34
	A	5.20	6.37	4.76	1.33	7.29	8.07
12/ 7/80	M	4.21	7.16	4.67	4.00	6.19	5.65
	A	1.17	8.98	4.74	4.66	6.80	4.78
12/ 8/80	M	8.09	3.70	5.17	8.78	8.22	2.52
	A	0.15	9.65	5.01	1.53	9.22	3.56
12/ 9/80	M	22.00	3.94	3.09	18.25	7.10	2.30
	A	-0.44	9.84	2.63	0.50	9.20	6.28
12/10/80	M	19.34	3.33	3.47	3.77	1.97	8.69
	A	45.93	5.13	1.90	8.71	1.75	5.75
12/11/80	M	62.00	0.21	2.36	7.93	-4.28	7.99
	A	13.31	0.00	5.08	7.78	0.38	6.52
12/12/80	M	47.13	-7.77	3.65	3.55	-5.76	12.47
	A	29.71	2.62	2.90	7.43	-1.52	7.31
12/13/80	M	11.14	-4.09	6.66	31.04	-3.45	3.89
	A	15.33	2.63	4.05	64102.97	1.72	0.07
12/14/80	M	22.97	-1.63	4.20	11.95	4.82	3.84
	A	33.35	5.87	2.02	99999.99	-0.76	0.00
12/15/80	M	9.08	1.23	5.78	5.46	-4.80	9.73
	A	67.01	0.60	2.19	3.00	5.69	6.90
12/16/80	M	26.03	-3.44	4.23	9.00	0.00	6.18
	A	13.64	3.19	4.09	1.72	0.56	13.63
12/17/80	M	40.21	-8.91	4.05	3.93	-4.16	11.14
	A	13.85	3.40	4.00	7.17	-1.88	7.52
12/18/80	M	101.31	-3.46	2.15	3.55	1.72	8.97
	A	42.92	7.60	1.32	4.80	2.46	7.31
12/19/80	M	35.25	-2.83	3.55	10.89	1.72	5.11
	A	16.91	6.40	2.63	136.07	6.65	0.89
12/20/80	M	95.53	-2.85	2.16	19.83	3.26	3.41
	A	7.27	6.21	4.11	2.40	6.30	7.14
12/21/80	M	219.19	-3.88	1.49	3.68	3.45	7.80
	A	6.66	6.61	4.05	1.58	6.87	8.03
12/22/80	M	2.66	3.23	9.28	1.33	8.05	6.70
	A	1.89	7.78	5.99	1.50	5.90	9.52
12/23/80	M	2.81	1.62	10.10	0.14	9.65	4.97
	A	2.43	9.46	2.01	-0.27	9.85	3.18

Table F6.
Same as Table E5 but for Boise.

		900mb to 850mb 215m to 673m			850mb to 800mb 673m to 1162m		
		Ri Number	Lapse Rate	Wind Shear	Ri Number	Lapse Rate	Wind Shear
12/ 6/80	M	0.21	8.73	13.05	-0.48	10.04	4.71
	A	14.50	6.61	2.80	99999.99	7.98	0.00
12/ 7/80	M	6.28	0.67	7.31	49.75	3.39	2.17
	A	1.50	8.69	5.09	3.51	2.97	8.46
12/ 8/80	M	5.40	3.15	6.72	16.45	-1.27	4.98
	A	10.01	3.56	4.76	3.72	-1.89	10.71
12/ 9/80	M	3.33	2.46	8.96	24.54	-7.95	5.13
	A	9.91	3.77	4.69	4.86	-1.67	9.24
12/10/80	M	M	M	M	M	M	M
	A	19.40	-7.03	5.59	3.50	-5.11	12.31
12/11/80	M	135.29	-11.65	2.39	2.38	-9.72	16.99
	A	34.64	-8.75	4.38	70.13	-4.24	2.65
12/12/80	M	79.23	-2.41	2.35	6.50	-10.63	10.57
	A	8.91	-8.10	8.48	159.11	-8.94	2.04
12/13/80	M	64.54	-9.91	3.32	M	M	M
	A	25.20	-20.39	6.58	53.25	-8.35	3.47
12/14/80	M	46.82	-10.02	3.94	16.62	-15.46	7.38
	A	6.92	-23.52	13.19	1.75	-0.81	14.65
12/15/80	M	9.66	-23.01	10.98	1.19	3.82	13.22
	A	139.76	-18.28	2.67	5.30	-0.60	8.25
12/16/80	M	33.51	-12.96	4.90	21.89	-7.55	5.24
	A	1.83	-12.50	20.73	12.77	-5.38	6.42
12/17/80	M	122.75	-6.74	2.19	15.00	-7.27	6.32
	A	38.46	-10.61	4.34	18.28	-1.81	4.71
12/18/80	M	60.03	-9.59	3.40	8.28	-5.67	8.11
	A	51.06	-18.78	4.48	11.91	-3.43	6.24
12/19/80	M	38.49	-10.72	4.38	3.39	-4.49	12.22
	A	31.80	-9.45	4.67	16.69	-7.93	6.13
12/20/80	M	19.16	-14.44	6.74	44.54	-2.24	3.09
	A	45.42	-14.41	4.37	20.45	3.04	3.40
12/21/80	M	M	M	M	0.00	0.40	28630.40
	A	1.25	3.60	13.09	0.37	5.85	19.24
12/22/80	M	0.45	4.63	19.85	1.67	8.65	4.79
	A	0.07	9.57	9.35	1.09	7.54	8.49
12/23/80	M	0.24	8.82	11.61	5.28	7.19	4.16
	A	1.33	8.17	6.47	1.63	5.33	9.84

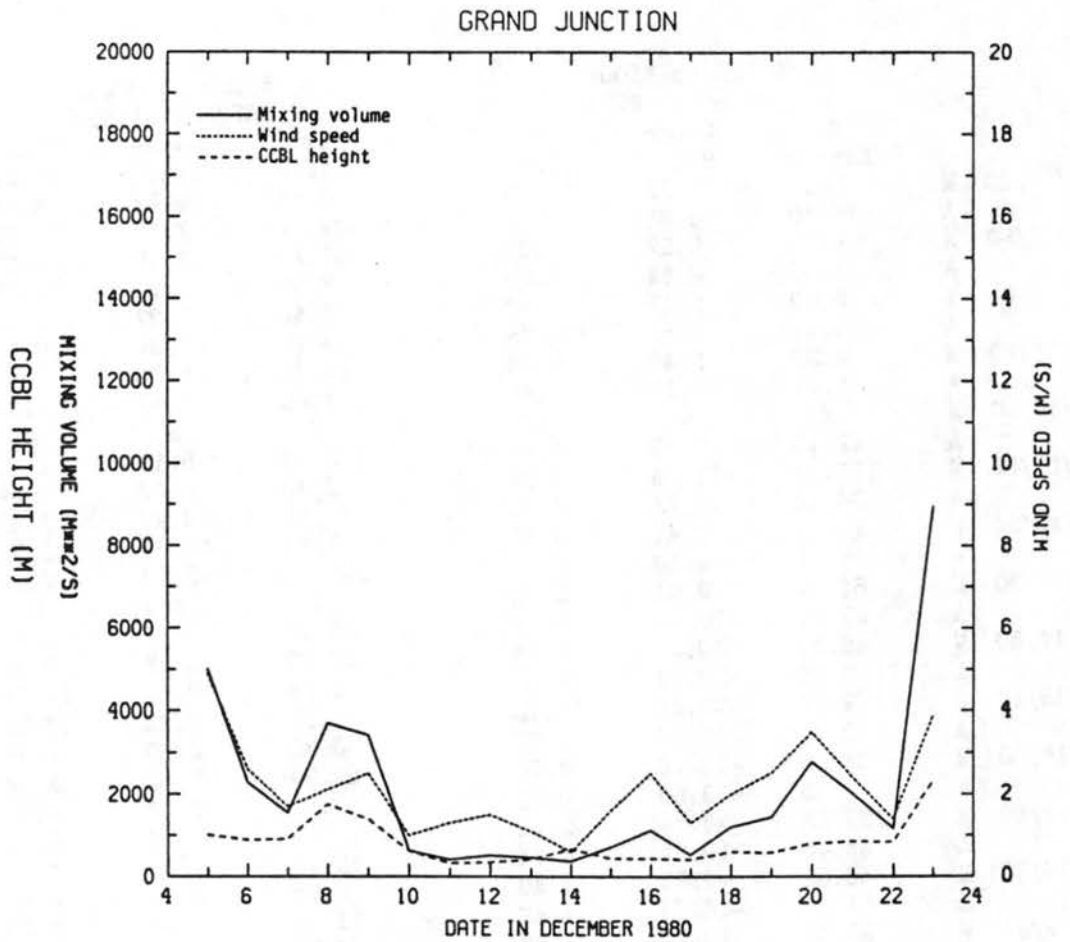

Figure F1. The CCBL height (m), mean wind speed below the CCBL (ms^{-1}), and mixing volume (m^2s^{-1}) from December 5-23, 1980 at Grand Junction.

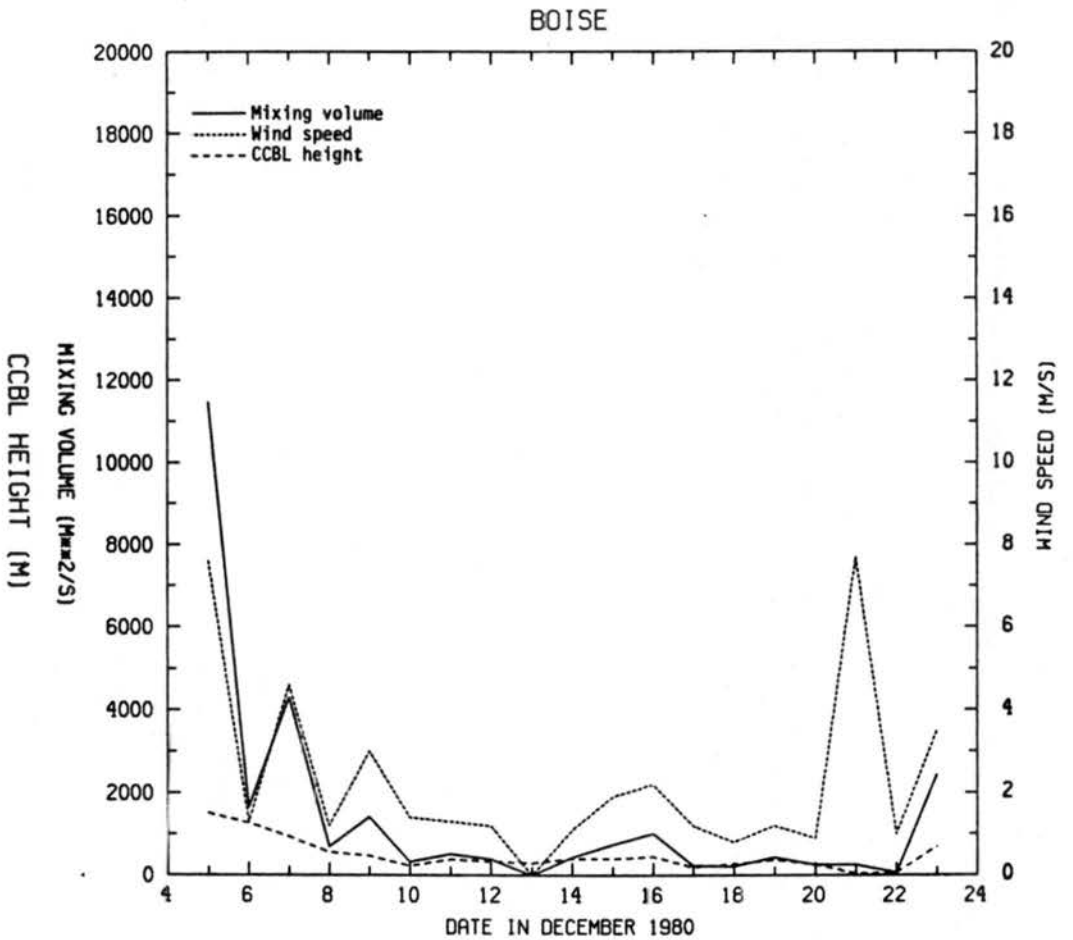

Figure F2. Same as Figure F1 but for Boise.

BIBLIOGRAPHIC DATA SHEET	1. Report No. Atmospheric Science Paper 409	2.	3. Recipient's Accession No.

4. Title and Subtitle

AN EXAMINATION OF DEEP STABLE LAYERS IN THE INTERMOUNTAIN REGION OF THE WESTERN UNITED STATES.

5. Report Date: December 1986

6.

7. Author(s): Paul G. Wolyn and Thomas B. McKee

8. Performing Organization Rept. No. 409

9. Performing Organization Name and Address

Department of Atmospheric Science
Colorado State University
Fort Collins, CO 80523

10. Project/Task/Work Unit No.

11. Contract/Grant No.

NSF ATM83-04328

12. Sponsoring Organization Name and Address

National Science Foundation
Washington, DC

13. Type of Report & Period Covered

14.

15. Supplementary Notes

16. Abstracts

The definition of a deep stable alyer used in this report is 65% of the lowest 1.5 km of the 120GMT sounding having a lapse rate of 2.5^{o}Ckm^{-1} or less. Deep stable layers are associated with one important group of days which can potentially cause poor regional air quality in the intermountain region of the western U.S. At Grand Junction, CO; Salt Lake City, UT; Winnemucca, NV; and Boise, ID; they cause low daytime convective boundary layer heights and can allow for light winds near the surface even if moderate or strong synoptic scale winds aloft are present. A climatology of deep stable layer days showed that at the four intermountain region stations most of the days with deep stable layers occurred in Dec and Jan. Using a strict deep stable layer definition and episode criteria, episodes of three days or longer occurred on the average at least once every two years at Salt Lake City and Winnemucca, and at lease once a year at Boise and Grand Junction. An analysis of the mixing volumes for five consecutive Decembers at the four intermountain region stations shows that all the deep stable layer days had low mixing volumes.

(continued on next page)

17. Key Words and Document Analysis. 17a. Descriptors

Inversions
Synoptic-scale influences in complex terrain
Cold-air stagnation in complex terrain
Air pollution potential

17b. Identifiers/Open-Ended Terms

17c. COSATI Field/Group

18. Availability Statement	19. Security Class (This Report) UNCLASSIFIED	21. No. of Pages 177
	20. Security Class (This Page) UNCLASSIFIED	22. Price

BIBLIOGRAPHIC DATA SHEET

An Examination of Deep Stable Layers in the Intermountain Region of the Western United States.

16. Abstract continued.

A deep stable layer episode, which occurred from December 6-23, 1980 at the four intermountain region stations, was examined in-depth to study the life cycle of a deep stable layer episode and to study the importance of different meteorological factors to the initiation, continuation, and termination of the episode. The initiation of the episode is associated with the movement of a warm ridge aloft into the region and is accompanied by a descending region of rapid warming and strong stability. Synoptic-scale warm air advection and subsidence are both important mechanisms for causing the warming aloft. Weak incoming solar radiation resulting in modest surface heating is important to prevent the destruction of the descending stable region.

When the region of rapid warming descended to 0.5-1.5 km it formed a capping stable layer. In this part of the episode called the continuation phase, a disturbance was able to weaken the deep stable layer but not terminate it. The longwave radiative effects of fog may be importnat in this phase of the episode.

The termination of the episode is associated with the destruction of the warm ridge aloft and the movement of disturbances into the region. Surface heating may be important for aiding in the termination of the episode. The presence of a thick fog layer can require a stronger disturbance to terminate the episode.